Ship Design for Damage Survivability

by

Dharmaraj Subramani

Submitted as a Thesis for the Degree of Doctor of Philosophy

Department of Marine Technology

University of Newcastle upon Tyne

November 1995

Abstract

This thesis presents a new set of methods to assist the process of ship design for safety with particular reference to collision damage. The study has two principal objectives:

- investigations into subdivision aspects of passenger ships to improve their overall survival index
- investigations into the subdivision of oil tankers in order to improve the effectiveness against spillage in the event of collision damage.

In order to investigate the ship subdivision aspect a damage stability model was needed. A pre-requisite for developing the damage stability software was a robust but flexible method to define the hull and the compartments of subdivision. B-splines have been a popular representational tool in computer aided design over the past three decades. This method, though more complex than other spline techniques such as cubic splines, was adopted with a fourth order basis function in this work. A complete set of spline manipulation libraries and associated numerical solvers were developed for this purpose. In addition to this, a method to define the intersection between the hull and the waterplane in the form of a closed B-spline curve for any given orientation of the vessel in terms of heel, trim and draught was developed to aid the damage stability calculations.

Though the earlier regulations stipulate fixed trim assessments to ease the computational process, it is clearly unsatisfactory and research has confirmed this to be a flawed approach. Free trim calculations on the other hand require an iterative and time consuming process to arrive at the equilibrium trim position for each heel angle. Pawlowski proposed a new method for the stability calculations of a freely floating rig when the unit is arbitrarily orientated to the wind direction. It uses the Euler theorem on the properties of equivolume waterplanes to arrive non-iteratively at the new inclined position. This theory was adapted for use in damage stability calculations and was numerically tested and proved to be sound.

Damage stability calculations, though combinatorially large, are also inherently parallel. Parallel Virtual Machines (PVM) is a Message Passing Interface (MPI) developed jointly by ORNL, University of Tennessee, Carnegie Mellon University and the

Pittsburgh Supercomputing centre. PVM enables a "virtual configuration" so that a collection of serial, parallel and vector processing machines appear as one large distributed memory computer. PVM was compared with another MPI called Network Linda where the advantage of PVM's user controlled message passing was demonstrated. PVM was used to implement the MIMD Distributed Memory paradigm to exploit this inherent parallelism in damage stability calculations and to obtain speed-ups.

A systematic exploration of the search space for this design problem involves the generation of a large number of internal subdivision configurations. This, coupled with the fact that the design space was multimodal in nature made it suitable to the application of a class of heuristic search algorithms called Genetic Algorithms (GA). A brief description of the mechanisms behind GA is presented along with their mathematical basis in the form of two theorems: the schema theorem and the building block hypothesis. Various techniques for solving constrained optimisation problems with GA was explored. The penalty function method was found to be the most suitable and was finally adopted.

The above techniques were applied to the optimisation of the internal subdivision of passenger ships and cargo ships, oil tankers in particular. For passenger ships, the nature of the 's'-factor formulation on the local index was shown. The multimodal nature of the subdivision problem was highlighted and a GA was used to investigate the optimal subdivision characteristics of the vessel. The 's' factor formulation for cargo ship rules is different to that described by the A.265 set of regulations for passenger vessels. In addition, the cargo ship rules describe a factor 'v' which accounts for the probabilities of vertical extents of damages. However this formulation does not assign any credit for horizontal subdivision below the waterline. Data on vertical extents and vertical location of damages for cargo ships was collected and analysed in earlier studies done at Newcastle University. This data was used to develop a probability function akin to that developed for the longitudinal extent and longitudinal location so as to give credit for any horizontal subdivisions. The principal objective of this part of the study was to explore the search space for subdivision configurations that would minimize net oil outflow.

Conclusion

Acknowledgements

First and foremost, I would like to thank Dr. P. Sen of the Department of Marine Technology, Newcastle University. He has not only been my guru but has also been a guardian and a friend. I deeply appreciate his efforts to ease my financial burden while undertaking this research.

There are many people who have made my stay at Newcastle a pleasant experience. I would like to thank Dave "old goat" Thomas who taught me everything from how to climb rocks and fell-walking to how to hold a pint, Brian "bam" Murray for teaching me the subtleties of the highland malts, Ian Applegarth and Claude Labrie for letting me endure pain during our long and torturous bike rides which culminated in the tour de Espanol. Many thanks to Christine "bionic" Barbier, Barbara "babs" Keating, Edmond "eddy" Chadwick, Jonathan Horn, Eko "Mr. E" Pannungal, Tri Achmadi, Hartanta "tari" Tarigan, Daniel Rosyid, Hang Sub Urm, Seong-Gi Seo, Peter Atkinson, Rauf "cream" Kattan, Helen Clough, to mention a few, for their wonderful company during the last four years. Thanks also to Paul Binks to appear unfailingly whenever we had to move house and for the "laundry keys" that helped me stay clean and to Christos "tictoc" Atalianis for being an accommodating flatmate and colleague (and to Lisa McEntee for the same). Special thanks to Chris, Aideen, Ronan, Connor and Orla (also known as the Forker household) for being my family away from home for all these years. I would also like to thanks my colleagues in the EDC (Pravir, Anjula, Yang-bo and many others) for their company.

Above all thanks to Shila for waiting for me so patiently for all these years and then making that awful mistake of marrying me. Her support and encouragement was always forthcoming in times of need.

My late father and my mother have been a constant source of inspiration. I would like to thank them for everything that they have done for me and would like to dedicate this effort to them.

Chapter 1

Introduction

The history of transition from a deterministic to a more probabilistic approach towards ship safety has been a long and painful one. The fatal encounter between *Titanic* and an iceberg on her maiden voyage in April 1912 was made even more damning by the fact that the ship complied fully with the applicable British Board of Trade requirements in force at the time [Payne'94]. It has often taken a maritime disaster of significant proportions to bring home the fact that rules and regulations based on previous experience and eras have not kept sufficient pace with modern technology.

> "Weak correlation between legislation and moral values has been normal in forming requirements for the design of ships for very many years. Laws to protect the sea traveller has been driven rather by disaster and public outrage" [Rawson'90].

Safety regulations are not just dependent on casualty potential but are also influenced by engineering, economics, politics, philosophy and publicity. It has been said that,

> "Safety regulations appear to the designer to be restrictive; to the shipowner expensive; to the press either bureaucratic or inadequate; and to the legislator unreasonable one day and insufficient the next" [Pawlowski'92].

The philosophy behind the "one-compartment standard" [Tagg'82] was to make ships safer by requiring sufficient compartmentation in the transverse direction so as to keep the ship afloat in an upright condition when any of the main compartments is breached. The fundamental assumption behind this standard was that all damages would occur only between transverse bulkheads thereby limiting the loss to only one compartment at any given time. This rule seemed to forget that ships involved in collision have very little respect for the positions of transverse bulkheads.

Comstock [Comstock'60] pointed out some of the major faults that were present in the 1960 SOLAS convention,

- the inability of the conference to address a fundamental error, the assumption that closer spacing of bulkheads by and of itself, increases the probability of a ship surviving collision damage.
- the fact that a majority of the passenger vessels had a factor of subdivision between 0.5 and 1.0 and therefore need not be designed to survive even a minor damage in the way of a transverse bulkhead and thus flood two adjacent compartments.
- generally a ship with greater number of passengers should have a higher standard of safety. Under the factorial system, in a given ship an increase in the number of passengers generally results in a decrease in the factor of subdivision.
- over-optimistic assumptions such as the damage extent and damage penetration would not exceed the limits set by the convention and that at the time of collision the ship will be ballasted so as to have the required stability without the requirements for such ballast spaces being built into the provision.

Probabilistic analysis procedures for estimation of ship subdivision was first introduced by Wendel [Wendel'60], [Wendel'68]. For the first time in the history maritime regulations evaluations of subdivision damage was proposed without any prior assumptions as to the lengths and locations of damage but rather on damage statistics and mathematical probability theory. The probabilistic rules provide the basis for the most effective passive means of protection for ships against collision damage.

> "It seems that many results related here and by other authors make it advisable to change fundamentally the regulations for subdivision prescribed by the International Convention" [Wendel'68].

It wasn't until 1973 that the International Maritime Organisation [IMO] (then known as the Intergovernmental Maritime Consultative Organisation [IMCO]) incorporated these probabilistic rules into the regulations for passenger ship subdivision.

In spite of the rational basis of the probabilistic evaluation methods, very few ships have been designed globally on these basis. This is partly due to the "grandfather clause" [Payne'94] whereby the applicable regulations under which a ship was built could be maintained to the day the ship was scrapped without significant modifications and partly due to the fact that the new regulations were consider to be "equivalent" to the provisions of part B of chapter II of SOLAS'60. This in many ways turned out to be the opt out clause for most designers who found the applications of the rules new more difficult. In a sense, this is probably true because the probabilistic regulations do involve a greater degree of computation and are cloaked in a language which is not particularly endearing to engineers.

One of the perceived advantages of the floodable length method was its ability to not just check the adequacy of a design but to determine how the design ought to be in that the rules were capable of simple inversion. Unfortunately the probabilistic method are not prescriptive in nature due to their mathematical and computational complexities. Hence it is left to the designer to do whatever is necessary to attain an acceptable value of A.

The attained index of subdivision A as defined by the regulations is a value lying between 0 and 1 and is representative of the probability of survival of a vessel under damaged conditions. The local index of subdivision (for passenger vessels) [Pawlowski'92] is a measure of the contribution that an individual compartment makes to the overall index A and is given by the formula

$$A_k = \frac{\sum_{i \in K} a_i p_i s_i}{\sum_{i \in K} a_i p_i}$$

where K is the set of all legal combinations that includes compartment k. In a similar manner, the local outflow index for oil tanker subdivision is defined as

$$e_j = \frac{\sum_{i \in J} p_i v_i}{\sum_{i \in J} p_i}$$

where a_i - probability of damage location in the longitudinal direction

p_i - probability of flooding a given compartment group

s_i - accounts for the probability of survival after flooding

v_i - volume of oil contained in the compartment group

and J is the set of all legal combinations that includes compartment j.

The use of local indices to arrive at the "best" subdivision arrangement is the main themes that was explored in the first part of this thesis. Since the amount of "survivability" available for a vessel is finite and fixed, the local index can be used as a measure to estimate the distribution of this survivability along the length of the vessel. The philosophy behind the probabilistic regulations is that no part of the ship should be excessively vulnerable which could be seen to imply that the distribution of "survivability" along the ship's length should be as uniform as possible. The local index could be used to prevent ships from having compartments with excessive lengths and breadths. The local index in effect could provide a handle for designers to make the probabilistic rules more manageable.

The basic outline of the thesis is thus as follows:

In chapter 2 the techniques of hullform generation is introduced. The pre-requisite for modelling the behaviour of a vessel under damaged condition was a robust and flexible technique of defining the hullform and the compartments. B-splines have been a popular tool in computer aided design over the past three decades. The formulation of the B-spline method along with the solver is described. In addition, the development of spline libraries along with the definition of the intersection between the waterplane and the hull is shown. The latter was required for damage stability calculations.

Chapter 3 describes the damage stability theory based on equi-volume waterplanes as proposed by Pawlowski [Pawlowski'91]. GZ-curves estimated using fixed trim methods have proven to be unsatisfactory due to the error in the estimation of the GZ values. Free trim methods on the other hand require an iterative process to arrive at the equilibrium position for each heel angle. Pawlowski's equi-volume theory used the Euler theorem on the properties of equivolume waterplanes to arrive non-iteratively at the new inclined position.

Chapter 4 describes a new class of heuristic search algorithm called Genetic Algorithms (GA). A brief description of the mechanisms behind GA is presented along with the mathematical basis in the form of two theorems: the schema theorem and the building block hypothesis. Various techniques used with GA for constrained optimisation problems are also discussed.

Damage stability calculations, though computationally large, are also inherently parallel. Parallel Virtual Machines (PVM), a message passing interface (MPI) developed

by a group of academic institutions in the United States was used to "farm" the damage stability calculations to a cluster of Unix machines to obtain speed ups. The philosophy behind such distributed computing paradigms is discussed in chapter 5. The comparative performance between PVM and another MPI called Network Linda is also discussed.

Chapter 6 shows how the techniques defined in chapters 2, 3, 4 and 5 are combined in order to solve the problem of ship subdivision and thus sets the scene for the computational foundation for the problem.

Chapter 7 describes the application of the above technique to explore passenger ship subdivision.

Chapter 8 describes the subdivision configurations explored for an oil tanker on the basis of the local outflow index. Also, a mathematical formulation of the vertical extent of probability is described, as this is relevant for tankers with some horizontal subdivision.

Finally, chapter 9 summarises the work done with concluding remarks.

Chapter 2

Hullform Generation

2.1 Introduction

In drafting technology, a spline is a flexible strip used to produce a smooth curve through a designated set of points. The term *spline curve* referred to a curve drawn with several small weights (ducks) distributed along the length of the strip to hold it in position on the drafting table as the curve is drawn.

In computer graphics, the term *spline curve* now refers to any composite curve formed with polynomial sections satisfying continuity conditions at the boundary of the pieces [Hearn'94].

2.2 Parametric representation and continuity

The most common functional form used for modelling curves and surfaces is the *parametric* or *vector-valued* function [Newman'79]. In the parametric form a curve is represented as a vector,

$$P(u) = [x(u) \quad y(u) \quad z(u)]$$

where u is the parameter value, usually normalised between zero and one.

The advantage of parametric representation is that the curve becomes axis-independent [Rogers'90] since a point on the curve is now specified by just a single parameter u. The length and the termination points of the curve are fixed by the parameter range.

If an object exists in a space which is free of a coordinate system, such that, the object is coordinate free or coordinate independent, then mathematically such a space is called an *affine space* and the geometry involved is called *affine geometry* [Farin'88]. Transformations such as rotations and translations performed in the affine space are called affine transformations. Parametric curves, due to their virtue of being axis-independent, are easily manipulated using affine manipulation transformations.

Given a complex curve, it is generally not possible to devise a simple function that specifies the shape of the entire curve or surface. However the procedure becomes much simpler if the parametric function has to define a small section of that curve, the entire shape is then defied by a series of functions, pieced together. Such *piecewise* approximations require methods that would ensure continuity at the joints. Conditions that ensure such continuity are known as parametric continuity conditions [Hearn'94] and are defined as,

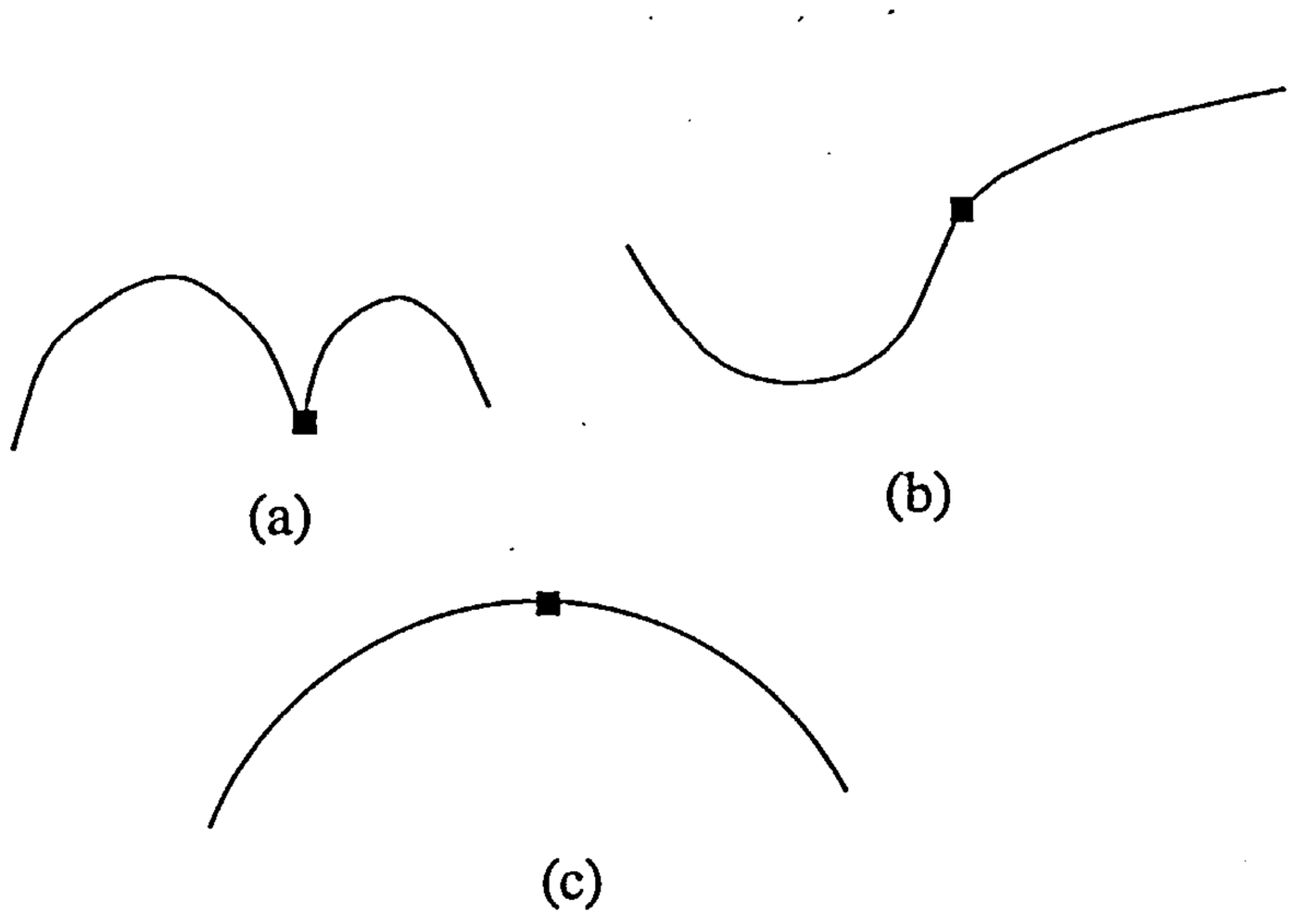

FIGURE 2.1. Parametric continuity (a) C^0 (b) C^1 (c) C^2

Zero order parametric continuity, described as C^0 continuity, ensures that the two ends of the curves meet, Figure 2.1 (a).

First order parametric continuity, C^1 continuity, ensures that the first derivatives of the parametric functions at their common joining point are equal, Figure 2.1 (b).

Second order parametric continuity, C^2 continuity, ensures that the second derivative is the same at the joining ends of the two curves, Figure 2.1 (c).

2.3 Spline Curves

Natural Cubic Splines were one of the first curves to be developed for graphics application [Hearn'94].

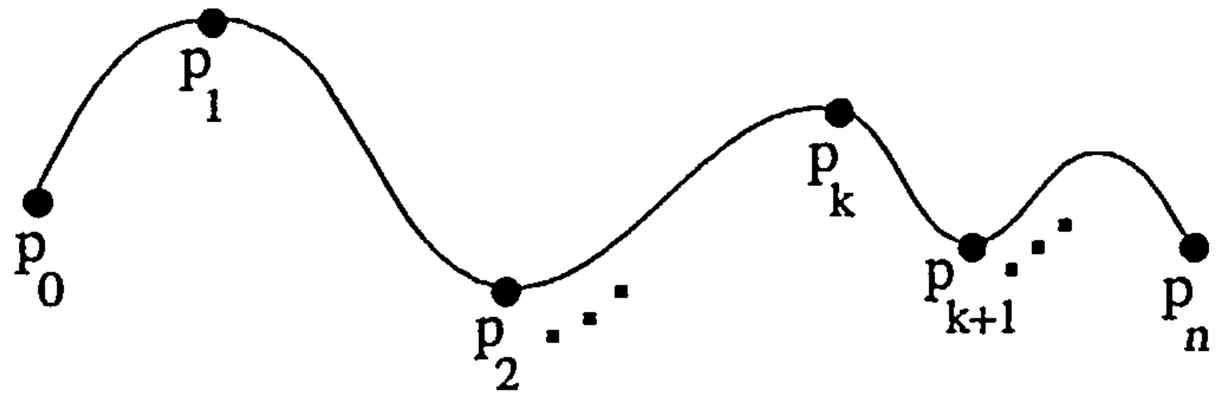

FIGURE 2.2. Piecewise continuous cubic interpolation spline

$$\begin{aligned} x(t) &= a_x(t) + b_x(t) + c_x(t) + d_x \\ y(t) &= a_y(t) + b_y(t) + c_y(t) + d_y \\ z(t) &= a_z(t) + b_z(t) + c_z(t) + d_z \end{aligned} \qquad \text{(EQ 2.1)}$$

The parametric cubic polynomial to be fitted to a set of control points is given in EQ 2.1. $n+1$ control points resulting in n curve sections gives $4n$ unknown coefficients to be determined. For each interior point, of which there are $n-1$ in total, four boundary conditions need to be satisfied

- The end of one curve segment and the beginning of the next must share a common point, i.e. C^0 continuity
- C^1 continuity
- C^2 continuity

giving a total of $4n-4$ equations. C^0 continuity for the end points yield a further two equations. For the two additional equations, there are two approaches

- set the second derivative at p_0 and p_n to zero
- add two dummy control points, p_{-1} and p_{n+1} so that all the original control points are now interior points with the necessary $4n$ boundary conditions.

The inability of allowing local control, wherein any change in position of a control point would not affect the shape of the entire curve in natural cubic splines is sought to be

overcome by other formulations such as *Hermite* formulation, *Cardinal* formulation and the *Kochanek-Bartels* formulation.

However a number of disadvantages exist with respect to cubic splines [Rogers'90]

- non-rational parametric cubics never reduce exactly to a conic section (except obviously quadratic curves such as parabolas).
- they poorly approximate asymptotic curves
- if not carefully controlled they frequently exhibit spurious oscillations, since the cubic spline is influenced locally by each data point
- discontinuities in the third derivative induce unwanted inflection points at certain locations along the curve

The Bézier curve developed by Pierre Bézier, a French engineer, is a popular and versatile spline approximation method. Consider the following expression

$$(1)^3 = ((1-t)+t)^3 \qquad \text{(EQ 2.2)}$$

$$1 = (1-t)^3 + 3(1-t)^2 t + 3(1-t)t^2 + t^3$$

Given four control point positions: $p_k = (x_k, y_k, z_k) \cdot k = 0, 1, 2, 3$, these coordinate positions can be combined with the Bézier blending functions (EQ 2.2) to describe the path of an approximating Bézier polynomial function between p_0 and p_3

$$P(t) = p_o(1-t)^3 + 3p_1(1-t)^2 t + 3p_2(1-t)t^2 + p_3 t^3 \qquad \text{(EQ 2.3)}$$

This is a cubic Bézier formulation. (EQ 2.2) can be extended to any degree yielding a generalised Bézier blending function which are in effect Bernstein polynomials

$$B_{n,i}(t) = C(n,i)t^n(1-t)^{n-i} \qquad \text{(EQ 2.4)}$$

where $C(n, i)$ represents the binomial coefficient

$$C(n,i) = \frac{n!}{i!(n-i)!}$$

The fact that the Bernstein functions always add up to one has connotations for the Bézier curve transformations. Consider the mapping

$$\Phi(x) = A\ P(t) + \underset{\sim}{V}$$

where A is a matrix (involving either rotation, shear, scaling or rotation) and $\underset{\sim}{V}$ is a translation vector. From (EQ 2.2)

$$\underset{\sim}{V} = \underset{\sim}{V}[(1-t)^3 + 3(1-t)^2 t + 3(1-t)t^2 + t^3]$$

and substituting this and (EQ 2.3) in the above equation,

$$\begin{aligned}\Phi(t) = {} & A[p_o(1-t)^3 + 3p_1(1-t)^2 t + 3p_2(1-t)t^2 + p_3 t^3] \\ & + \underset{\sim}{V}[(1-t)^3 + 3(1-t)^2 t + 3(1-t)t^2 + t^3]\end{aligned}$$

$$\begin{aligned}\Phi(t) = {} & [Ap_0 + \underset{\sim}{V}](1-t)^3 + [Ap_1 + \underset{\sim}{V}]3p_1(1-t)^2 t \\ & + [Ap_2 + \underset{\sim}{V}](3(1-t)t^2) + [Ap_0 + \underset{\sim}{V}]t^3\end{aligned} \qquad \text{(EQ 2.5)}$$

(EQ 2.5) implies that the transformation Φ can be applied to the coefficients p_0, p_1, p_2 and p_3 leaving the nature of the polynomial functions unchanged. This is a direct consequence of the fact that the Bernstein functions add up to one. This property has profound implications in computer graphics since the number of operations in transforming an object in a three dimensional space is reduced to the manipulation of the control vertices defining that object.

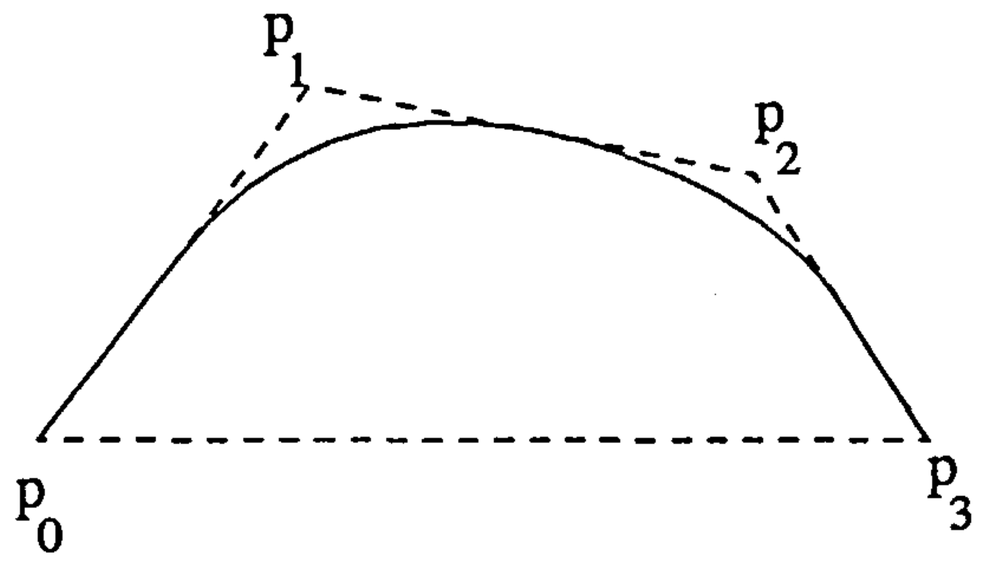

FIGURE 2.3. The convex hull

Another important feature of barycentric combinations can be demonstrated with Bézier curves. The term "barycentric combinations" is derived from " barycentre", meaning centre of gravity. Barycentric combinations are a set of weights with the following properties [Farin'88],

- they are all non-negative.
- the sum of the weights add up to one.

When the Bézier is evaluated for a parametric variation of $0 \le t \le 1$, then $P(t)$ in (EQ 2.3) is a weighted sum of the polygon points (p_0, p_1, p_2, p_3) where all the weights are positive and the sum of the weights equals one. Hence the polygons joining these

polygon points encloses a curve defined by these polynomials, i.e., it defines a convex hull within which $P(t)$ lies. Some of the other interesting features of Béziers are

- a Bézier curve always passes through the first and last control points, i.e. $p(0) = p_0$ and $p(1) = p_n$
- the slope at the beginning of the curve is along the line joining the first two control points, and the slope at the end of the curve is along the line joining the last two control points.

However Béziers suffer from the following two drawbacks

- Béziers do not allow local control over the shape of the curve
- the number of control points to be approximated and their relative positions determine the degree of the Bézier polynomial. (This drawback can to a certain extent be overcome by the spline make up of Bézier polynomials. However additional complications are then introduced, viz. mapping each Bézier curve to a global parameter, ensuring end conditions of continuity etc.).

2.4 B-spline Curves

B-splines have been a popular tool for hullform definition [Rogers'77], [Izumida'79], [Munchmeyer'79], [Fog'85] due to some of their positive characteristics

- the B-spline basis function is positive for all parameter values and sums up to one thereby exhibiting the convex hull property
- a B-spline curve with a d^{th} order basis function is a polynomial with degree $d - 1$ with C^{d-2} continuity over the knot set range
- B-splines exhibit the variation diminishing property which means that the curve does not oscillate about any straight line more often than its defining polygon
- any affine transformation can be applied to the curve by applying it to the defining polygon vertices
- the degree of the polynomial is independent of the number of control points
- B-spline curves demonstrate local control characteristics (Bézier splines are a sub-set of B-splines when the knot set is uniform)

The theory of B-splines was first suggested by Schoenburg [Rogers'90] but the recursive definition of the basis function for numerical computation was independently discovered by Cox [Cox'71] and by de Boor [de Boor'72]. The application of the B-spline basis to curve definition technique was carried out by Gordon and Riesenfeld [Riesenfeld'73].

The locus of a B-spline polynomial is defined as

$$P(s) = \sum_{i=0}^{n} p_i N_{i,d}(s) \quad (k_{min} \le s \le k_{max}) \quad (2 \le d \le n+1)$$

where p_k, $k = 0, \ldots, n$ are the $n+1$ control points and N is the basis (or B-spline blending) function. The Cox-deBoor recursion formula for this blending function is given as

$$N_{i,1}(s) = \begin{cases} 1 & if(k_i \le s \le k_{i+1}) \\ 0 & otherwise \end{cases}$$

(EQ 2.6)

$$N_{i,d}(s) = \frac{s - k_i}{k_{i+d-1} - k_i} N_{i,d-1}(s) + \frac{k_{i+d} - s}{k_{i+d} - k_{i+1}} N_{i+1,d-1}$$

The procedure for the formulation of a fourth order basis function (third degree polynomial) is explained below.

Consider a set of control vertices through which a B-spline curve needs to be passed. Construct a knot set $\{k_0, k_1, k_2, k_3, k_4, k_5, k_6, k_7\}$ and build the basis function using (EQ 2.6) as follows:

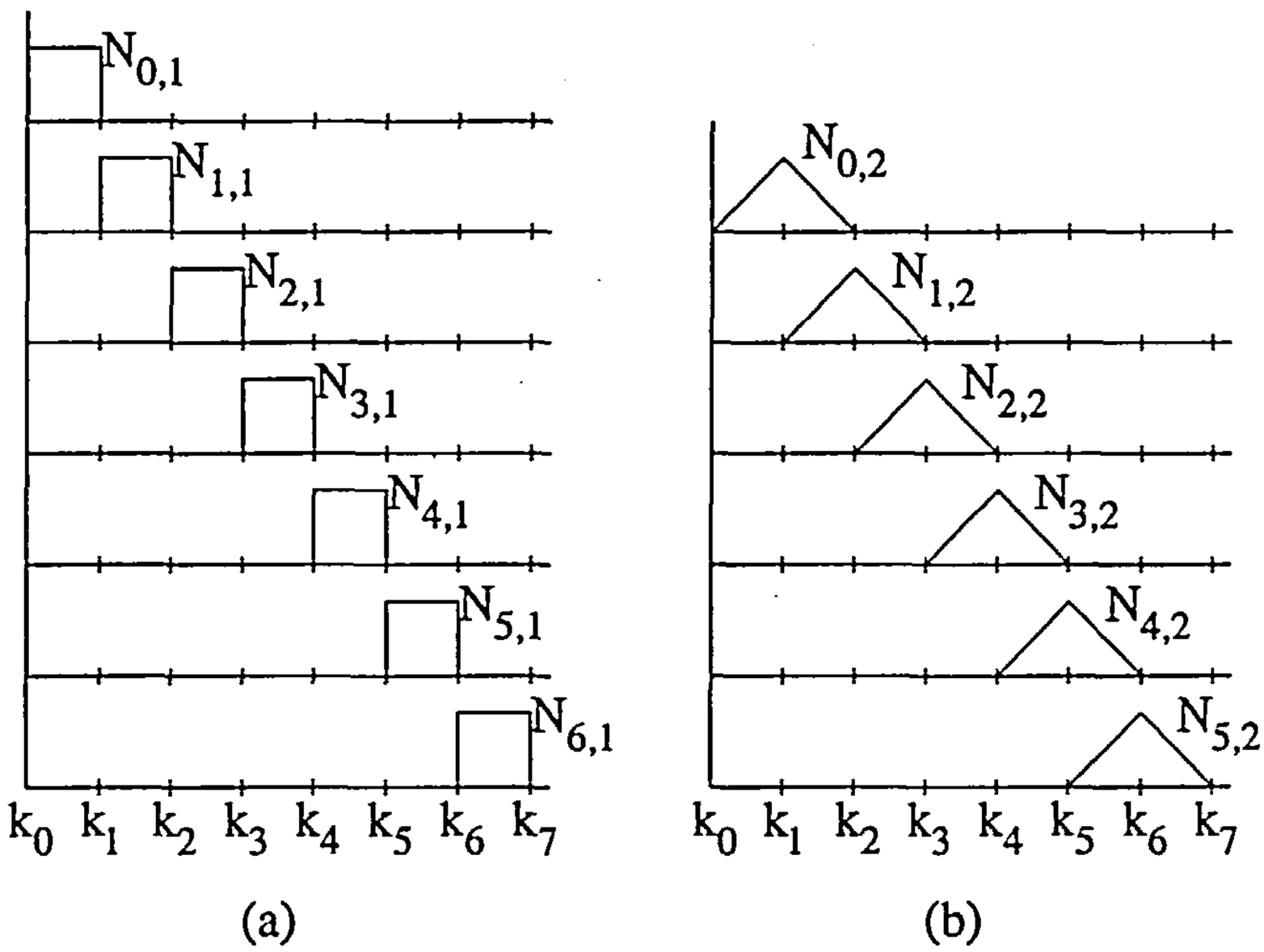

FIGURE 2.4. Basis function build up

Figure 2.4 (a) shows the first order basis functions, with the basis function values as $N_{i,1}(s) = 1$ for $k_i \le s \le k_{i+1}$, $i = 0, \ldots, 6$. The first order basis functions are defined over one sub-interval of the total range of k starting at k_0.

Figure 2.4 (b) shows the variation in the second order basis functions, $d = 2$, which are now defined over two sub-intervals of k. From (EQ 2.6)

$$N_{i,2}(s) = \frac{s - k_i}{k_{i+1} - k_i} N_{i,1} + \frac{k_{i+2} - s}{k_{i+2} - k_{i+1}} N_{i+1,1} \qquad i = 0, \ldots, 5$$

The third order basis functions are

$$N_{i,3}(s) = \frac{s - k_i}{k_{i+2} - k_i} N_{i,2} + \frac{k_{i+3} - s}{k_{i+3} - k_{i+1}} N_{i+1,2} \qquad i = 0, \ldots, 4$$

and finally the fourth order basis functions are

$$N_{i,4}(s) = \frac{s - k_i}{k_{i+3} - k_i} N_{i,3} + \frac{k_{i+4} - s}{k_{i+4} - k_{i+1}} N_{i+1,3} \qquad i = 0, \ldots, 3$$

Considering the knot interval $[k_3, k_4]$ alone, $N_{3,1}(s) = 1$ for $k_3 \le s \le k_4$ and $N_{i,1} = 0 \quad i = 0, 1, 2, 4, 5, 6$. Substituting these values in the higher order basis functions, the four fourth order basis function for the interval $[k_3, k_4]$ are given as,

$$N_{0,4} = \frac{D_4^3}{T_{41} T_{42} T_{43}} \qquad \text{(EQ 2.7a)}$$

$$V_{1,4} = -\frac{D_1 D_4 D_4}{T_{41} T_{42} T_{43}} - \frac{D_2 D_4 D_5}{T_{42} T_{43} T_{52}} - \frac{D_3 D_3 D_5}{T_{43} T_{52} T_{5:}} \qquad \text{(EQ 2.7b)}$$

$$V_{2,4} = -\frac{D_2 D_2 D_4}{T_{42} T_{43} T_{52}} - \frac{D_2 D_3 D_5}{T_{43} T_{52} T_{53}} - \frac{D_3 D_3 D_6}{T_{43} T_{53} T_{6:}} \qquad \text{(EQ 2.7c)}$$

$$N_{3,4} = -\frac{D_3^3}{T_{43} T_{53} T_{63}} \qquad \text{(EQ 2.7d)}$$

where $D_i = (k_i - s)$ and $T_{ij} = (k_i - k_j) \quad i, j = 1, \ldots, 6$.

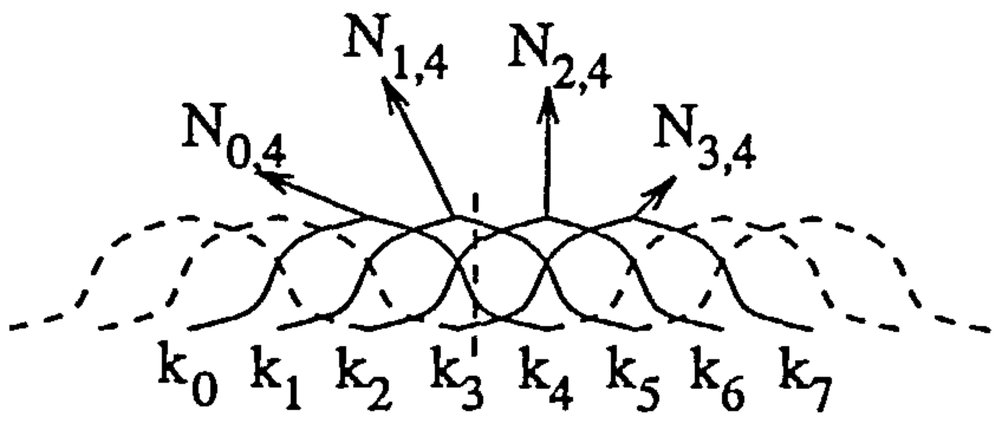

FIGURE 2.5. Fourth order B-spline basis function distribution

As seen from Figure 2.5, for a given pair of knots, four basis functions span that knot interval and hence the coordinate position for a B-spline curve maybe stated as

$$P(s) = p_1 N_{0,4}(s) + p_2 N_{1,4}(s) + p_3 N_{2,4}(s) + p_4 N_{3,4}(s) \qquad \text{(EQ 2.8)}$$

(EQ 2.8) shows that at least four points are required to define a B-spline with a fourth order basis function. Also, to construct the basis function between two knots k_i and k_{i+1}, the two adjacent knots on either side, viz. k_{i-2} and k_{i-1} to the left of k_i and k_{i+2} and k_{i+3} to the right of k_{i+1}, are required.

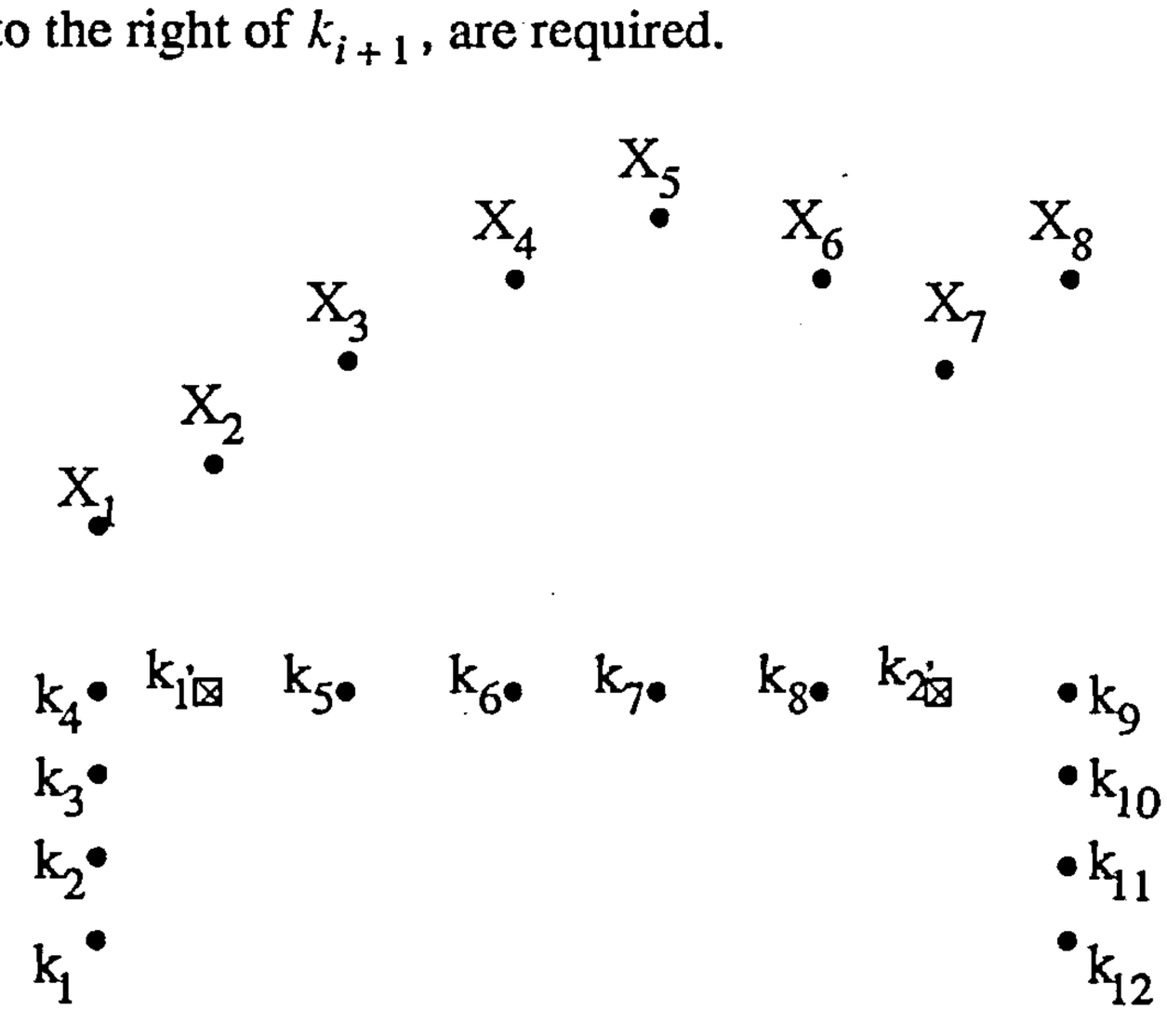

FIGURE 2.6. Coordinate points for B-spline fitting

Figure 2.6 shows a set of eight points through which a B-spline curve needs to pass.

First, a knot set for the set of data points needs to be constructed. The knot set range is divided into $n + d$ intervals giving the total number of knots as $n + d + 1$ where $n + 1$ is

the total number of data points and d is the order of the basis function. In this case $n+1 = 8$ and hence the total number of knots is $n+d+1 = 7+4+1 = 12$, i.e. $\{k_1, k_2, \ldots, k_{12}\}$. Since open uniform and non-uniform B-splines have knot multiplicity at the ends which equals the order of the basis function, $k_1 = k_2 = k_3 = k_4$ and $k_9 = k_{10} = k_{11} = k_{12}$ in this particular case (Figure 2.6). It is usual to set the first set of multiple knots to zero, i.e. $k_1 = k_2 = k_3 = k_4 = 0$. For non-uniform knot sets, a knot value can be taken as the cumulative distance between consecutive coordinate data points up to the coordinate point under consideration, which is an approximation to the length of the curve up to that data points

$$k_{1'} = k_4 + |\underset{\sim}{X}_1 - \underset{\sim}{X}_2|$$

$$k_5 = k_4 + |\underset{\sim}{X}_1 - \underset{\sim}{X}_2| + |\underset{\sim}{X}_2 - \underset{\sim}{X}_3|$$

$$k_6 = k_5 + |\underset{\sim}{X}_3 - \underset{\sim}{X}_4|$$

$$k_7 = k_6 + |\underset{\sim}{X}_4 - \underset{\sim}{X}_5|$$

$$k_8 = k_7 + |\underset{\sim}{X}_5 - \underset{\sim}{X}_6|$$

$$k_{2'} = k_8 + |\underset{\sim}{X}_6 - \underset{\sim}{X}_7|$$

$$k_9 = k_8 + |\underset{\sim}{X}_6 - \underset{\sim}{X}_7| + |\underset{\sim}{X}_7 - \underset{\sim}{X}_8| = k_{10} = k_{11} = k_{12}$$

The values of $k_{1'}$ and $k_{2'}$ are retained to determine the control vertices as shown below.

The second step is to determine the values of the control vertices (or polygon points) so as to ensure that the B-spline passes through the above set of points. In this example eight control points have to be determined in the X, Y and Z direction.

The eight blending functions (Figure 2.7) can be determined from the constructed knot sets $\{k_1, k_2, \ldots, k_{12}\}$ using (EQ 2.7a-d).

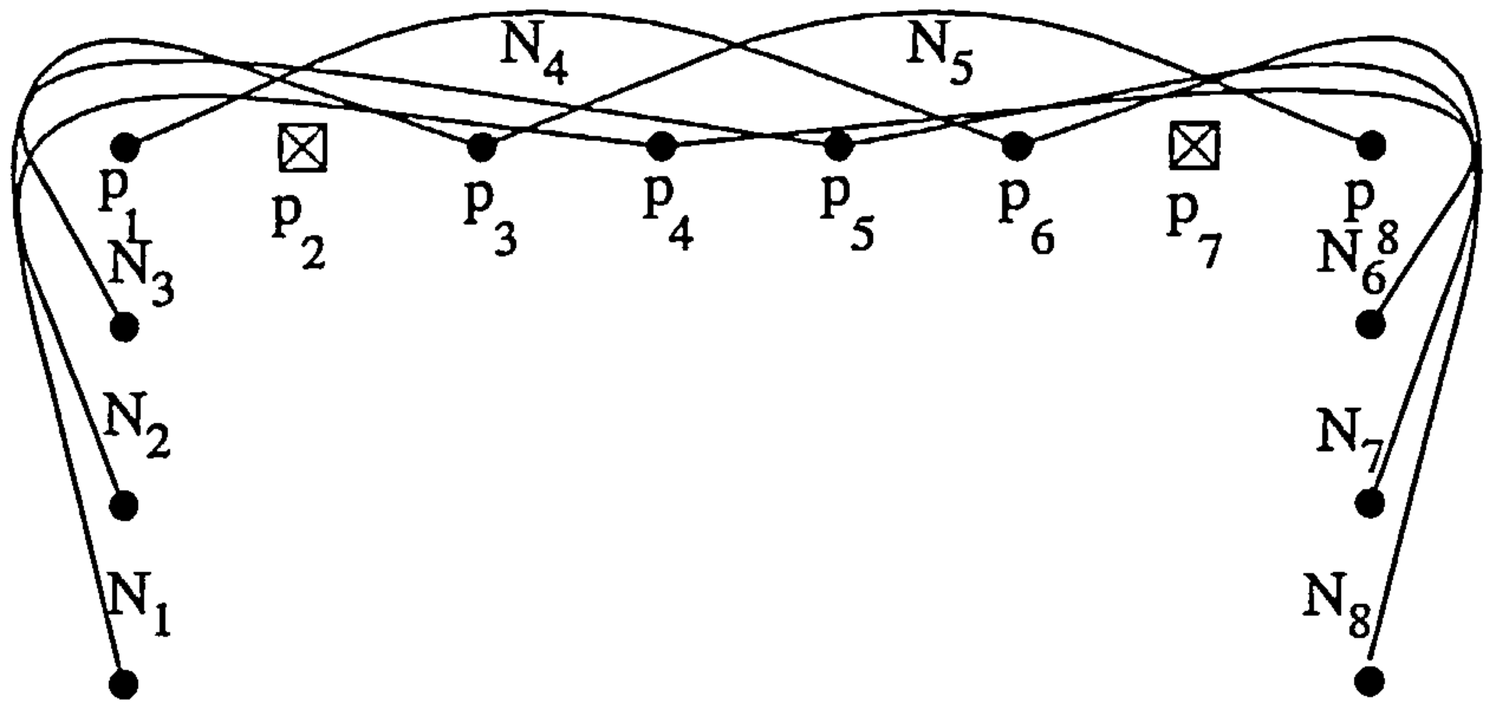

FIGURE 2.7. Blending function spanning the knot sets

Considering initially the x-component of $\underset{\sim}{P}$

$$p_1^x N_1(s) + p_2^x N_2(s) + p_3^x N_3(s) + p_4^x N_4(s) = \underset{\sim}{x}_1 \qquad s = k_4 \qquad \text{(EQ 2.9a)}$$

$$p_1^x N_1(s) + p_2^x N_2(s) + p_3^x N_3(s) + p_4^x N_4(s) = \underset{\sim}{x}_2 \qquad s = k_{1'} \qquad \text{(EQ 2.9b)}$$

$$p_2^x N_2(s) + p_3^x N_3(s) + p_4^x N_4(s) + p_5^x N_5(s) = \underset{\sim}{x}_3 \qquad s = k_5 \qquad \text{(EQ 2.9c)}$$

$$p_3^x N_3(s) + p_4^x N_4(s) + p_5^x N_5(s) + p_6^x N_6(s) = \underset{\sim}{x}_4 \qquad s = k_6 \qquad \text{(EQ 2.9d)}$$

$$p_4^x N_4(s) + p_5^x N_5(s) + p_6^x N_6(s) + p_7^x N_7(s) = \underset{\sim}{x}_5 \qquad s = k_7 \qquad \text{(EQ 2.9e)}$$

$$p_5^x N_5(s) + p_6^x N_6(s) + p_7^x N_7(s) + p_8^x N_8(s) = \underset{\sim}{x}_6 \qquad s = k_8 \qquad \text{(EQ 2.9f)}$$

$$p_5^x N_5(s) + p_6^x N_6(s) + p_7^x N_7(s) + p_8^x N_8(s) = \underset{\sim}{x}_7 \qquad s = k_{2'} \qquad \text{(EQ 2.9g)}$$

$$p_5^x N_5(s) + p_6^x N_6(s) + p_7^x N_7(s) + p_8^x N_8(s) = \underset{\sim}{x}_8 \qquad s = k_9 \qquad \text{(EQ 2.9h)}$$

where $N_i(s)$, $i = 1, \ldots, 8$ are the eight blending functions whose values are determined for given values of s and p_i^x, $i = 1, \ldots, 8$ are the eight control vertices to be determined. Due to the nature of the blending function formulation, (EQ 2.7a-d), the values of $N_2 = N_3 = N_4 = 0$ in (EQ 2.9a) and $N_5 = N_6 = N_7 = 0$ in (EQ 2.9h).

Also the value of N_5, N_6, N_7 and N_8 in (EQ 2.9c), (EQ 2.9d), (EQ 2.9e) and (EQ 2.9f), respectively, reduce to zero. The final matrix is of the form

$$\begin{bmatrix} N_1(k_4) & 0 & 0 & 0 & 0 & 0 & 0 & 0 \\ N_1(k_{1'}) & N_2(k_{1'}) & N_3(k_{1'}) & N_4(k_{1'}) & 0 & 0 & 0 & 0 \\ 0 & N_2(k_5) & N_3(k_5) & N_4(k_5) & 0 & 0 & 0 & 0 \\ 0 & 0 & N_3(k_6) & N_4(k_6) & N_5(k_6) & 0 & 0 & 0 \\ 0 & 0 & 0 & N_4(k_7) & N_5(k_7) & N_6(k_7) & 0 & 0 \\ 0 & 0 & 0 & 0 & N_5(k_8) & N_6(k_8) & N_7(k_8) & 0 \\ 0 & 0 & 0 & 0 & N_5(k_{2'}) & N_6(k_{2'}) & N_7(k_{2'}) & N_8(k_{2'}) \\ 0 & 0 & 0 & 0 & 0 & 0 & 0 & N_8(k_9) \end{bmatrix} \begin{bmatrix} p_1^x \\ p_2^x \\ p_3^x \\ p_4^x \\ p_5^x \\ p_6^x \\ p_7^x \\ p_8^x \end{bmatrix} = \begin{bmatrix} \underline{x}_1 \\ \underline{x}_2 \\ \underline{x}_3 \\ \underline{x}_4 \\ \underline{x}_5 \\ \underline{x}_6 \\ \underline{x}_7 \\ \underline{x}_8 \end{bmatrix}$$

Since from the first and last equations the values of p_1^x and p_8^x are known the matrix reduces to the form

$$\begin{bmatrix} N_2(k_{1'}) & N_3(k_{1'}) & N_4(k_{1'}) & 0 & 0 & 0 \\ N_2(k_5) & N_3(k_5) & N_4(k_5) & 0 & 0 & 0 \\ 0 & N_3(k_6) & N_4(k_6) & N_5(k_6) & 0 & 0 \\ 0 & 0 & N_4(k_7) & N_5(k_7) & N_6(k_7) & 0 \\ 0 & 0 & 0 & N_5(k_8) & N_6(k_8) & N_7(k_8) \\ 0 & 0 & 0 & N_5(k_{2'}) & N_6(k_{2'}) & N_7(k_{2'}) \end{bmatrix} \begin{bmatrix} p_2^x \\ p_3^x \\ p_4^x \\ p_5^x \\ p_6^x \\ p_7^x \end{bmatrix} = \begin{bmatrix} \underline{x}'_2 \\ \underline{x}_3 \\ \underline{x}_4 \\ \underline{x}_5 \\ \underline{x}_6 \\ \underline{x}'_7 \end{bmatrix} \qquad \text{(EQ 2.10)}$$

where $x'_2 = x_2 - p^x{}_1 N(k'_1)$ and $x'_7 = x_7 - p^x{}_8 N(k'_2)$. Solving (EQ 2.10) involves solving a tri-diagonal matrix with extra corner points to yield the x-component of the control vertices.

The y and z components of the control vertices can be determined in a similar manner.

2.5 The Tridiagonal Solver

The two main families of methods which may be employed in solving a matrix systems of equations are:

- **direct methods** which give an exact solution (apart from the numerical roundoff errors) if the solution exists and is unique, after a finite number of steps. The most common ones are:

  Cramer's rule: The least efficient of the direct methods.

  Adjoint method: The most obvious method involving calculation of the inverse matrix, not only inefficient but also unstable.

  Gaussian method: Otherwise known as the 'LU-factorisation' followed by simple stages of forward and backward substitution. To avoid instabilities that could occur even in non-singular systems 'pivoting' between the relevant rows (partial pivoting) or between the rows and columns (complete pivoting) is performed. The more drastic alternative of scaling is difficult to implement in a sensible manner and when badly implemented could easily make the system more unstable. There are three ways in which the 'LU-factorisation' can be performed:

  Doolittle's method - main diagonal elements of the lower triangle are all one.

  Crout's method - main diagonal elements of the upper triangle are all one.

  Choleski's method - both upper and lower main diagonal elements are one.

  For the latter of these methods the system must, first, be symmetric with the upper triangular matrix then being the transpose of the lower. Secondly, it must be positive definite (i.e. all its eigenvalues are greater than zero) such that all the values on the main diagonals are also greater than zero. However, this gives rise to a stable method which gives the solution in less than half the computations of the Gaussian method

- **iterative methods** are restricted to well-determined (i.e. square) systems and begin with initial estimation (usually some form of educated guess although this could even be chosen at random) and refine this on each step in a sequence of approximations hopefully converging to the exact solution. A major advantage of such schemes are their ability to exploit sparsity when direct methods cannot or when, for any other reason, an iterative approach is more appropriate. There are several drawbacks to these methods ranging from the choice of initial approximation to the point at which a solution is said to be 'acceptable'. Indeed the sequence may not converge at all and if it does it sometimes cannot be guaranteed to be to the desired solution. The most well known iterative methods are:

  Jacobi/Gauss-Seidel: This utilises the expression of the original matrix into a sum of a diagonal matrix with an upper and a lower triangular matrix. Each step of each iteration exploits the use of the values from the previous steps combined with the solution of the previous iteration.

  Relaxation Schemes: These are in essence based on the Gauss-Seidel method but each successive iteration is weighted to increase (Under Relaxation) or decrease (Over Relaxation) the rate of convergence or divergence.

  Conjugate Gradient: Probably one of the most researched of method strategies (particularly in relation to optimization techniques). These require the systems to be both symmetric and positive definite. The approach is based on combining

the efficiency of 'steepest descent' algorithms (i.e. always reducing the error by means of the highest gradient) and the reliability of conjugate direction algorithm (i.e. closer to a direct method, changing direction by 90 degrees on each iteration until eventually 'homing in' to the solution). These methods can easily exploit sparsity and pre-conditioning (i.e. prior multiplication by some approximation to the inverse of the original matrix). In fact these approximations may be chosen via direct schemes such as Choleski's or another iterative scheme such as Over Relaxation.

Direct methods are usually the first choice although, when the degree of computation and data manipulation involved is taken into account, it is iterative methods that are generally the more promising. It is at this point that sub-block structuring and sparsity properties of a system become vital in the choice of strategy for its solution.

For the case of tridiagonal systems (i.e. those with only the three main diagonals as non-zero elements) the choice is more straightforward. Taking into account the difficulties of specifying an initial approximation and tolerance for the iterative schemes, together with the possible delays in convergence, a direct approach seems more straightforward. However, should the matrices become either very much larger or more complex or both, iterative methods should be considered once more. Since the system considered here is known to be reasonably small, and taking into account the fact that many thousands of systems such as these are to be solved, the direct method was the obvious choice. Given that these systems may or may not be symmetric, a choice was made between Crout's method and a modified version of Crout's method which exploits the fact that, $l(i, j) = u(i, j)$ for all i, j. This is exploited throughout the factorisation and substitution stages. Also if it is known that the matrix is positive definite (strict diagonal dominance being a good indication), this can then be further exploited by the increased stability of Choleski's method.

Of course, examination of the systems (EQ 2.10) shows that there are non-zero elements other than those on the three main diagonals (in this case the two elements to give the x-component of the control vertices). Since these occur at only a few (a pair in this case) of known positions it does not significantly affect the choice of direct tridiagonal matrix solvers but a certain amount of pre-conditioning is required. This can be done by a combination of gaussian elimination and pivoting techniques although a careful check is kept on the stability of this process to control the accuracy of the solution element as well as the inherited stability (and symmetry) of the resulting reduced system of equations.

2.6 B-spline manipulations

A complete B-spline library, containing various operations and procedures to manipulate B-spline curves was developed to incorporate flexibility into the hullform and compartment form definitions and enhance the capabilities of the software. Some of the more important of these procedures were:.

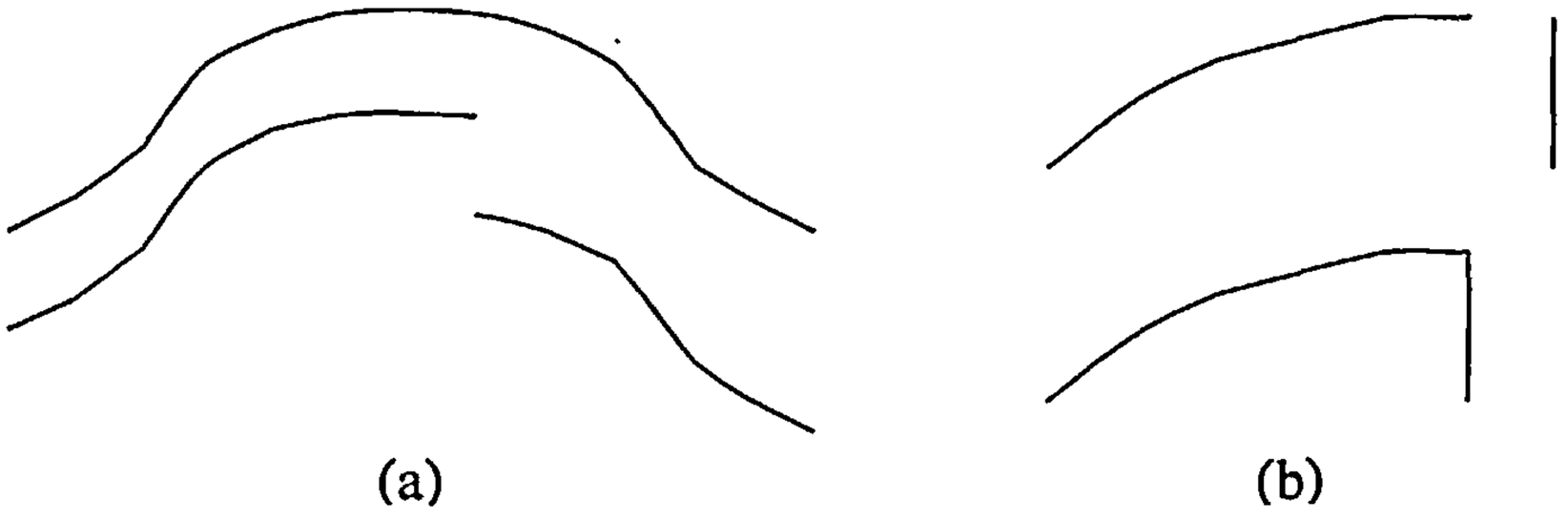

FIGURE 2.8. Splitting and merging of B-spline curves

- the ability to split a spline at a specific knot value with the component B-spline curves retaining their original shapes, Fig 2.8 (a)
- the ability to merge two B-spline curves whereby the new curves retains the shapes of the component curves, Fig 2.8(b)

It is the coordinate points, about which the split must occur, that is usually known. the first step, therefore is to determine the knot value corresponding to this coordinate point. In order to achieve this, the plane containing the spline curve is rotated in space so as to make it lie parallel to the XY-plane and the point of the split to lie on the Y-axis. The rotation is done in two stages. Fig 2.9 shows the rotation sequence. Z' is the normal to the plane in which the B-spline curve lies. The first rotation, γ_y, is about the Y'-axis and the second, γ_x, along the X'-axis.

The rotation can therefore be expressed as,

$$\left[M_x\right]\left[M_y\right]\left[\underset{\sim}{P}\right] \qquad \text{(EQ 2.11)}$$

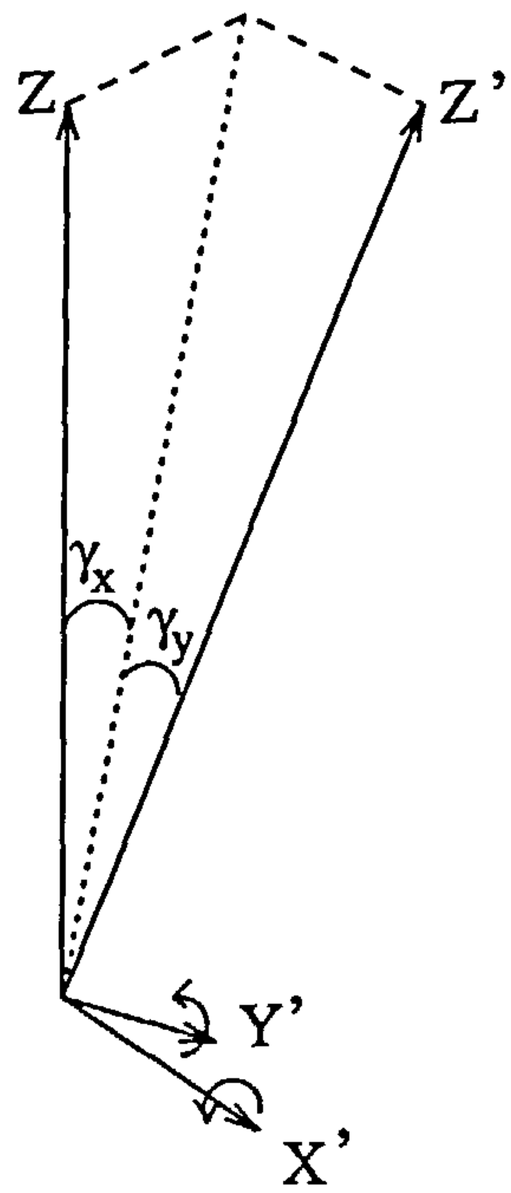

FIGURE 2.9. Spline rotation sequence

where

$$\left[M_x\right] = \begin{bmatrix} 1 & 0 & 0 \\ 0 & \cos\gamma_x & \sin\gamma_x \\ 0 & -\sin\gamma_x & \cos\gamma_x \end{bmatrix}$$

$$\left[M_y\right] = \begin{bmatrix} \cos\gamma_y & 0 & -\sin\gamma_y \\ 0 & 1 & 0 \\ \sin\gamma_y & 0 & \cos\gamma_y \end{bmatrix}$$

and $\left[\underset{\sim}{P}\right]$ represents the coordinates of the control vertices. If the equation of the plane on which the spline curve lies is given as

$$\frac{a}{d}x + \frac{b}{d}y + \frac{c}{d}z = 1$$

then

$$\text{sign of } \gamma_y = \left(\text{sign of } \frac{a}{d}\right)\left(\text{sign of } \frac{c}{d}\right)$$

$$\text{sign of } \gamma_x = (-1)\left(\text{sign of } \frac{b}{d}\right)\left(\text{sign of } \frac{c}{d}\right)$$

Applying (EQ 2.11) to the B-spline polygon vertices ensure that the spline now lies parallel to the XY-plane. Applying the translation operator to the x coordinates of the polygon vertices results in the point of split to lie on the Y-axis. Identifying the segment at which the intersection occurs reduces to finding a change in the sign in the transformed x coordinates of the polygon vertices. The knot value can then be determined by solving the cubic polynomial, since the B-spline has a fourth order basis function. This knot value can then be used to split the spline curve.

In order that the component B-spline curves retain their shapes as the original curve, the new polygon vertices at the ends of the component curves is determined by ensuring zeroth, first, second and third order continuity (giving four equations to solve for the four new end polygon vertices). Due to the property of B-splines, the last coordinate point coincides with the last polygon vertex, the system reduces to a three-by-three, which can be solved using direct methods such as Cramer's rule.

The process of merging two spline curves, in contrast is a much simpler process. Consider two B-splines, with six polygon vertices and ten knot vectors each (due to a fourth order basis function). The merged B-spline curve has twelve polygon vertices and consequently only sixteen knot vectors. This is achieved by equating the last four knots of the first spline with the first four on the second (and adding k to each subsequent knot vector on the second spline, where k is the value of the last knot on the first component B-spline curve). It must be noted that though the end knot sets are equated to derive the new knot set for the merged spline, the polygon vertices are retained as they are. This means the new spline could have a discontinuity along its locus but still be defined by a single B-spline curve definition.

2.7 Hullform generation

The basic hullform is generated by fitting fourth order B-spline curves through the offset data. Offset data is specified in input files for a series of waterlines starting from the keel.

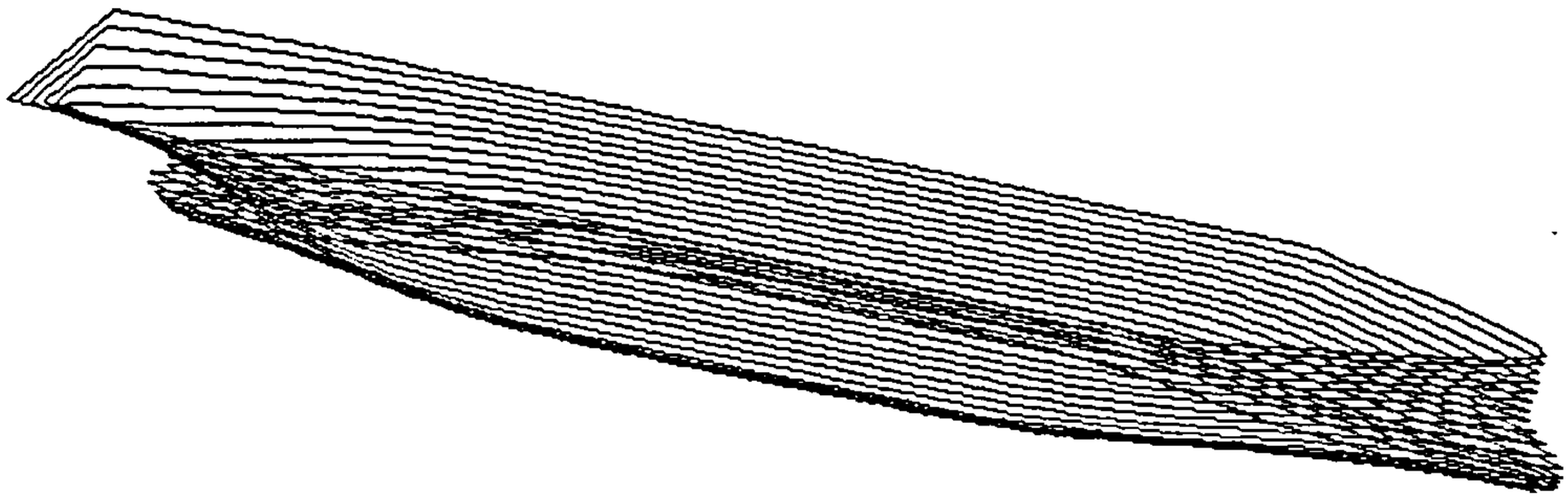

FIGURE 2.10. Hullform representation with waterlines

Fig 2.8 shows the waterline representation of a hullform. The offsets for one half of the waterline is entered in the input data file, thereby restricting the analysis to symmetric hullforms only.

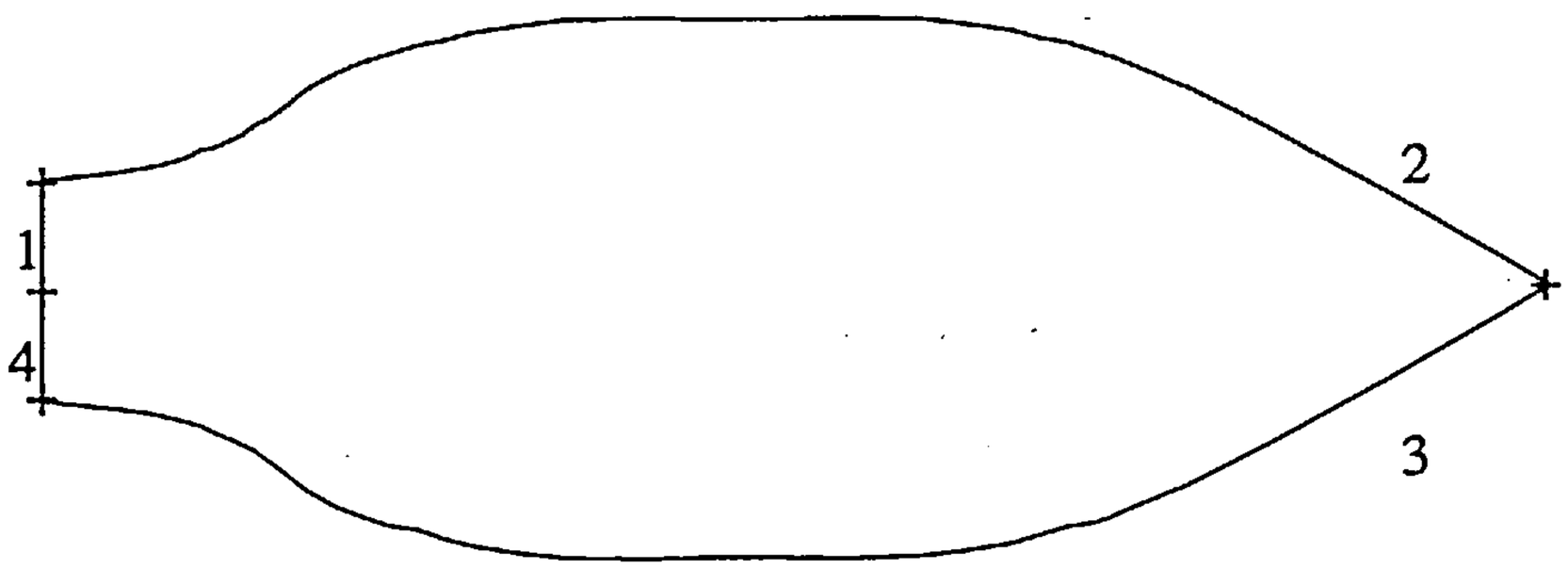

FIGURE 2.11. The construction of a waterline

Each waterline B-spline is made up by merging four independent B-spline curves as shown in Fig 2.11. For waterlines that begin at the centreplane in the aft section (especially true of waterlines that lie below the transom), they are assumed to begin (at the aft end) at a small hypothetical distance from the centreline. This was done so as to maintain the four spline make up of a waterline (as shown in Fig 2.11).

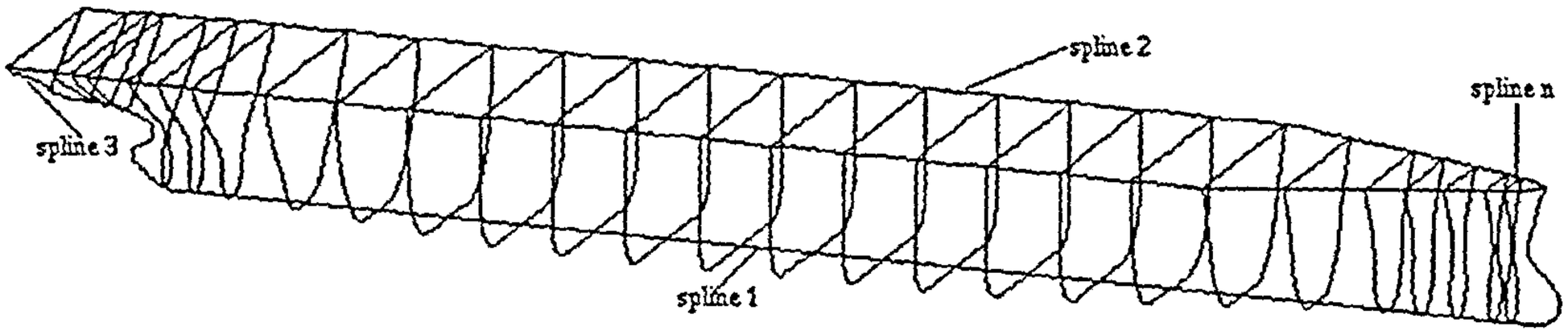

FIGURE 2.12. Hullform representation with bodylines

The hullform representation in the form of bodyline is as shown in Fig 2.12. The hullform described in this way has a central spline, spline 1, which runs from the spline that defines the transom, spline 3. The deck is defined as spline 2.

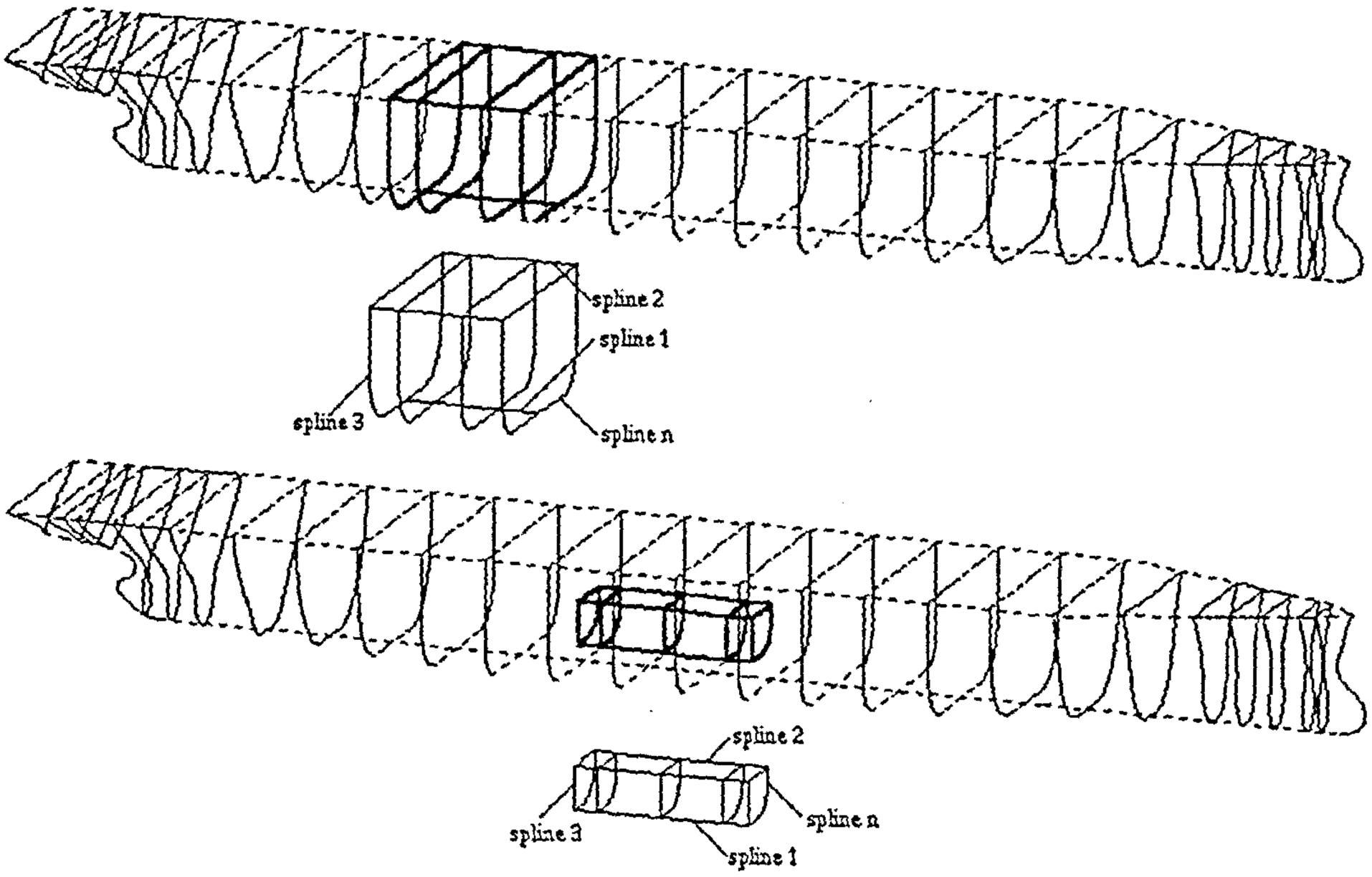

FIGURE 2.13. Compartment definition

The format used above to define the hullform is also maintained when defining the compartments of subdivision as shown in Fig 2.13. Any operation that can be legally performed on the hull can also be performed on the compartments of subdivision since they all conform to the same definition as an "object" known as "compartment".

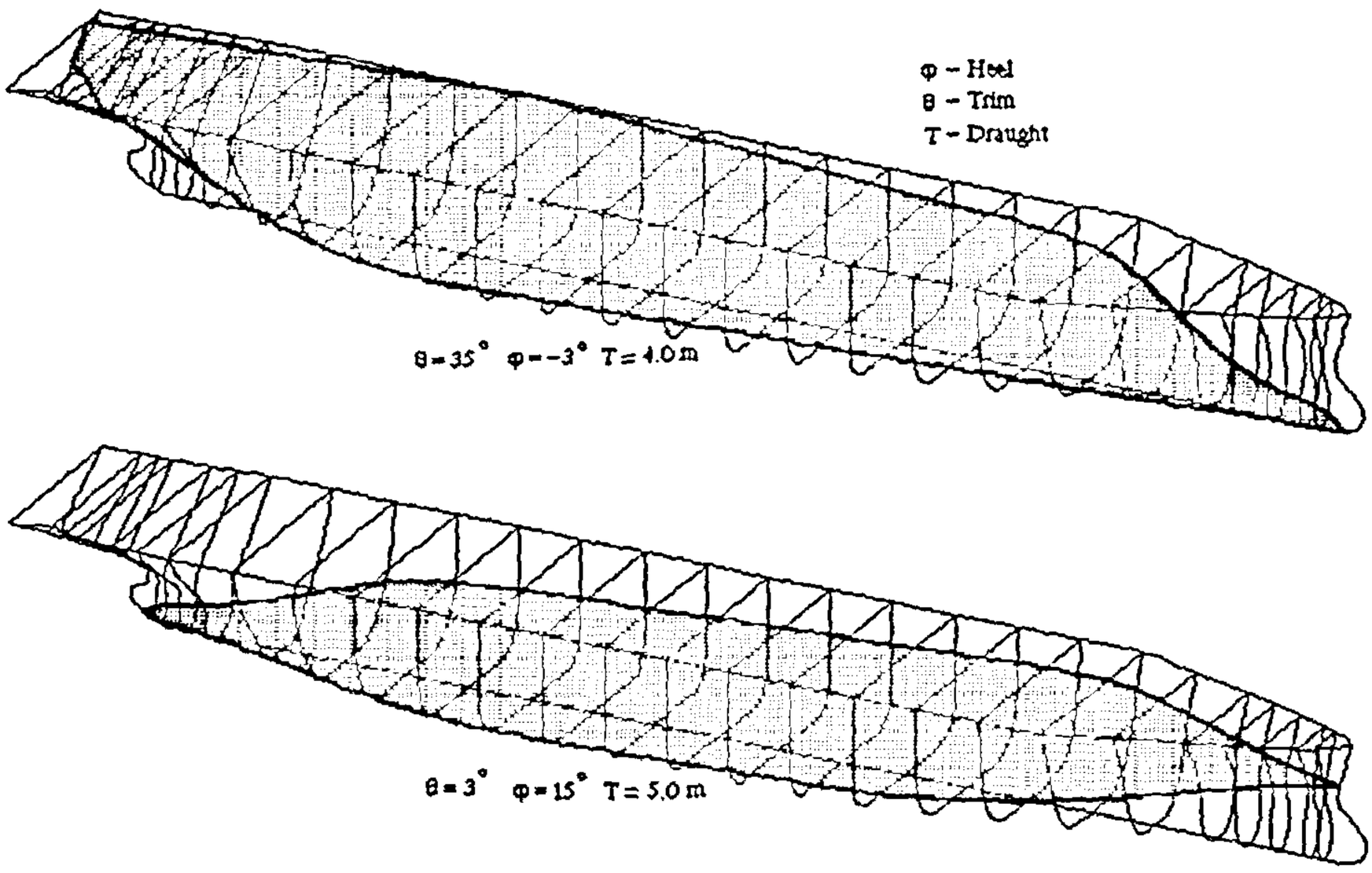

FIGURE 2.14. Waterplane definition

Procedures were also developed to enable the construction of a waterplane, the intersection between the object compartment and the waterline, for any angle of heel and trim and for any draught (where draught is the value of the z-intercept of the waterplane). The procedure for construction of the waterplane involved finding the intersection(s) of each station defining the compartment and ordering them in a logical sequence. B-spline curves were then fitted through these sets of ordered points and then merged together to form the closed "waterplane" spline curve. This feature of enabling the description of waterplanes is very crucial in damage stability calculations as explained in Chapter 3.

There was however one difficulty encountered with the numerical evaluation of the moment of inertia of these waterplanes as required by the damage stability theory. The moment of inertia for a waterplane is defined as

$$I = \iint x^2 dA$$

where $dA = dxdy$. Since both x and y are defined by a cubic function of the knot vector t (since a fourth order basis function was used to define the B-spline), the above equation could be expressed as,

$$I = \iint f(t^6)\left(\frac{dx}{dt}dt\right)\left(\frac{dy}{dt}dt\right)$$

$$I = \iint g(t^{10})dtdt$$

$$I = h(t^{12})$$

All the information in a digital computer is presented in coded form by means of so-called bits, that is, by elements that can take only one of the two values 0 or 1. With floating point numbers, the numbers are represented in the form $m \cdot a^p$, where m is the mantissa, a is the basis of the number system in use (usually 2), and p is the integral exponent with a + or - sign. Since the machines used were Unix workstation which were mainly 32 bit machines, the double precision specifications for the compilers in use was a 52 bit mantissa, a 11 bit exponent, and a 1 bit sign. This implied that the largest number (before the decimal digit for floating point numbers) was $2^{51} - 1$ which works out to 2251799813685247. It is not unusual to have knot vectors that go up to 1000 or more. Even for a knot value of 200, the moment of inertia value works out to a large number 4096000000000000000000000000. This caused a lot considerable degree of truncation error resulting in exceptions in the damage stability routines.

One solution to this problem was to use a set C-libraries that allowed for arbitrary precision floating-point arithmetic[Motteler'93] across a variety of hardware and software platforms. This, however, caused a dramatic increase in the run-time for the application. The second option (which was finally adopted) was to split the spline into small segments so that the knot size did not exceed 15 and to evaluate the moments of inertia of the closed curve in sections (it is also possible to convert the double integral into a line integral by using Green's first identity and then using the above). The overheads in terms of time with this method was considerably lower than that using arbitrary precision.

However with the new generation of 64 bit processors like the INTEL Pentium, this may not be a problem in the future. The possible use of non-uniform rational b-spline surfaces (NURBS) could also improve the performance of the damage stability routine.

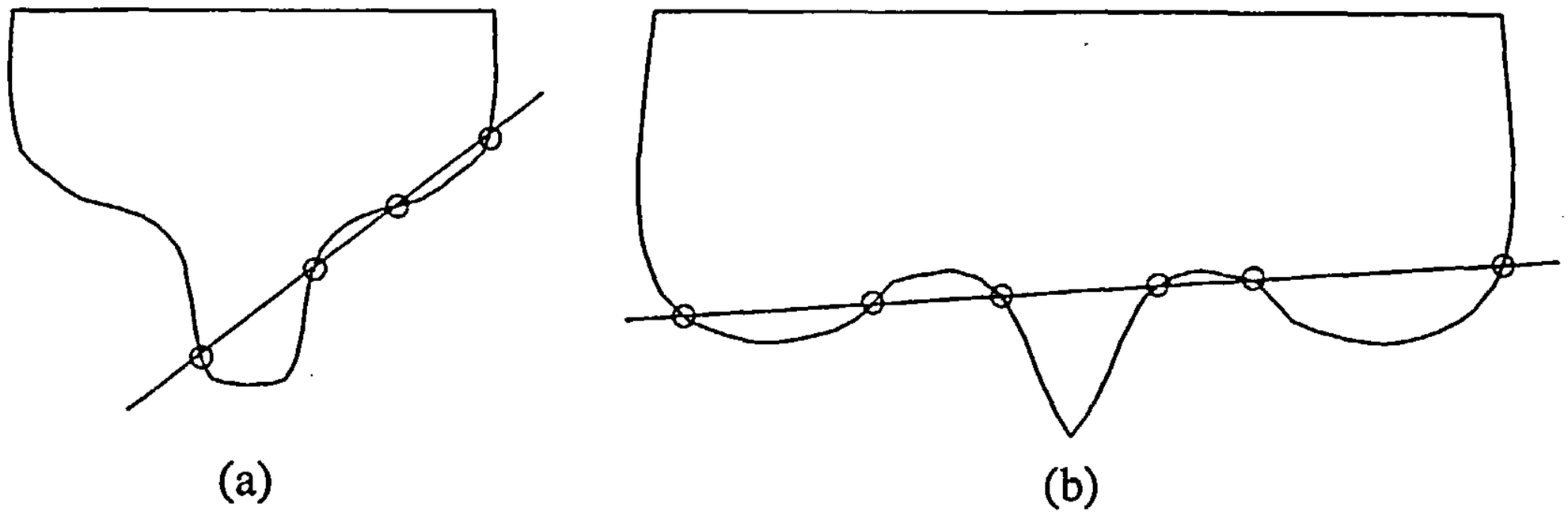

FIGURE 2.15. Limitations in aft form descriptions

Also the waterplane representational approach imposes some restriction on the kinds of aftforms that the software can handle. The permissible aftform is shown in Fig 2.15 (a), where the maximum number of intersections (between the waterline and the station) is limited to four. Aftforms of the kind defined in Fig 2.15 (b), having greater than 4 intersection points (six in this case) are not permissible in the current version of the software.

Finally, volumetric and hydrostatic procedures also used the waterplane spline construction for their calculations. The Newton-Cotes formula (trapezoidal rule) is given as,

$$\int_{x_1}^{x_2} f(x)dx = h\left[\frac{1}{2}f_1 + \frac{1}{2}f_2\right] + O(h^3 f'') \qquad \text{(EQ 2.12)}$$

where f_1 and f_2 are the values of $f(x)$ at x_1 and x_2 and $O(\ )$ signifies the integration error estimate. Press et al [Press'92] showed that if the trapezoidal rule is evaluated with N steps to give a result S_N, and then again used with 2N steps, getting a result S_{2N} then the combination

$$S = \frac{4}{3}S_{2N} - \frac{1}{3}S_N \qquad \text{(EQ 2.13)}$$

reduces to an expression where the error estimate is the same as that given by Simpson's rule.

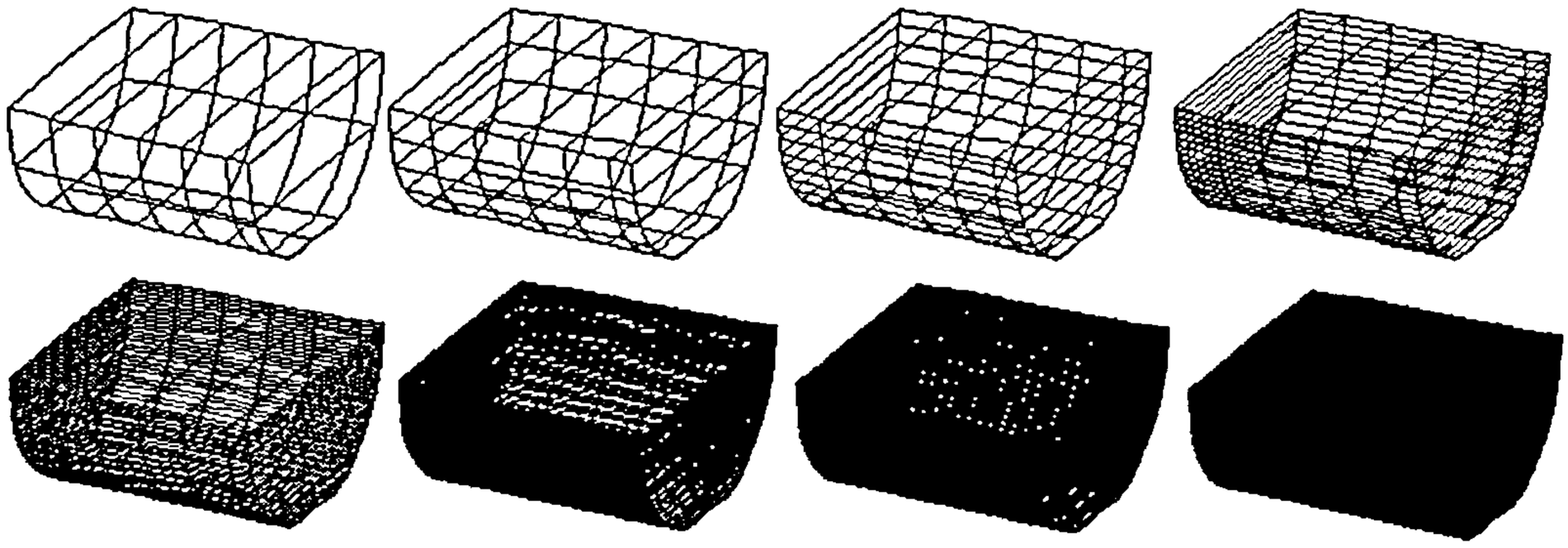

FIGURE 2.16. Compartment hydrostatics calculation sequence

This principle is used to determine the volume of a compartment as demonstrated by the sequence of figures in Fig 2.16. (EQ 2.12) is used as a workhorse, harnessed by (EQ 2.13) to produce a Simpson's rule type numerical integration scheme is a particularly good one for light-duty work. Parameters are provided to set the accuracy of the convergence criteria and flags trap non-convergent cases.

2.8 Conclusion

Space curves such as b-spline have occupied a pivotal role in the development of modern aids to computer aided design. The added complexity of using b-spline methods is offsets by their efficiency and the degree of flexibility that they allow. The generation of the hull-waterplane intersection was a complex process involving the generation and alignment of points in space in the right sequence to produce a sensible closed curve. The ease of achieving this depended largely on the use of b-splines which made the process of obtaining the points of intersection both simple and robust. B-spline curves also facilitated the graphical visualisation capabilities which were very crucial to the development and implementation of the damage stability theory as will be seen in the next chapter.

Chapter 3

Damage Stability

3.1 Introduction

Stability is the ability of a ship, when displaced from the position of equilibrium, to return towards the original position under the action of restoring forces. A vessel is classified as stable or unstable depending on whether this condition is satisfied or not. Stability is often further classified as *Statical stability* and *Dynamical stability* [Shansky'63]. When a stable vessel is disturbed from the horizontal axes by external forces, it resists this inclination by generating an internal restoring couple formed by its weight and the buoyancy forces, called the *righting moment*. The external forces do work against this righting moment. Statical stability is characterised by the magnitude of the righting moment which is brought into play by the inclination of the ship. Dynamical stability is characterised by the amount of work done by the righting moment during the process of inclination [Shansky'63].

The estimation of the righting lever can be performed under *fixed trim* or *free trim* conditions. Fixed trim assumes that the equilibrium trim remains the same during inclination. Usually this assumption does not incur heavy penalties for intact stability calculations. Wimalsiri [Wimalsiri'91] demonstrated, with the help of examples, how

free trim calculations deviate from fixed trim calculations for damaged vessels, Figure 3.1.

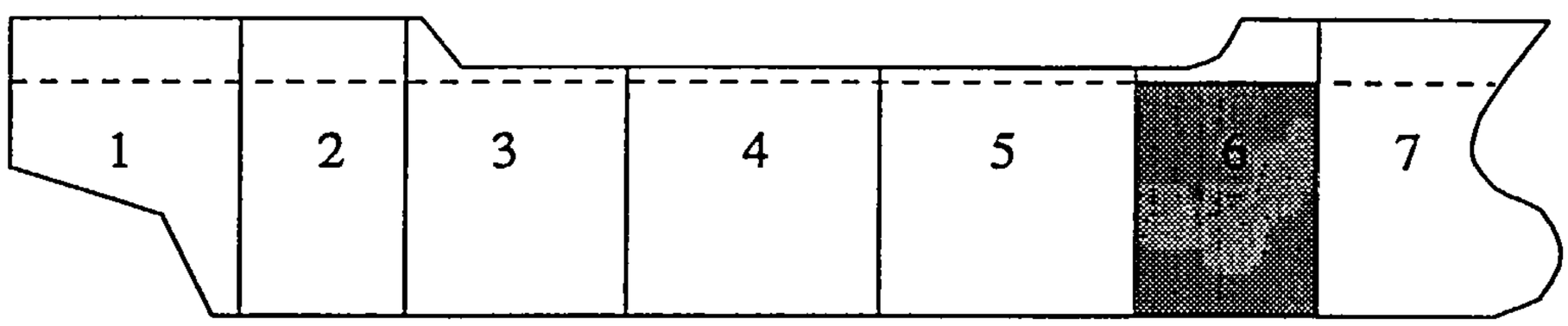

FIGURE 3.1. Damaged ship (shaded damaged portion)

The problem becomes particularly acute when the damaged compartments are located at the fore or aft ends of the ship.

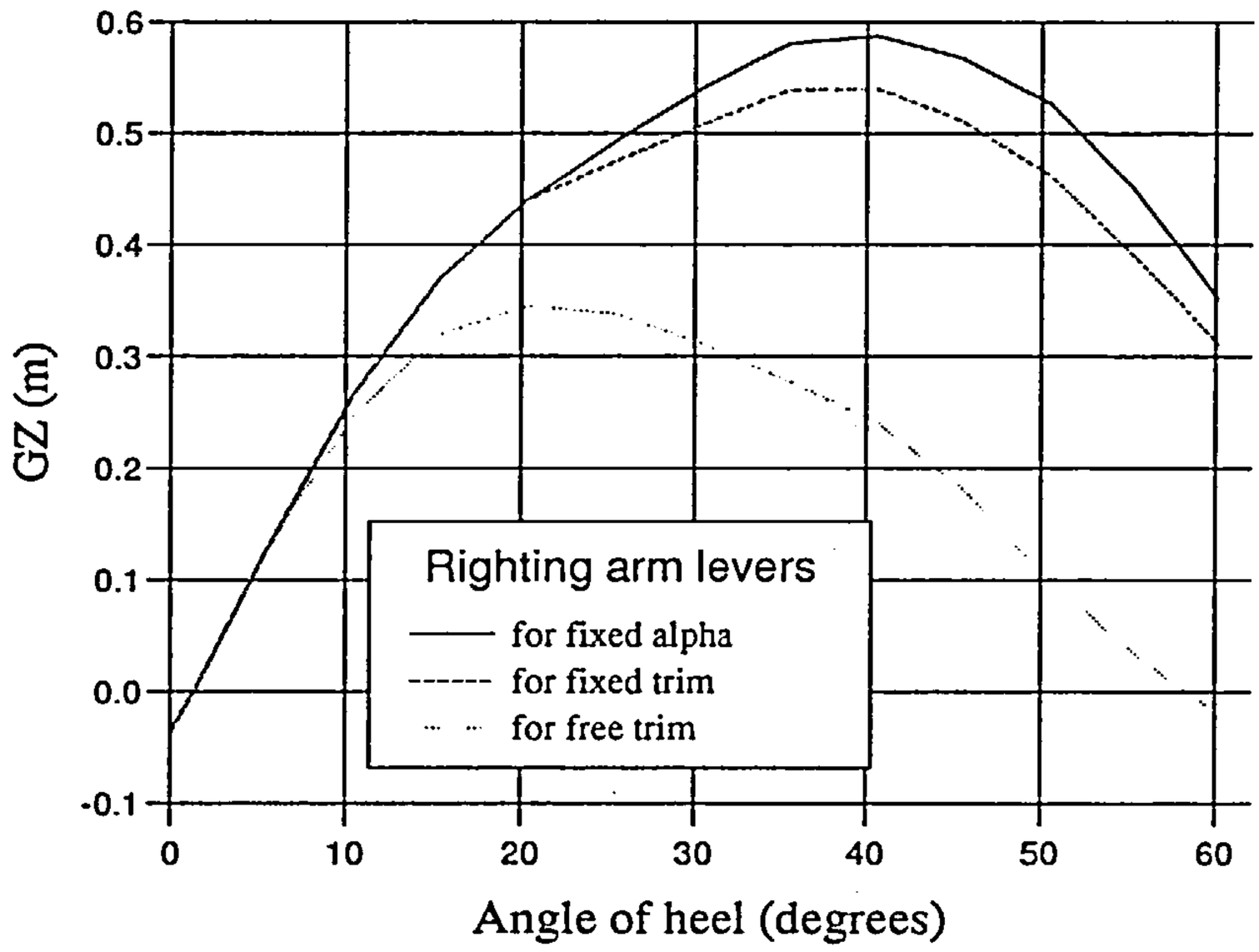

FIGURE 3.2. Variation in the GZ curves

Figure 3.2 shows the variation in the GZ curves for the three cases:

i. fixed longitudinal (or centreplane, see figure 3.3) inclination (fixed α).

ii. fixed trim (fixed β).

iii. free trim

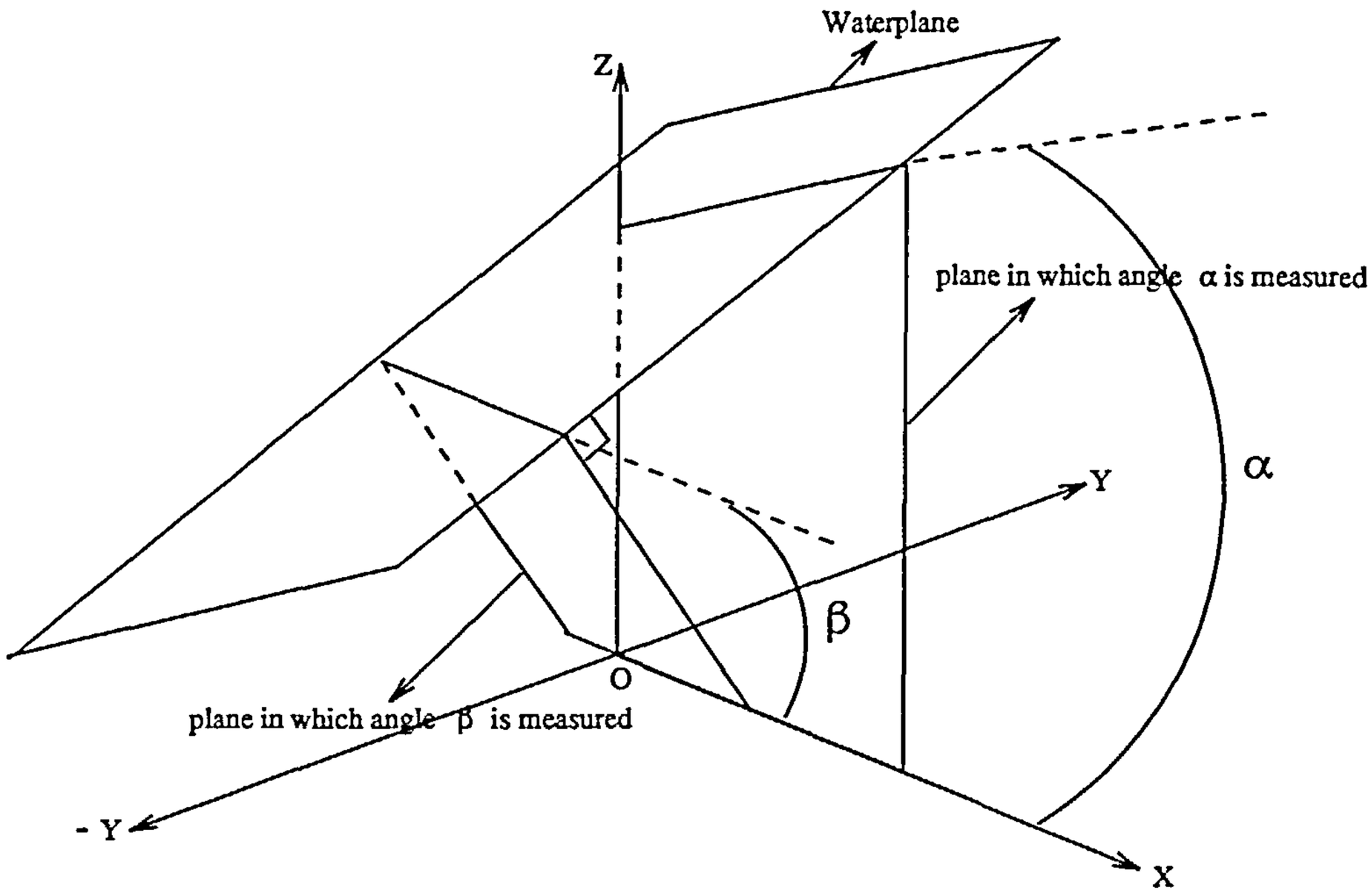

FIGURE 3.3. The planes for measuring α and β

where,

α is the angle between the trace of the waterplane on the ZOX plane and the X-axis, Figure 3.3.

β is measured on a plane perpendicular to the waterplane and passing through the X-axis.

Hence, in general, $\alpha \neq \beta$.

Pawlowski [Pawlowski'91] proposed a new methodology for the calculations of a freely floating rig under conditions of free trim when the unit is arbitrarily orientated to the wind direction. This method clearly defines what is commonly understood as the angle of inclination, for this arbitrary orientation, and showed its importance with respect to stability calculations. It uses the Euler theorem on the properties of equivolume waterplanes to arrive non-iteratively at new inclined equivolume positions. The non-iterative nature of the calculations saves computation time by eliminating unnecessary integrations. It also provides an algorithm for the GZ-curve calculations. This theory was adapted to make it amenable to stability calculations of damaged vessels. This theory and the background to it are discussed in the following sections.

3.2 Euler's theorem on equivolume waterplanes

A vessel subjected to the action of external forces [Shansky'63] can be resolved into a resultant force and a couple. If the force has a vertical component it will result in a change in draught and consequently in the displacement of the vessel. If the force has only horizontal components then the vessel would move horizontally giving rise to a resultant resistance force from the water over a wetted surface area which would give rise to additional couples. Hence in the absence of a vertical force component the resultant couples acting on the ship would cause it to incline with no change in displacement. Such inclinations are called *equivolume*.

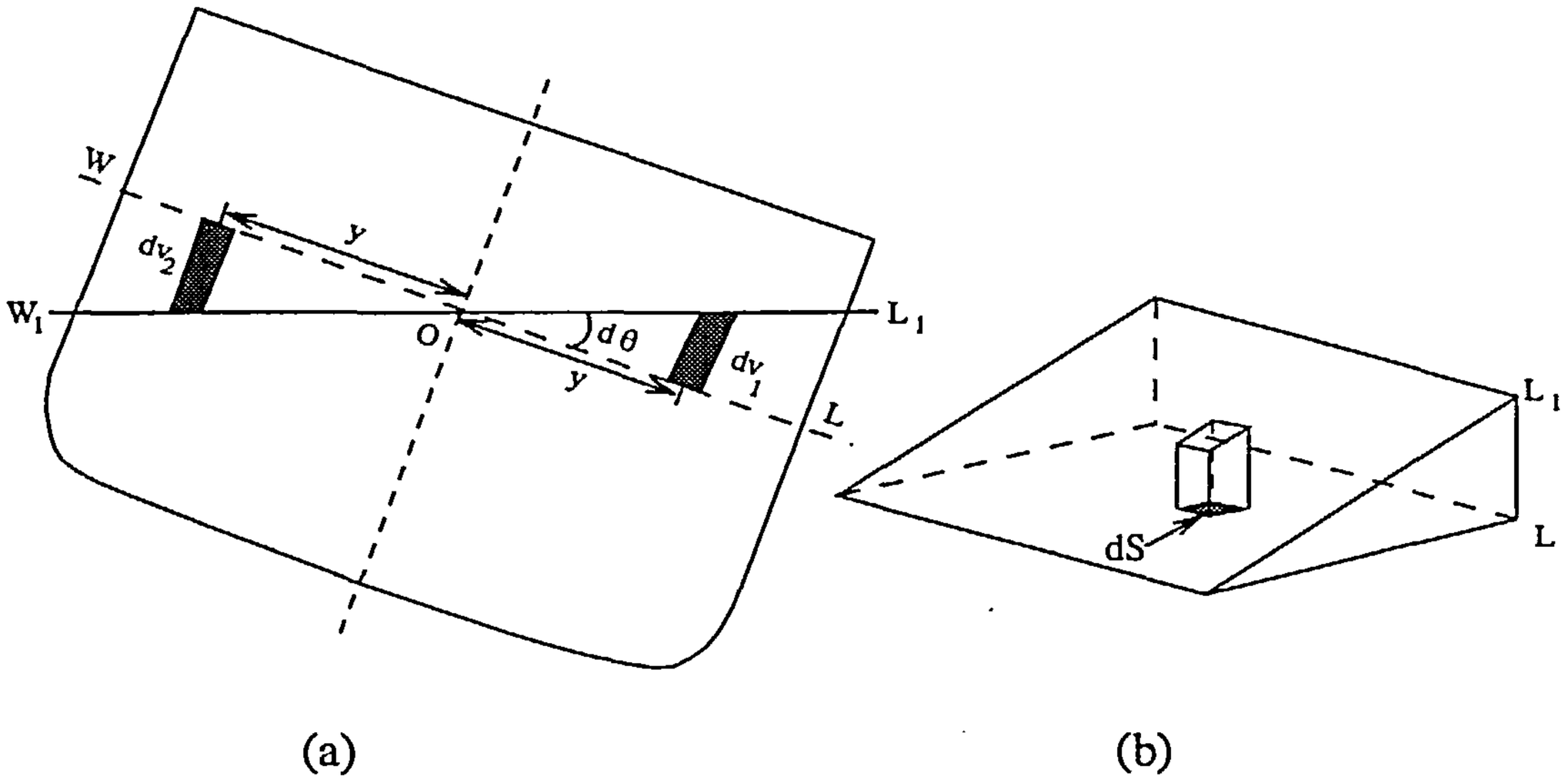

FIGURE 3.4. Equivolume inclinations

Figure 3.4 (a) shows an equivolume waterplane W_1L_1 inclined to waterplane WL by an infinitesimally small angle $d\theta$. The emerged and immersed wedges formed are equal in volume and hence,

$$dv_1 = dv_2 \qquad \text{(EQ 3.1)}$$

Consider a small prismatic element, Figure 3.4 (b), with its base resting on waterplane WL and with an area dS and height $yd\theta$ (Figure 3.4 (a)). y denotes the absolute value of the distance from the centroid of the prismatic element to the point O, the intersection of the equivolume waterplanes. If the immersed portion of waterplane WL is denoted as S_1 and the emerged portion as S_2, then

$$dv_1 = \int_{S_1} y d\theta \, dS = d\theta \int_{S_1} y \, dS = M_{S_1} \, d\theta \qquad \text{(EQ 3.2a)}$$

$$dv_2 = \int_{S_2} y d\theta \, dS = d\theta \int_{S_2} y \, dS = M_{S_2} \, d\theta \qquad \text{(EQ 3.2b)}$$

where M_{S_1} and M_{S_2} denote the absolute values of the static moments of the areas S_1 and S_2 about the line of intersection of the equivolume waterlines WL and W_1L_1. Combining (EQ 3.1) with (EQ 3.2a) and (EQ 3.2b)

$$M_{S_1} = M_{S_2}$$

$$M_{S_1} - M_{S_2} = 0$$

$$M_S = 0 \qquad \text{(EQ 3.3)}$$

where M_S is the net moment of the waterplane about the line of intersection of the equivolume waterlines WL and W_1L_1. (EQ 3.3) states that the static moments of the whole area of the waterplane S about the line of intersection of the equivolume waterlines WL and W_1L_1 is zero. This is possible if and only if the line of intersection of the two waterlines WL and W_1L_1, about which the static moment is evaluated, passes through the centroid of the waterplane WL.

> Euler's Theorem: *The line of intersection of two equivolume waterlines, the angle between them being infinitesimally small, must pass through the centroids of both waterlines.*

The Euler's theorem can also be stated as,

> *If a floating ship is turned through an infinitesimal angle about any axis passing through the centroid of the waterplane, the volume of the immersed portion of the ship is unchanged.*

3.3 The curves of centre of buoyancy

During equivolume inclinations of the vessel, though the underwater volume remains the same, the form of the immersed and emerged wedges are no longer identical. Since the centre of buoyancy is the centroid of this underwater volume, its position changes too.

The theorem of moments in theoretical mechanics states that if a body, which is a member of a system, moves in any direction, the centre of gravity of the system moves in the same direction parallel to the shift in the centre of gravity of that body. The magnitude of this shift is inversely proportional to the ratio of their weights.

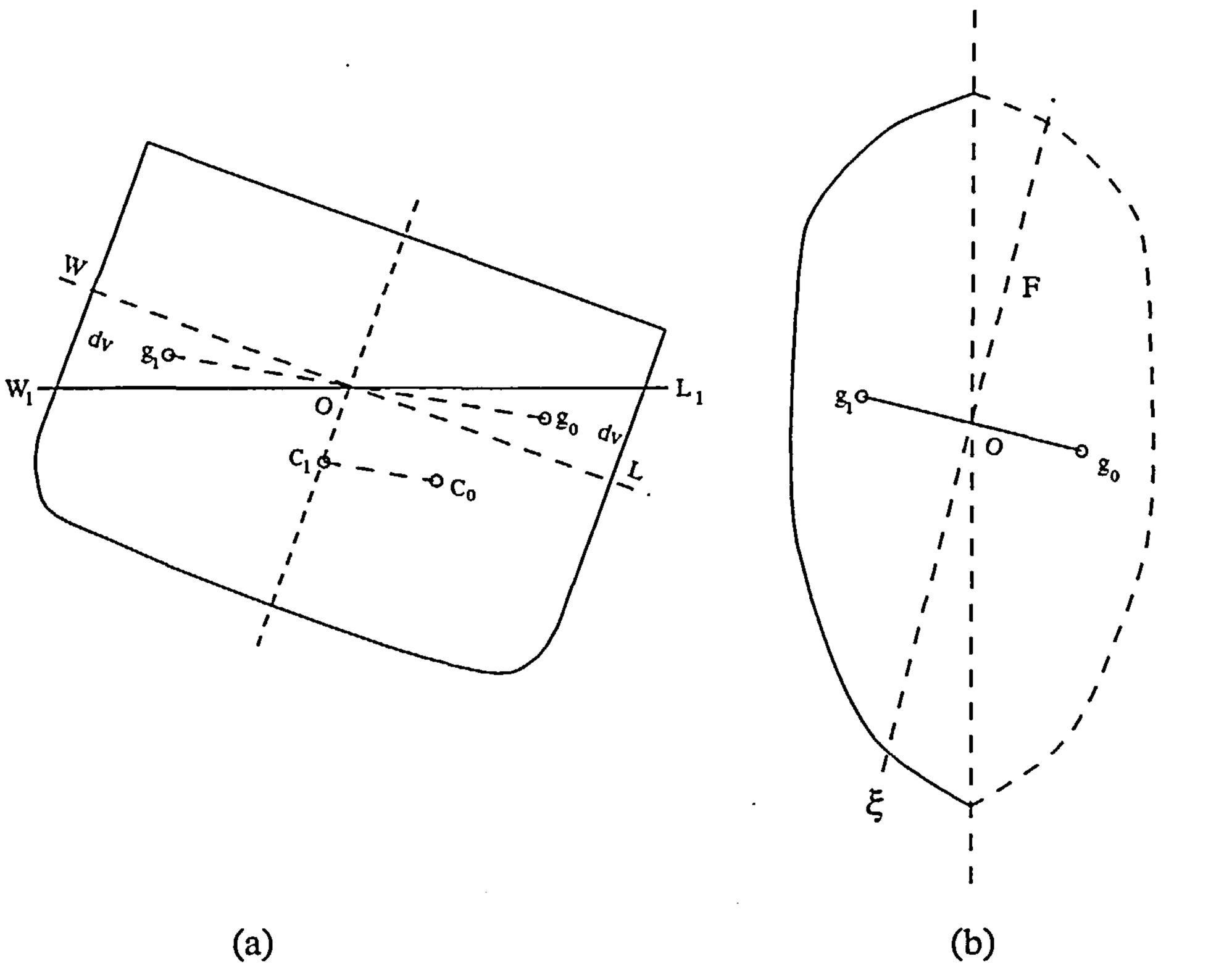

FIGURE 3.5. Shift in the centre of buoyancy (2-D)

In Figure 3.5 (a) the immersed and emerged wedges have equal volumes dv each. g_0 and g_1 are the centroids of these volumes. $\overline{g_0 g_1}$ is the vector that represents the shift in the centroids of the volume dv. The shift in the centre of buoyancy of the underwater volume $\overline{C_0 C_1}$ from the theorem is therefore

$$C_0 C_1 = \overline{g_0 g_1} \frac{dv}{V} \qquad \text{(EQ 3.4)}$$

where V is the total underwater volume.

This expression can be rewritten as

$$V\ C_0C_1 = \overline{g_0g_1}dv. \qquad \text{(EQ 3.5)}$$

The left hand side represents the increment in the static moment of volume with respect to a plane perpendicular to g_0g_1 while the right hand side represents the moment of transference of the wedge of volume dv.

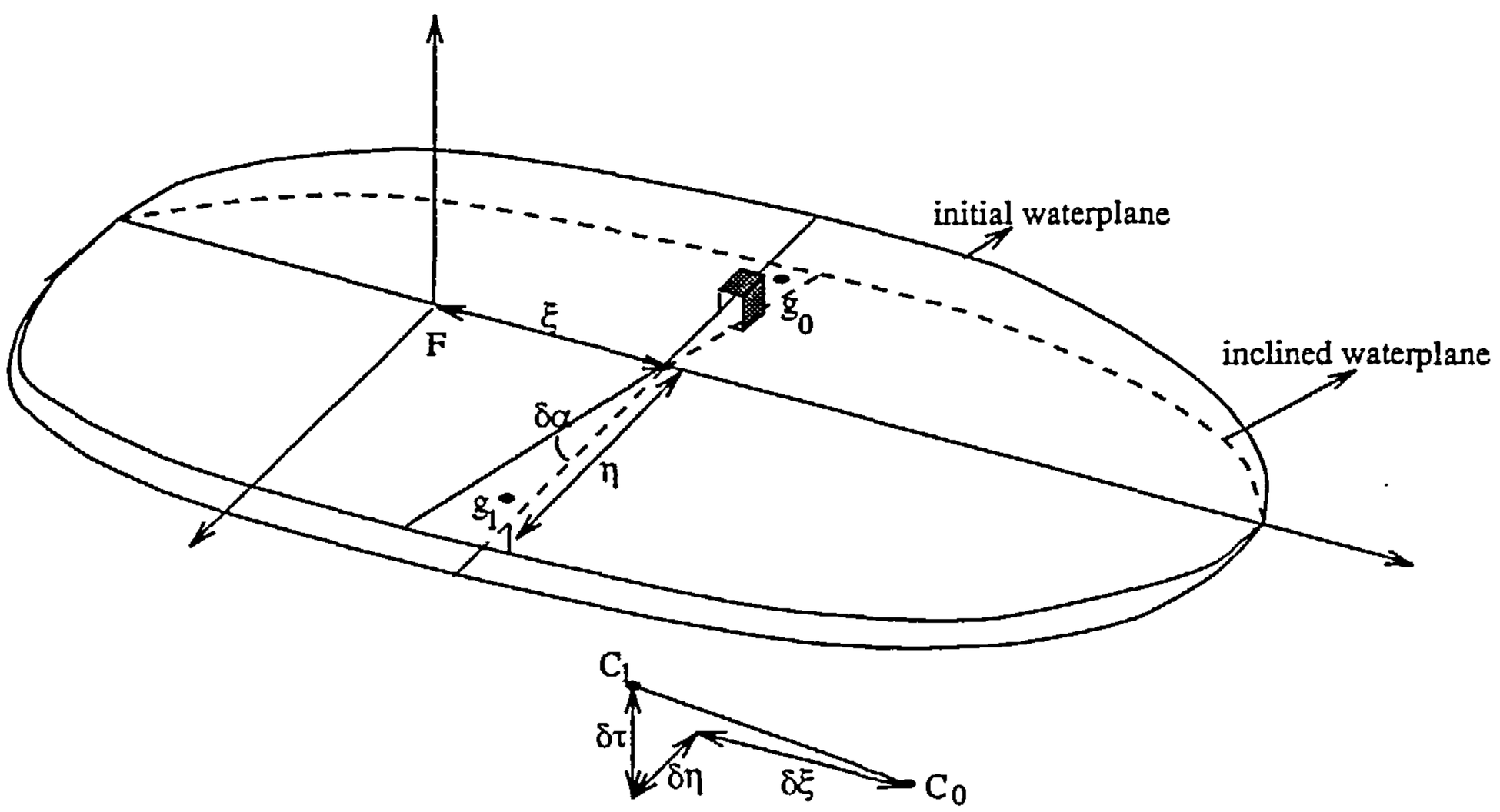

FIGURE 3.6. Shift in the centre of buoyancy (3-D)

Figure 3.5 (b) and Figure 3.6 shows the general case of a shift in the centre of buoyancy. Let the waterplanes WL and W_1L_1 be inclined through an angle $d\alpha$ about an axis $F\xi$ lying on the original waterplane WL and passing through the centroid F of that waterplane. Taking F as the origin draw an axis $F\eta$ perpendicular to $F\xi$ on the waterplane and an axis $F\tau$ perpendicular to $F\xi$ and normal to the waterplane. The shift in the centre of buoyancy can now be resolved into components parallel to the $F\xi$, $F\eta$ and $F\tau$ axes denoted as $d\xi$, $d\eta$ and $d\tau$ respectively.

The volume of an elementary prism (Figure 3.6) would then be,

$$dv = \eta\ d\alpha\ dS$$

and the distance of its centroid from the coordinate palnes would be $\left(\xi, \eta, \frac{1}{2}\eta d\alpha\right)$ where,

ξ - is the distance from the centroid of the prism to the $\eta F\tau$ plane

η - is the distance from the centroid of the prism to the $\xi F\tau$ plane

$\frac{1}{2}\eta\, d\alpha$ - is the distance from the centroid of the prism to the $\xi F\eta$ plane

Integrating over the whole area S, the increments of the moment of volume V in accordance with (EQ 3.5) can be written as

$$dM_{\eta\tau} = V\, d\xi = d\alpha \int_S \xi\eta\, dS \qquad \text{(EQ 3.6)}$$

$$dM_{\xi\tau} = V\, d\eta = d\alpha \int_S \eta^2\, dS \qquad \text{(EQ 3.7)}$$

$$dM_{\xi\eta} = V\, d\tau = \frac{(d\alpha)^2}{2} \int_S \eta^2\, dS \qquad \text{(EQ 3.8)}$$

The integral

$$\int_S \eta^2\, dS = I_\xi \qquad \text{(EQ 3.9)}$$

represents the equatorial moment of inertia about the centroidal axis ξF while the integral

$$\int_S \xi\eta\, dS = I_{\xi\eta} \qquad \text{(EQ 3.10)}$$

is the product inertia about the centroidal axes ξF and ηF. Substituting (EQ 3.9) and (EQ 3.10) in (EQ 3.6) to (EQ 3.8),

$$d\xi = \frac{I_{\xi\eta}}{V} d\alpha \qquad \text{(EQ 3.11)}$$

$$d\eta = \frac{I_\xi}{V} d\alpha \qquad \text{(EQ 3.12)}$$

$$d\tau = \frac{1}{2}\frac{I_\xi}{V}(d\alpha)^2 \qquad \text{(EQ 3.13)}$$

(EQ 3.11) to (EQ 3.13) represents the changes in the coordinates of the centre of buoyancy during the equivolume inclination. Also comparing (EQ 3.12) and (EQ 3.13), $d\tau = \frac{1}{2}\, d\eta\, d\alpha$. Therefore $d\tau$ is a small quantity of high order when compared to $d\eta$.

Considering all possible equivolume inclinations with no impositions on the direction of the axis of inclination or its magnitude, the centre of buoyancy corresponding to these positions will lie on a closed surface which is the locus of the centres of buoyancy for a given equivolume inclination. In ship theory, this surface is known as the *C surface*.

When the ship is inclined in a particular plane, the centre of buoyancy moves along a particular trajectory which lies on the C surface. This is known as the *C trajectory* which is, in general, a curve of double curvature. Its projection on the plane of inclination is termed as the curve of centre of buoyancy or the *C curve* which is obviously planar.

Corresponding to each point on the C surface, there is a particular position of the waterplane. (EQ 3.11) to (EQ 3.13) give the change in the centre of buoyancy in a coordinate system arranged so that the ξF and ηF axes lie in the waterplane. When the centre of buoyancy shifts, the element of the arc of the C trajectory is

$$dS = \sqrt{d\xi^2 + d\eta^2 + d\tau^2}$$

$d\tau^2$ being negligibly small when compared to $d\xi^2$ and $d\eta^2$,

$$dS = \sqrt{d\xi^2 + d\eta^2} \qquad \text{(EQ 3.14)}$$

(EQ 3.14) shows that the displacement dS takes place in a plane parallel to the $\xi F\eta$ plane, i.e. to the waterplane. Hence an important property of the C surface is obtained which can be stated as,

> *a plane tangential to the C surface at any point C is always parallel to the waterplane corresponding to the point C*

and since the C trajectory lies on the C surface

> *a tangent to the C curve is parallel to the trace of the corresponding waterplane on the plane of inclination.*

3.4 The geometry of a vessel's arbitrary attitude

The left handed coordinate system that describes the geometry of a vessel is shown in Figure 3.7.

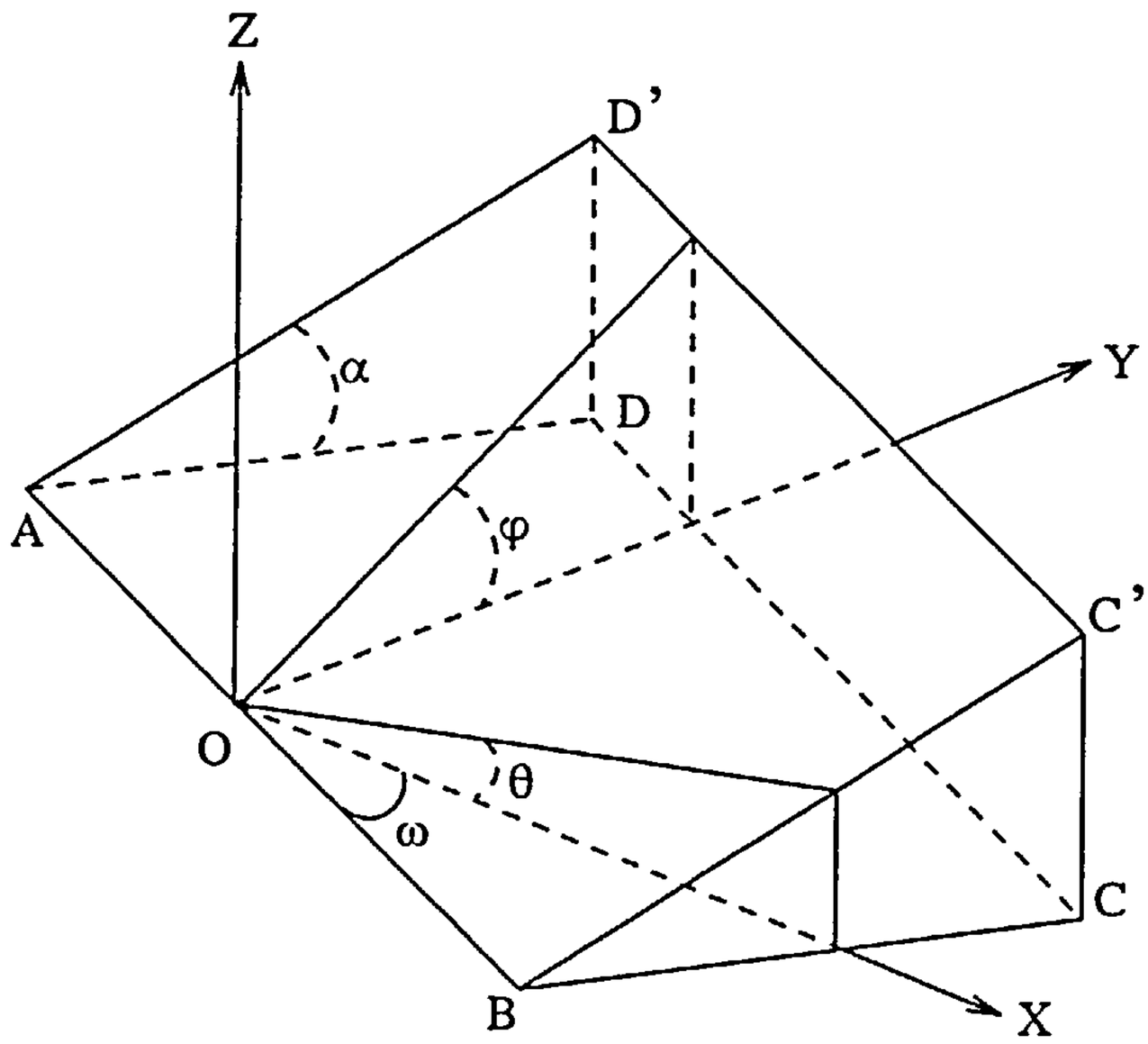

FIGURE 3.7. Analytical and statical angles of heel and trim

α - the angle between the base plane (or the XOY plane) and the inclined waterplane $ABC'D'$

φ - the theoretical angle of heel. It is the angle between the trace of the waterplane $ABC'D'$ on the YOZ plane and the Y axis

θ - the theoretical angle of trim. It is the angle between the trace of the waterplane $ABC'D'$ on the XOZ plane and the X axis

φ and θ are measured positive in the anticlockwise direction. The equation of the waterplane in this coordinate system is given as,

$$z = x\tan\theta + y\tan\varphi + T \qquad \text{(EQ 3.15)}$$

where T is the draught on the Z-axis. The vector normal to the waterplane (from plane geometry) is

$$\bar{R} = (\tan\theta, \tan\varphi, -1)$$

and its magnitude is

$$|\bar{R}| = \sqrt{1 + \tan^2\theta + \tan^2\varphi}$$

Therefore the unit normal vector to the waterplane directed vertically upwards (away from the origin) is,

$$\bar{n} = -\frac{\bar{R}}{|\bar{R}|}$$

or

$$\bar{n} = -\frac{1}{|\bar{R}|}(\tan\theta, \tan\varphi, -1) \qquad \text{(EQ 3.16)}$$

The base plane and the waterplane intersect each other along a line (line AB, Figure 3.7) which is called the axis of inclination. The direction of this axis is described by the angle ω, measured from the X axis on the XY plane. Putting $z = 0$ in (EQ 3.15)

$$\tan\omega = -\frac{\tan\theta}{\tan\varphi}$$

Taking a dot product between the normal $\bar{n}$ and the Z axis

$$\bar{n} \cdot \bar{k} = |\bar{n}||\bar{k}|\cos\alpha$$

Since the direction cosines for $\bar{k} = (0, 0, 1)$,

$$\cos\alpha = \frac{1}{|\bar{R}|}$$

$$\cos\alpha = \frac{1}{\sqrt{1 + \tan^2\theta + \tan^2\varphi}}$$

$$\tan\alpha = \sqrt{\tan^2\theta + \tan^2\varphi} \qquad \text{(EQ 3.17)}$$

$$|\bar{R}| = \sqrt{1 + \tan^2\theta + \tan^2\varphi} = \sqrt{1 + \tan^2\alpha} = \frac{1}{\cos\alpha} \qquad \text{(EQ 3.18)}$$

From (EQ 3.16) and (EQ 3.18), the normal $\bar{n}$ can now be expressed as

$$\bar{n} = (-\tan\theta\cos\alpha, -\tan\varphi\cos\alpha, \cos\alpha) \qquad \text{(EQ 3.19)}$$

Pawlowski [Pawlowski'91] described a wind impact screen or a δ-plane, an imaginary plane, which is fixed in the global sense (earth coordinates) and perpendicular to the base plane and to the wind direction.

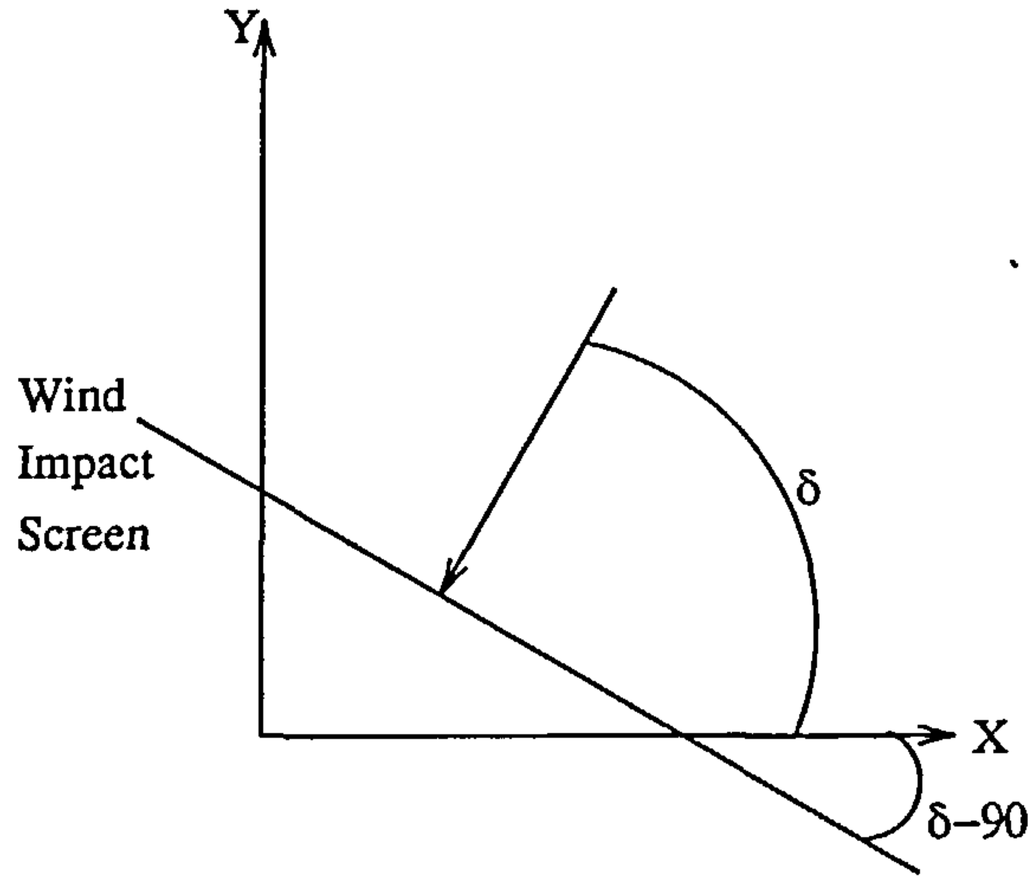

FIGURE 3.8. *Wind impact screen*

Figure 3.8 shows the wind direction at an angle δ with respect to the X axis. A plane perpendicular to this wind direction and the XOY plane making an angle $-(90 - \delta)$ with respect to the X axis is the wind impact screen. Since this plane is fixed in space, the trace of the waterplane with this wind impact screen does not change its direction (earth coordinates) and is called the *axis of rotation*, whose unit vector is denoted by $\bar{e}$, Figure 3.9.

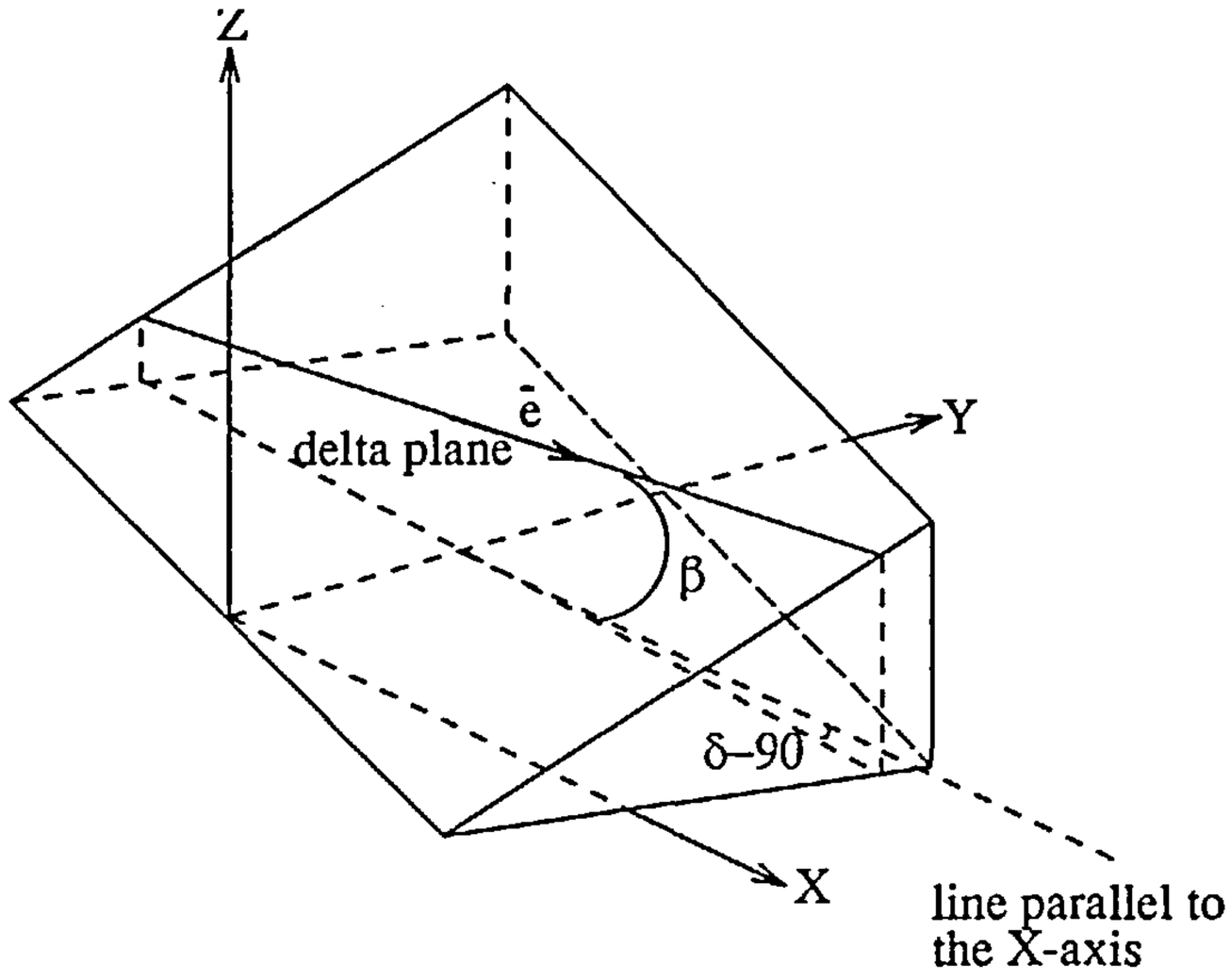

FIGURE 3.9. *Axis of rotations*

It is worthwhile emphasizing that unlike the axis of inclination, that has been described previously, the axis of rotation is at all times perpendicular to the wind direction and is coincident with the wind heeling moment vector.

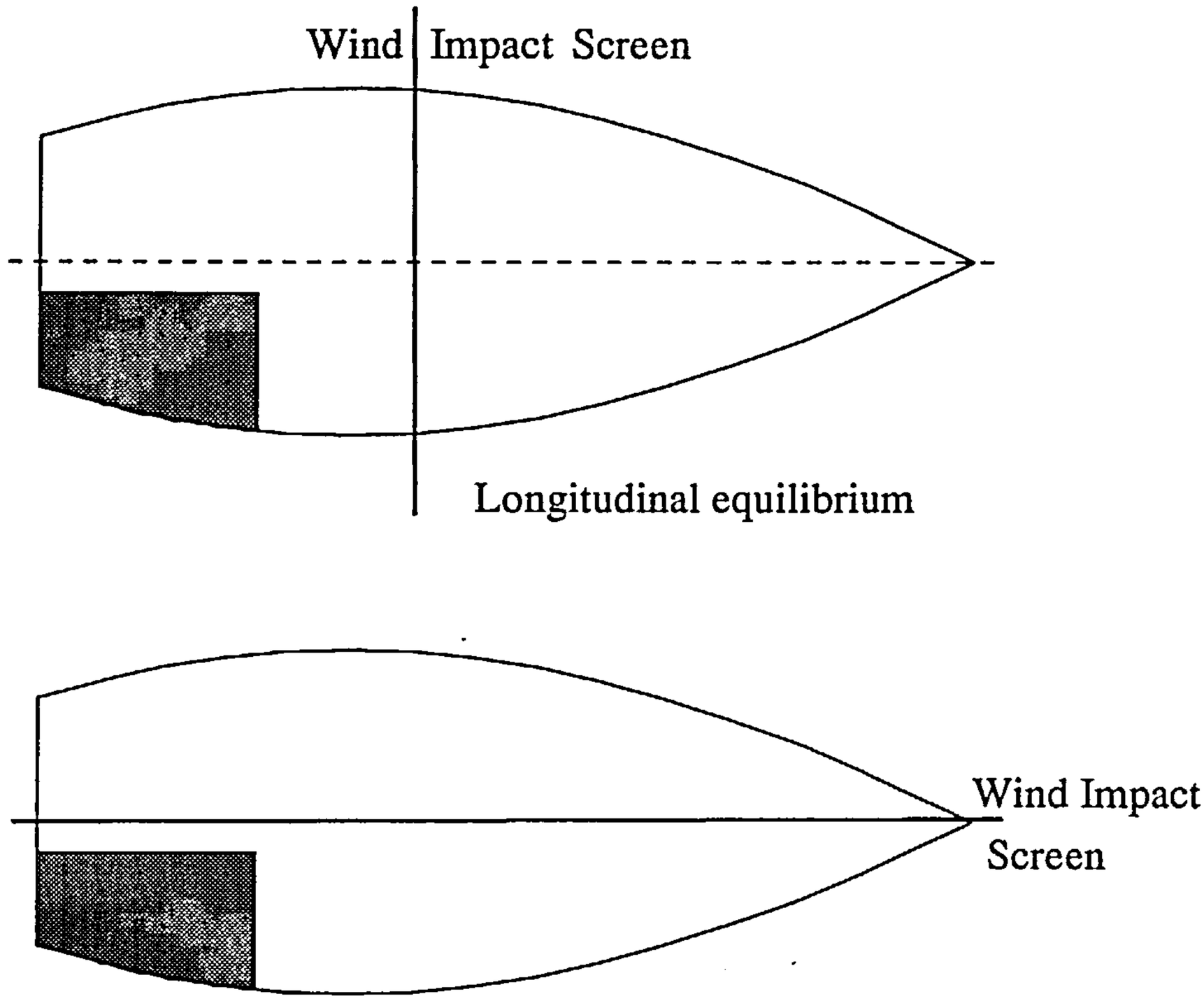

FIGURE 3.10. Axis of rotation definition for monhull damage stability calculations

For the damage stability case, for non-symmetric damage scenarios, the wind impact screen is the midship plane during longitudinal equilibrium, Figure 3.10. After longitudinal equilibrium has been achieved, the internal righting moment is directed along the centre plane, the wind impact screen can now be taken as the centreplane (beam case, $\delta = 90$).

Figure 3.11 describes the angle of rotation ϕ (the roll angle) which is measured perpendicular to the δ-plane.

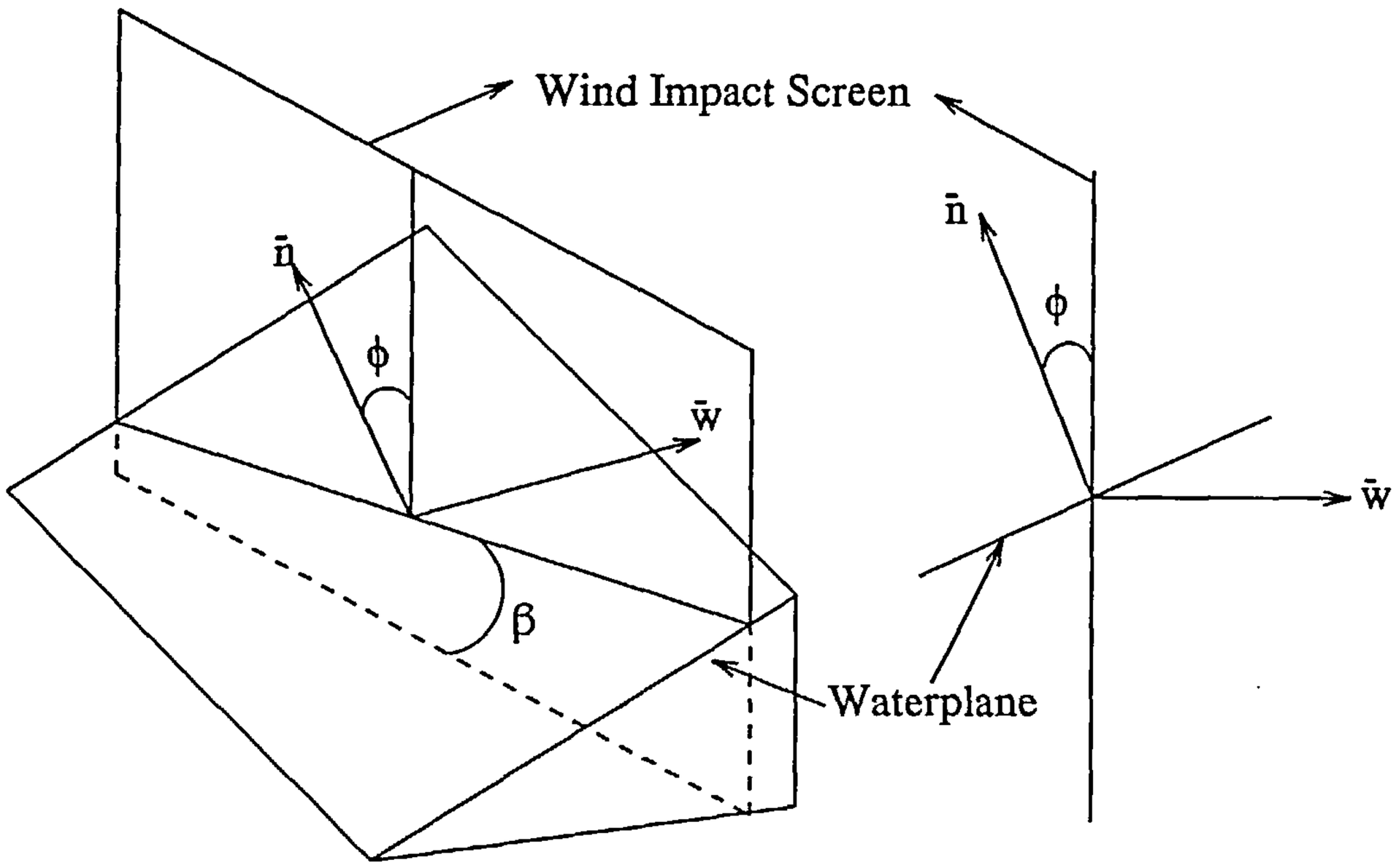

FIGURE 3.11. The angle of rotation

$\bar{w}$ is a unit vector which represents the wind speed such that,

$$\bar{w} = (\cos\delta, \sin\delta, 0) \qquad \text{(EQ 3.20)}$$

The dot product between $\bar{w}$ and $\bar{n}$ would give,

$$\bar{w} \cdot \bar{n} = \cos(90 + \phi)$$

Substituting from (EQ 3.19) and (EQ 3.20)

$$\sin\phi = -\bar{w} \cdot \bar{n} = \cos\alpha(\cos\delta\tan\theta, \sin\delta\tan\varphi) \qquad \text{(EQ 3.21)}$$

If the axis of inclination (line AB, Figure 3.7) is rotated so as to be aligned with the δ-plane, i.e. $\omega = \delta - 90$, then (EQ 3.21) yields, $\phi = \alpha$. This means that only in situations where the axis of inclination is parallel to the axis of rotation does the angle of inclination α become the angle of roll, ϕ.

For a beam case (as in the case of monohulls), $\delta = 90$, then ϕ denotes the roll angle of the unit due to beam wind and from (EQ 3.21)

$$\sin\phi = \cos\alpha\tan\varphi$$

Referring to Figures 3.9 and 3.11, as the vessel inclines through an angle ϕ, the trace of the waterplane on the δ-plane changes through an angle β. Thus though the axis of rotation is fixed in space (earth coordinates), it does change its position with respect to the vessels coordinate system. The direction of the axis of rotation is described by the line of intersection between the still waterplane and the δ-plane and is given by the cross product $\bar{w} \times \bar{n}$, Figure 3.11, where,

$$|\bar{w} \times \bar{n}| = |\bar{w}||\bar{n}|\sin(90 + \phi)$$
$$|\bar{w} \times \bar{n}| = \cos\phi$$

and

$$\bar{w} \times \bar{n} = \bar{e}\cos\phi$$

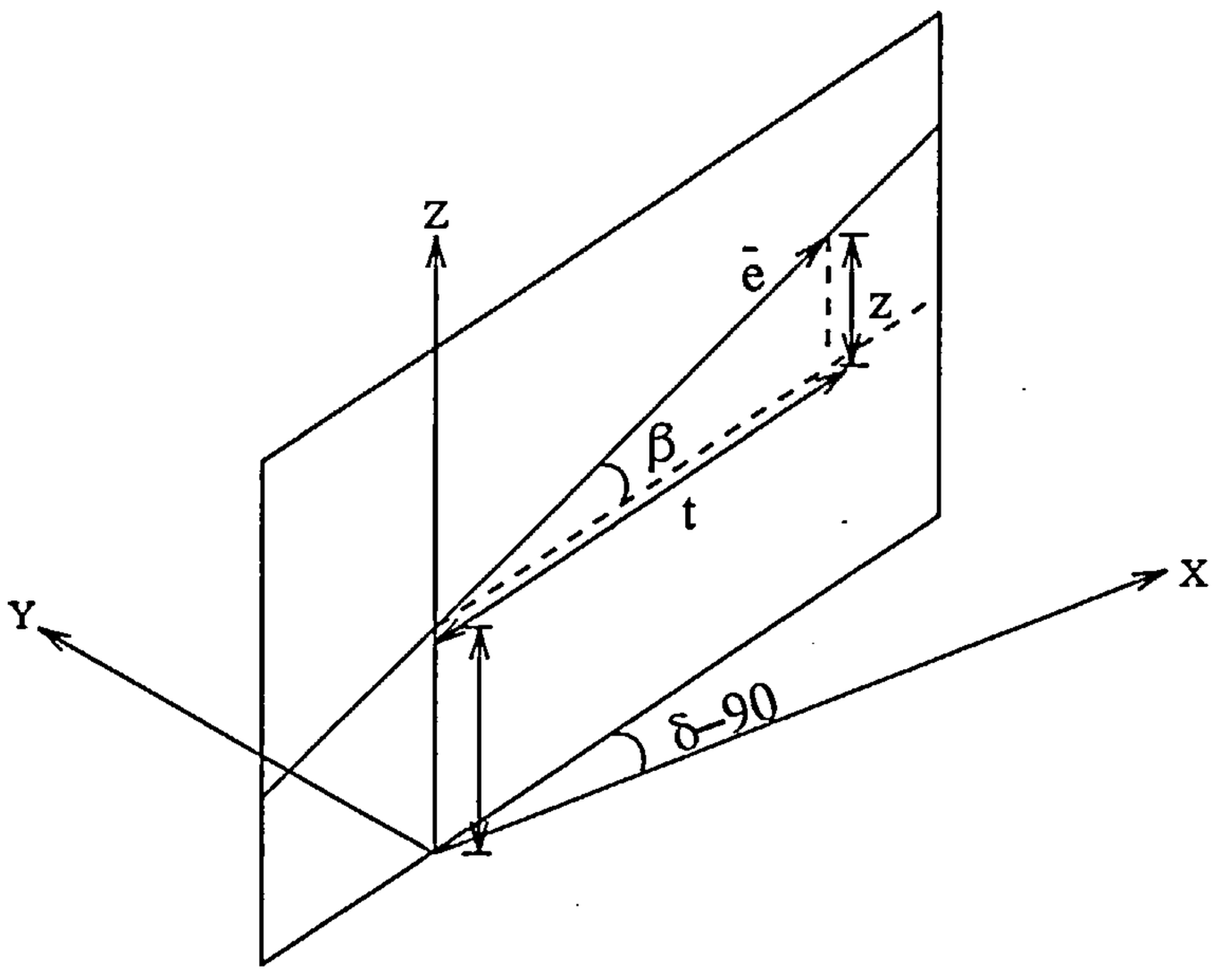

FIGURE 3.12. Direction cosines of the axis of rotation

The parametric equation of the axis of rotation as a line of intersection between the waterplane and the δ-plane is,

$$x = t\sin\delta$$
$$y = t\cos\delta$$
$$z = t(\sin\delta\tan\theta - \cos\delta\tan\varphi) + T$$

where z results from (EQ 3.15) and t is a parameter that varies along the δ-plane. The axis of rotation is inclined to the base plane by angle β, Figure 3.12, hence,

$$\tan\beta = \frac{z}{t} = \sin\delta\tan\theta - \cos\delta\tan\varphi \qquad \text{(EQ 3.22)}$$

T being a constant. The angle β is nothing but the angle of trim measured on the δ-plane. Solving (EQ 3.21) and (EQ3.22) simultaneously,

$$\tan\theta = R\sin\phi\cos\delta + \tan\beta\sin\delta \qquad \text{(EQ 3.23a)}$$

$$\tan\varphi = R\sin\phi\sin\delta - \tan\beta\cos\delta \qquad \text{(EQ 3.23b)}$$

where $R = \frac{1}{\cos\alpha}$. Substituting (EQ 3.23a) and (EQ 3.23b) in (EQ 3.17) and solving,

$$\cos\alpha = \cos\beta\cos\phi \qquad \text{(EQ 3.24)}$$

The directions cosines of the axis of rotation unit vector $\bar{e}$ can now be stated in terms of the trim angle β as,

$$\bar{e} = (\cos\beta\sin\delta, -\cos\beta\cos\delta, \sin\beta) \qquad \text{(EQ 3.25)}$$

There are in effect three ways to describe the arbitrary attitude of a vessel, with three pairs of independent angles of inclination, viz. (θ, φ), (ω, α) or (β, ϕ). (θ, φ) are the classical definitions of trim and heel. (ω, α) are described with respect to the axis of inclination. (β, ϕ) are described with respect to the axis of rotation. (β, ϕ) could be regarded as the Euler angles of rotation and could be called the semi-dynamic angles of heel.

3.5 Free trim inclinations

For a given heel angle ϕ, the free trim condition implies the determination of the trim angle β which results in the buoyancy force vector $\overline{B}$ and the weight force vector $\overline{W}$, both in the direction of $\bar{n}$, to lie in the same transverse plane to the axis of rotation.

This is subject to the assumption that the vector of wind heeling moment is parallel to the axis of rotation $\bar{e}$. Thus, for any angle of rotation ϕ the following the equivolume relationship holds:

$$\nabla = \nabla_0 \qquad \text{(EQ 3.26)}$$

$$\bar{e} \cdot \bar{r} = 0 \qquad \text{(EQ 3.27)}$$

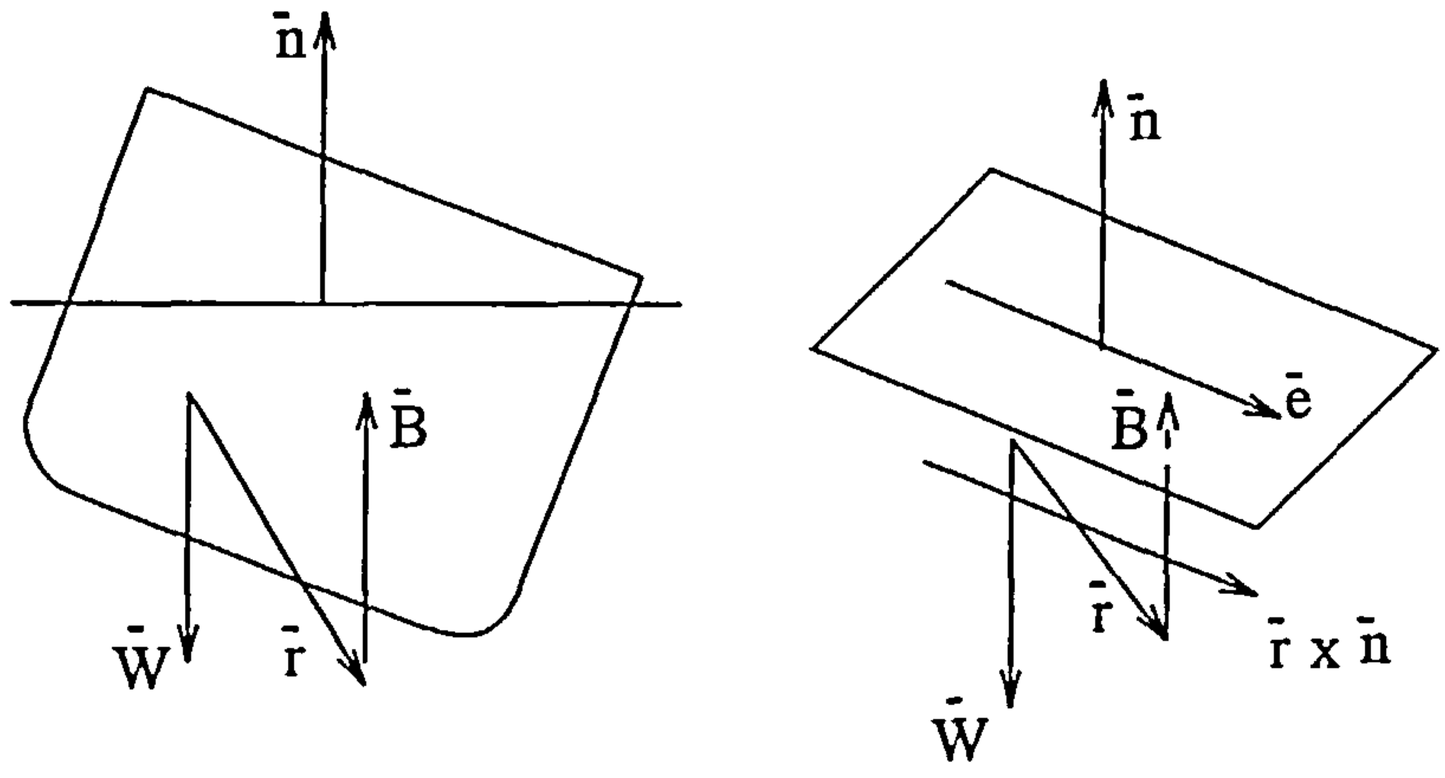

FIGURE 3.13. Longitudinal equilibrium in free trim calculations

where $\bar{r}$ is the coordinate vector of the centre of buoyancy relative to the centre of gravity, Figure 3.13, such that

$$\bar{r} = (x_B - x_G, y_B - y_G, z_B - z_G)$$

Since the axis of rotation is fixed in space (earth coordinates), it follows from (EQ 3.26) that

> *the centre of buoyancy during free trim rotations moves along a strictly flat curve lying on a plane fixed in space, perpendicular to the axis of rotation.*

The restoring moment

$$\overline{M_R} = (\bar{r} \times \bar{n})\rho g \nabla$$

is then parallel to the axis of rotation $\bar{e}$, hence

$$M_R = \bar{e} \cdot (\bar{r} \times \bar{n})\rho g \nabla$$

and the righting arm curve $GZ = M_R/\rho g \nabla$ is given by,

$$GZ = \bar{e} \cdot (\bar{r} \times \bar{n}) \qquad \text{(EQ 3.28)}$$

The calculation of this righting arm under free trim conditions, based on (EQ 3.27) usually implies an iterative procedure which involves, for each angle of rotation ϕ, adjustment of β and draught, aiming to satisfy (EQ 3.26) and (EQ 3.27). To simplify this tedious procedure Euler's theorem on equivolume waterplanes can be used.

The first step involves the determination of an instantaneous axis of inclination which lies on the waterplane and passes through its centre of flotation. This axis is called the *axis of flotation* denoted as ξ'. The direction of the ξ' - axis is defined by the angle χ,

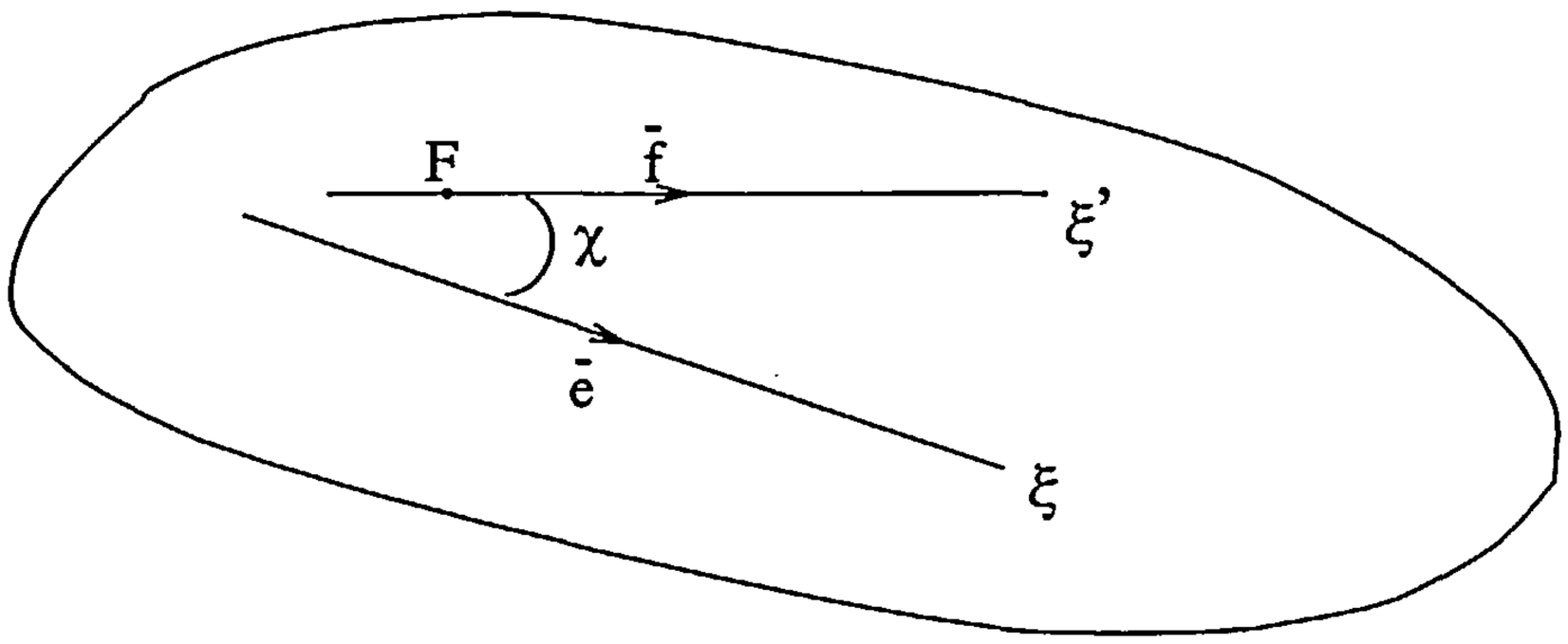

FIGURE 3.14. The axis of flotation

measured positive in the anticlockwise direction when measured from the axis of rotation $\bar{e}$ on the waterplane (denoted as the ξ- axis), Figure 3.14. Differentiating (EQ 3.27)

$$d\bar{e} \cdot \bar{r} + \bar{e} \cdot d\bar{r} = 0 \qquad \text{(EQ 3.29)}$$

The axis of rotation $\bar{e}$ though fixed in space (earth coordinates) does move with respect to the vessels coordinate system. This implies that the term $d\bar{e} \cdot \bar{r}$ is generally different from zero and that the displacement of the centre of buoyancy is not entirely normal to the axis of rotation $\bar{e}$.

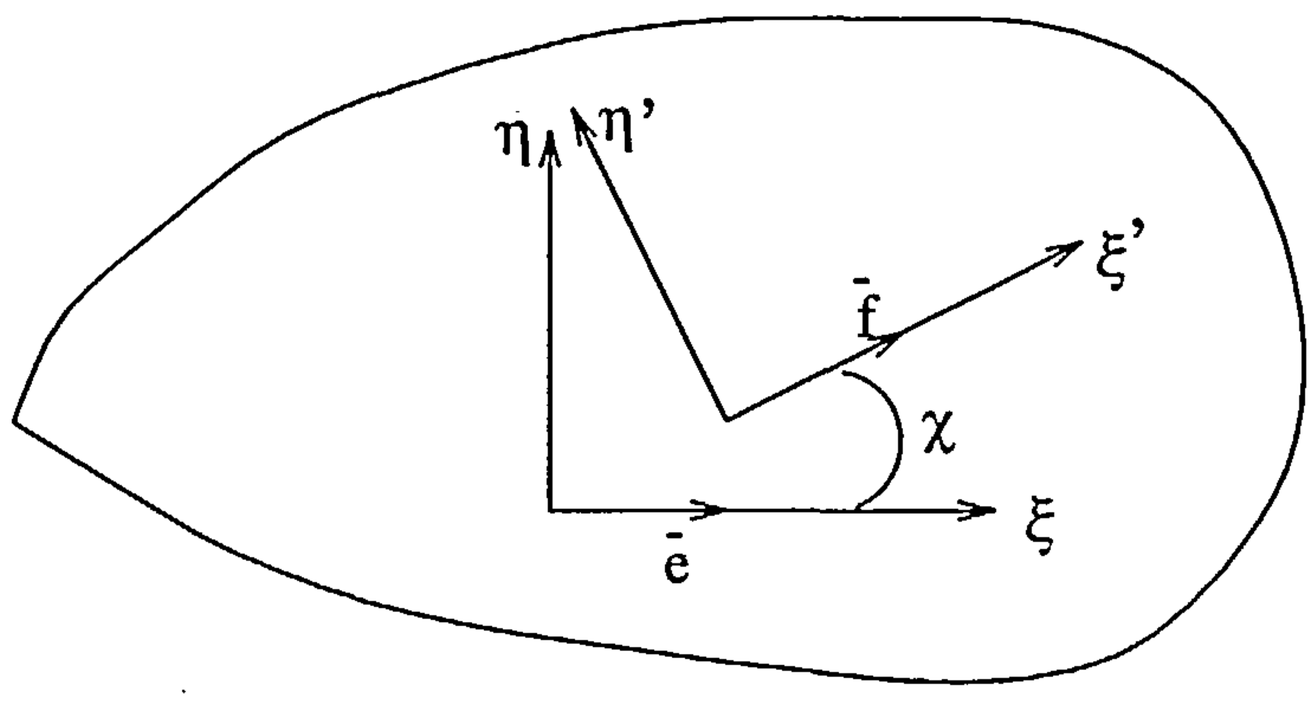

FIGURE 3.15. The $\bar{f}$ and $\bar{e}$ coordinate systems

The (ξ', η') system (Figure 3.15) is the coordinate system associated with the axis of flotation $\bar{f}$ whereas the (ξ, η) system is the coordinate system associated with the axis of rotation $\bar{e}$. The angle between these two systems is obviously χ. The following therefore holds

$I_{\xi\xi}, I_{\eta\eta}$ moments of inertia about the longitudinal and transverse axis of the waterplane, associated with the axis of rotation, $\bar{e}$

$I_{\xi'\xi'}, I_{\eta'\eta'}$ moments of inertia about the longitudinal and transverse axis of the waterplane, associated with the axis of flotation, $\bar{f}$

$D = I_{\xi\eta}$ deviation moment (or product moment) of inertia of the waterplane, associated with the axis of rotation $\bar{e}$

$D' = I_{\xi'\eta'}$ deviation moment (or product moment) of inertia of the waterplane, associated with the axis of flotation, $\bar{f}$

The displacement $d\bar{r}$ in (EQ 3.29) due to an infinitesimal rotation $d\alpha_1$ about the axis of flotation $\bar{f}$ can be analysed as transverse and parallel components to that axis. These components of $d\bar{r}$ would be proportional to the moments of inertia of the still waterplane $I_{\xi'\xi'}$ and $I_{\xi'\eta'}$ respectively.

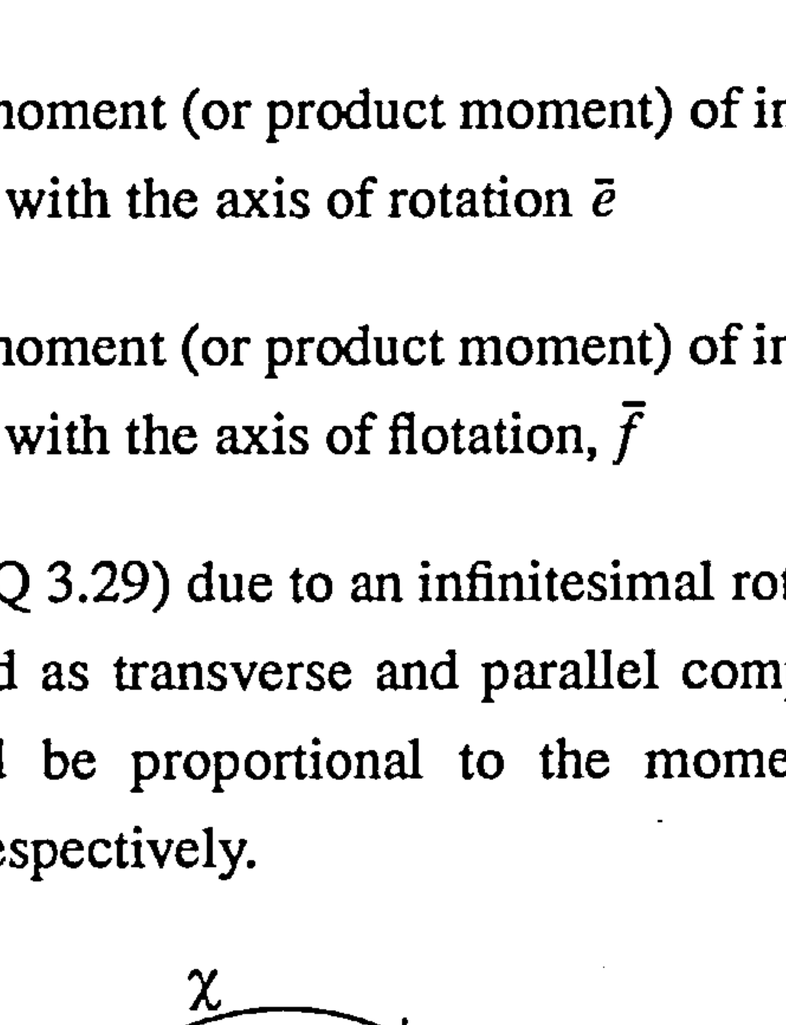

FIGURE 3.16. $d\bar{r}$ **with respect to** $\bar{f}$ **and** $\bar{e}$

Therefore (refer Figure 3.16)

$$\tan\chi_f = \frac{I_{\xi'\eta'}}{I_{\xi'\xi'}} \qquad \text{(EQ 3.30)}$$

and

$$d\bar{r} = \frac{I_{\xi'\xi'}}{\nabla} d\alpha_1 (\bar{n} \times \bar{f}) + \frac{I_{\xi'\eta'}}{\nabla} d\alpha_1 \bar{f}$$

where $\bar{n} \times \bar{f}$ is the component of $d\bar{r}$ perpendicular to $\bar{f}$. Therefore the magnitude of $d\bar{r} = |d\bar{r}|$ which gives the length of the displacement of the centre of buoyancy ds is

$$ds = r' d\alpha_1 \qquad \text{(EQ 3.31)}$$

where $r' = \frac{1}{\nabla}\sqrt{(I_{\xi'\xi'})^2 + (I_{\xi'\eta'})^2}$

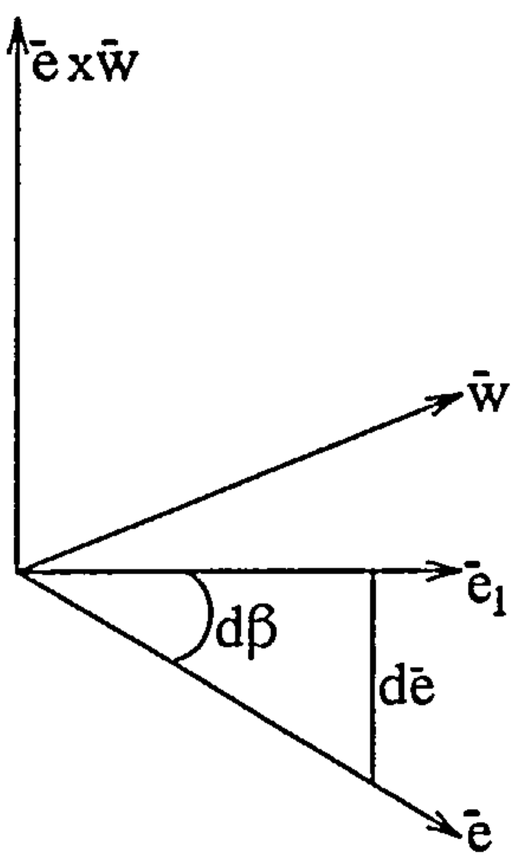

FIGURE 3.17. Change in the axis of rotation $d\bar{e}$

Since the axis of rotation remains on the δ-plane at all times (Figure 3.17),

$$d\bar{e} = d\beta(\bar{e} \times \bar{w}) \qquad \text{(EQ 3.32)}$$

Also from Figure 3.16,

$$\bar{e} \cdot d\bar{r} = |d\bar{r}| \sin\upsilon = |d\bar{r}| \sin(\chi - \chi_f)$$

$$\bar{e} \cdot d\bar{r} = ds \sin(\chi - \chi_f) \qquad \text{(EQ 3.33)}$$

Substituting (EQ 3.32) and (EQ 3.33) in (EQ 3.29)

$$ds\sin(\chi - \chi_f) = d\beta(\bar{e} \times \bar{w}) \qquad \text{(EQ 3.34)}$$

Now the axis of flotation $\bar{f}$ may be thought of as a resultant axis due to the simultaneous rotation of the δ-plane about the axis of rotation $\bar{e}$ (by angle $d\phi$) and about the unit normal vector to the δ-plane $\bar{w}$ (by the angle $d\beta$), Figure 3.18.

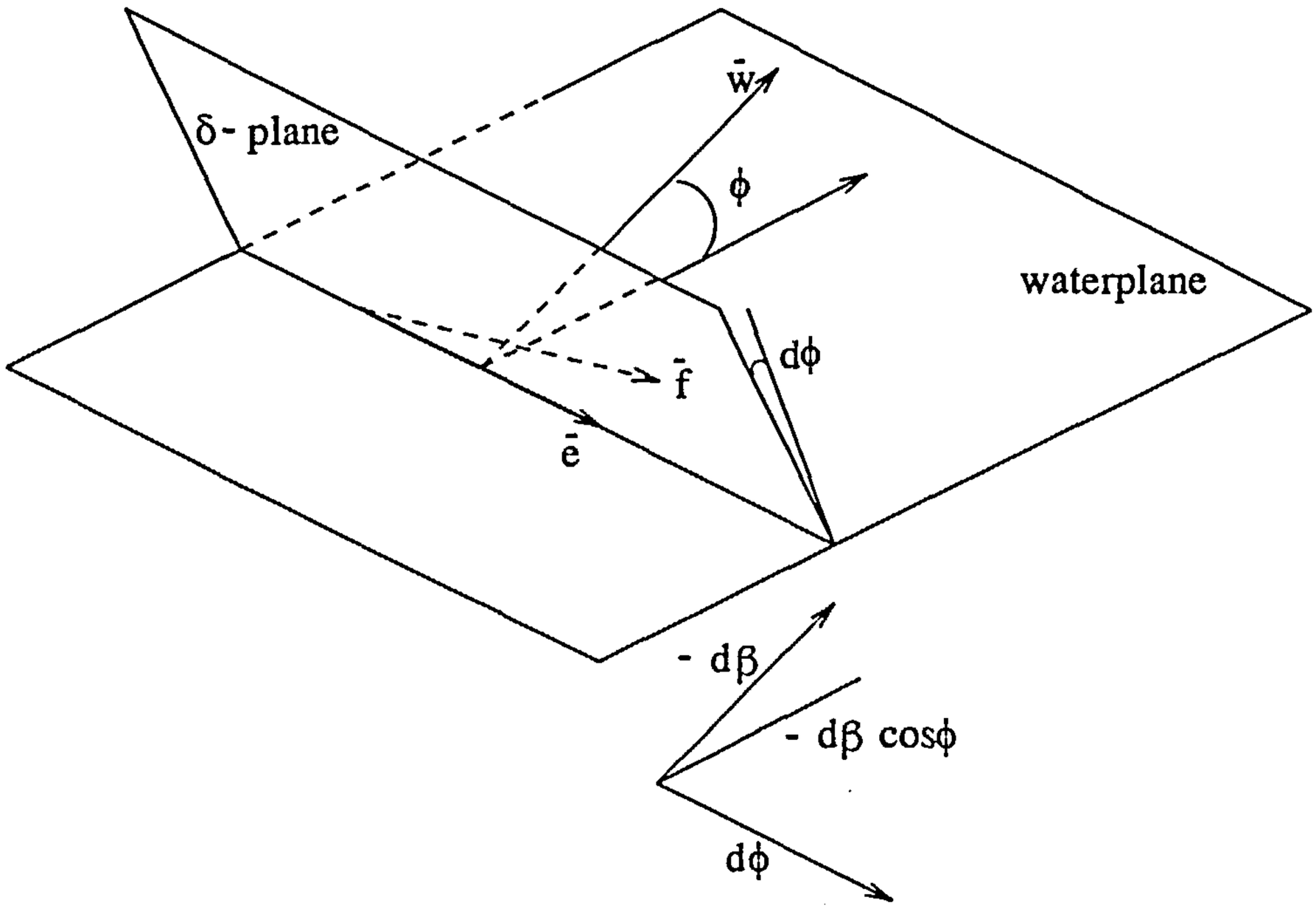

FIGURE 3.18. Alternative direction cosines for $\bar{f}$

Since $\bar{w}$ is inclined to the baseplane by an angle ϕ, the instantaneous rotation of the waterplane, $\bar{f}d\alpha_1$, may be decomposed into parallel and normal components to the axis of rotation $\bar{e}$:

$$\bar{f}d\alpha_1 = (d\phi, -d\beta\cos\phi)$$

The negative sign of $d\beta$ appears because for an anticlockwise rotation resulting in a positive trim angle, the $d\bar{\beta}$ vector would point along the $-Y$ axis (right hand rule).

But since the angle between $\bar{f}$ and $\bar{e}$ axis has been defined as χ, two useful relationships arise from this decomposition

$$\frac{d\phi}{d\alpha_1} = \cos\chi \qquad \text{(EQ 3.35)}$$

$$-\frac{d\beta\cos\phi}{d\alpha_1} = \sin\chi \qquad \text{(EQ 3.36)}$$

Substituting (EQ 3.36) and (EQ 3.31) in (EQ 3.34)

$$r'\sin(\chi-\chi_f) = -\frac{\bar{r}\cdot(\bar{e}\times\bar{w})}{\cos\phi}\sin\chi \qquad \text{(EQ 3.37)}$$

The relationship between the moments of inertia with respect to the (ξ,η) and the (ξ',η') coordinate systems can be represented in the form similar to the Mohr's circle representation (Figure 3.19) commonly used in strength of materials (see Appendix A).

r' and χ_f in (EQ 3.37) are functions of $I_{\xi'\xi'}$ and $I_{\xi\eta'}$, and therefore are functions of χ.

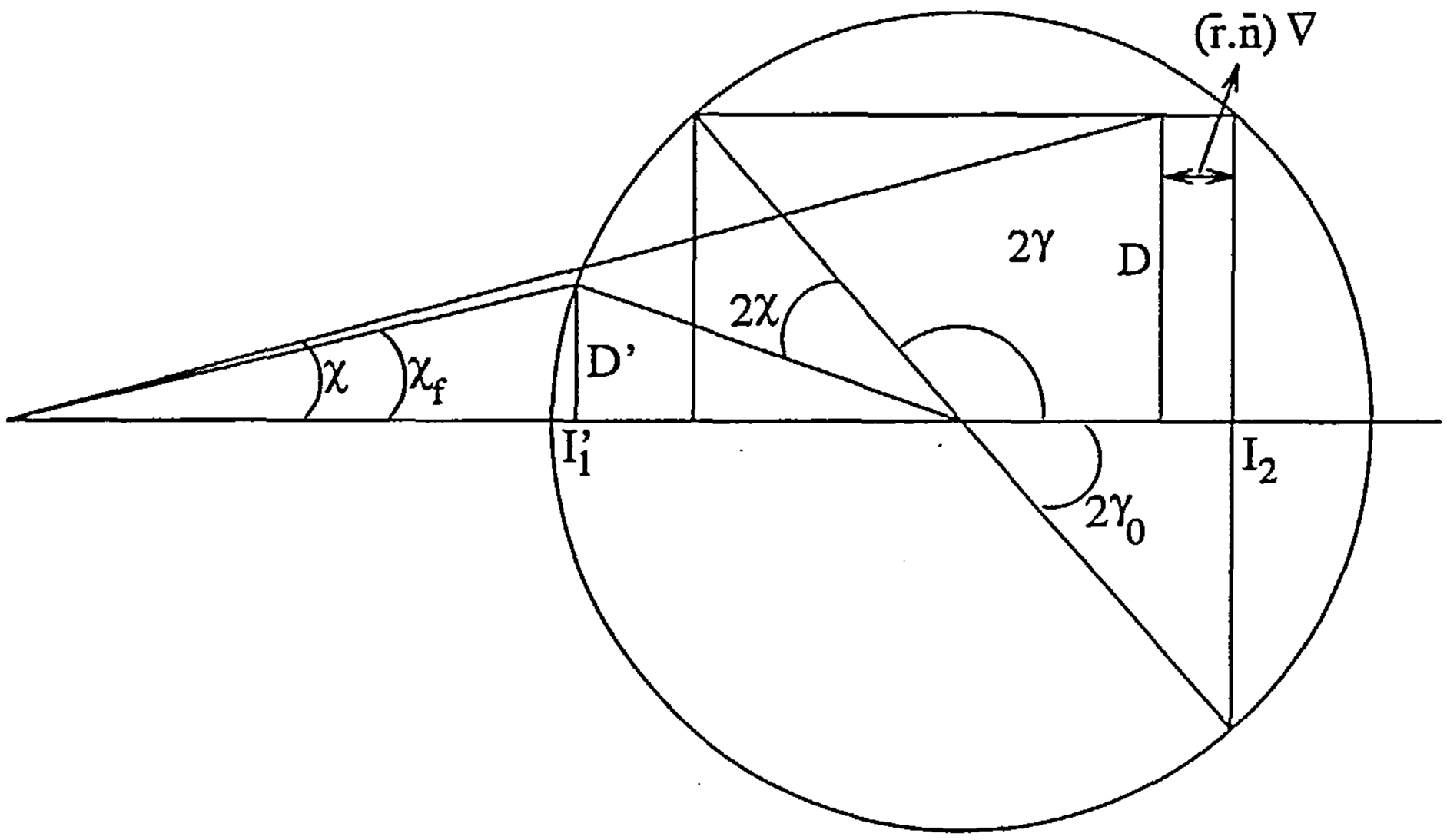

FIGURE 3.19. Mohr's circle interpretation of the angle χ

The expression for χ can be obtained by resorting to physical considerations thereby eliminating the need for a numerical solution. This solution is

$$\tan\chi = \frac{D}{I_{\eta\eta}+(\bar{r}\cdot\bar{n})\nabla} \qquad \text{(EQ 3.38)}$$

$R = \frac{I_{\eta\eta}}{\nabla}$, the longitudinal metacentric radius, is usually substantially larger than $\bar{r}\cdot\bar{n}$ (the vertical distance between the centre of gravity G and the centre of buoyancy B) particularly in the case of monohull ships. Hence $\chi \approx \chi_f$ and $\nu \approx 0$. This implies that the

displacement of the centre of buoyancy $d\bar{r}$ under free trim considerations is nearly exactly normal to the axis of rotation $\bar{e}$ and its deviation from the normal direction may be conveniently ignored.

Therefore,

$$\tan\chi = \frac{D}{I_{\eta\eta}} \qquad \text{(EQ 3.39)}$$

Having determined the angle χ, the unit vector $\bar{f}$ of the ξ'-axis is simply obtained from the rotation of $\bar{e}$ on the still waterplane by the angle χ as,

$$\bar{f} = \bar{e}\cos\chi + \bar{a}\sin\chi \qquad \text{(EQ 3.40)}$$

where $\bar{a} = \bar{n} \times \bar{e}$.

3.6 Cone of axis of flotation

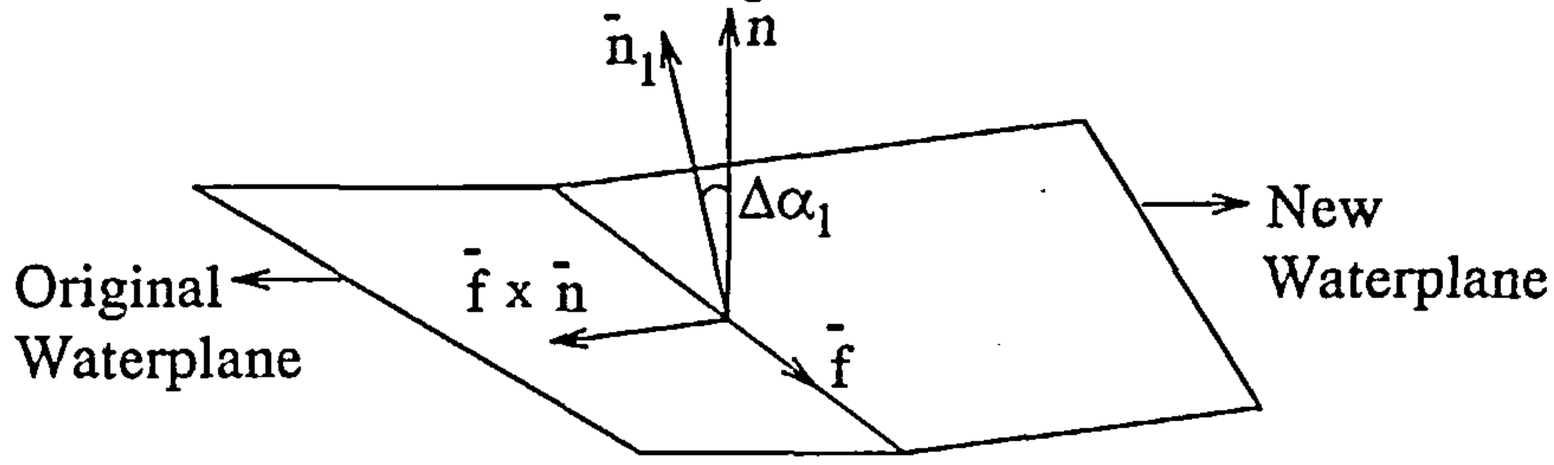

FIGURE 3.20. The normal $\bar{n}_1$ to the new waterplane

Having determined $\bar{f}$, the instantaneous axis of rotation, from (EQ 3.40), the normal to the new waterplane, inclined to the previous one by an angle $\Delta\alpha_1$ can be found by rotating the normal $\bar{n}$ about the ξ'-axis by an angle $\Delta\alpha_1$, Figure 3.20. Thus,

$$\bar{n}_1 = \bar{n}\cos\Delta\alpha_1 + (f \times \bar{n})\sin\Delta\alpha_1 \qquad \text{(EQ 3.41)}$$

Having determined $\bar{n}_1$, (EQ 3.19) can be solved to obtain the new α, θ and φ. The new angle of roll ϕ and the new trim angle β on the δ-plane can be obtained from (EQ 3.21)

and (EQ 3.22) respectively. The direction cosines of the new axis of rotation $\bar{e}_1$ can be obtained from (EQ 3.25).

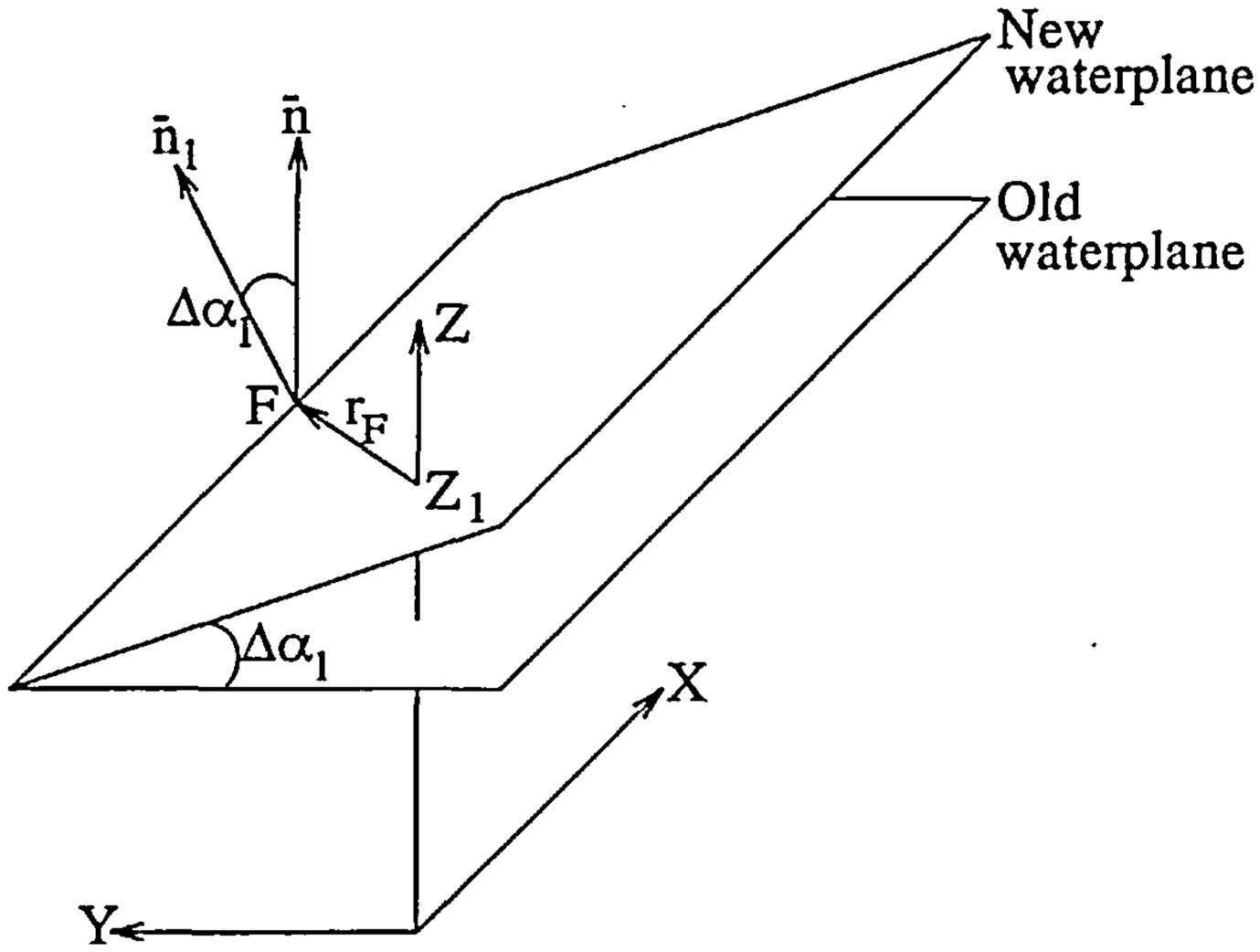

FIGURE 3.21. New draught T_1 of the new waterplane

The draught T_1 for the new waterplane is defined by its intersection with the Z-axis. If this point on the Z-axis is Z_1 (Figure 3.21) then the coordinates of OZ_1 are $(0, 0, T_1)$ where T_1 is the z intercept. The position vector of the centre of flotation F is (x_F, y_F, z_F) and is the centre of flotation for the original waterplane. Therefore,

$$r_F = \overline{OF} - \overline{OZ} = (x_F, y_F, z_F - T_1)$$

The value of T_1 can be found from,

$$\bar{n}_1 \cdot \bar{r}_F = 0 \qquad \text{(EQ 3.42)}$$

However the equation of the new waterplane can also be give by

$$\bar{n}_1 \cdot (\bar{r} - \bar{p}_F) = 0 \qquad \text{(EQ 3.43)}$$

where $\bar{r}$ is a position vector of any point lying on the new waterplane and $\bar{p}_F$ is the position vector of the point F. The advantage of (EQ 3.43) is that since it does not use the draught T, it can be applied to all cases including that when the angle of heel is 90°.

Having determined the new waterplane, a new centre of flotation F_1 and a new axis of flotation $\bar{f}_1$ can be determined for this waterplane using (EQ 3.39) and (EQ 3.40).

Although this new waterplane rotates about the previous axis of flotation, it is no longer an equivolume waterplane as, in general, the new axis of flotation is different from the old one. Therefore this new waterplane is called the auxiliary waterplane and may be used for finding the equivolume waterplane without iterations.

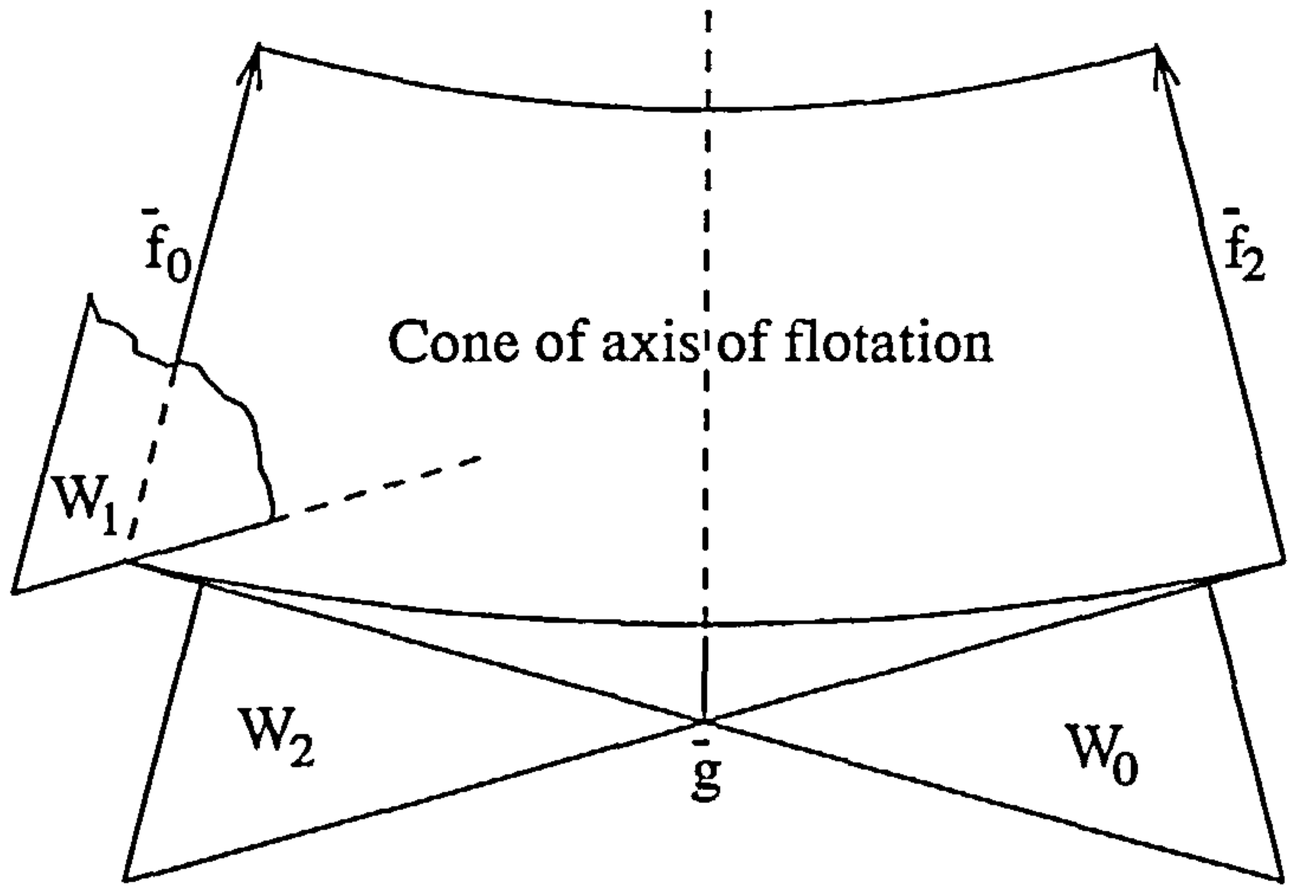

FIGURE 3.22. Cone of axis of flotation

From Figure 3.22, the following holds,

$W0$ - the previous equivolume waterplane

$W1$ - the auxiliary waterplane

$W2$ - the sought equivolume waterplane.

The procedure for finding $W2$ is based on the assumption that within a small interval of the angle of rotation, equivolume waterplanes roll over the side surface of a cone and the line of tangency between this cone and the waterplanes coincides with the instantaneous axis of flotation. In other words, the axes of flotation are generating lines of this cone (Figure 3.22).

Figure 3.23 shows the geometrical construction used for finding the equivolume waterplane $W2$ from $W0$. The waterplane $W0$ and $W2$ intersect each other along line $\bar{g}$ which is equidistant from the two axes of flotation $\bar{f}_0$ and $\bar{f}_2$. The line $\bar{g}$ is called the *axis of finite rotation.*

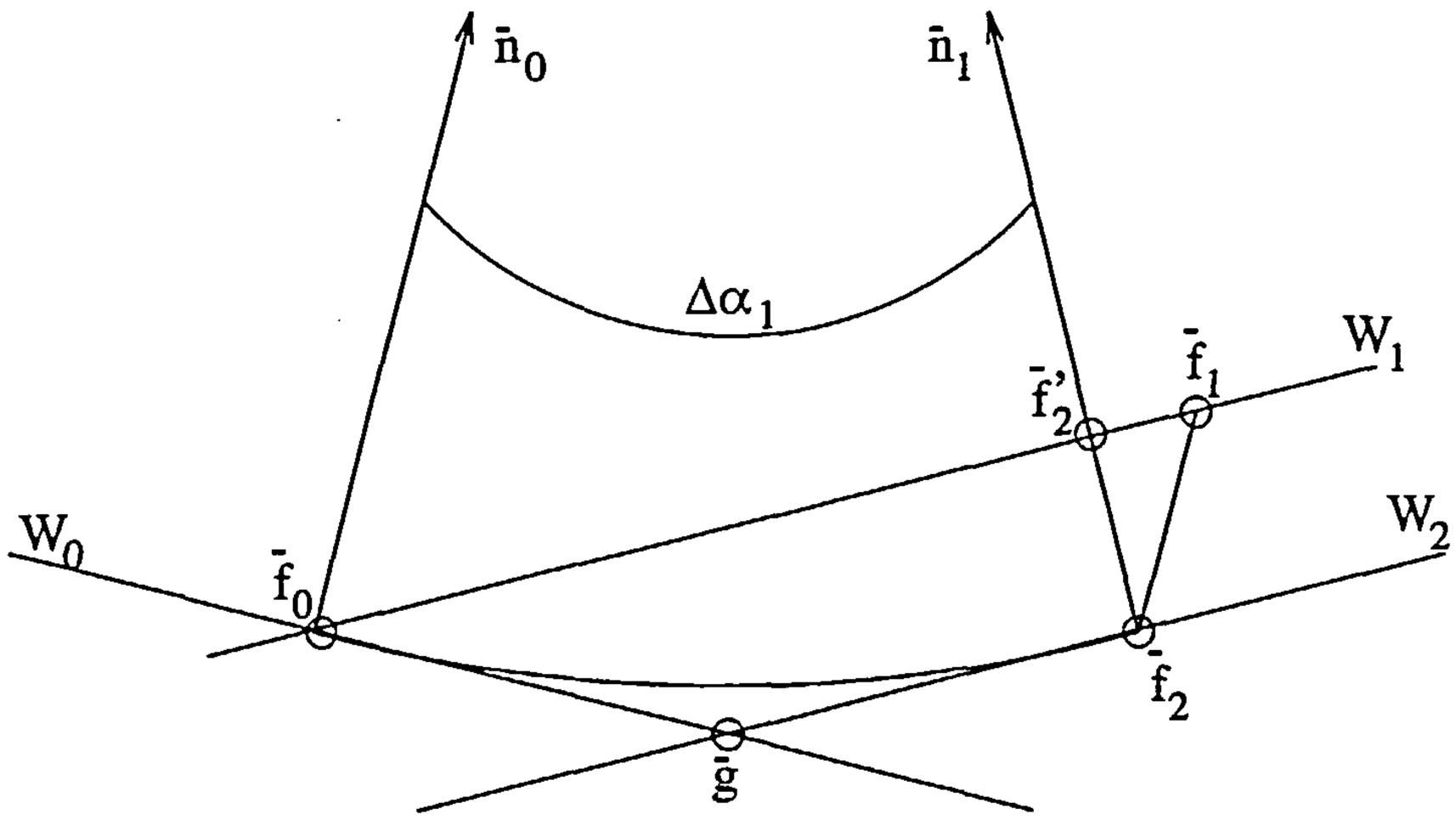

FIGURE 3.23. The mechanism of equivolume inclinations

3.7 Axis of finite rotations and equivolume waterplanes

The angle between $\bar{g}$ and the axis of flotation $\bar{f}_0$ is defined as ψ, the unit vector $\bar{g}$ can be obtained from the rotation of $\bar{f}_0$ by this angle on the waterplane $W0$,

$$\bar{g} = \bar{f}_0 \cos\psi + (\bar{f}_0 \times \bar{n}_0)\sin\psi \qquad \text{(EQ 3.44)}$$

Also since $\bar{f}_0$ and $\bar{f}_1$ both lie on the auxiliary waterplane $W1$, Figure 3.23,

$$\bar{f}_0 \times \bar{f}_1 = \bar{n}_1 \sin 2\psi \qquad \text{(EQ 3.45)}$$

The angle 2ψ can also be found directly from the formula

$$2\psi = (\chi_1 - \chi_0) - \sin\left(\frac{\chi_0 + \chi_1}{2}\right)\tan\left(\frac{\phi_1 + \phi_0}{2}\right)\Delta\alpha_1 \qquad \text{(EQ 3.46)}$$

This formula, however, becomes ill conditioned for angle of ϕ close to $90°$.

The next step is to determine the axis of finite rotation $\bar{g}$, from which the sought equivolume waterplane can be determined. The problem of finding $\bar{g}$ reduces to the problem of finding any point P on the waterplane $W0$, equidistant from $\bar{f}_0$ and $\bar{f}_1$ such that

$$|\bar{f}_0 \times \overline{F_0 P}| = |\bar{f}_1 \times \overline{F_1 P}| \qquad \text{(EQ 3.47)}$$

where,

$\overline{F_0}, \overline{F_1}$ - centre of flotations of waterplanes $W0$ and $W1$ respectively

P - a point on $W0$ at a distance d from $\bar{f}_0$ at the centre F_0 such that $P = F_0 + (\bar{n}_0 \times \bar{f}_0)d$

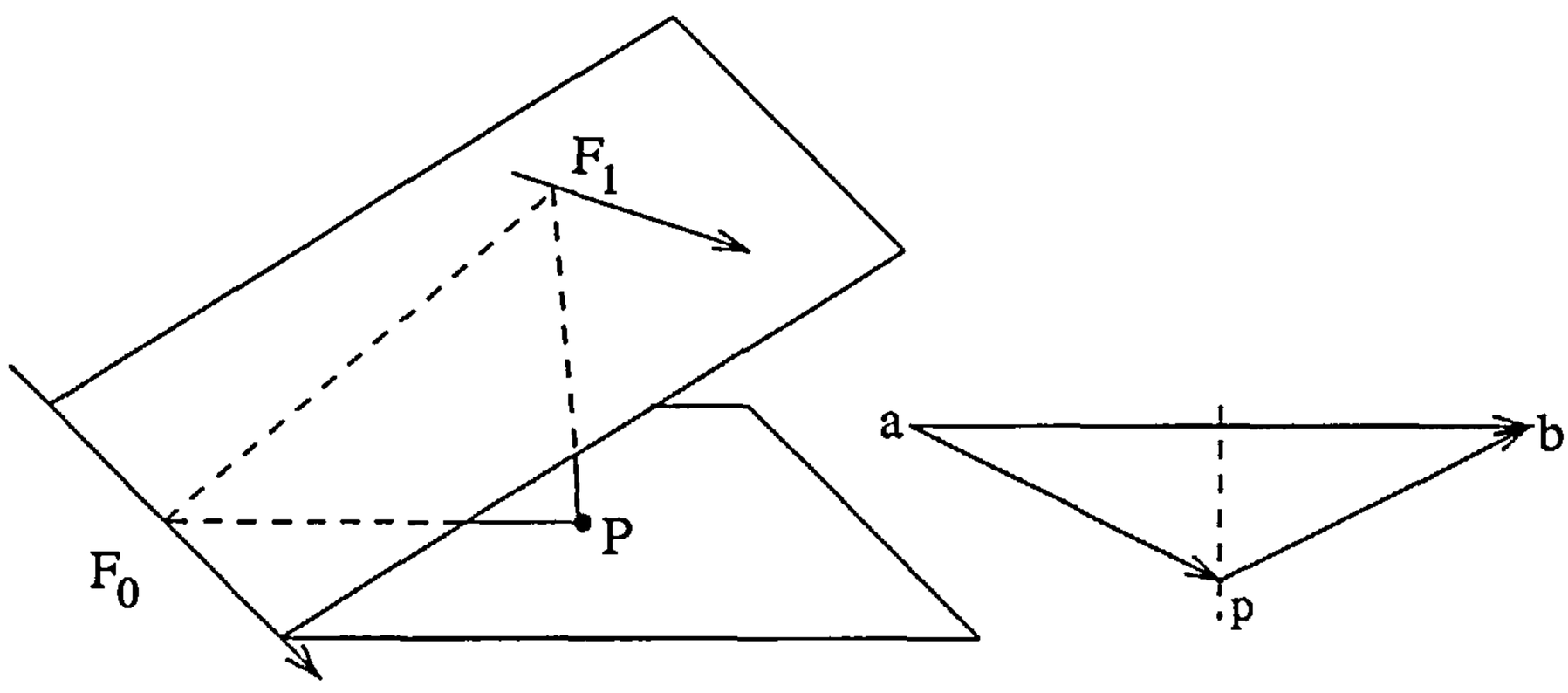

FIGURE 3.24. Postion of the axis of finite rotation $\bar{g}$

The problem of finding point P formulated as an optimisation problem can be stated as,

$$\text{minimize} \qquad \text{f: } (x_p - x_{f_0})^2 + (y_p - y_{f_0})^2 + (z_p - z_{f_0})^2 \qquad \text{(EQ 3.48)}$$

$$\text{subject to} \qquad g_1\text{: } \overline{ap} \cdot \overline{ab} = \overline{pb} \cdot \overline{ba} \qquad \text{(EQ 3.49)}$$

$$g_2\text{: } Ax_p + By_p + Cz_p = D \qquad \text{(EQ 3.50)}$$

where

$\overline{OP}(x_p, y_p, z_p)$ - the position vector of point P

$\bar{a}(x_{f_0}, y_{f_0}, z_{f_0})$ - the position vector of F_0

$\bar{b}(x_{f_1}, y_{f_1}, z_{f_1})$ - the postion vector of F_1

The objective function f, is to minimize the distance between P and F_0 subject to the constraint functions g_1 and g_2. Constraint g_1 states that the point P should be equidistant from F_0 and F_1. Constraint g_2 states that the point P must lie on waterplane $W0$, where $Ax + By + Cz = D$ is the equation of the waterplane $W0$.

Constraint g_1 in terms of the coordinate positions of $\bar{a}$, $\bar{b}$ and $\bar{P}$ is

$$2(x_{f_1} - x_{f_0}) + 2(y_{f_1} - y_{f_0}) + 2(z_{f_1} - z_{f_0}) + \{(x_{f_0}^2 + y_{f_0}^2 + z_{f_0}^2) - (x_{f_1}^2 + y_{f_1}^2 + z_{f_1}^2)\} = 0$$

Constraint g_2 from using (EQ 3.15) become,

$$(-\tan\theta)x_p + (-\tan\varphi)y_p + z_p - T = 0$$

A lagrange multiplier formulation for this problem would be of the form

$$L\{\bar{P}(x_p, y_p, z_p)\} = f + \lambda_1 g_1 + \lambda_2 g_2 \qquad \text{(EQ 3.51)}$$

Differentiating L with respect to x_p, y_p, z_p, λ_1 and λ_2, a system is obtained of the form,

$$[A][X] = [B]$$

where

$$[A] = \begin{bmatrix} 2 & 0 & 0 & 2(x_{f_1} - x_{f_0}) & -\tan\theta \\ 0 & 2 & 0 & 2(y_{f_1} - y_{f_0}) & -\tan\varphi \\ 0 & 0 & 2 & 2(z_{f_1} - z_{f_0}) & 1 \\ 2(x_{f_1} - x_{f_0}) & 2(y_{f_1} - y_{f_0}) & 2(z_{f_1} - z_{f_0}) & 0 & 0 \\ -\tan\theta & -\tan\varphi & 1 & 0 & 0 \end{bmatrix}$$

$$[X] = \begin{bmatrix} x_p \\ y_p \\ z_p \\ \lambda_1 \\ \lambda_2 \end{bmatrix}$$

$$[B] = \begin{bmatrix} 2x_{f_0} \\ 2y_{f_0} \\ 2z_{f_0} \\ (x_{f_0}^2 + y_{f_0}^2 + z_{f_0}^2) - (x_{f_1}^2 + y_{f_1}^2 + z_{f_1}^2) \\ T \end{bmatrix}$$

Since $[A]$ is a symmetric matrix, this linear system can be solved by using robust, standard numerical solvers. The solution gives the coordinates of point $\bar{P}(x_p, y_p, z_p)$ from which the axis of finite rotation $\bar{g}$ can be determined.

Having determined $\bar{g}$, the unit vector $\bar{n}_2$ of the sought equivolume waterplane can be found by rotating the normal $\bar{n}_0$ about the axis $\bar{g}$ by an angle $\Delta\alpha_1$, i.e. $\bar{n}$ and $\bar{f}$ in (EQ 3.41) is to be replaced by $\bar{n}_0$ and $\bar{g}$. Having obtained $\bar{n}_2$, (EQ 3.19) can be used again to obtain α, θ and φ. ϕ and β can be obtained from (EQ 3.21) and (EQ 3.22) respectively. The direction cosines of the new axis of rotation $\bar{e}_2$ can be determined from (EQ 3.25).

The whole procedure for determining the equivolume waterplanes can be set in the form similar to a flow chart as follows:

(A) For original waterplane W0, determine:
n_0 - normal to the waterplane
e_0 - the axis of rotation on the waterplane
a_0 - $n_0 \times e_0$

(B) Determine the following angle for W0:
α - angle between n_0 anf the Z-axis
β - the trim angle on the δ-plane
ϕ - the angle of roll

(C) Determine χ, the direction of instantaneous axis of flotation f_0 on W0, from (EQ 3.39)

(D) Determine $f_o \times n_0$

(E) Determine n_1 from (EQ 3.41) for an incremental angle of inclination $\delta\alpha$. Knowing n_1, the draught (or Z-intercept) for the new waterplane W1 can be determined using (EQ 3.42)

(F) Get the description of the new waterplane W1 using (EQ 3.43). Determine all the properties described in (A) and (B) for W1

(G) Find χ_1 for W1 using (EQ 3.39)

(H) Knowing χ_1, determine the instantaneous axis of flotation f_1 on W1

(I) Determine angle ψ using (EQ 3.45) or (EQ 3.46)

(J) Knowing ψ, determine the axis of finite rotation $\bar{g}$ using (EQ 3.44)

(K) Determine the point P which lies equi-distant from f_0 and f_1 on W0

(L) Determine the new normal n_2 and draught to the new waterplane W2 as in (E)

(M) As in (F), get the description of the new equivolume waterplane W2

(N) Set W0 = W2
Go to (A)
Repeat the procedure

3.8 The GZ-curve

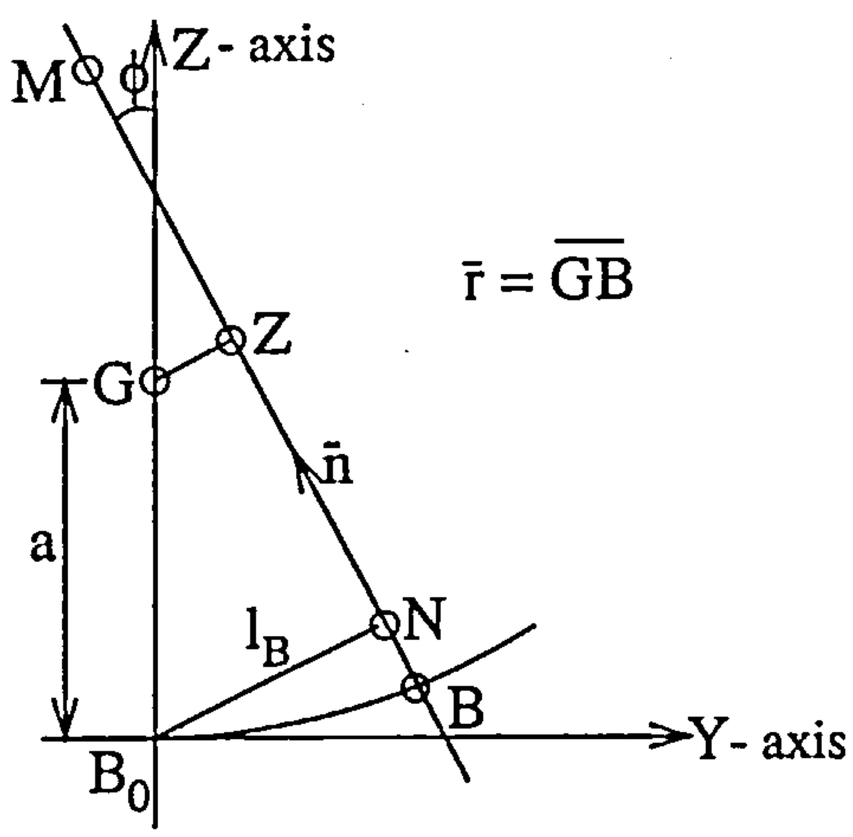

FIGURE 3.25. The righting arm lever

For a given inclination ϕ, (EQ 3.28) holds for the righting arm lever. From figure 3.25,

$$ZM = BM - BZ \qquad \text{(EQ 3.52)}$$

where BZ is the projection of the distance between the centre of gravity G and the centre of buoyancy B on the normal to the waterplane $\bar{n}$. BZ can therefore be expressed as

$$BZ = -\bar{r} \cdot \bar{n} \qquad \text{(EQ 3.53)}$$

The coordinates of the centre of buoyancy can be calculated without calculating the static moments of the immersed volume of the vessel provided its initial position is known.

A YZ coordinate system may be introduced, normal to the axis of rotation $\bar{e}$ with the Z-axis lying on the plane of symmetry. The Z-axis also passes through the centre of gravity G and the origin of this coordinate system is at a distance a below G (Figure 3.25). The coordinates of the centre of buoyancy for this system is:

$$Y = \int_0^{\phi} BM \cos\phi d\phi \qquad \text{(EQ 3.54)}$$

$$Z = \int_0^{\phi} BM \sin\phi d\phi \qquad \text{(EQ 3.55)}$$

GZ can now be expressed in terms of Y and Z as

$$GZ = Y\cos\phi + (Z - a)\sin\phi \qquad \text{(EQ 3.56)}$$

3.9 Validation

The software developed using the above theory (called *ImoPsngr*) was bechmarked with the help of another damage stability software developed by Wimalsiri [Wimalsiri'91] called *dammod2*. Wimalsiri benchmarked *dammod2* with a commercial damage stability package called *SIKOB* [SIKOB'87].

A box barge with the following particulars was used for this purpose:

Length = 156.7m

Beam = 24.6 m

Depth = 13.6 m

Draught = 6.74 m

KG = 8.03 m

Volume displacement = 25981.0 m^3

The configuration of the damage compartments is shown in figure 3.25.

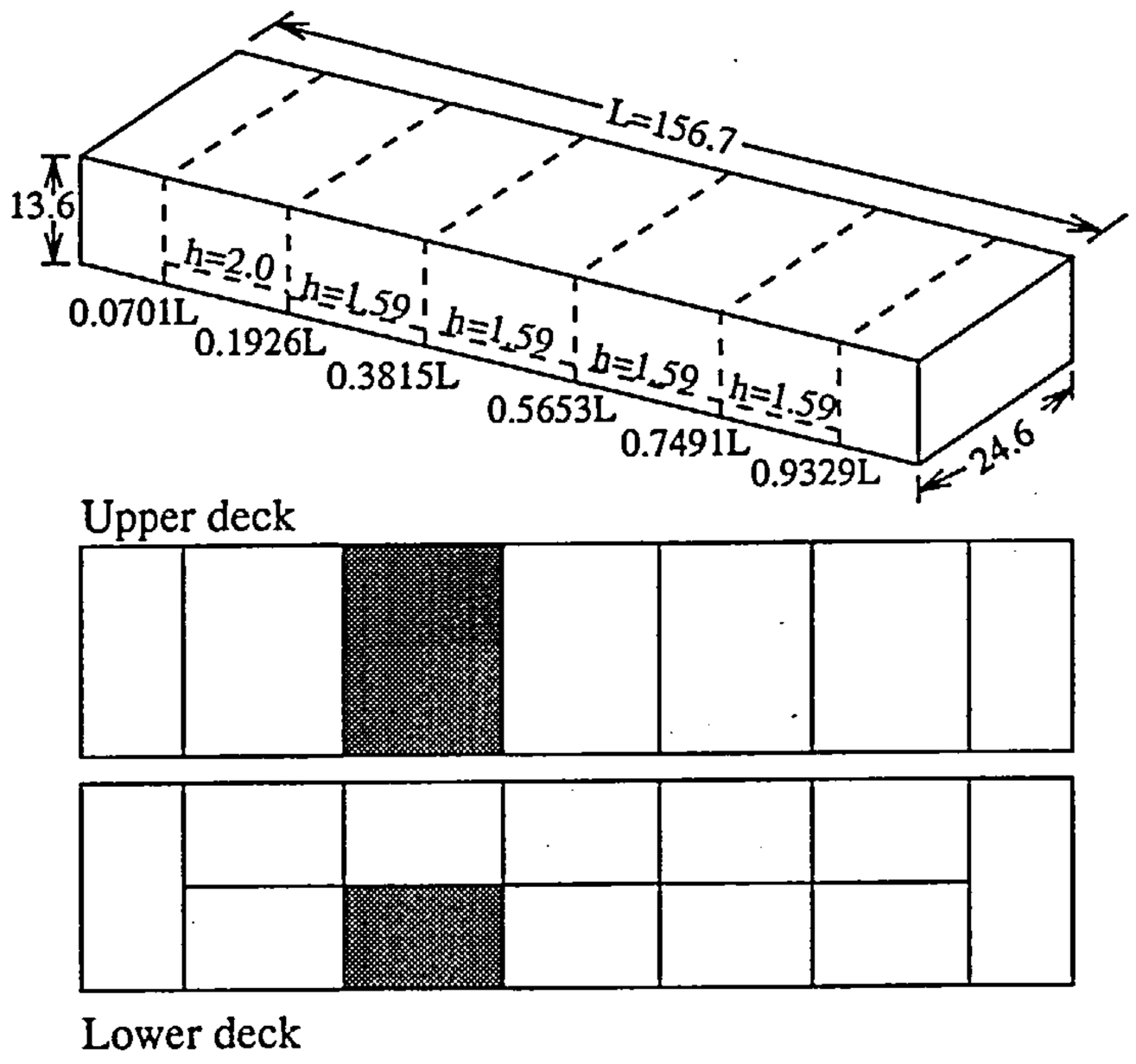

FIGURE 3.26. Damage combination (1)

The damage stability levers genetrated using *ImoPsngr* and *dammod2* are shown in figure 3.26. Table 3.1 gives the volume and trim angle during the inclination process for *dammod2* and *ImoPsngr*.

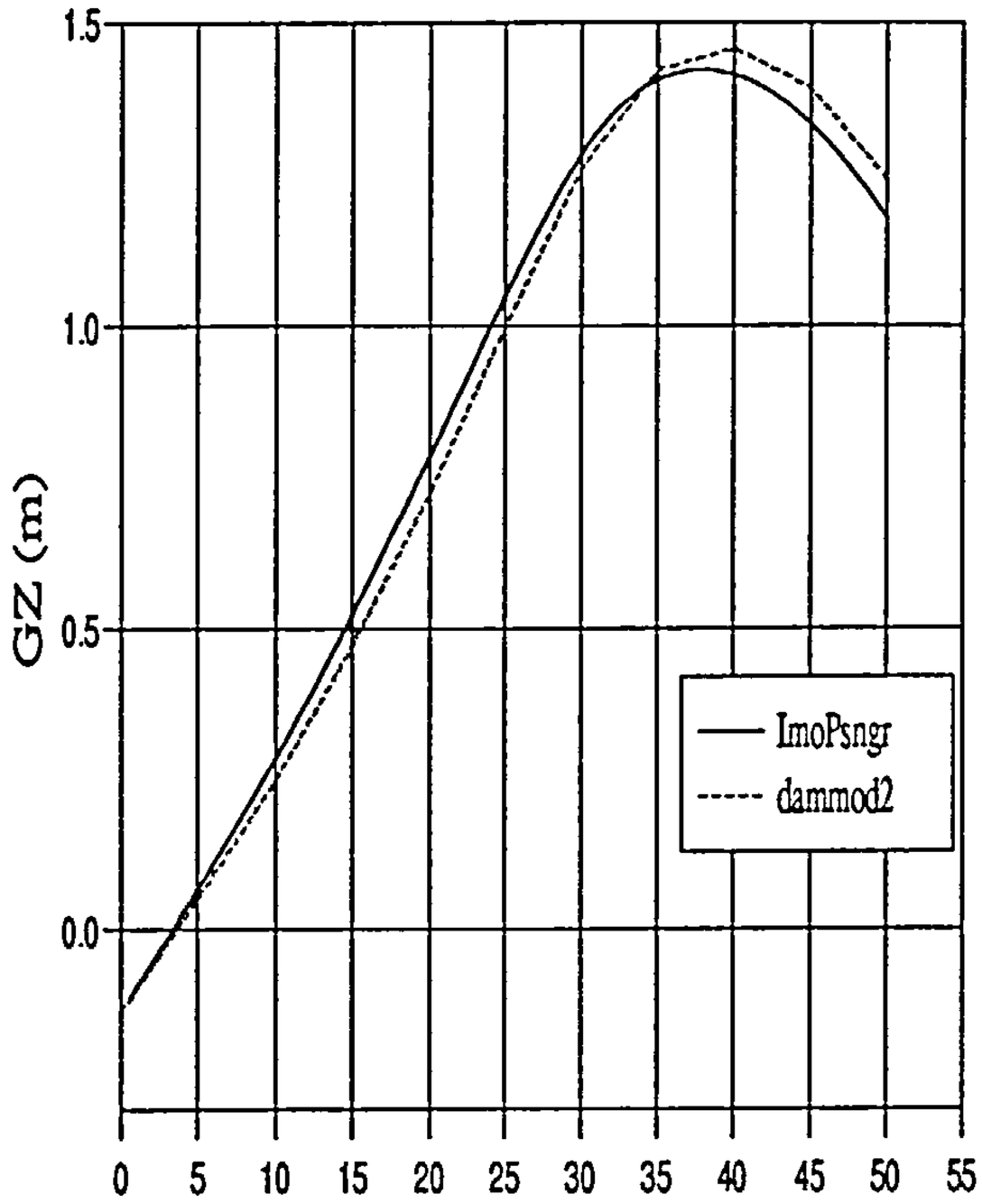

FIGURE 3.27. Damage levers for combination (1)

TABLE 3.1 Volume and trim history for damage combination (1)

heel (degrees)	dammod2		ImoPsngr	
	trim (degrees)	Volume (m^3)	trim (degrees)	Volume (m^3)
0.0	-1.444	25981.49	-1.515	25981.10
2.0	-1.444	25981.49	-1.515	25981.10
5.0	-1.444	25981.49	-1.515	25981.10
10.0	-1.442	25982.07	-1.514	25981.10
15.0	-1.442	25981.64	-1.514	25981.11
20.0	-1.450	25982.81	-1.536	25981.16
25.0	-1.505	25981.48	-1.623	25981.19
30.0	-1.631	25980.40	-1.783	25981.14
35.0	-1.851	25981.73	-2.022	25913.62
40.0	-2.169	25980.30	-2.361	25703.09
45.0	-2.596	25981.22	-2.811	25697.56

The second damage combination involved two transverse zones, as shown in figure 3.28, involving four compartments.

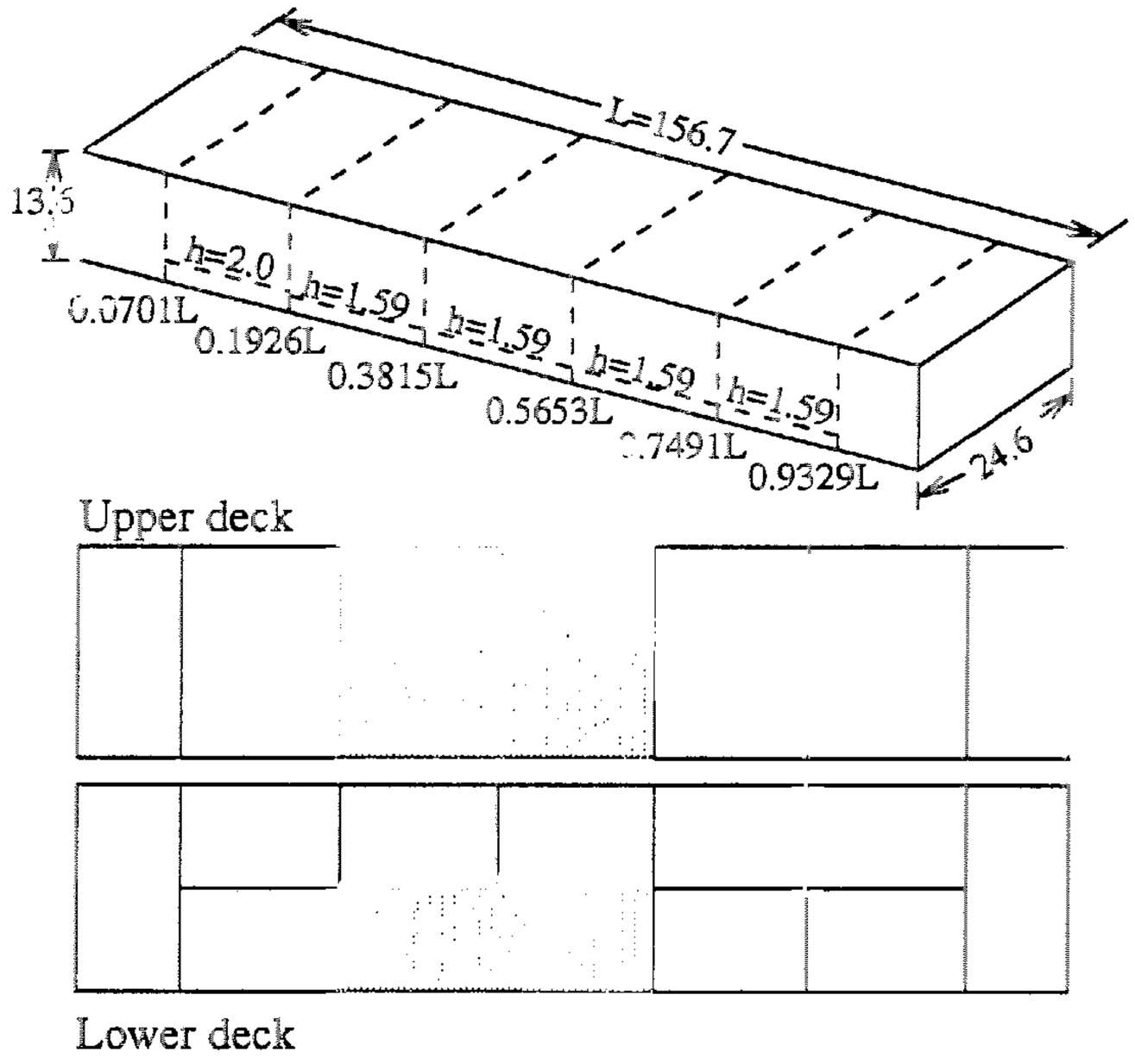

FIGURE 3.28. Damage combination (2)

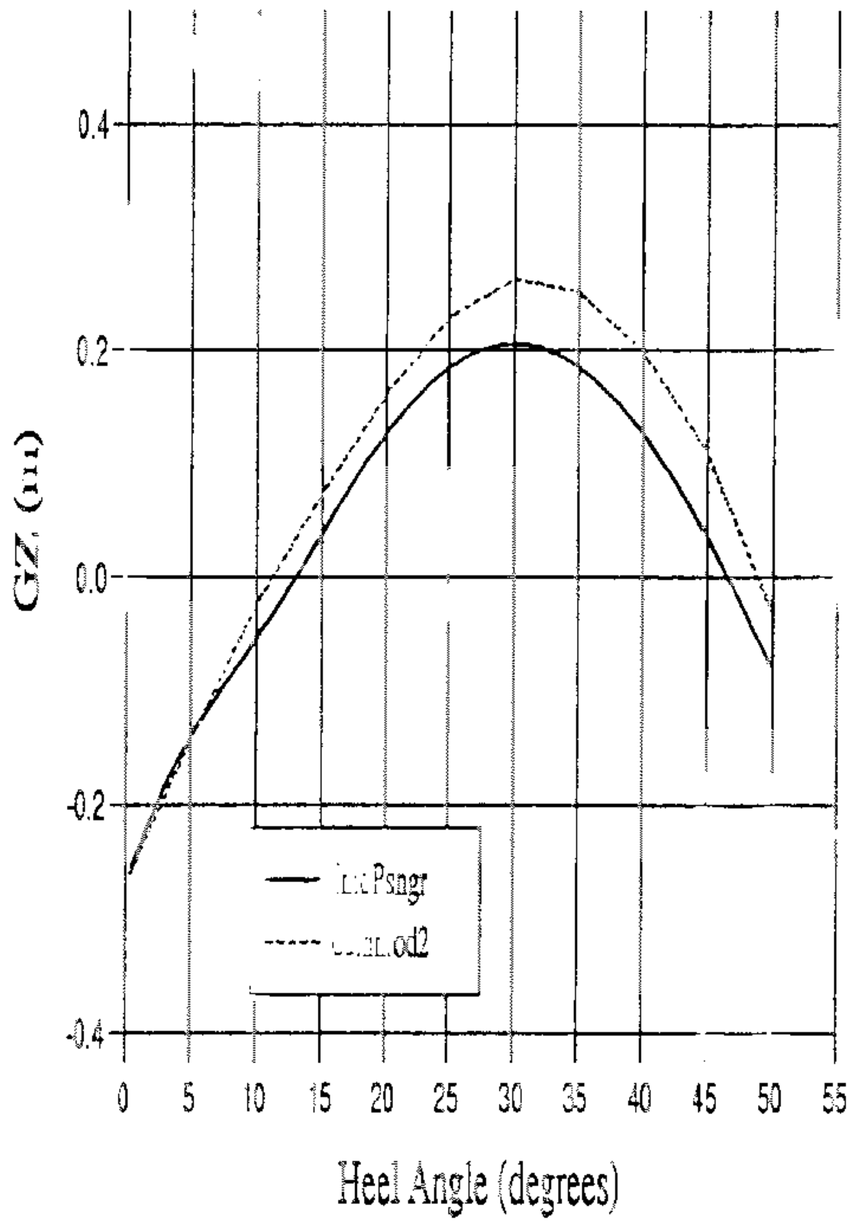

FIGURE 3.29. Damage levers for combination (2)

TABLE 3.2 Volume and trim history for damage combination (2)

heel (degrees)	dammod2		ImoPsngr	
	trim (degrees)	Volume (m^3)	trim (degrees)	Volume (m^3)
0.0	-2.166	25982.80	-2.257	25981.80
2.0	-2.192	25980.76	-2.274	25981.69
5.0	-2.237	25981.32	-2.353	25981.49
10.0	-2.347	25981.62	-2.589	25981.32
15.0	-2.547	25982.09	-2.879	25981.31
20.0	-2.810	25982.58	-3.218	25981.34
25.0	-3.121	25981.83	-3.609	25981.33
30.0	-3.464	25981.84	-4.027	25981.27
35.0	-3.833	25981.48	-4.479	25981.13
40.0	-4.249	25981.94	-5.000	25980.94

The damage stability levers genetrated for combination (2) using *ImoPsngr* and *dammod2* are shown in figure 3.29. Table 3.2 gives the volume and trim angles during the inclination process as estimated by *dammod2* and *ImoPsngr*. The results show a very good correlation between the two programs, particularly at smaller heel angles which are of great interest for the purpose of this study.

3.10 Conclusion

This method requires a clear visualisation of the behaviour of the vessel as it undergoes the process of inclination under conditions of free trim. The method clearly defines the angle of heel in terms of the planes in which they are measured which is vitally important in order to obtain a correct estimate of the GZ-curve.

Since the process is based on the properties of equivolume waterplanes, the process of inclination under free trim conditions is no longer an iterative process and the next equivolume waterplane is obtained in one single step. Also the method continuously maps the position of the centre of buoyancy as the vessel inclines thereby generating the GZ-curve without the need for any further iterative procedures.

Chapter 4

Genetic Algorithms

4.1 Introduction

> "Few technical terms have gained such rapid notoriety as the appellation 'NP-complete'. In the short time since its introduction in the early 1970's, this term has come to symbolize the abyss of inherent intractability that algorithm designers increasingly face as they seek to solve larger and more complex problems", [Garey'79].

Algorithm designers resort to the study of the frequency of execution of the statements in an algorithm in order to establish apriori the computing time required by that algorithm. If $T(n)$ is the time for an algorithm of n inputs, then $T(n) = O(f(n))$ defines the upper bound on the computation time for the algorithm. $f(n)$ is a function of n, the input to the algorithm.

Due to reasons not yet fully known, the best algorithms for most problems divide into two neat classes [Horowitcz'84]. The first group consists of problems whose solutions are bounded by a polynomial of small degree, e.g.: ordered searching $O(\log n)$, polynomial evaluation $O(n)$, sorting $O(n\log n)$ and matrix multiplication $O(n^{2.81})$

The second group consists of problems whose best known algorithms are nonpolynomial, e.g.: travelling salesman problem $O(n^2 2n)$ (TSP). The parameters of this problem consists of a finite set $C = \{c_1, c_2, \ldots c_m\}$ of "cities" and, for each pair of cities (c_i, c_j) in C, the distance $d(c_i,c_j)$ between them.

A solution is the ordering $(c_{\pi(1)}, c_{\pi(2)}, \ldots c_{\pi(m)})$ of the given cities that minimizes

$$\left\{\sum_{i=1}^{m-1} d(c_{\Pi(i)},c_{\Pi(i+1)})\right\} + d(c_{\Pi(m)},c_{\Pi(1)})$$

This expression gives the length of the "tour" that starts at $c_{\pi(1)}$, visits each city in sequence, and returns directly to $c_{\pi(1)}$ from the last city, $c_{\pi(m)}$. The computation time for an *exact* solution for this problem increases with N as $e^{(const \times N)}$, becoming rapidly prohibitive in cost as N increases. TSP belongs to a class of problem that are often referred to as NP-complete problems. The "N" stands for nondeterministic and the "P" stands for polynomial. A comprehensive mathematical definition of NP-completeness and NP-hardness can be found in textbooks dealing with algorithmics [Roberts'84], Harel'87],[Horowitz'84].

The algorithmic notion of efficiency, in the broadest terms, may be considered to involve all the various computing resources needed for executing an algorithm. However increasingly the use of the term "most efficient" has come to signify the term "fastest" since time seems to be the dominant factor determining whether an algorithm is efficient or not.

Discovering a problem to be NP-complete does provide some valuable information about what lines of approach have the potential of being the most productive. For instance the designer would accord looking for exact, efficient solutions a relatively low priority and concentrate more on a search for faster algorithms that would meet most of the problem specifications. In other words he would direct his search towards finding satisfactory solutions rather than optimal ones.

A class of heuristic search algorithms based on the principles of natural physical processes has evolved in the past three decades to tackle an interesting class of large

scale combinatorial optimization problems, many of which have been proved to be NP-hard. The development of these methods, being largely dependent on computers, have been spurred on by the emerging advancements in computer technology.

These methods, in the form of specialist manifestations like Simulated Annealing, Evolutionary Strategies, Genetic Algorithms, to mention a few, share the same underlying probabilistic search mechanism directed towards "satisficing" [Simon'69] the level of performance.

> "In the real world we usually do not have a choice between satisfactory and optimal solutions, for we only rarely have a method of finding the optimum" [Simon'69].

These methods have a high probability of locating the "most satisfactory" solution in a multimodal [multiple-peaked] search landscape.

The principle of natural evolution for parameter optimization used by Schwefel [Schwefel'81], Fogel's Evolutionary Programming [Fogel'66] for searching through a space of small finite-state machines, Glover's scatter search techniques [Glover'77], Holland's Genetic Algorithm [Holland'75], Koza's Genetic Programming methods [Koza'90] and simulated annealing methods based on principles of thermodynamics by Kirkpatrick, Gelatt and Vecchi [Kirkpatrick'83] are some of the often quoted and pioneering work in the field of heuristic computation.

Though these methods share the underlying principles of probabilistic search methodologies there are still some fundamental features that distinguish one method from another. Simulated Annealing, for instance, uses a cooling schedule akin to an actual annealing process to converge towards the optimum. Evolutionary strategies rely more on the mutation operator to direct its search towards a more productive landscape. Genetic Algorithms on the other hand rely more heavily on the crossover of helpful "genetic" information between parents to direct its search.

In general the task of optimization can be perceived as a search through a space of potential solutions. Problems involving small search spaces where the objective and constraint equations are defined by means of continuous or even piece-wise continuous functions have successfully used classical exhaustive or numerical search methods.

The emerging class of combinatorial problems (including NP-complete ones), be it in VLSI chip design or ship subdivision, due to the magnitude of the search spaces involved, render the application of traditional optimization techniques ineffective and inefficient. Coupled with this fact are additional problems of discontinuous or ill-defined functions and integer (or discrete) variables.

A significant body of literature is available as introductory material to the world of Genetic Algorithms [Goldberg'89], [Michalewicz'92], [Srinivas'94]. However a brief illustration of the workings of Genetic Algorithms is provided below before discussing the mathematical foundations on which they are based.

4.2 Genetic Algorithms [GA]: How do they work?

The example of a Simple Genetic Algorithm (SGA) [Goldberg'89] which optimizes a function $f(x) = x^2$ is used to demonstrate the workings of genetic algorithms. The problem is as follows:

$$Max \qquad f(x) = x^2 \qquad 0 \le x \le 31$$

Assuming that a acceptable values of x are to be generated using binary strings, a randomly generated population of strings (with a string size n=5) can be taken, as shown in Table 4.1, as

01101, 11000, 01000, 10011

TABLE 4.1: A simple genetic algorithm

column 1	column 2	column 3	column 4	column 5	column 6	column 7	column 8
initial pop	$f(x)$	$f/(\sum f)$	roulette count	interim pop	Xover sites	New pop	$f(x)$
01101	169	0.14	1	01101	0110 | 1	01100	144
11000	576	0.49	2	11000	1100 | 0	11001	625
01000	64	0.06	0	11000	11 | 000	11011	729
10011	361	0.31	1	10011	10 | 011	10000	256
	$\sum f$ = 1170						$\sum f$ = 1754

It is obvious that a 5-bit binary string can represent any number in the range 0 [00000] to 31 [11111]. Genetic algorithms use the concept of fitness to advance the search. Since

the aim here is to maximise $f(x)$ it would be sensible to take the value of x^2 for a given x to represent its fitness, so that strings representing bigger x values are perceived to represent fitter solutions. Using a binary coding/decoding method the absolute fitness $f(x)$ and percentage fitness $f/(\sum f)$ of each string is given in Table 4.1 in columns 2 & 3.

The reproduction process in a genetic population is easiest to create using a biased roulette wheel where the roulette wheel is divided into areas proportional to the fitness of each string (see Figure 4.1)

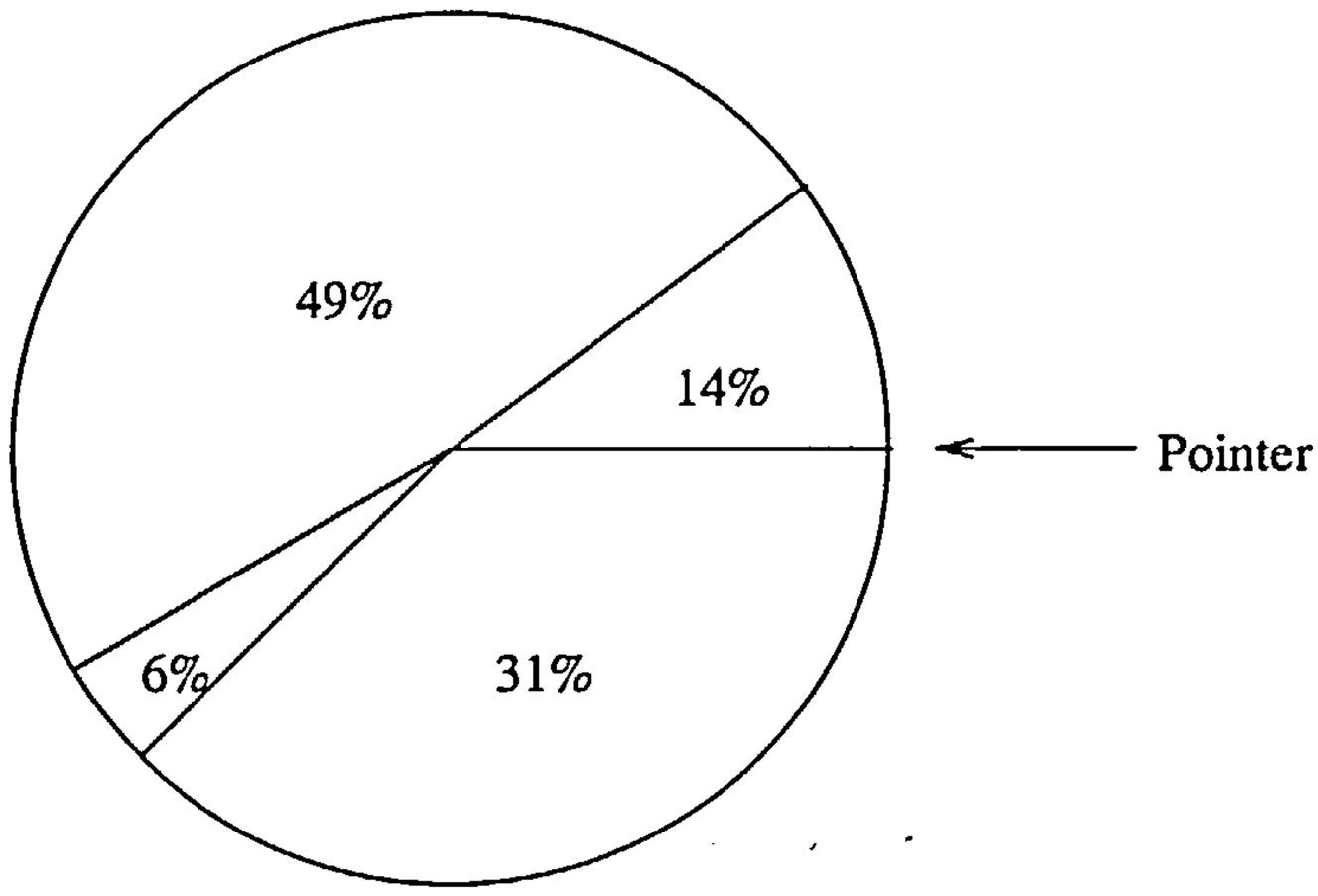

FIGURE 4.1. A biased roulette wheel

Now to produce a new population, the roulette wheel is spun and the resulting string pointed to by the pointer is selected as a member of the new population. In this case the roulette count is given in column 4 of Table 4.1 and the resulting intermediate population is given in column 5.

To apply the crossover operator, a pair of strings are selected from the intermediate population and a crossover site is selected for each of these pair at random (using a random number generator). The crossover sites for the strings in the intermediate population is given in column 6. A pictorial working of crossover is shown in Figure 4.2

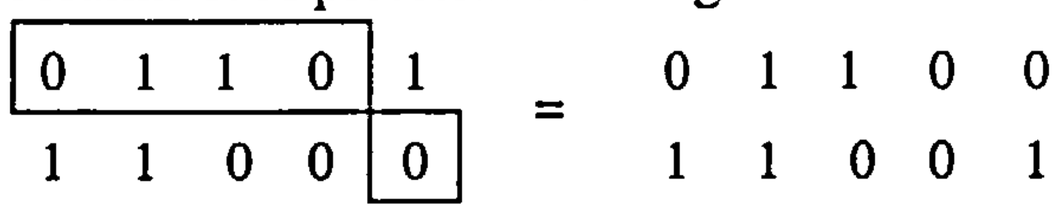

FIGURE 4.2. Schematic representation of crossover

Column 7 in Table 4.1 shows the new population attained after crossover. The fitness of the new population is given in column 8. The total fitness (and hence the average fitness) of the population has increased after one generation from 1170 to 1754. If this procedure is applied repeatedly to this population its average fitness can be expected to grow with each successive generation with the results converging to some maximum value for an individual string (close to 931 or 31^2 which is the maximum in this case).

Another operator (not described in the above demonstration) used in GA's is the mutation operator. Mutation is applied after crossover by which a binary flip occurs at certain bit positions within a a string with a certain probability (mutation probability). Mutation in GA's occupies a less important role when compared to crossover for exploiting the search space. This is to ensure that potentially valuable genetic material is not lost and as in most natural regenerative processes the mutation probability is necessarily low

4.3 GA: Why do they work?

The mathematical foundations for GA was laid by Holland [Holland'75] with the description of the Schemata. Here Holland used a to describe the set of possible structures that an adaptive system could attain. To quote Holland:

"The adaptive system must, as an integral part of its search of a, persistently test and incorporate structural properties associated with better performance".

Schemata was described using a tenary alphabet set {0,1,*} where the * denotes the *don't care* symbol. Essentially schemata can be thought of as a pattern matching device. In a genetic population highly fit individuals having certain important similarities could give the search more fruitful directions and schemata or similarity templates [Goldberg'89] help highlight these characteristics.

4.3.1 The order of schema

The *order* of a schema, denoted by $o(S)$, is the number of *fixed* positions present in the schema. In other words, order can be defined as the length of the template minus the number of *don't care (*)* symbols.

For example, the following schema, all of length 7,

$S_1 = (1 * 1\ 0\ 1 * *)$

$S_2 = (* * 1 * 0\ 0 *)$

$S_3 = (1\ 1\ 0 * 1 * 0)$

have the following orders:

$o(S_1) = 4$

$o(S_2) = 3$

$o(S_3) = 5$

The order of a schema is useful in estimating the survival probability when applying the crossover operator.

4.3.2 The defining length of a schema

The *defining length* of a schema is the distance between the first and the last fixed string positions and is denoted as $\delta(S)$. Defining length is a measure of the compactness of a schemata, that is, the smaller the defining length the more compact it is. For example, the defining length of the schema defined above are,

$\delta(S_1) = 5 - 1 = 4$

$\delta(S_2) = 6 - 3 = 3$

$\delta(S_3) = 7 - 1 = 6$

4.3.3 Schema theorem and the building block hypothesis

Consider a genetic population of size, N. Let each string in the population be denoted as $v_i \ \ (i = 1, \ldots N)$ .We define the following:

$\xi(S, t)$ - the expected number of strings in a population at time t, matched by schema S.

$eval(S, t)$ - the average fitness at time t of the schema S. Assuming p strings in the population $\{v_{i_1}, v_{i_2}, \ldots, v_{i_p}\}$ match schema S at time t

$$eval(S, t) = \frac{\sum_{j=1}^{p} eval(v_{i_j})}{p}$$

where

$eval(v_{i_j})$ is the fitness evaluated for string v_{i_j}.

As seen in section 4.2, the probability p_i of a string v_i being selected during the selection process is given by,

$$p_i = \frac{eval(v_{i_j})}{F(t)}$$

where $F(t) = \sum_{i=1}^{N} eval(v_i)$ is the total fitness of the population at time t.

The expected number of schema S in the population at time t+1, $\xi(S, t+1)$ therefore depends upon:

1. the probability of selecting schema $S = \frac{eval(S, t)}{F(t)}$
2. the number of strings in the population at time t that matches schema S, $\xi(S, t)$
3. the total number of selections made, N.

Therefore

$$\xi(S, t+1) = \xi(S, t)\frac{eval(S, t)}{(F(t))/N} \quad \text{or,}$$

$$\xi(S, t+1) = \xi(S, t)\frac{eval(S, t)}{F(t)}N$$

$$\xi(S, t+1) = \xi(S, t)\frac{eval(S, t)}{\bar{F}(t)} \qquad \text{(EQ 4.1)}$$

where $\bar{F}(t)$ is the average fitness of the population.

The implications of (EQ 4.1) is clear. An "above average" schema receives increasing number of strings in the next generation, a "below average" schema receives decreasing numbers of strings, and an average schema stays at about the same level from generation to generation. If the schema S is above average by $\varepsilon\%$ then,

$$\xi(S, t) = \bar{F}(t) + \varepsilon\bar{F}(t)$$

and (EQ 4.1) can be rewritten as,

$$\xi(S, t) = \xi(S, 0)(1+\varepsilon)^t \qquad \text{(EQ 4.2)}$$

(ε is < 0 for below average schemata).

Since (EQ 4.2) defines a geometric progression it can now be said that *above average schemata receive exponentially increasing numbers of strings in the next generation.* (EQ 4.1) is sometimes known as the reproductive schema growth equation [Michalewicz'92].

The selection procedure on its own does not introduce any new points into the search space since the selection procedure just copies the selected strings from the previous generation into an intermediate population pool. It is only by applying recombination operators that new points appear in the gene pool. Two genetic operators perform this function - crossover and mutation.

Its is obvious that the defining length of a schemata S, $\delta(S)$ (section 4.3.2) plays an important role in the probability of destruction or survival of S. If $p_d(S)$ is defined as,

$$p_d(S) = \frac{\delta(S)}{m-1} \qquad \text{(EQ 4.3)}$$

then (EQ 4.3) states that the probability of destruction of a schemata of length m. For a schema of length m, there are m-1 crossover sites to choose from.

For a schema $S_1 = (* * * 1 * * *)$ with defining length $\delta(S_1) = 0$, the probability of crossover destroying S_1 is zero. Similarly for $S_2 = (0\ 1\ 1\ 0\ 0\ 0\ 1)$, the probability of S_2 being destroyed is 1. Now if p_c is the probability with which crossover is applied to any schema S then the probability of destroying S due to crossover is,

$$\{p_d(S)\}_x = p_c \frac{\delta(S)}{m-1}$$

The probability of survival of schema S,

$$\{p_s(S)\}_x = 1 - \{p_d(S)\}$$

$$\{p_s(S)\}_x = 1 - p_c \frac{\delta(S)}{m-1} \qquad \text{(EQ 4.4)}$$

(EQ 4.4) defines the lower limit on the probability of survival of S. This is because a schema could survive crossover even if the crossover site is between fixed positions. Consider two schema

$S_1 = (1\ 1\ *\ *\ |\ *\ *\ 0)$
$S_2 = (1\ 1\ *\ *\ |\ *\ *\ 0)$

with the crossover site as shown. The crossover operation does not destroy the schema in this instance since the two schema are identical. This probability, however small, is still finite. Hence (EQ 4.4) should really be written as

$$\{p_s(S)\}_x \geq 1 - p_c \frac{\delta(S)}{m-1} \qquad \text{(EQ 4.5)}$$

Combining (EQ 4.1) & (EQ 4.5), the expected numbers of schema S in the next generation is

$$\xi(S, t+1) \geq \xi(S, t) \frac{eval(S, t)}{\bar{F}(t)} \left[1 - p_c \frac{\delta(S)}{m-1}\right] \qquad \text{(EQ 4.6)}$$

The last operation to be considered is mutation. Let p_m be the probability of mutation.

The probability of mutation destroying schema S is,

$$\{p_d(S)\}_m = (p_m)^{o(S)}$$

This can be explained as follows. If S_1=(* * 1 0 1 *) then schema S_1 would be destroyed if the mutation operation alters either of the fixed position in S_1, i.e., the 1 0 1 bit of the string. The probability of destruction is therefore

$$\{p_d(S_1)\}_m = p_m \times p_m \times p_m$$

$$\{p_d(S_1)\}_m = (p_m)^3$$

Now the order of the schema S_1, $o(S_1)$ (see 4.2.1 for definition), is given as the number of fixed positions in S_1, i.e. $o(S_1) = 3$. Hence

$$\{p_d(S_1)\}_m = (p_m)^{o(S_1)}$$

Applying binomial expansion to the above expression and neglecting higher order terms since $p_m \ll 1$,

$$\{p_d(S)\}_m \approx o(S) \cdot p_m$$

Therefore the probability of survival of schema S,

$$\{p_s(S)\}_m \approx 1 - o(S) \cdot p_m \qquad \text{(EQ 4.7)}$$

The total probability after crossover and mutation, combining (EQ 4.4) & (EQ 4.7) is

$$p_s(S) = 1 - p_c \frac{\delta(s)}{m-1} - o(S) \times p_m \qquad \text{(EQ 4.8)}$$

Combining (EQ 4.1) & (EQ 4.8)

$$\xi(S, t+1) \geq \xi(S, t) \frac{eval(S, t)}{\bar{F}(t)} \left[1 - p_c \frac{\delta(s)}{m-1} - o(S) \times p_m\right] \qquad \text{(EQ 4.9)}$$

This is the final form of the growth equation and is known as the schema theorem.

Schema theorem: *Short, low-order, above-average schemata receive exponentially*

increasing trials in subsequent generations of a genetic algorithm.

One of the immediate consequences of the schemata theorem which always favours the short, low-order schemata is called the *Building Block Hypothesis*

Building Block Hypothesis: *A genetic algorithm seeks near-optimal performance through the juxtaposition of short, low-order, high performance schemata, called building blocks.*

4.4 Genetic Operators

Figure 4.3 summarizes the working of a Simple Genetic Algorithm (SGA).

The inner 'while' loop consists of the genetic operators selection, crossover and mutation which determine the extent of the search space Evaluation calculates fitness performance and consequently the convergence criteria.

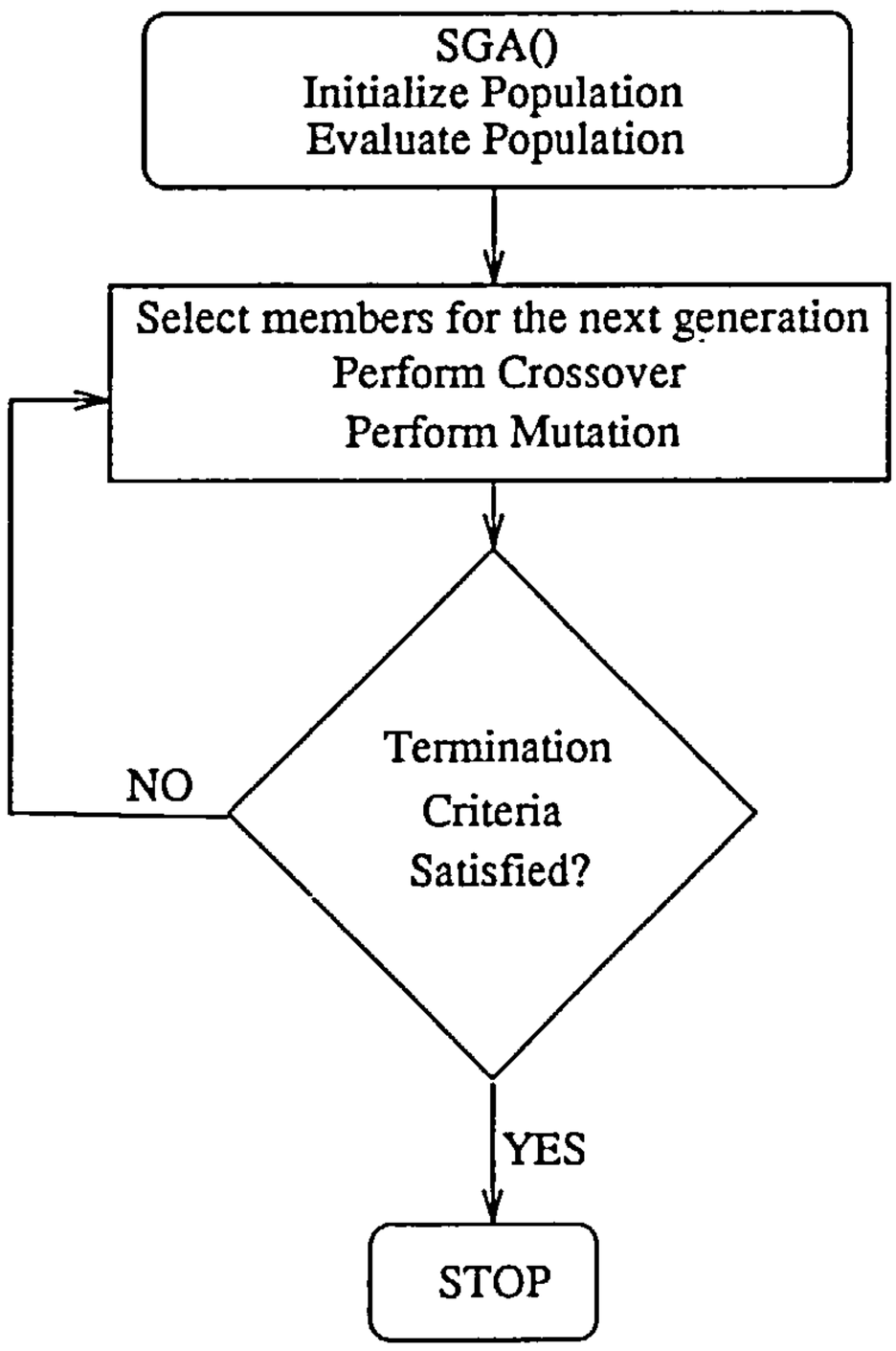

FIGURE 4.3. A Simple Genetic Algorithm

The outer loop monitors the progression from one generation to another.

4.4.1 Selection

Selection is a procedure by which fitter members of the current generation are copied on to the next generation for propagation. It in effect mimics the Darwinian survival-of-the-fittest paradigm. Some of the earliest work done by DeJong {DeJong'75] consisted of four sampling mechanisms.

- *elitist model* - The *elitist model* preserves the best chromosome
- *expected value mode*l - It reduces the stochastic errors of the selection routine. A count c is introduced for each chromosome where $c = f(c)$. Each time a chromosome is selected its value is reduced by 0.5 or 1. When $c < 0.0$, the chromosome is no longer available for selection.
- *elitist expected value model* - a variation that combines the first two.
- *crowding factor model* - In the CF model, when one individual was born, another dies, where the dying individual is selected from a subset of CF members chosen from the full population at random. The dying individual is chosen such that it most closely resembles the new offspring using a simple bit-by-bit similarity count.

Brindle [Brindle'81] introduced a few more schemes

- *deterministic sampling*
- *remainder stochastic sampling without replacement*
- *stochastic tournament*
- *remainder stochastic sampling with replacement*

Baker [Baker'87] studied these selection schemes and compared them on the basis of three measure: bias, spread and efficiency. Baker then introduced a new scheme called *stochastic universal sampling* (SUS) which is shown to have zero bias and a minimum spread. On a standard roulette wheel (see Figure 4.1), proportional selection uses a single pointer which indicates the "winner". SUS is analogous to a spinning wheel with N equally spaced pointers. Hence a single spin results in N "winners".

4.4.2 Crossover

Crossover is the most important operator in GA's. Some of the crossover variations are:

- *One-point crossover* - Single point crossover involves the random selection of one crossover point in each string. The strings to the right of the crossover point are swapped.
- *Two-point crossover* - here two points are randomly chosen and segments of strings between them are swapped. Two point crossover eliminates the bias towards bits at the ends of strings.
- *Uniform crossover* - Bits of a strings rather than segments are exchanged in this method. At each string position, the bits are probabilistically exchanged with some fixed probability. The exchange of bits at one string position is independent of the exchange at other positions.

4.4.3 Mutation

In mutation any one bit of a string gets flipped, so that mutation changes a 0 to a 1 or a 1 to a 0. In Simple Genetic Algorithms bits of strings are independently mutated, that is, mutation of one bit does not affect the probability of mutation of other bits. Mutation, in GA's, plays the secondary role of restoring lost genetic material. As an extreme example, if all the strings in a given population have converged to a 0 at a particular position and say if the optimal at that position was a 1. In such cases, crossover could not generate a 1 at that position as readily as mutation could.

Usually genetic algorithms are considered to have two phases, the exploratory phase and the exploitation phase. The exploratory phase usually occurs during earlier generations where search spaces need to be wide and possibilities of premature convergence are few. Exploitation is a phenomena for latter generations when regions of relative efficiency have been identified and convergence rates need to be higher. Higher mutation probabilities lead to greater variation in the gene pool resulting in a wider search space. Adaptive mutation schemes [Schwefel'88], [Baeck'91] have been proposed that make use of such schemes.

4.5 Incorporating constraints in GA

It should be apparent from the description of the workings of a GA that they could be adopted readily to unconstrained minimisation (or maximisation problems as any maximisation problem can be converted to a minimisation problem). For an

unconstrained problem, fitness function evaluation involves evaluating the objective function at a particular state in the search space.

Though incorporating constraints is a convoluted process in GA's, many schemes have been proposed. One approach concentrates on the use of special representation mappings (decoders) which guarantee (or at least increase the probability of) the generation of a feasible solution and these apply special repair algorithms to "correct" any infeasible solutions so generated. However some of the drawbacks of this approach lie in the fact that decoders are frequently computationally intensive to run [Davis'87a] and that not all constraints can be easily implemented in this way.

Michalewicz [Michalewicz'92] introduced a method for handling linearly constrained problems called GEnetic algorithm for Numerical Optimization for COnstrained Problems [GENOCOP]. Equality constraints (if any) are first eliminated, the number of variables is reduced by expressing all equations in terms of independent variables and inequalities are modified appropriately. Since the resultant set consists only of linear inequality constraints, the search space is convex and with properly designed "closed operators" this search space can be searched efficiently. However the drawbacks of GENOCOP are that it cannot handle non-linear constraints.

4.5.1 Unconstrained minimization

Classical optimization methods divide constrained optimization techniques into direct search methods and indirect methods [Rao'78]. Two methods that fall under the heading of indirect methods - the *Augmented Lagrangian method* and *Exterior Penalty functions methods* are of particular interest in the context of GA's.

Augmented Lagrangian The augmented lagrangian method [Minoux'86] combines the two concepts of penalty (from the penalty function methods) and duality (from the Lagrangian method). This method was originally proposed by Hestenes [Hestenes'69] and Powell [Powell'69] for equality constraints. The generalisation of the Hestenes & Powell function to inequality constraints was carried out by Rockafeller [Rockafeller'73]. For a general minimization problem:

$Minimize \qquad f(x)$

subject to $g_i(x) \leq 0 \qquad i = 1, \ldots m\ ,\ x \in R^n$

The Hestenes & Powell formulation of the augmented lagrangian for equality constraints was

$$\underset{x}{Min}\ L(x, \lambda, r) = f(x) + \sum_{i=1}^{m} \lambda_i g_i(x) + r \sum_{i=1}^{m} [g_i(x)]^2$$

where λ is unrestricted in sign and r is the penalty term such that $r > 0$.

To extend the formulation to inequality constraints Rockafeller introduced slack variables $s_i \geq 0$ and the problem was described as,

$Minimize \qquad f(x)$

subject to

$g_i(x) + s_i = 0 \qquad i = 1, \ldots m\ ,\ x \in R^n$

$s_i \geq 0\ ,$

The problem at each stage is then reduced to,

$$\underset{x \in R^n}{Min} \qquad L(x, \lambda, r) = f(x) + \sum_{i=1}^{m} \lambda_i [g_i(x) + s_i] + r \sum_{i=1}^{m} [g_i(x) + s_i]^2 \qquad \text{(EQ 4.10)}$$

where λ is unrestricted in sign.

Given, x, the minimization for $s_i \geq 0$ can be carried out for each s_i independently. Assembling all the terms containing s_i

$$r \cdot s_i^2 + (2 \cdot r \cdot g_i(x) + \lambda_i) s_i \qquad \text{(EQ 4.11)}$$

Assuming $r > 0$, the minimum for $s_i \geq 0$ is obtained by differentiating (EQ 4.11) w.r.t s_i

$$2rs_i + 2rg_i(x) + \lambda_i = 0$$

therefore

$$s_i = -g_i(x) - \frac{\lambda_i}{2r}$$

and therefore the minimum for $s_i \geq 0$ is obtained either for

a. $s_i = -g_i(x) - \frac{\lambda}{2r}$, if $g_i(x) \leq \frac{-\lambda_i}{2r}$ or for

b. $s_i = 0$ if $g_i(x) > \frac{-\lambda_i}{2 \cdot r}$. In this case the slack variables are set to zero.

In case(a), $g_i(x) \leq \frac{-\lambda_i}{2 \cdot r}$ implies that the slack variables s_i are always greater than or equal to zero (≥ 0), thus keeping the solutions to the feasible region. Substituting the values of s_i into the augmented lagrange formulation, (EQ 4.10),

$$\underset{x \in R^n}{Min} \quad L(x, \lambda, r) = f(x) + \sum_{i=1}^{m} \lambda_i \left[-\frac{\lambda_i}{2r}\right] + r \sum_{i=1}^{m} \left[\frac{\lambda_i}{2r}\right]^2$$

which can be written as $\underset{x \in R^n}{Min} \quad L(x, \lambda, r) = f(x) + \sum_{i=1}^{m} \left(\frac{-\lambda_i^2}{4r}\right)$

For case(b), when $g_i(x) > \frac{-\lambda_i}{2 \cdot r}$, the solution goes into the infeasible region (s_i are set to zero). In these situations the penalty function term starts to penalize the solution. Substituting the values of $s_i = 0$ into (EQ 4.10), the augmented formulation reduces

to, $\underset{x \in R^n}{Min} \quad L(x, \lambda, r) = f(x) + \sum_{i=1}^{m} \lambda_i [g_i(x)] + r \sum_{i=1}^{m} [g_i(x)]^2$

Hence the problem reduces to minimizing for x at each stage the function

$$\underset{x \in R^n}{Min} \qquad L(x, \lambda, r) = f(x) + \sum_{i=1}^{m} G(g_i(x), \lambda, r)$$

where

$$G(g_i(x), \lambda, r) = \begin{cases} \dfrac{(-\lambda_i)^2}{4 \cdot r} & r > 0,\ g_i(x) \le \dfrac{-\lambda_i}{2 \cdot r} \\ \lambda_i g_i(x) + r[g_i(x)]^2 & r > 0,\ g_i(x) \ge \dfrac{-\lambda_i}{2 \cdot r} \end{cases}$$

This is the augmented lagrangian formulation derived by Rockafellar [Rockafellar'73]. The steps involved in an augmented lagrangian are as shown in Figure 4.4

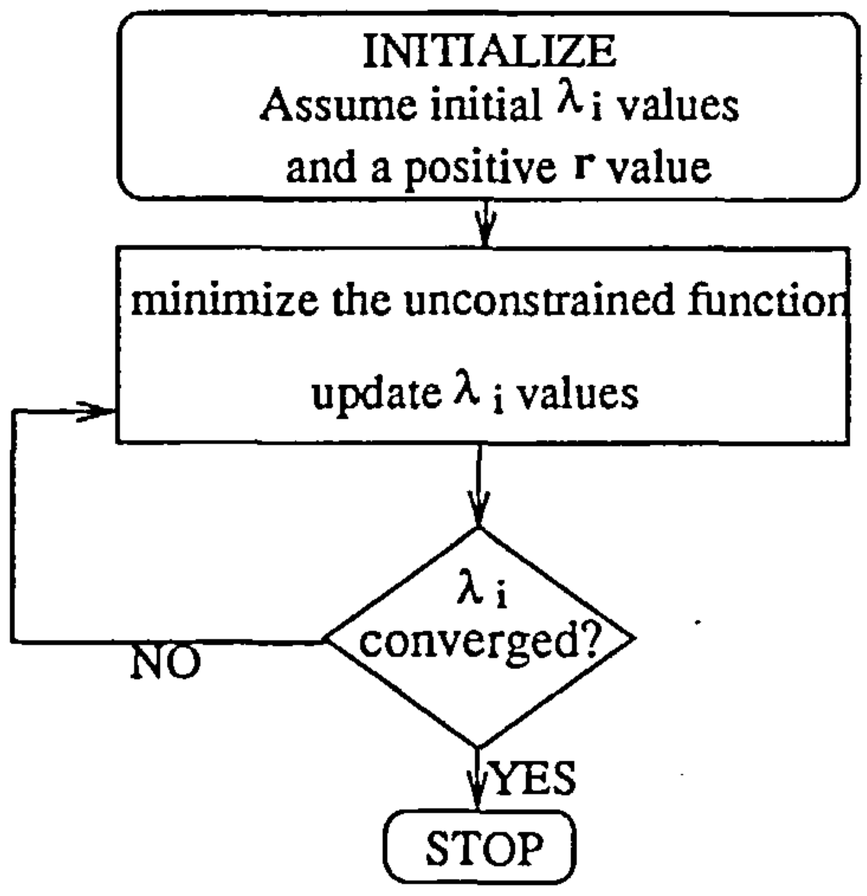

FIGURE 4.4. The augmented lagrangian method

Hestene suggested the following algorithm for updating the λ_i values

- for a given λ, find $\hat{x}(\lambda, r)$, the minimum in x of $\hat{L}(x, \lambda, r)$
- replace the vector λ by $\lambda' = \lambda + 2 \cdot r \cdot g[\hat{x}(\lambda, r)]$

Since $g_i(x) \le 0 \qquad i = 1, \ldots m$, the updating scheme progressively reduce the values of the λ_i's. As seen from case(a), $g_i(x) \le \dfrac{-\lambda_i}{2r}$ implies that the solution remains in the feasible region, the updating scheme ensure that this condition can be met more readily.

Augmented lagrangians overcome the drawback of function ill-conditioning that is seen to occur in penalty function formulations especially at high penalty values. The augmented lagrangian was tested using genetic algorithms for the following problems [Rao'78].

1. *Minimize* $f(x_1, x_2) = \frac{1}{3}(x+1)^3 + x_2$

subject to

$$g_1(x_1, x_2) = -x_1 + 1 \le 0$$
$$g_2(x_2) = -x_2 \le 0$$

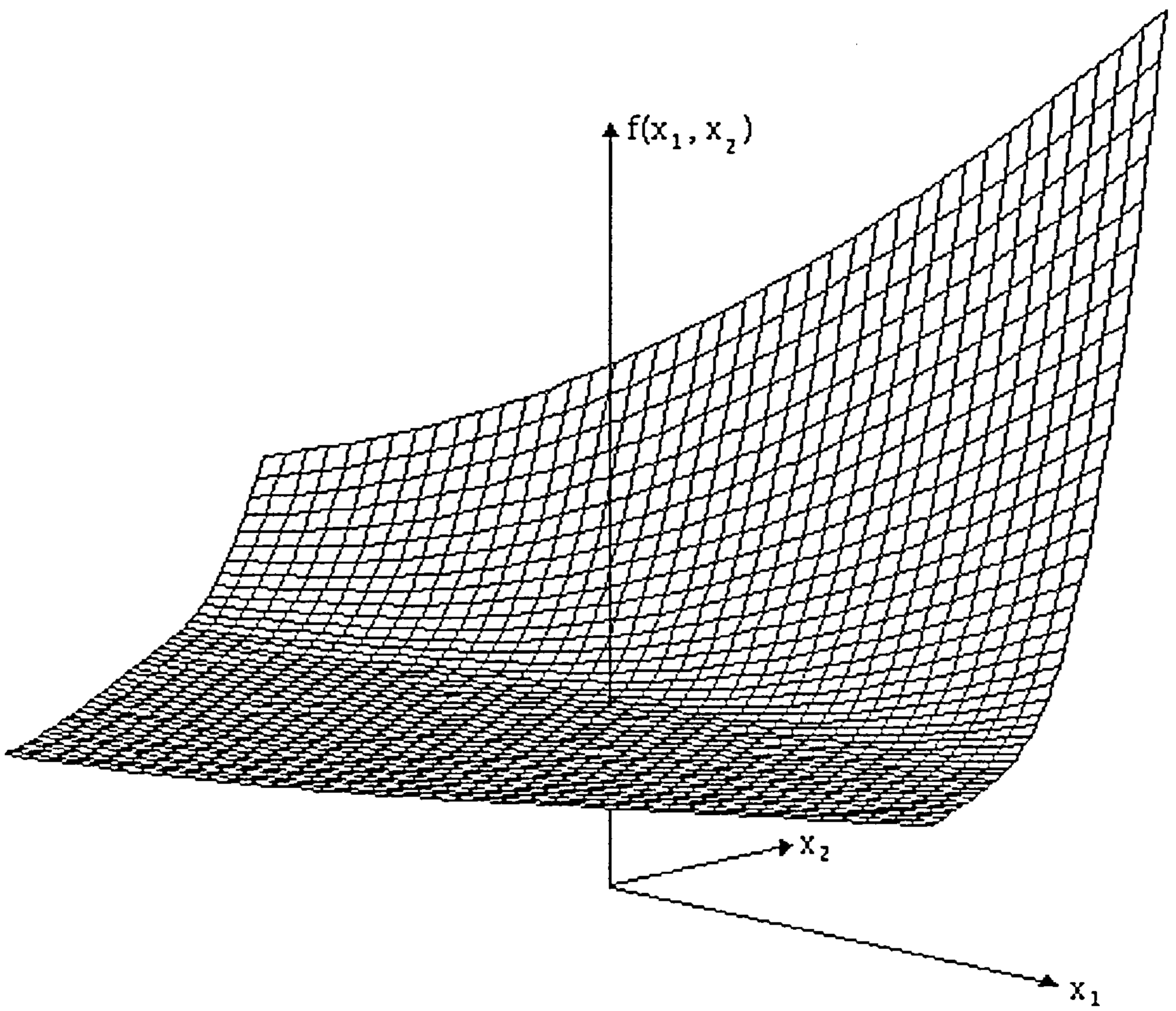

FIGURE 4.5. Augmented Lagrangian for $f(x_1, x_2) = \frac{1}{3}(x+1)^3 + x_2$

2. *Minimize* $f(x_1, x_2) = x_1^2 + x_2^2 - 2x_1 - 4x_2$

subject to

$$g_1(x_1, x_2) = x_1 + 4x_2 - 5 \leq 0$$

$$g_2(x_1, x_2) = 2x_1 + 3x_2 - 6 \leq 0$$

$$g_3(x_1) = -x_1 \leq 0$$

$$g_4(x_2) = -x_2 \leq 0$$

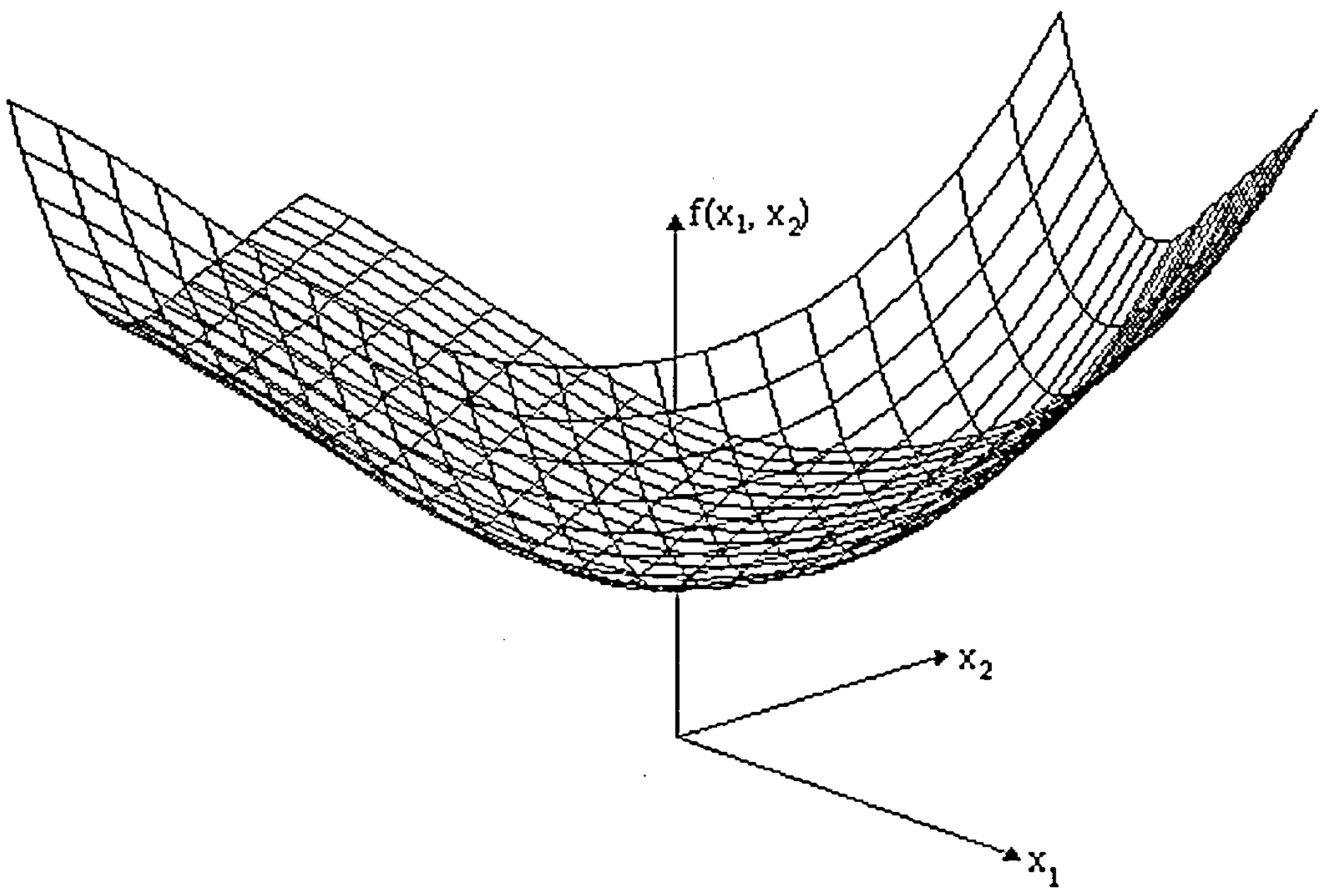

FIGURE 4.6. Augmented Lagrangian for $f(x_1, x_2) = x_1^2 + x_2^2 - 2x_1 - 4x_2$

The augmented lagrangian formulation in each of the two cases resulted in modified single objective functions. The nature of the resulting surfaces is shown in Figures 4.5 and 4.6 respectively.

The minimization procedure depicted in Figure 4.3 was adopted for finding the optimal

solution for the dual problem in each case.

Problem 1 (Figure 4.5) was run with a genetic population size of 50 and with a maximum limit of 50 generations per iterative (inner) loop (see Figure 4.4). The solution never converged to a minimum for these parameters. The reasons are obvious from the nature of the surface as seen in Figure 4.5. The Genetic Algorithms tends to descend quickly into the flat region of the function and then converges at a very gradual rate. Convergence was achieved for population sizes of 2000 and maximum generation limits of 500. Problem 2 (Figure 4.6) being highly unimodal in nature, converged quickly to the optimum solution with population size of 50 and a maximum generation limit of 50.

There was however one drawback to using the augmented lagrangian formulation making them unsuitable for the subdivision problem being investigated. In the subdivision problem, single damage zones are defined by the two transverse bulkheads that limit this zone. Multiple damage zones involve combinations of such single zones. The optimization involves searching the design space with varying bulkhead positions, and since the total number of combinations depends on the actual bulkhead positions, this total varied from (bulkhead) configuration to configuration. Consequently the number of constraints, which depends on the number of combinations, varied for each internal configuration. The augmented lagrange formulation allocates one λ_i value to each constraint equation. The method does not permit varying the number of λ_i values between two iterations because the scheme for updating the λ_i values depend on λ_i values from the previous iteration.

Exterior Penalty function method: The exterior penalty function [Rao'78] is defined as,

$$\phi(X, r_k) = f(x) + r_k \sum_{j=1}^{m} \langle g_j(X) \rangle^q$$

where r_k is the positive penalty factor, the exponent q is a non-negative constant, usually 2, and $g_j(x),\ j = 1, \ldots m$ are the m constraints. $\langle g_j(X) \rangle^q$ is defined as

$$\langle g_j(X) \rangle = max\langle g_j(X), 0 \rangle = \begin{cases} g_j(X) & if(g_j(X) > 0) \\ 0 & if(g_j(X) \leq 0) \end{cases}$$

Essentially the penalty function formulation penalizes constraint violations by reducing the achievements in terms of the evaluation function so that a constrained problem is transformed to an unconstrained one by associating a penalty with all constraint violations and the penalties are included in the function evaluation.

Some of the often cited drawbacks of incorporating high penalties [Davis'87b] in the evaluation routine when the domain (search space) is one in which the occurrence of individual solutions violating the constraints is likely is that the GA spends a lot of its time evaluating illegal individuals. Furthermore, the generation of a legal individual under such conditions tends to guide the genetic optimization towards premature convergence.

For a given internal subdivision configuration, a large number of single and multiple combination of compartments needs to be evaluated. But with the need to keep computing times down, those combinations which have very small probabilities of damage are not considered since their contribution to the overall index would also be negligibly low. However, even amongst the combinations evaluated, those involving multiple zones or larger compartments (or both) tend to violate certain constraints. This violation would nevertheless reflect adversely on the overall performance fitness of that particular gene. Hence the penalty factor is kept to relatively low values since constraint violation need not be a sign of an illegal individual. Also the objective and constraint function values are normalised to within certain maximum and minimum bounds which alleviates the problem of premature convergence.

4.6 Conclusion

Genetic algorithms (GA's) differ from other heuristic search methods in that they use crossover as the primary search mechanism. GA's have gained considerable popularity as a general purpose robust optimization technique especially when dealing with vast payoff landscapes riddled with multimodality.

The ship subdivision problem is one such example. In addition, the subdivision problem involves constraints of the "if ... then ... else" kind. GA's are particularly suited to handling such complex constraints. Hence even though GA's are inherently wasteful they offer the best probability of reaching efficient solutions under the given circumstances.

Chapter 5

Distributed Computing

5.1 Introduction

The area of parallel and distributed computing which fall under the broader category of concurrent programming [Andres'91] has become an area of renewed activity. This emanates partly from the need to solve the plethora of large complex combinatorial problems in many real-life situations and partly from the recent technological advances in both hardware and software which has made concurrent programming feasible and more accessible for a large number of applications.

5.2 Architectures

Flynn's taxonomy of computer architectures [Flynn'72] is still the most generalized method of classifying parallel computers. Flynn divided computers according to whether they used single or multiple "streams" of data, and (orthogonally) single or multiple "streams" of instructions. The four broad categories that emerge from such a classification are SISD, MISD, SIMD and MIMD architectures.

- SISD - Single Instruction Single Data or the conventional von Neumann architecture which carries out one instruction on one datum at a time.

- MISD - Multiple Instructions Single Data architectures would apply several instructions to each datum it fetches from memory. No computers conforming to this model have yet been constructed.

- SIMD - Single Instruction Multiple Data. In an SIMD computer, many processes simultaneously execute the same instructions, but on different data. For example.: for the instruction ADD A B, each processor adds its own value of A and B. SIMD machines are made up of processing elements (PE's). The PE's are controlled by a single task master which broadcasts program instructions to the PE's. PE's can also perform data transfer amongst themselves. One of the strengths of SIMD computers is scalability. As more PE's are added, so are more interprocessor links, so that the total communications bandwidth of the machine rises in proportion to its size. SIMD's are very good at certain things but very poor at others. In image processing the same operation needs to be carried out on each pixel of the image, such as taking the weighted average of its value and its four nearest neighbours. If each pixel were mapped to a PE, an SIMD could process the image in much less time that a serial machine. On the other hand if the task is not well load-balanced, i.e. when certain atomic tasks require much larger processing times than others, some PE's must wait for others to finish with a resultant loss in efficiency.

- MIMD - Multiple Instructions Multiple Data. A MIMD computer contains several independent processors (usually equi-powerful) in which each executes its "individual program". "Individual program" usually implies different paths of execution through the same piece of code resting on these machines.

5.3 MIMD Processing

MIMD processing has been the growth area of concurrent engineering over the recent past. Technology has evolved a variety of MIMD systems, the two important ones being

- Shared memory / Tightly coupled [Hwang'85] systems

- Distributed memory / Loosely coupled / Message-passing [Betsekas'89] systems with many hybrid designs lying in between

5.3.1 Shared memory MIMD systems

Figure 5.1 typifies a shared memory model of a MIMD system. Individual processors (denoted as P_i) have direct access to any part of the whole machines memory. In less extreme examples the individual processors have a private memory called buffers or caches

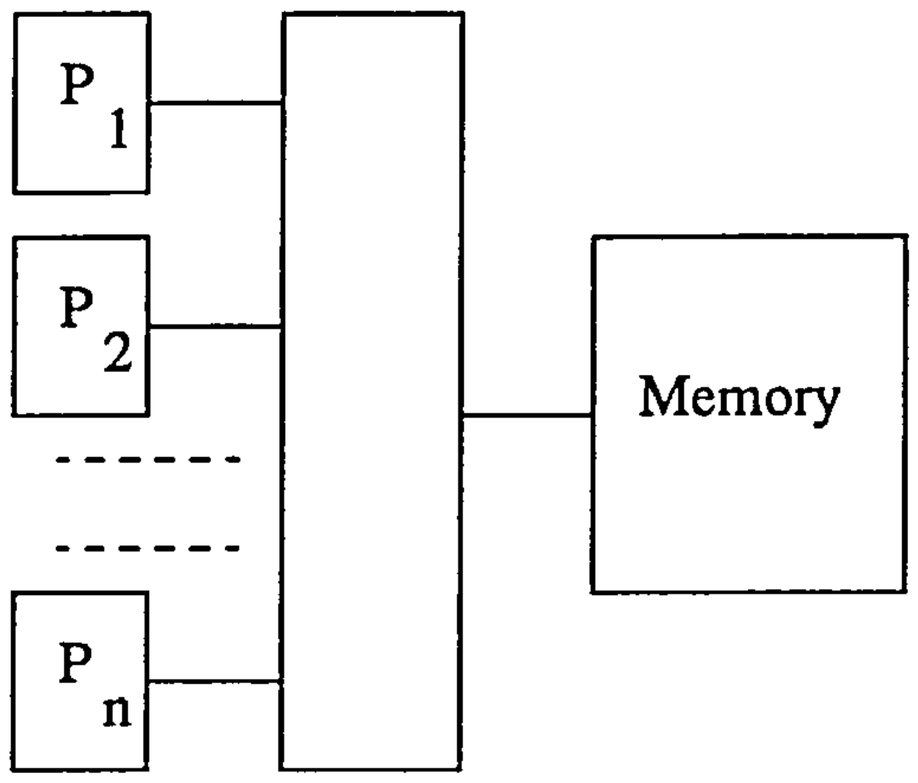

FIGURE 5.1. Shared memory MIMD model

Memory access time in shared memory systems can be either uniform (UMA) or non-uniform (NUMA). Shared-memory architectures are attractive because they are relatively simple to program. Interprocessor communication is via the global memory, that is, one processor writes into the global memory and the second processor reads from that location. However one drawback of shared memory systems is that they cannot be scaled indefinitely. As the number of processor trying to access the memory increases, so do the odds that processors will be contending for such access. Eventually (and in fact, very rapidly), access to memory becomes a bottleneck limiting the speed of the computer. The use of local cache memory can alleviate this problem to a certain extent and this concept taken to the extreme distributes all the memory between the processors resulting in an MIMD distributed system.

5.3.2 Distributed memory MIMD systems

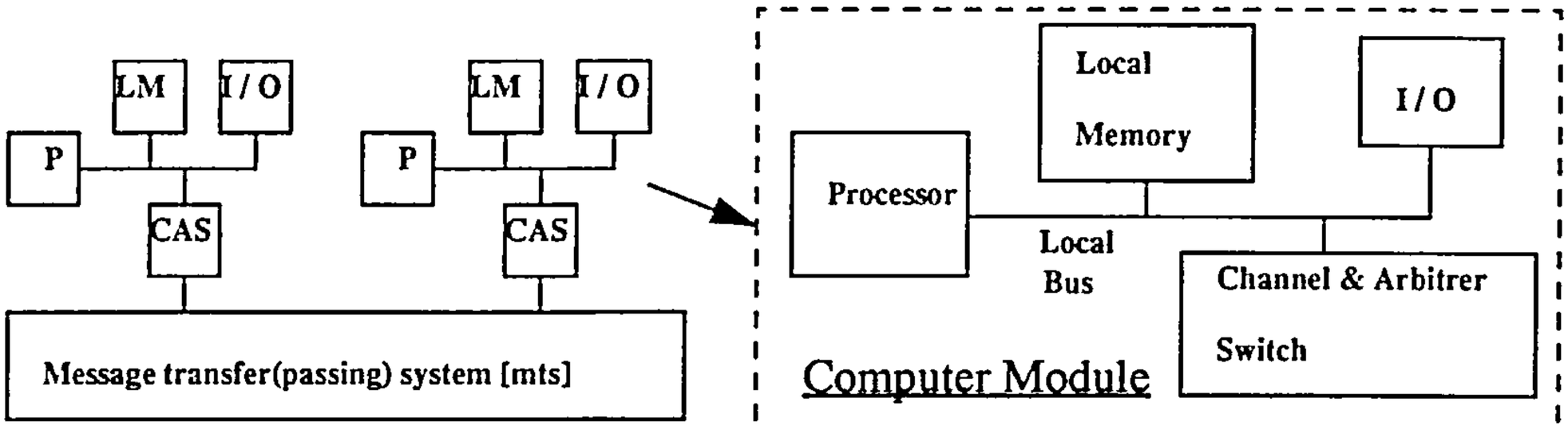

FIGURE 5.2. A MIMD distributed system

In a loosely coupled or distributed system, the degree of memory conflicts is not as severe as in a tightly coupled system. In a typical distributed system each processor has a set of input/output (I / O) devices and a large local memory where it accesses most of its instructions and data. Such a unit is shown in Figure 5.2 and is referred to as a computer module. The processors communicate by exchanging messages through a message passing interface (MPI) (also sometimes referred to as a message transfer system (MTS)) and reside as nodes sharing a communication network, e.g, an Ethernet.

5.4 Basic Concepts

The taxonomy on MIMD computers [Hockney'88] describe the various MIMD networks as

- *star*
- *mesh*
- *cube*
- *reconfigurable*
- *hierarchical*

These configurations describe the way in which the computer modules are interconnected. For instance, in *star*, the simplest network, several hosts are connected to a common host (i.e. a star like configuration). Network topologies are usually chosen with some particular application in mind [Bertsekas'89] since each topology exhibits certain regularities and consequently certain properties suitable to that application. The

suitability of a topology to a communication task is measured in terms of some typical criteria such as

- diameter - the maximum distance between any pair of nodes
- connectivity - network connectivity provides a measure of the number of "independent" path connecting a pair of nodes
- flexibility - the broad-baseness of the topology in being able to run a variety of algorithms

In distributed systems a significant proportion of the total computing time is spent on interprocessor communication. Typically the communication delay can be split into

- communication processing time - the time required to prepare information for transmission
- queuing time - packets (of information) ready for transmission may end up waiting in a queue (for various reasons)
- transmission time - time taken for the actual transmission of all the bits of a packet
- propagation time - time between the transmission of the last bit of a packet from the transmitting processor to when it is received by the receiving processor.

5.4.1 Load balancing

Load balancing or the scheduling parameter [Hockney'88] was one of the earliest problems studied in MIMD computation. If T_1 is the time required to perform a certain task on one processor of a kind and T_p is the time to perform the task on p identical processors of the same kind the *efficiency of scheduling*, E_p, is defined as,

$$E_p = \frac{T_1}{pT_p} \leq 1$$

Ideally $T_p = T_1/p$ and $E_p = 1$. However if some processors finish before others and become idle $T_p \geq (T_1/p)$ and $E_p < 1$.

5.4.2 Synchronization

In the concurrent implementation of any algorithm, it is necessary to co-ordinate the activities of different processors [Bertsekas'89]. This is often achieved by dividing the

algorithm into different phases. So a phase represents a sequence of computations done sequentially such that within each phase the computations are divided among n processors of a computing system. During a phase t each processor i does some computation using the problem data, together with information that it received from other processors during phases $1, 2, \ldots t-1$. An implicit assumption made here is that the computations of different processors can be carried out "independently" within a phase. If the computation of phase $t+1$ can be started only after the completion of all the computation at phase t on all i processors then such an act of synchronization will take a certain time. This time represents the time lost which could otherwise have been used for useful computation.

5.4.3 Granularity

For an effective utilisation of parallelism, one needs to consider carefully the run-time "cost" of the synchronisation mechanism available on the system. The higher the run-time cost of a particular mechanism, the longer the intervals between synchronisation have to be, in order to amortize the synchronisation overheads over the parallelism that is gained. In categorising parallelism from this point of view, the term "granularity" is often used. It is the number of instructions between the synchronisation events of parallel activities and represents the length of the period between synchronisation. It is a useful measure, when compared with system capability, to estimate the effectiveness of a parallelisation scheme.

Granularity	Nos. of instructions between synchronisation
Fine	less than 20
Medium	20 to 200
Coarse	200 to 2000
Very coarse	2000 to 1 million

5.4.4 Types of parallelism

- **Algorithmic parallelism** - In algorithmic parallelism the program or process is partitioned and distributed across the network of processors. Each partition executes its own data or data received from other partitions in parallel. Algorithmic parallelism is usually difficult to implement.

- **Geometric parallelism** - Geometric parallelism involves the partitioning of data rather than code. If the nature of the algorithm is such that it can process large data structure concurrently, then it can be partitioned and distributed over the network. In this case each processor in the network would run the same algorithm (or a copy of it) but the path through the algorithm would change, being data dependent.

- **Task farming** - Task farming is one of the simplest methods of exploiting parallelism. Farming consists of a master processor that produces a number of independent tasks which are broadcast to slave processors for independent processing. The results are collected by the master. Load balancing is easily achieved in the task farming since if one processor comparatively slower, then the other processors can get on with processing the remainder of tasks in parallel.

5.5 System Modelling

The probabilistic analysis of ship subdivision involves evaluation of survivability characteristics of the vessel for single and multiple damage zones. The evaluations of the characteristics of one particular internal configuration has no bearing on the evaluations for any other configuration. Added to this is the fact that the evaluation for a given internal configuration takes a fair amount of time. This make the whole task ideally suited for MIMD coarse-grained distributed task farming. Factor such as

- availability of a wide variety of powerful UNIX workstations (SUN's, HP's)
- availability of a network (Ethernet)
- ease of access to commercial and public domain software (Linda, PVM)

were also helpful in implementing this methodology.

A task farming model is shown in Figure 5.3

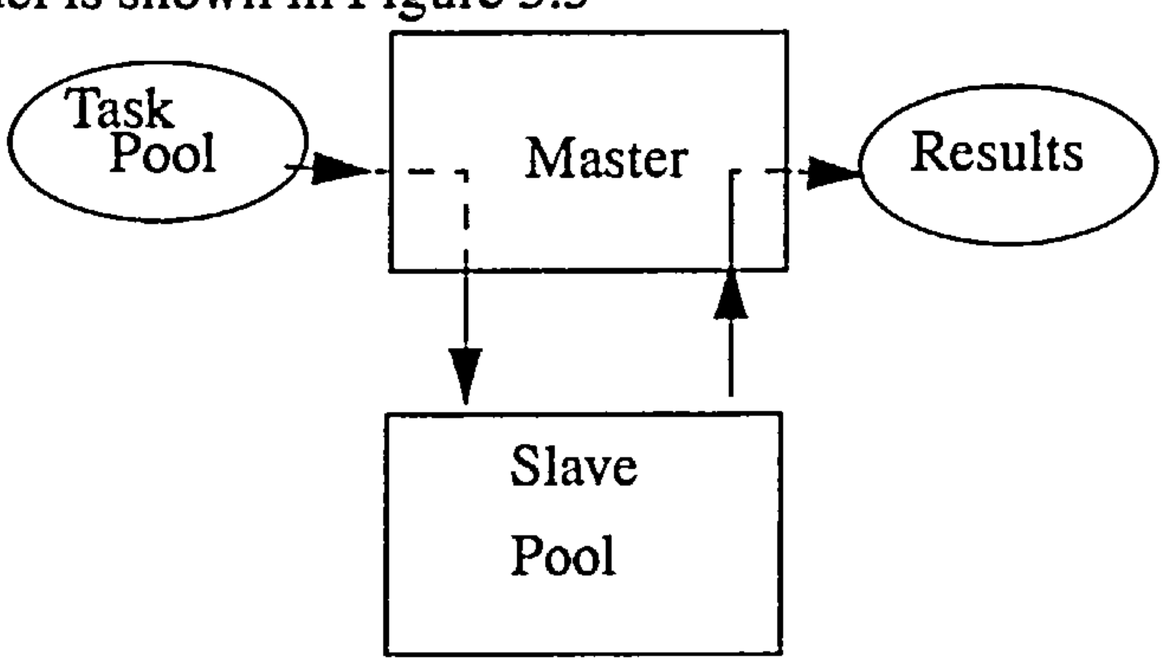

FIGURE 5.3. A task farming model

A task (in the pool) represents a given internal configuration of the vessel. Since each member of the genetic population decodes to an (unique) internal configuration (i.e. transverse bulkhead positions and positions of decks and longitudinals) the pool of tasks in effect represents the gene pool at any given generation (of the GA). The overall (or outer) loop of the GA is implemented by the master processor. The genes get farmed out to individual slaves which return, on completion, the vessel characteristics for that configuration as shown in Figure 5.4.

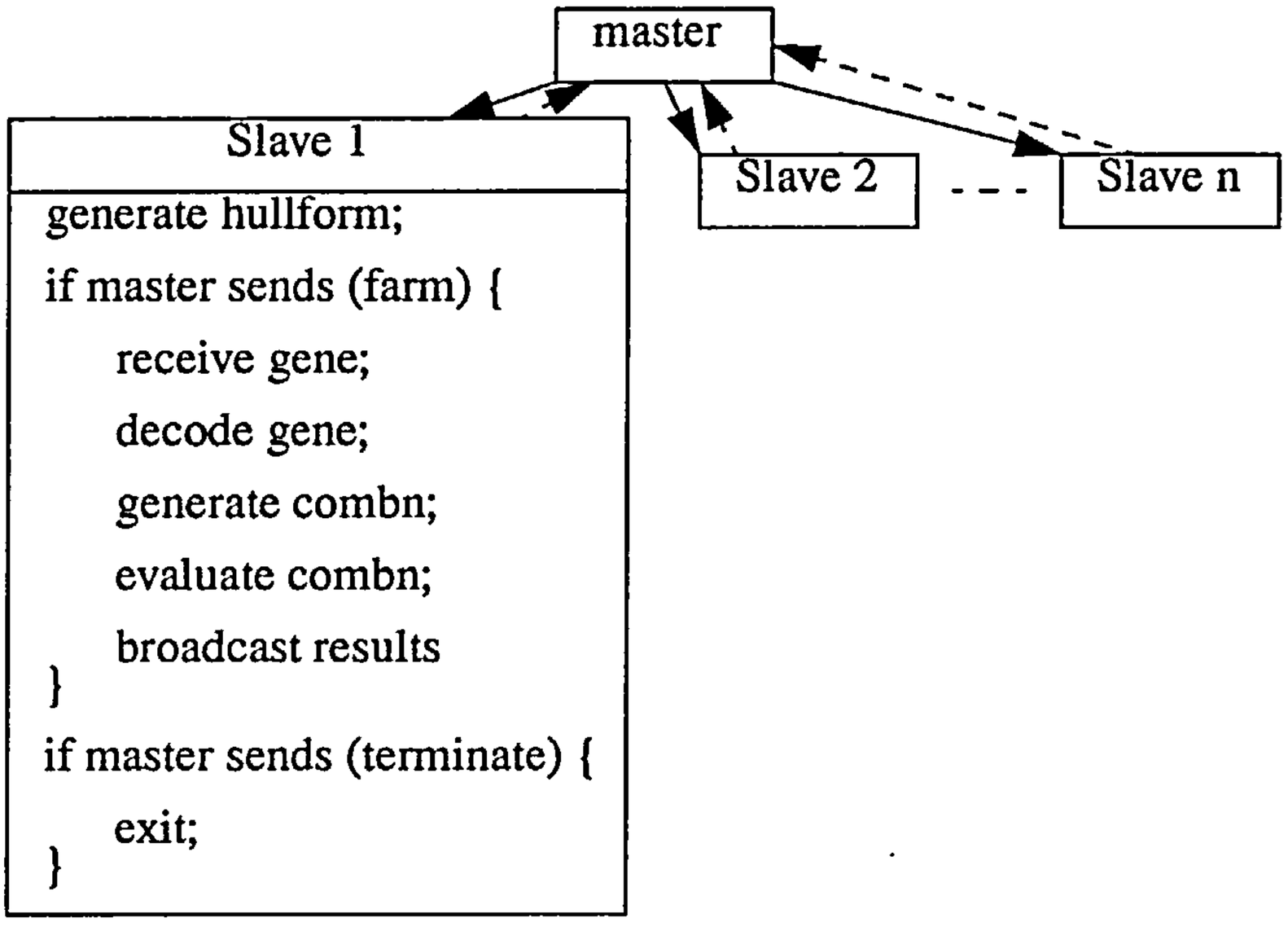

FIGURE 5.4. Fitness farming

As shown, the slaves carry replicated pieces of code. The slaves first generate the hullform and read in initial data such as vessel KG, subdivision draught etc. and then enter into a continuous "non-blocking" receive mode. In this mode, the slave is in a "wait" state, waiting for a message from the master to arrive. When that happens, the received message is placed in an active receive buffer. It unpacks the message, decodes the string and translates that into the various bulkhead and deck positions. The damage zone combinations are determined and stability and other characteristics for each combination are evaluated. These are than used to evaluate the fitness function of that gene which is then broadcast back to the master. The slave process then reverts back to its "non-blocking" receive state and waits for the arrival of the next message.

5.6 Network Linda

Linda is a co-ordination language (written in a higher level programming language such as Fortran or C) to enable the description of parallel computations [Petrie'94]. Linda was developed as part of a research project by David Gelernter at Yale University and is now available as a commercial product from Scientific Computing Inc., USA. Linda uses the distributed data structure paradigm [C-Linda'92] in which the method decouples the data required for calculations. The program then uses this shared data space, with individual processes reading data from it and placing results in it. In Linda this space is often referred to as the "tuple space". The tuple space in effect behaves as a virtual shared memory in that interprocessor communication is achieved by "writing to" and "reading from" the tuple space. Linda tuples are of two kinds. *Active tuples* are processes that become passive on completion of execution and *Passive tuples* are the data for the processes. Linda provides six operations on the tuple space to support interprocessor communication, shared data structures and process creation.

- *out(t)* - *out(t)* adds a passive tuple *t* to the tuple space using *out(t)*. All fields of the tuple are evaluated prior to the tuple being added to the tuple space.
- *in(s)* - *in(s)* causes precisely one tuple *t* which matches the template *s* to be with-drawn from the tuple space.
- *rd(s)* - similar to *in(s)*, except that instead of removing the matching tuple from the tuple space, a copy is made to instantiate formulae in s
- *inp(s)* & *rdp(s)* - predicate forms (or) non-blocking forms of *in(s)* & *rd(s)*, i.e., if no matching tuple is available these operations return failure rather than wait for a matching to become available.
- *eval()* - allows active tuples to be added to the tuple space. *eval()* is similar to out except that tuple's fields are evaluated after it is added to the tuple space rather than before.

5.7 PVM

Parallel Virtual Machine (PVM) is an ongoing research project at the Oak Ridge National Laboratory (ORNL) involving ORNL, Emory University, University of Tennessee, Carnegie Mellon University, Pittsburgh Supercomputer centre and funded by the U.S Department of Energy, the National Science Foundation and the state of

Tennessee. PVM is a public domain software, distributed freely in the interest of advancement of science and is being used in computational applications around the world [PVM'93]. PVM enables a "virtual configuration" so that a collection of serial, parallel and vector computers appear as a large distributed memory computer. Functions to set up tasks on the virtual machine, functions for communication and synchronization are all provided by PVM. PVM functions have been coded in C.

The first part of the PVM system consists of a daemon, called *pvmd3* that resides on all the computers that would make the virtual machine. During execution, the user starts the daemon on a machine which in turn starts *pvmd3* on each of the computers making up the user-defined virtual machine.

The second part of the system consists of library interface routines for message passing, spawning processes, task co-ordination, and virtual machine configuration modification.

5.8 Comparison between PVM & Network Linda

A comparative study was carried out by the Computing Laboratory, Newcastle University between Network Linda and PVM [Petrie'94]. The subdivision optimization problem was one of the algorithms amongst others, to be used to make the comparison. Interprocessor communication in Linda (section 5.5) was through the "virtual shared memory" (or tuple space) whereas in PVM this is done manually by the user. The message is first packed into a buffer and then broadcast to a processor where it received and then carefully unpacked in a sequence that mirrors the packing sequence. Each method has its own advantages and disadvantages. The following example highlights this point.

Consider a communication sequence that involves the transmission of three integer vectors IX, IY and IZ of length 10 each and three double precision vectors RX, RY and RZ of length 15 each.

In PVM,

(master) Transmission sequence

```
bufid = pvm_initsend(PvmDataDefault);
if (bufid < 0) return -1;
pvm_pkint(IX, 10, 1);
pvm_pkint(IY, 10, 1);
pvm_pkint(IZ, 10, 1);
pvm_pkdouble(RX, 15, 1);
pvm_pkdouble(RY, 15, 1);
pvm_pkdouble(RZ, 15, 1);
if (pvm_send(tid, MASTER_SENDS) < 0) return -1;
else return 1;
```

(slave) Reception sequence

```
if (pvm_nrecv(parent_tid, SLAVE_RECEIVES) > 0)) {
        pvm_upkint(IX, 10, 1);
        pvm_upkint(IY, 10, 1);
        pvm_upkint(IZ, 10, 1);
        pvm_upkdouble(RX, 15, 1);
        pvm_upkdouble(RY, 15, 1);
        pvm_upkdouble(RZ, 15, 1);
}
```

In Linda,

(master) Transmission sequence

```
out('vectors', IX, IY, IZ, RX, RY, RZ);
```

(slave) Reception sequence

```
rd('vectors', ?IX, ?IY, ?IZ, ?RX, ?RY, ?RZ);
```

This example demonstrates the lassitude of interprocessor communication in PVM as opposed to that in Linda. In PVM each vector has to be individually packed (with its correct length) at the transmitting end and then unpacked in exactly the same sequence at the receiving end. If this sequence is not maintained then it would result in an error. This procedure can get very cumbersome especially when large amounts of data need to be transmitted or when the data structures have complex forms. For a complex data structure each element/vector/array has to be individually packed and unpacked. Linda procedures require just one call for transmission and reception and the vector lengths need not be specified.

The subdivision problem involves the movement of bulkheads to create an optimal internal configuration. The number of damage combinations depends on the bulkhead positions (as the maximum damage size is limited by regulations) and many of the variables used in the algorithm were functions of these damage combinations. A variation in the number of damage combinations meant that the vector lengths of variables that depended on it were not fixed, the memory allocated to such variables was done dynamically (as is possible in C). PVM was better suited for handling such dynamic variations in memory allocation in comparison to Linda simply because the overall control of the transmission/reception sequence was left in the hands of the user. The following example demonstrates this fact.

(master) Transmission sequence

```
bufid = pvm_initsend(PvmDataDefault);
.....
pvm_pkint(&tot_hull_zones, 1, 1);
for (i = 1; i <= tot_hull_zones; i++) {
    pvm_pkint(&hull_zone[i].nos_comp, 1, 1);
    pvm_pkint(hull_zone[i].comp_no, hull_zone[i].nos_comp+1, 1);
    pvm_pkdouble(&hull_zone[i].min, 1, 1);
    pvm_pkdouble(&hull_zone[i].max, 1, 1);
}
.....
if (pvm_send(tid, MASTER_SENDS) < 0) return -1;
else return 1;
```

(slave) Reception sequence

```
if (pvm_nrecv(parent_tid, SLAVE_RECEIVES) > 0)) {
    .....
    pvm_upkint(tot_hull_zones, 1, 1);
    *zne = MYALLOC(ZONE, (*tot_hull_zones)+1);
for (i = 1; i <= *tot_hull_zones; i++) {
    pvm_upkint(&zone[i].nos_comp, 1, 1);
    zone[i].comp_no = MYALLOC(int, zone[i].nos_comp+1);
    pvm_upkint(zone[i].comp_no, zone[i].nos_comp+1, 1);
    pvm_upkdouble(&zone[i].min, 1, 1);
    pvm_upkdouble(&zone[i].max, 1, 1);
}
```

```
        .....
    }
```

The master processor first transmits the total number of hull zones that have been generated for this internal vessel configuration. It then transmits the vectors whose memories have been allocated dynamically for that number of hull zones. At the slave end, the number of zones to be formed is the first information that is received and then the dynamic allocation is performed locally for the various variables in the slave process. The pvm buffer is then unpacked for that vector length.

In Linda the tuple fields are atomically and automatically transferred to their destinations, this means that some ingenuity has to be exercised in order to recover the length of an array before transferring its data. Several possibilities exist to achieve this but these at best compromise Linda's elegance and expressiveness, and involves fragmentation accompanied by awkward devices to preserve the logical association between related fragments. Due to these reasons PVM was adopted as the message passing interface for this particular problem.

5.9 Conclusion

Since computers were first invented in the 1940's they have followed a similar plan: a single processor in conjunction with a single memory cache, executing a series of instruction one after another. The technological advances of the recent past has been responsible for a paradigm shift in the philosophy of design of computer architectures, in the 90's, where multithreading, parallelism and distributed computing have become the norm.

This is of particular benefit for tackling problems that are combinatorially large such as the ship subdivision problem. The availability of ready-to-use software such as PVM has also enabled users with non-specialised computing background access to distributed computing methods. Its is evident that with the growing need to solve larger and more complex problems, the use of distributed computing software will become imperative if the solutions are to be achieved in realistic time frames.

Chapter 6

Computational Foundations to the Subdivision Problem

The deterministic regulations based on the factor of subdivision approach not only set the required standards for safety but also provided naval architects with design guidance as to the placement of internal subdivision members. The advantage of using the floodable length curves was that not only did they provide a measure of the effectiveness of a subdivision scenario but actually prescribed the choice of the "best" possible location for the subdivision members.

The probabilistic rules of subdivision are designed to apply when used to evaluate the effectiveness of a given subdivision scenario. They are however much more difficult to "invert", that is, to use the rules to arrive at an "optimal" internal configuration. There are three principal reasons for this.

i. Probabilistic regulations are computationally more intensive.

ii. The rules are in the form on an "if...., then....., else....." format which makes them difficult to model mathematically in a closed form.

iii. The optimal landscape is highly multi-modal in nature. In other words, vastly different internal configurations result in almost the same A-index value.

B-spline curves have been used in computer aided design for over three decades. B-splines curves are numerically more robust and stable than either power series curves or Bézier curves. However b-spline curves are more complex in their formulation and require the use of a robust (non-standard) numerical solver. B-spline curves are stable under conditions of affine transformations such as rotations and translations and allow for local control along the curve which is useful for obtaining faired lines. Therefore fourth order b-spline curves were used for hullform generation and for the description of the internal compartments of subdivision. The use of b-spline curves also allowed for the efficient generation of the intersection between the hull and the still waterplane, known as the hull waterplane. The description of this hull waterplane was essential for the development of the damage stability theory which was based on the theory of equivolume waterplanes. The description of the hull (and compartment) waterplane areas was also useful in developing routines for generating the tank sounding data in an efficient manner.

Traditional damage stability calculations under conditions of free trim involves an iterative process. For each incremental angle of heel of the damaged vessel, in the upright (non-trimmed) position, the draught and the angle of trim has to be adjusted in such a way so as to maintain longitudinal equilibrium and the total displacement volume a constant.

The theory of equivolume waterplanes as applied to damage stability calculations, on the other hand, provides the position of the next equivolume waterplane in a single step. Since the probabilistic regulations on ship safety involves repeated damage stability calculations for different damage scenarios, this reduces the computational burden involved in such calculations by a considerable extent. In addition, the method also maps the locus of the centre of buoyancy as the vessel inclines thereby yielding the GZ-curve for the damaged vessel as it heels. The position of the next equivolume waterplane depends largely on the magnitude of the longitudinal (centreplane) moment of inertias and the cross-product moment of inertias. With the description of the hull waterplane in the form of a b-spline, it is possible to evaluate the moments of inertias of the waterplane in a closed form manner thereby eliminating the need for an iterative integration method (as proposed in the original theory). This also helps to reduce the computational time required during each incremental heel of the damaged vessel.

The "optimal" landscape for the subdivision problem is multi-modal in nature. Conventional optimisation techniques which rely largely on the gradients of the landscape to be searched tend to get entrapped in regions of local optima under such situations. The Genetic Algorithm (GA) is a heuristic search technique based on the principles of natural physical processes which has proved to be efficient in searching through multi-peaked performance landscapes. GA combine the twin roles of exploration and exploitation. The preliminary stages of a GA are of exploration where the algorithm explores for pockets of efficient regions. As the algorithm progresses and the pockets of efficiency gets largely identified, the GA shifts to the exploitation stage. In other words fitter members begin to dominate the gene pool as less fit members die.

GA's are admittedly more wasteful than conventional search methods in terms of the time lost in evaluating less fit members. However given the nature of the performance landscape, GA's have the highest probability of locating the "most satisfactory" solution or solutions. Also the probabilistic regulations have a lot of the rules in the form of "if...., then...., else...." statements. These often lead to a stepwise variation in the parameters which can readily be handled by the use of GA's.

A damage zone is defined as a compartment which is bound by two transverse (parallel to midship plane) members. The evaluation of a given subdivision configuration involves evaluating the damage stability characteristics of a vessel for single and multiple (two, three etc.) zones of damage. If a zone has any longitudinal (parallel to centreplane) subdivision members then each zone has to be evaluated first for wing damage only and then for wing and central compartment damages. For cargo ships (and in this case for oil tankers in particular), the presence of vertical (parallel to baseplane) subdivision members results in even greater number of damage combinations to be evaluated.

In order to arrive at a "satisfactory" subdivision configuration, the locations of internal subdivision members have to be varied and the damage characteristics of the vessel be evaluated for every such variation. Even with the use of efficient tools such as b-spline curve fitting methods in combination with a quick damage stability evaluation using equivolume waterplanes, the number of damage combinations tends to grow very rapidly to make the problem almost computationally intractable. However the fact that the evaluation of a particular damage combination for a given internal subdivision configuration is completely independent of that for another configuration makes the

problem ideally suited to the application of distributed computing paradigms such as task farming.

With the current state-of-the-art in Unix workstations, an average damage combination takes around twenty minutes to evaluate. For a average of twenty five damage combinations per configuration, the total evaluation time on a serial machine would be of the order of eight hours. The same task when distributed to a cluster of ten workstations could be completed in less than sixty minutes, a speed up factor of eight. Also given a population size of seventy, the time taken for the evaluation of an entire generation of genes requires the use of distributed computing methods in order to comprehensively analyse a given scenario. Parallel virtual machines (PVM), developed in the United States, is a freely available (public domain) software package that allows a collections of serial machines (Unix workstations in this case) to appear as a large distributed memory computer.

The tools described so far, namely,

- the method of b-splines
- damage stability calculations based on equivolume waterplanes
- genetic algorithms
- distributed computing using PVM

can now be combined together in order to investigate the ship subdivision problem in general to arrive at "satisfactory" internal configurations based on the probabilistic regulation of ship subdivision.

Chapter 7

Investigations into

Passenger ship subdivision

7.1 Introduction

The first conference on the safety of life at sea (SOLAS) was held in 1913. The incident that led to the convening of this conference was the sinking of the *Titanic* on her maiden voyage in April 1912 when more than fifteen hundred passengers and crew lost their lives. The conference was interrupted by the First World War and its results remained inconclusive.

Work, however, resumed after the war and the second SOLAS conference was held in 1929. This conference was mainly concerned with the problems of buoyancy and subdivision requirement of passenger ships based on empirical methods. Methods to obtain bulkhead spacing were formulated on the floodable length principle. The methods developed did not consider the stability of vessels during and after damage nor did it systematically take into account the extent of damage.

The third SOLAS conference which was convened in 1948 introduced further regulations on stability by introducing damage stability requirements. These were in the form of added impositions on the amount of heel permissible after flooding and

asymmetrical flooding requirements. The sinking of the *Andrea Doria* as a result of collision damage in 1956 called for a critical review of the SOLAS requirements.

The fourth SOLAS conference convened in 1960 (SOLAS'60) was the first to be convened under the auspices of the International Maritime Organisation [IMO] (known then as Intergovernmental Maritime Consultative Organisation [IMCO]). On the whole the recommendations made by SOLAS'60 were not too different from SOLAS'48.

In preparation for SOLAS'60, leading naval architects from the United States of America, as a result of extensive studies, concluded that there was a need for a new probabilistic approach to damage stability based on actual damage statistics [Comstock'61]. The conference concluded with calls for continued studies on the passenger and cargo ship subdivision requirements and an IMO subcommittee on subdivision, stability and load lines (STAB) was formed as a result.

The 1974 SOLAS convention approved resolution A.265 as the probability based damage stability regulations for passenger ship, a result of work carried out by the subcommittee. The new rules were considered to be equivalent to the provisions of part B of chapter II of the 1960 convention and were therefore known as the "equivalent rules".

> "There is indeed a need for minimum standards of survivability along the ship length but this can be assured by using probabilistic principles. The subcommittee, however resorted to deterministic requirements, contained in regulation 5 of resolution A.265(VIII) [IMO'74], making the new regulations incoherent in this respect, necessarily more cumbersome to apply and in effect more stringent than the SOLAS requirement. As a result, the new regulations have hardly ever been used. This is made possible by the fact that the new regulations[IMO'74] are equivalent to the old one[IMO'60];they are not obligatory and the designer may choose either one of them. In such a situation the designer inevitably chooses those which are easier to use and comply with rather than those which provide higher standards of safety" [Pawlowski'92].

7.2 IMO Resolution A.265

Subdivision is the process of partitioning or compartmenting the internal volume of the vessel to limit the amount of water ingress in the event of that compartment becoming open to sea. This, in turn, determines the ability of the ship to survive in her damaged condition and limits the amount of hazardous cargo being released into the environment. Since safety is usually a relative measure one can, so far as it is practicable only try and increase the probability of survival. Wendel [Wendel'60] was the first to initiate the use of the probabilistic approach to the evaluation of subdivision for safety. This idea was further developed by Comstock & Robertson [Comstock'61], Volkov [Volkov'63], Wendel [Wendel'68] and by the IMO which finally resulted in Resolution A.265 [IMO'74].

Robertson et al. [Robertson'74] provided a thorough discussion of the philosophy, background and practical application of Resolution A.265. A brief description of some of the key elements of this resolution is presented here for completeness.

7.2.1 Intermediate draughts

The regulations specify three intermediate draughts d_1, d_2 and d_3 for evaluating any damage scenario which are in turn dependent upon d_0, the lightest service draught and d_s, the subdivision draughts. These are as follows.

$$d_1 = d_s - \frac{2}{3}(d_s - d_o)$$

$$d_2 = d_s - \frac{1}{3}(d_s - d_o) \qquad \text{(EQ 7.1)}$$

$$d_3 = d_s - \frac{1}{6}(d_s - d_o)$$

"Normally, d_0 is the anticipated draught with no cargo. That is to say, d_0 defines the lower limit of the ships' range of operating drafts. While it appears that an accurate determination (of d_0) is not possible, especially in the design stage, the probable degree of inaccuracy in establishing d_0 and the related intermediate drafts d_1, d_2 and d_3 should have little effect on the results of calculations called for by regulations"[Robertson'74].

7.2.2 Attained index A

Resolution A.265 states that a ships' attained index of subdivision A must be equal to or greater than its required subdivision index R. A is defined as the summation

$$A = \sum_{i \in J} a_i \, p_i \, s_i \qquad \text{(EQ 7.2)}$$

where a_i - accounts for the probability of damage location in the longitudinal direction

p_i - accounts for the probability of different longitudinal extents of damage

s_i - accounts for the probability of survival after flooding

J - is the set of all feasible combinations of compartments taken singly or as groups of adjacent compartments

7.2.3 Factor a & p

The probability theory and damage statistics on which factors a and p are based on has been discussed extensively by Hook [Hook'91], but a brief introduction is provided here.

Given a continuous random variable X [Ross'89], there exists a non-negative function $f(x)$, defined for all real $x \in (-\infty, \infty)$, having the property that for any set B of real numbers

$$p\{X \in B\} = \int_B f(x)dx \qquad \text{(EQ 7.3)}$$

where $f(x)$ is the probability density function (p.d.f). (EQ 7.3) states the probability of X being in B. Also

$$1 = p\{X \in -(\infty, \infty)\} = \int_{-\infty}^{\infty} f(x)dx$$

All probability statements about X can be assumed in terms of $f(x)$. If B=[a,b] then

$$p\{a \le X \le b\} = \int_a^b f(x)dx$$

and when a=b

$$p\{X = a\} = \int_{a}^{a} f(x)dx = 0$$

In other words the equation states that the probability that a continuous random variable will assume any particular value is zero. Two random variables X and Y are said to be jointly continuous if there exists a function $f(x, y)$, defined for all real x and y, having the property that for every sets A and B of real numbers

$$p\{X \in A, Y \in B\} = \int_{B}\int_{A} f(x, y)dxdy$$

where $f(x, y)$ is the joint probability distribution function of X and Y.

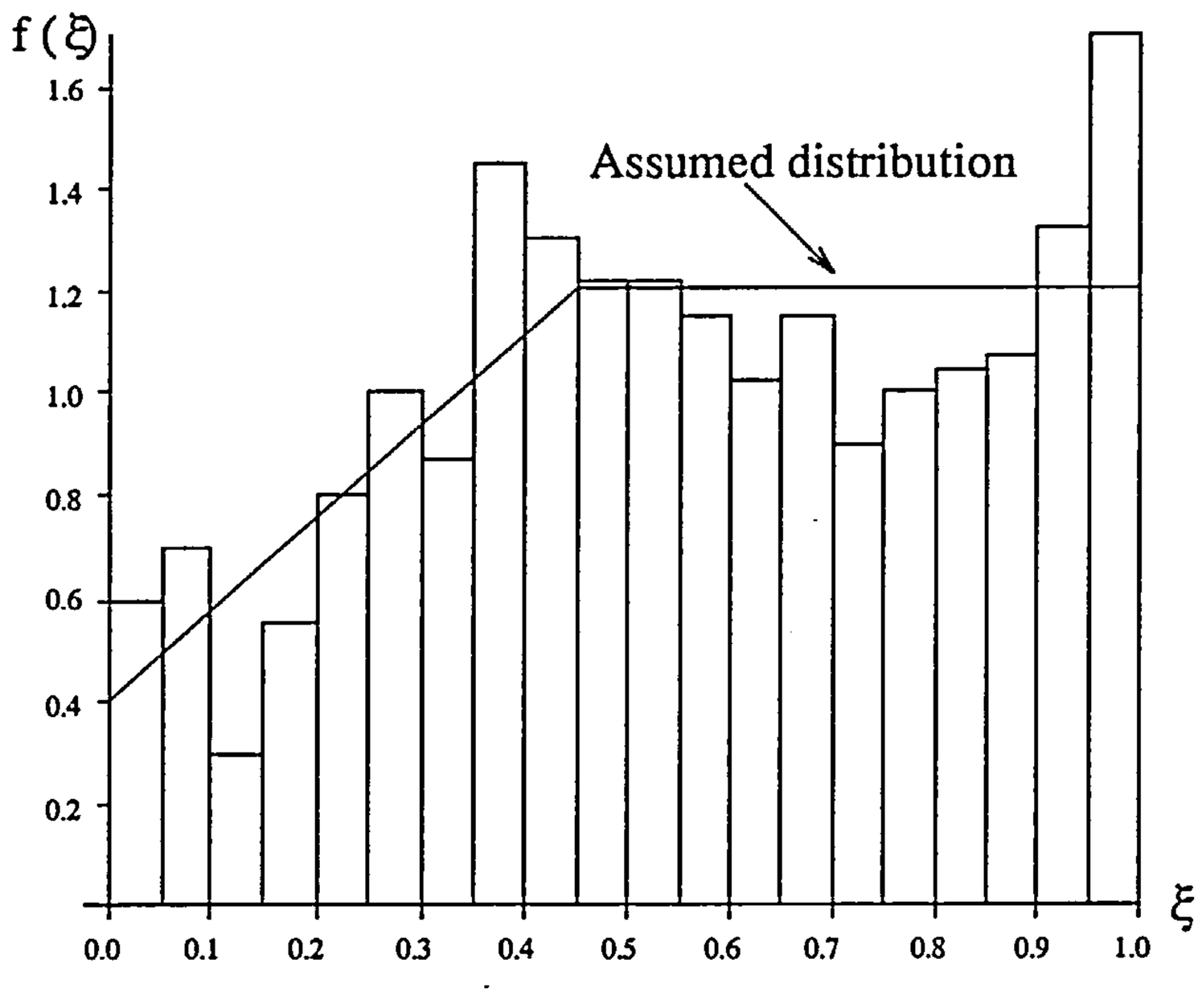

FIGURE 7.1. p.d.f of collision location

Figure 7.1 shows the p.d.f for the non-dimensional damage location $\xi = \frac{x}{L}$ and Figure 7.2 represents the p.d.f for the non-dimensional longitudinal extents of damage $\lambda = \frac{l}{L}$ where x is the location of damage, l is the length of damage and L is the ship length. ξ and λ are not independent variables [Pawlowski'92] and hence the joint density function can be expressed as

$$f(\xi, \lambda) = \begin{cases} f(\xi)f(\lambda|\xi) \\ f(\lambda)f(\xi|\lambda) \end{cases}$$

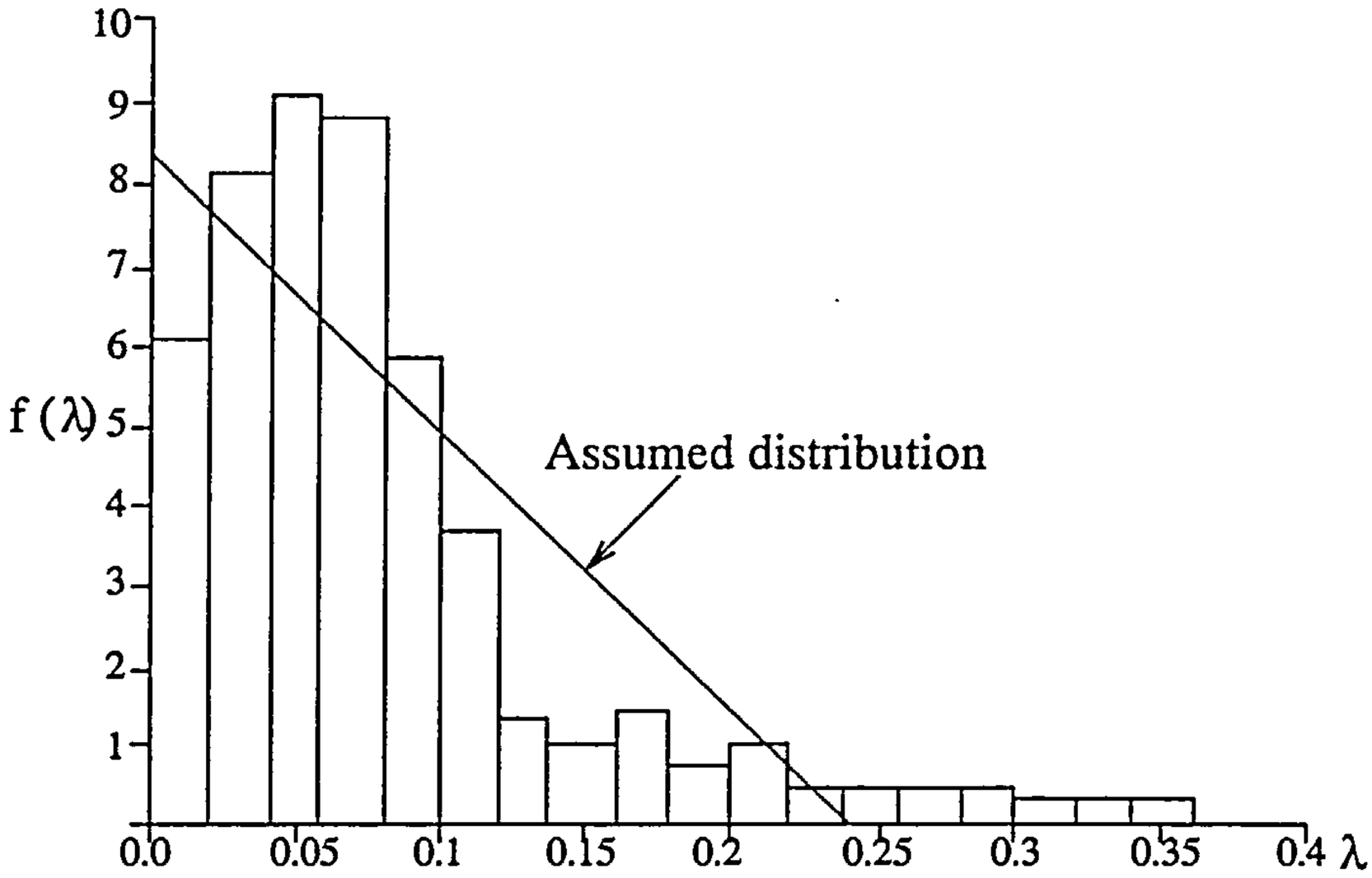

FIGURE 7.2. p.d.f for collision extents

It is therefore insufficient to know only the marginal distribution $f(\xi)$ or $f(\lambda)$ in order to find their joint density, the conditional distributions $f(\xi|\lambda)$ or $f(\lambda|\xi)$ also need to be determined. Due to the lack of statistical damage data, these distributions can be obtained from the marginal distributions only by making some assumptions [Pawlowski'92].

From the statistical distribution Figure 7.1 and Figure 7.2, the distribution functions assumed by IMO were

$$f(\xi) = \begin{cases} 0.4 + 1.6\xi & 0 \le \xi \le 0.5 \\ 1.2 & 0.5 \le \xi \le 1.0 \end{cases} \qquad \text{(EQ 7.4)}$$

$$f(\lambda) = \frac{1}{\lambda_{max}} 2(1 - y)$$

where $y = \dfrac{\lambda}{\lambda_{max}}$ - is the normalised damage length

λ_{max} - assumed maximum non-dimensional damage length, $\min(\dfrac{48}{L_s}$ or $0.48)$

Factor a in regulation A.265 is

$$a = 0.4[1 + \xi_1 + \xi_2 + \xi_{12}] \qquad \text{(EQ 7.5)}$$

where ξ_1 - minimum of 0.5 or χ_1/L_s

χ_1 - distance from aft terminal of L_s to the aft end of the considered compartment

ξ_2 - minimum of 0.5 or χ_2/L_s

χ_2 - distance from aft terminal of L_s to the forward end of the considered compartment

ξ_{12} - minimum of 1.0 or $(\chi_1+\chi_2)/L_s$

Factor 'p' is given in the form

$$p = W\left[4.46\left(\frac{l}{\lambda}\right)^2 - 6.20\left(\frac{l}{\lambda}\right)^3\right] \text{ if } \left(\frac{l}{\lambda} \le 0.24\right)$$

$$p = W\left[1.072\left(\frac{l}{\lambda}\right) - 0.086\right] \quad \text{if } \left(\frac{l}{\lambda} > 0.24\right) \qquad \text{(EQ 7.6)}$$

where l - length of compartments or group of compartments

$W = 1.0$ and $\lambda = L_s$ for $L_s \le 200$ metres

$W = \dfrac{184}{L_s - 16}$ and $\lambda = 200$ for $L_s > 200$ metre

All damages which open single compartments of length l_i are represented in Figure 7.3 by points in a triangle with base l_i [IMO'74]. Triangles with base $l_i + l_j$ (where $j = i+1$) enclose points corresponding to damages opening either compartment i or compartment j, or both of them. Correspondingly, the points in the parallelogram ij represents damages which open both compartment i and j.

Superimposing the two distribution functions shown in Figure 7.1 and Figure 7.2 on the joint density function shown in Figure 7.4, the total volume between the XY-plane and the surface given by $f(x, y)$ equals one and represents the probability that there is damage (which has been assumed to be certain). The volume above the triangle corresponding to a damage that opens a compartment represents the probability that this compartment only is opened, as shown for a given compartment in Figure 7.4.

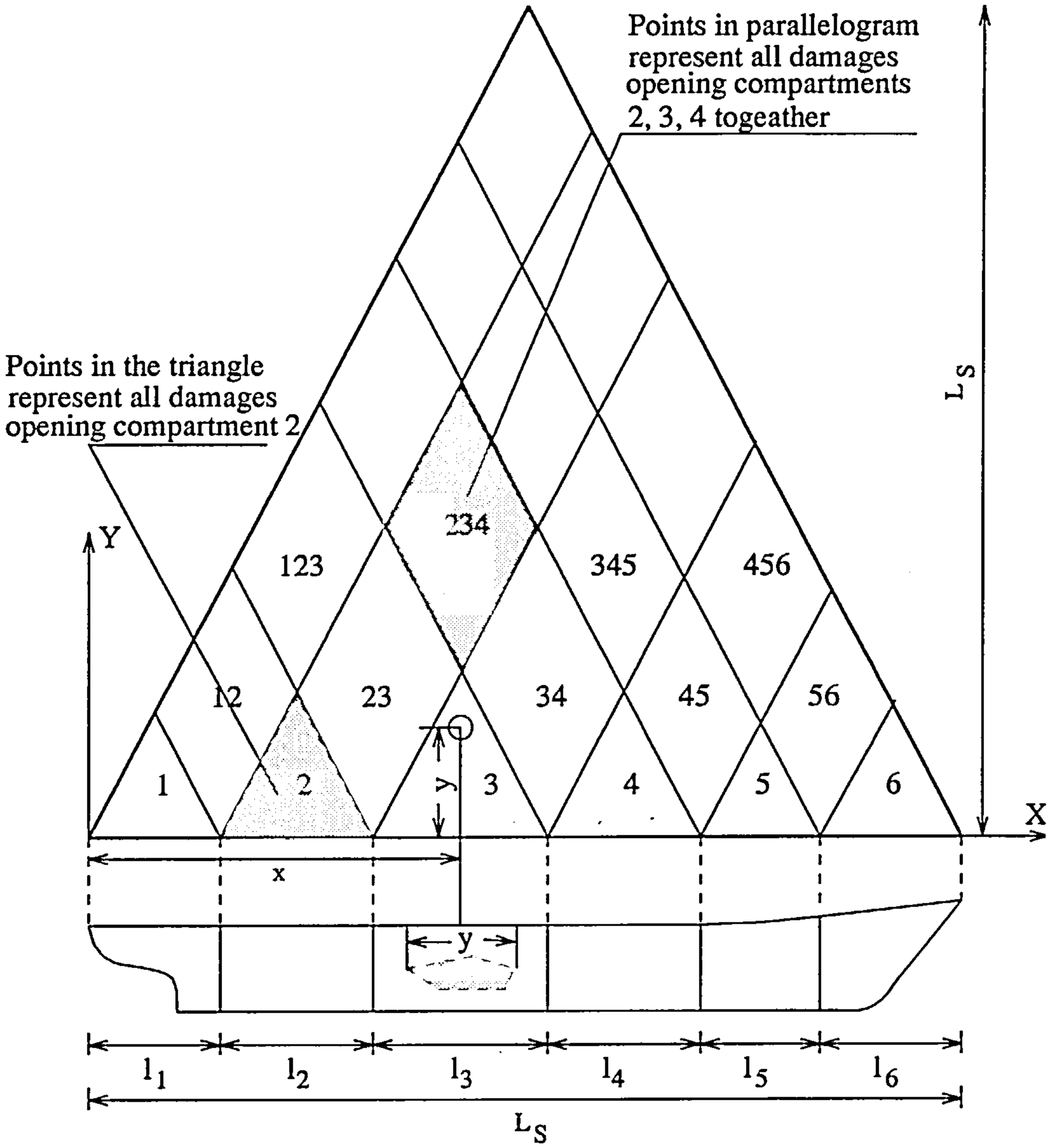

FIGURE 7.3. Triangular area of all possible combinations of damage lengths and locations

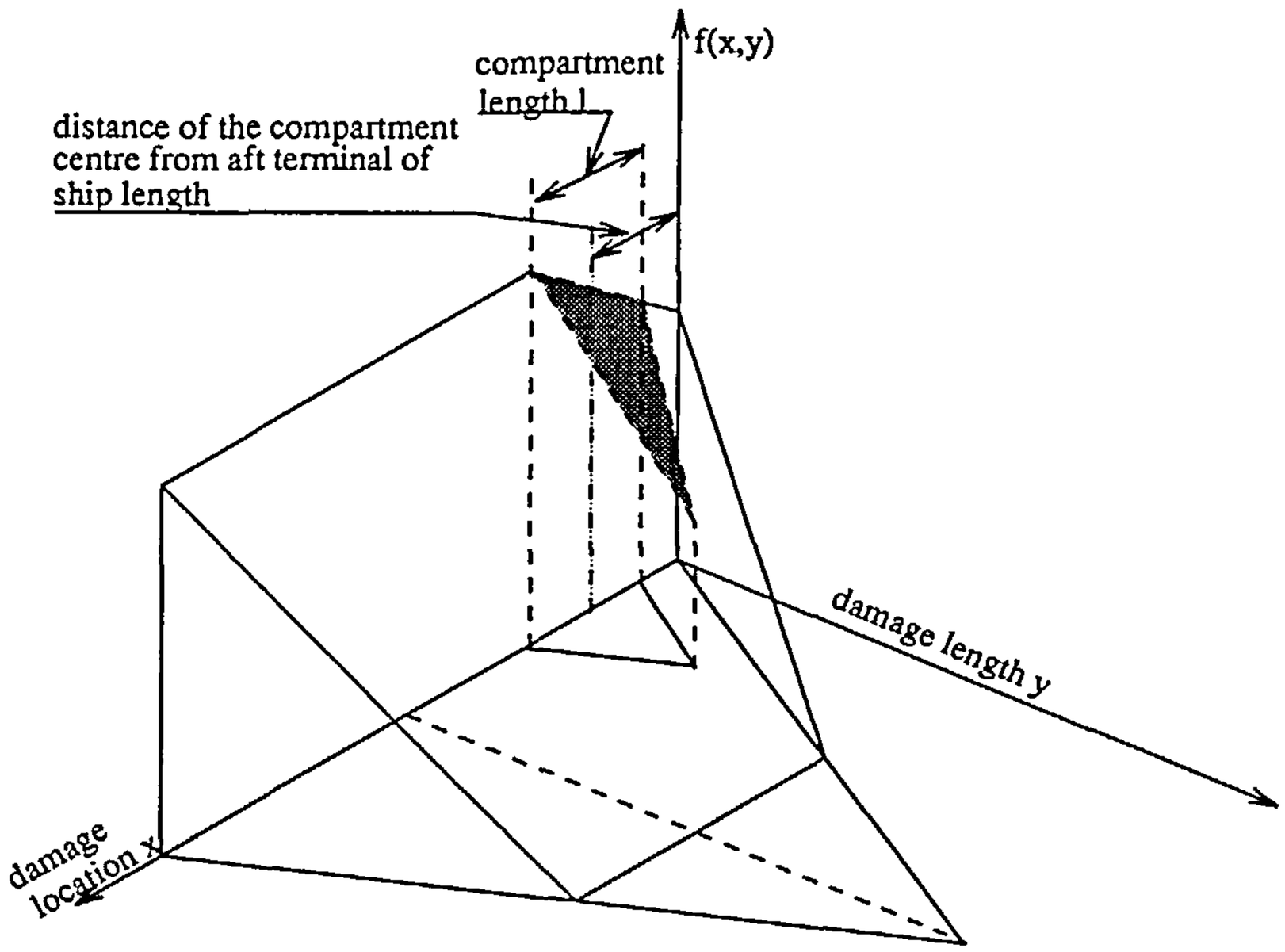

FIGURE 7.4. Joint density function of damage length and location

7.2.4 Factor s

It was a matter of some debate within IMO as to whether factor s should be based on metacentric height, freeboard, and beam or directly on the righting arm curve [Robertson'74]. The righting arm curve is a function of freeboard and metacentric height for a given intact vessel. Model test conducted for a damaged vessel showed that for a given sea state the righting arm depended on freeboard and other factors. For example the righting arm for leeward and windward sides were found to be different in the case of a vessel with a superstructure fitted on the bulkhead deck. It was thought furthermore that there were uncertainties associated with the values of the righting arms due to the effect of water which may be trapped on the deck. Furthermore, the limited experimental eveidence indicated a fairly determinate boundary between the stable and unstable region that could be represented in terms of the freeboard and metacentric height [Robertson'74]. Hence a fairly simple relationship of these latter parameters was established which approximated to the survival probability. The final form of factor s (for dimensions in meters) was obtained as:

$$\left\{ s_i = 4.9\left[\left(\frac{F_1}{B_2} - \frac{\tan\theta}{2}\right)(GM_R - MM_s)\right]^{\frac{1}{2}} \right\} \leq 1.0 \qquad \text{(EQ 7.7)}$$

where F_1 - the effective mean damage freeboard (as explained below)

B_2 - the extreme moulded breadth of the ship at midlength at the relevant bulkhead deck.

θ - the angle of heel due to unsymmetrical flooding in the final condition after cross flooding, if any.

GM_R - the highest required intact metacentric height at the relative draught (Regulation 5(e)[IMO'74]) or if a higher metacentric height is to be specified in the instructions to the master, that value may be used.

MM_s - the reduction in height of the metacentric height as a result of flooding calculated for the ship in the upright position in the final stage of flooding.

From EQ 7.7 it is obvious that s_i reduces to zero when $\tan\theta = F_1/(B_2/2)$. It is apparent from this relationship that, the angle θ at which the subdivision deck immerses, the s_i factor immediately reduces to zero leading to a step-wise variation of the s_i factor.

Also regulation 5(c)(i)(1) states that

> there shall be a positive metacentric height, GM, calculated by the constant displacement method and for the ship in the upright condition, of at least
>
> $$GM = 0.003\frac{B_2^2(N_1 + N_2)}{\Delta F_1} \text{ (metres)}$$
>
> or
>
> $$GM = 0.015\frac{B_2}{F_1} \qquad \text{(EQ 7.8)}$$
>
> or
>
> $$GM = 0.05 \text{ m}$$

where N_1 - number of persons for whom life boats are provided

N_2 - number of persons (including officers and crew) that the ship is

permitted to carry in excess of N_1.

This requirement is on the basis that about one third of the total number of persons (assuming 0.07 tons per person) are located at about $1/4B_2$ off the centreline. It prescribes that the heel under such circumstances should not immerse more than about F_1.

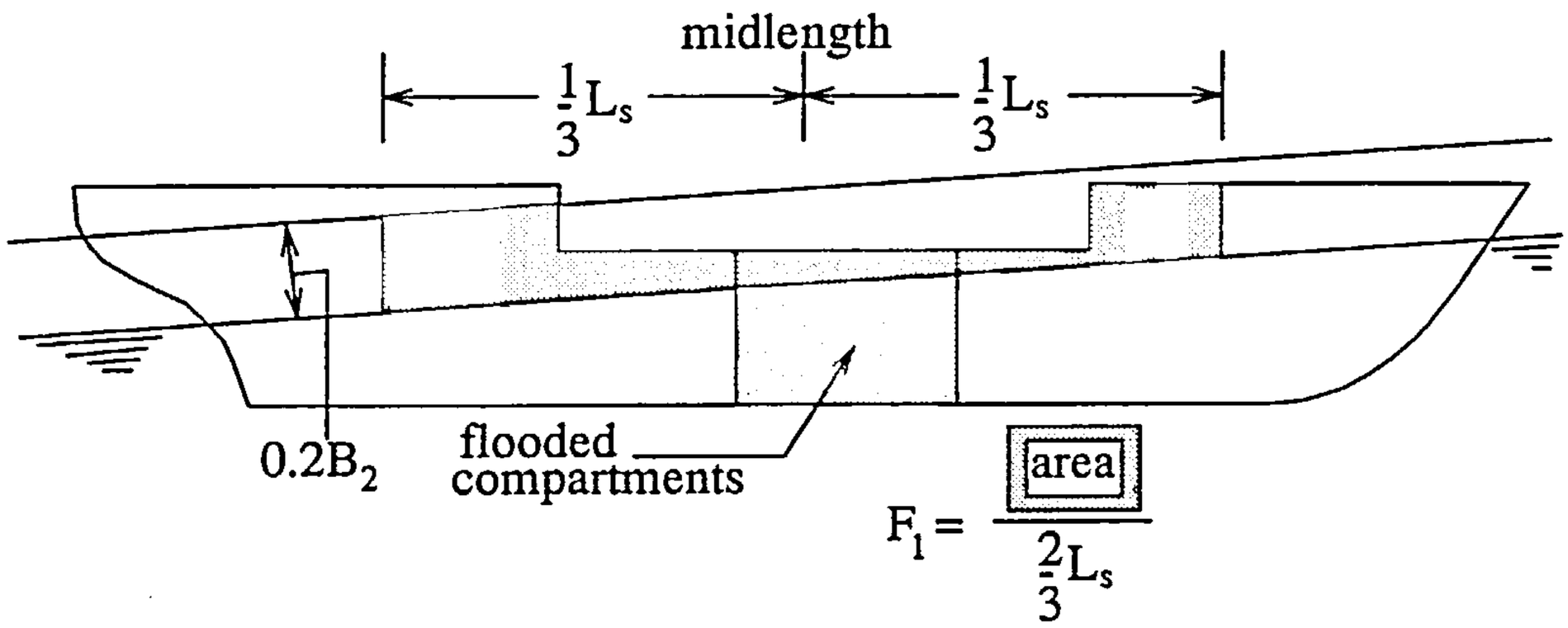

FIGURE 7.5. Illustration of the "effective mean damage freeboard", F_1

F_1 the effective mean damage freeboard, and is defined in Regulation(1)(h) as being equal to the projected area of that part of the ship taken in the upright position between the relevant bulkhead deck (or subdivision deck which defines the limit of watertight integrity in the flooded condition, Regulation(1)(e)), and the damaged waterline and between $\frac{1}{3}L_s$ forward and abaft the midlength divided by $\frac{2}{3}L_s$ (see Figure 7.5). In making this calculation no part of the area which is more than $0.2B_2$ above the damaged waterline shall be included.

Regulation 5(b)(i) states that ships must be able to withstand the event of flooding due to one side damage with a penetration of $0.2B_1$ (B_1 is the extreme moulded breadth at midlength at or below the deepest subdivision loadline Regulation(1)(d)(i)) at right angles to the centreline on the ship's side. The extent of longitudinal damage is $(3 + 0.03L_s)$ metres or 11 metres, whichever is less, located anywhere on the ships length but not including a transverse bulkhead.

However Regulation 5(b)(ii) extends the above to include transverse bulkheads occurring anywhere within a length equal to $\left(\frac{N}{600} - 1.0\right)L_s$ measured from the forward terminal of L_s, Figure 7.6.

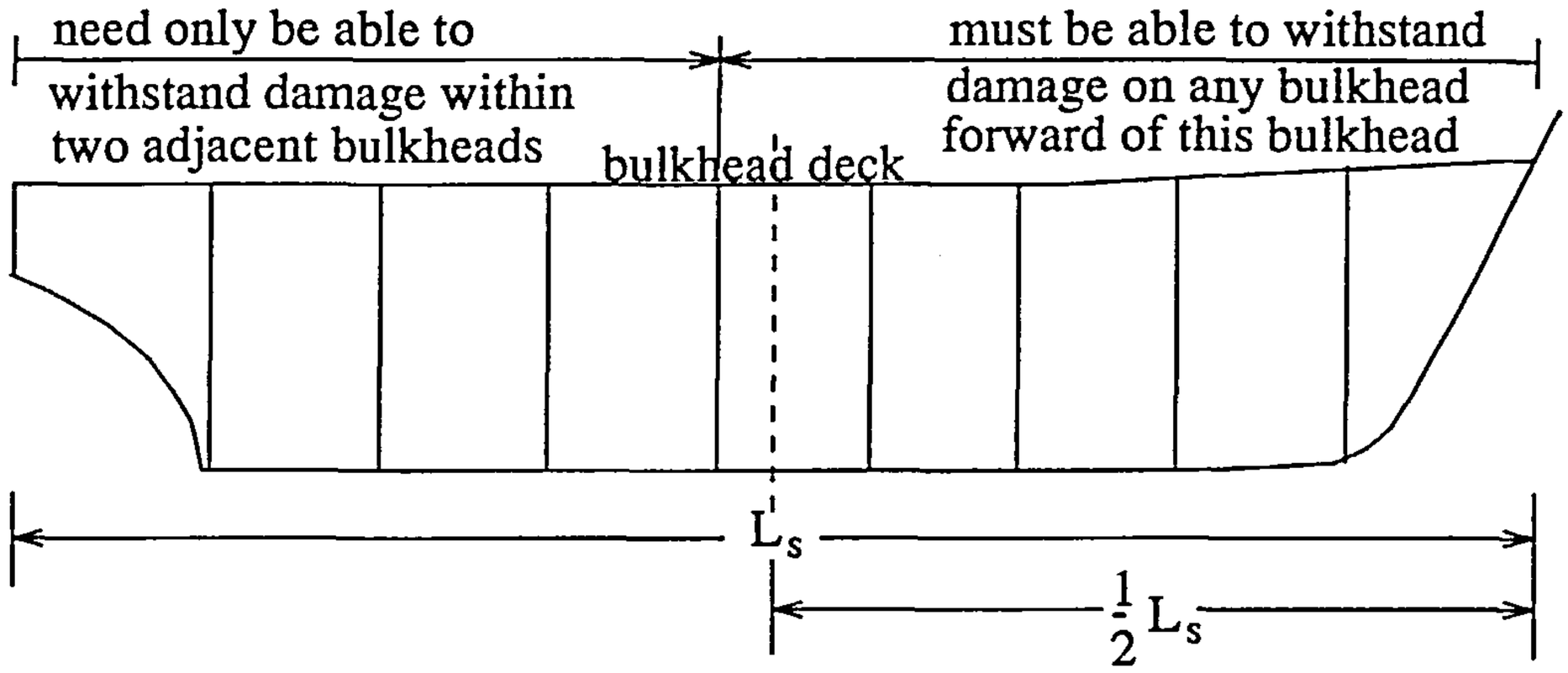

FIGURE 7.6. Illustration of regulation 5(b)(ii) for N=900

The value of $\left(\frac{N}{600} - 1.0\right)$ shall not be more than one. This may be interpreted literally to mean that N cannot be more than 1200. The intention of the regulations is that any ship for which N is 1200 or more be able to withstand the prescribed side damage at any point in its entire length [Robertson'74]. This is tantamount to a two compartment damage situation.

7.2.5 Factor r

The largest ratio of non-dimensional damage penetration to damage length should be in the case of right angle collisions, when the striking vessel has a rigid bow [Pawlowski'92].

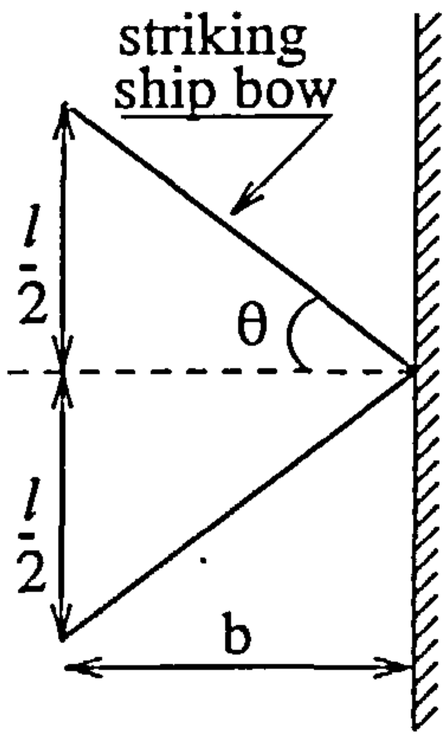

FIGURE 7.7. Damage penetration to damage length relationship

The following relationship therefore holds

$$l = 2b\tan\theta \leq B_{str}$$

where B_{str} is the breadth of the striking vessel

$$\frac{l}{L_s} = 2\frac{b}{B}\frac{B}{L}\tan\theta \leq \frac{B_{str}}{L_s}$$

$$\lambda = 2\zeta\frac{B}{L_s}\tan\theta \leq \frac{B_{str}}{L_s}$$

where ζ is the non-dimensional damage penetration.

Assuming that the smallest practical value of $2\frac{B}{L}\tan\theta$ equals 0.12,

$$\zeta = \begin{cases} \dfrac{\lambda}{0.12} & \text{if } \lambda < 0.12 \\ 1.0 & \text{otherwise} \end{cases} \qquad \text{(EQ 7.9)}$$

In other words the depth of damage is related to the longitudinal extent of damage.

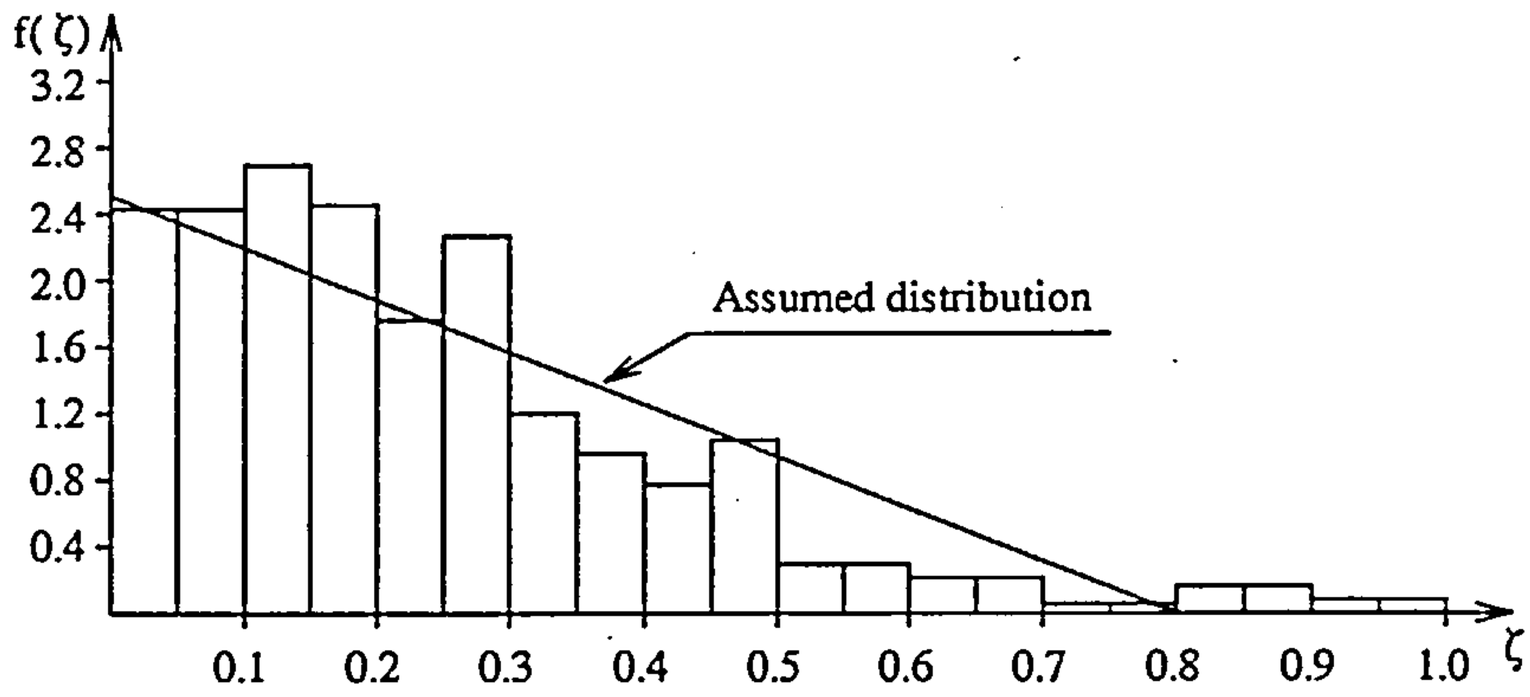

FIGURE 7.8. p.d.f of damage penetration

IMO approximates the distribution of damage penetration (Figure 7.8) very roughly, using a linear distribution whose distribution function is

$$f(\zeta) = \frac{2}{\zeta_{max}}(1 - z) \qquad \text{(EQ 7.10)}$$

where $z = \frac{\zeta}{\zeta_{max}}$ - the normalized damage penetration

ζ_{max} - assumed maximum non-dimensional damage penetration = 0.8

The factor r, which represents the probability that the inboard spaces will not be flooded as defined in A.265 is

$$r = \frac{b}{B_1}\left[2.8 + \frac{0.08}{\left(\frac{l}{L_s} + 0.02\right)}\right] \text{ if } \frac{b}{B_1} \leq 0.2 \qquad \text{(EQ 7.11)}$$

$$r = \frac{0.016}{\left(\frac{l}{L_s} + 0.02\right)} + \frac{b}{B_1} + 0.31 \text{ if } \frac{b}{B_1} > 0.2$$

when $\frac{l}{L_s} < 0.2\frac{b}{B_1}$, r shall be determined by linear interpolation between 1.0 for $\frac{l}{L_s} = 0$ and r value calculated by (EQ 7.11) for $\frac{l}{L_s} = 0.2\frac{b}{B_1}$.

7.3 The Required Index R

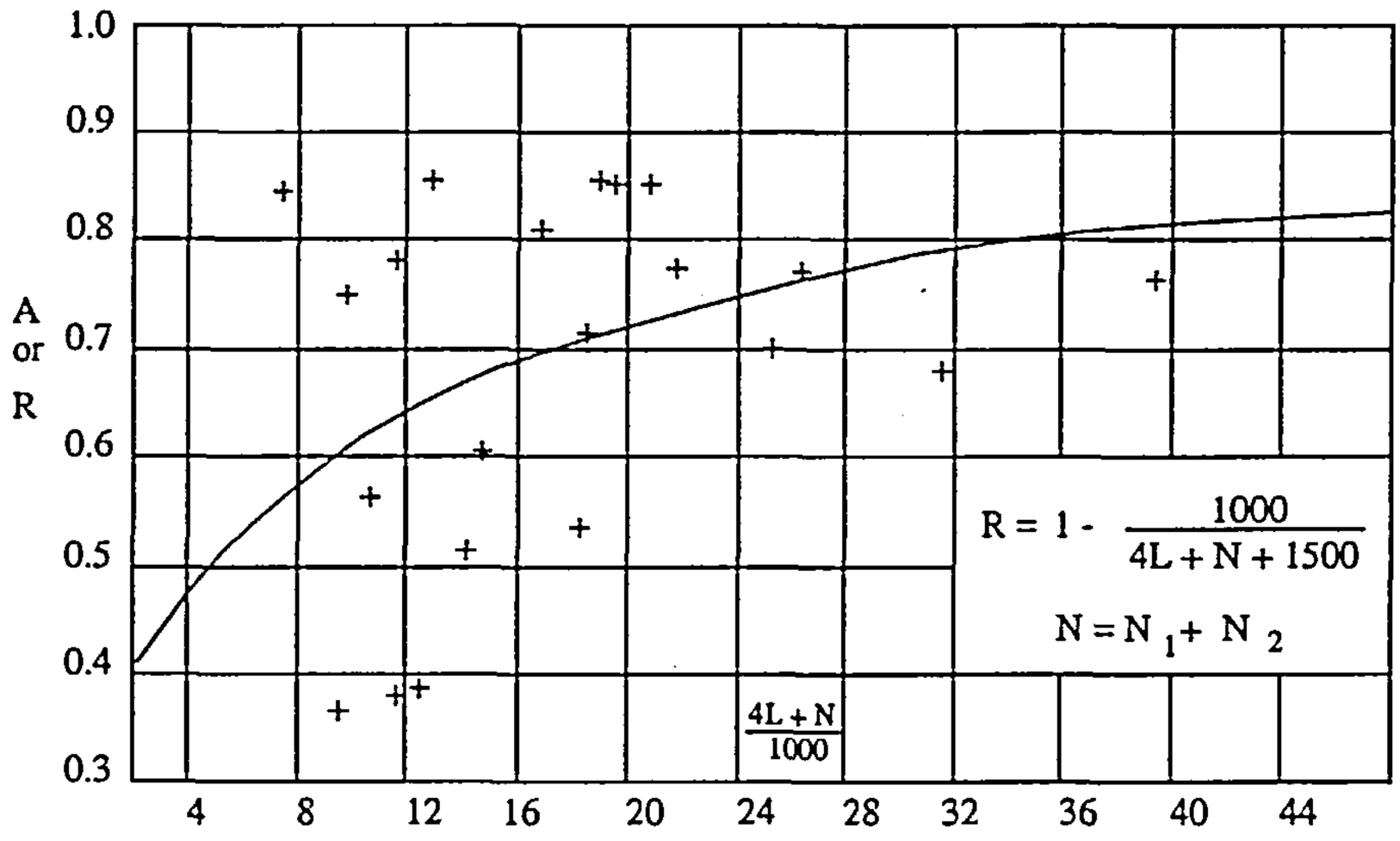

FIGURE 7.9. Comparison of R with calculated A values

Figure 7.9 shows the A values of some existing ships designed on the basis of the 1960 regulations and the R values prescribed in A.265 as,

$$R = 1 - \frac{1000}{4L_s + N + 1500}$$

where $N = N_1 + N_2$ (N_1, N_2 are as defined in section 7.2.4).

"Because the Regulations in the 1960 Safety convention under which these ships were constructed are illogical, it would be surprising if these A values did not show considerable scatter"[IMO'74].

It will be observed from Figure 7.9 that the required index value R has been pitched in the regulations at about the average value for existing ships. Though this left many delegations unhappy, who thought a higher standard was practical and necessary, it did help to complete the very extensive and drawn out work that went into drawing up these regulations. The regulations were therefore agreed upon with the belief that a higher standard of safety would eventually evolve as the experience in design of ships to the new regulations grew.

7.4 Local indices of Subdivision

In the probabilistic approach to subdivision, the attained index of subdivision A is computed for each design arrangement. The value of A, lying between 0 and 1, is representative of the probability of survival and is calculated according to (EQ 7.2).

The contribution of a given compartment to the overall index A can be estimated by adding up all the terms of the product of a, p and s involving that compartment, that is,

$$a_k = \sum_{i \in K} a_i \, p_i \, s_i \qquad \text{(EQ 7.12)}$$

where k is the compartment under consideration and K is the set of all combinations that include compartment k. The local index of subdivision for that compartment can therefore be expressed as

$$A_l = \frac{\sum_{i \in K} a_i \, p_i \, s_i}{\sum_{i \in K} a_i \, p_i} \qquad \text{(EQ 7.13)}$$

which represents the survivability contribution of all possible combinations involving the said compartment.

From (EQ 7.13) it can be concluded that the local index becomes zero for any compartment with excessive length and/or breadth, that is for which factor $s_i = 0$. As distinct from the local indices, the attained index of subdivision could be called the *overall* or *global* index of subdivision.

Pawlowski [Pawlowski'92] proposed that this concept of local indices of subdivision be incorporated into regulation 5 of A.265 in the form of a fraction of overall index. To quote Pawlowski,

> "Apart from being consistent with the probabilistic method, such a requirement is simple, clean and easy to handle. It prevents a ship from having compartments with excessive lengths & breadths, that is, ensures that no part of the ship is too vulnerable to flooding. On the other hand, contrary to the situation in the present regulations, there is no need for setting lower limits for bulkhead spacing nor for a standard depth of penetration, or in other words, for the prescribed size of damage".

TABLE 7.1 : Values of local indices required by (current) regulation 5 [IMO'74]

	100m	150m	200m	250m
One compartment	0.100	0.075	0.063	0.083
Two compartment	0.420	0.328	0.283	0.352

TABLE 7.2 : Fractions of the required (overall) indices of subdivision

One compartment N = 600	17%	12%	9.6%	12%
Two compartment N = 1200	62%	47%	40%	48%

Table 7.1 and Table 7.2 give the local index calculated by Pawlowski [Pawlowski'92] for different ship lengths. The variations of the local indices have no justification, and moreover the values particularly for ships with one compartment standard is set at a very low level which Pawlowski describes as being "unacceptable for the profession and the travelling public".

The overall index of subdivision can be considered as an average of the local indices, and hence small values at certain parts of the ship must be counteracted by high values at

other region to keep the overall index above a certain value. Since indices cannot be arbitrarily high, and high values are difficult to achieve, a large scatter can be symptomatic of an "non-optimal" overall index. Hence, in general, ships should be designed with a minimum scatter of the local index value so as to attain the best value of the overall maximum.

7.5 Knowledge based expert system

One of the ideas explored to achieve this [Sen'92] was the use of knowledge based system in order to examine the design space for designs improved from the subdivision point of view. The rationale behind this approach was to separate out the logical processing elements of computer aided design from the knowledge elements so that incremental advances in design expertise can be easily incorporated into the system as the expertise grows over a period of time.

The task of processing the knowledge domain is carried out by the inference engine. The inference engine of the knowledge based system developed was based on a combination of the backward chaining and the forward chaining system. The knowledge base consisted essentially of

- design formulae for estimating the characteristics of a design incorporating external procedures and databases.
- design rules which either control the sequence of execution of external routines or make decisions about changes in design layout.
- interfacing rules which control communication with the expert system.

The expert system used the concept of local indices built into the "expertise" as a system of rules to constitute the driving mechanism to change the bulkhead position.The rules were based on the insight that if compartments with low local index values are reduced in size then the overall A index will increase in magnitude due to a resultant smoother distribution of the local index values. However, as shown in the subsequent sections, the stepwise variation of the s-factor values made the use of expert system cumbersome and inefficient.

7.6 Variation in a, p and s

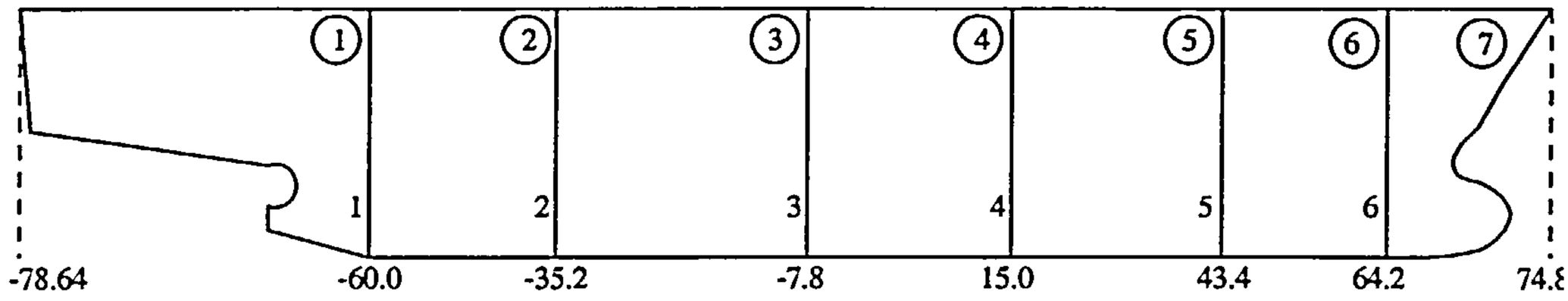

FIGURE 7.10. A passenger ferry type vessel

Figure 7.10 shows a passenger ferry type vessel, which is identical to that used in the development of the expert system [Sen'92] . The pricipal dimensions of the vessel were as follows:

L_s: 153.51 m
LBP: 148.0 m
B: 24.0 m
D: 13.9 m
d_o: 6.0 m
d_s: 9.0 m

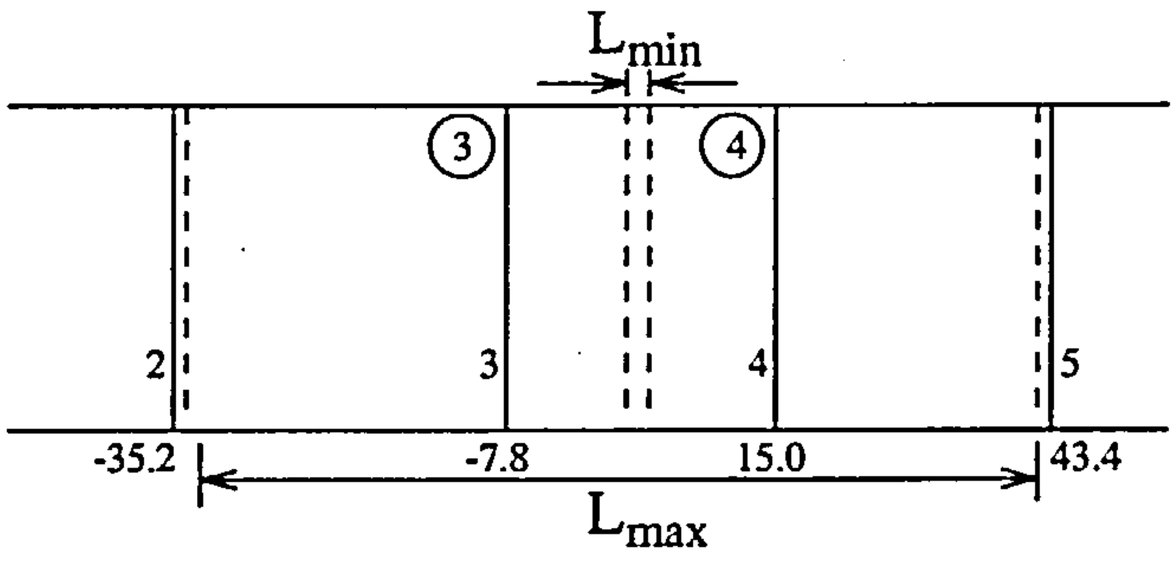

FIGURE 7.11. Variation in compartment lengths

The a, p and s values for each compartment was found by varying the bulkhead positions such that the compartment lengths varied in steps from a small value L_{min} to a maximum value L_{max}, bound by the adjacent bulkheads. Figure 7.11 shows the variation in the compartment length for compartment number 4.

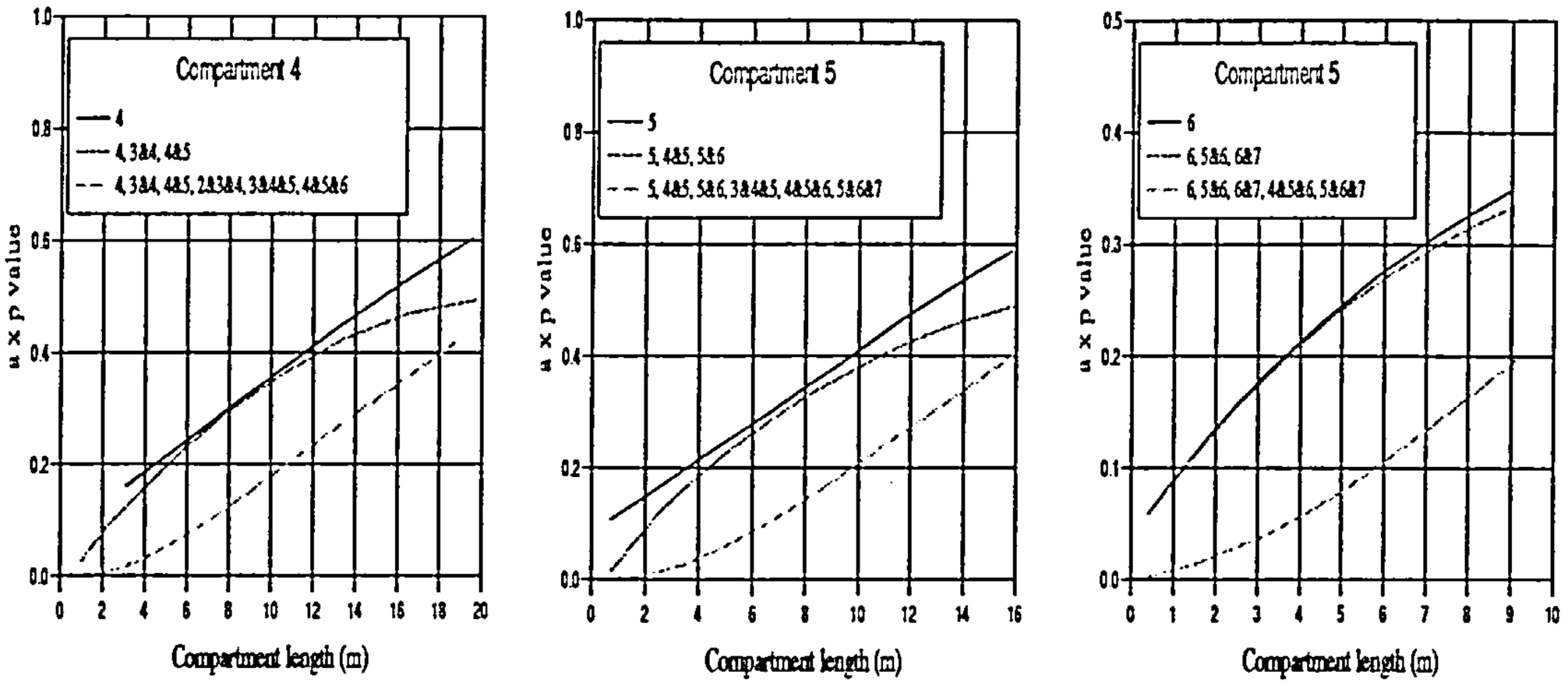

FIGURE 7.12. Variation of ap with length

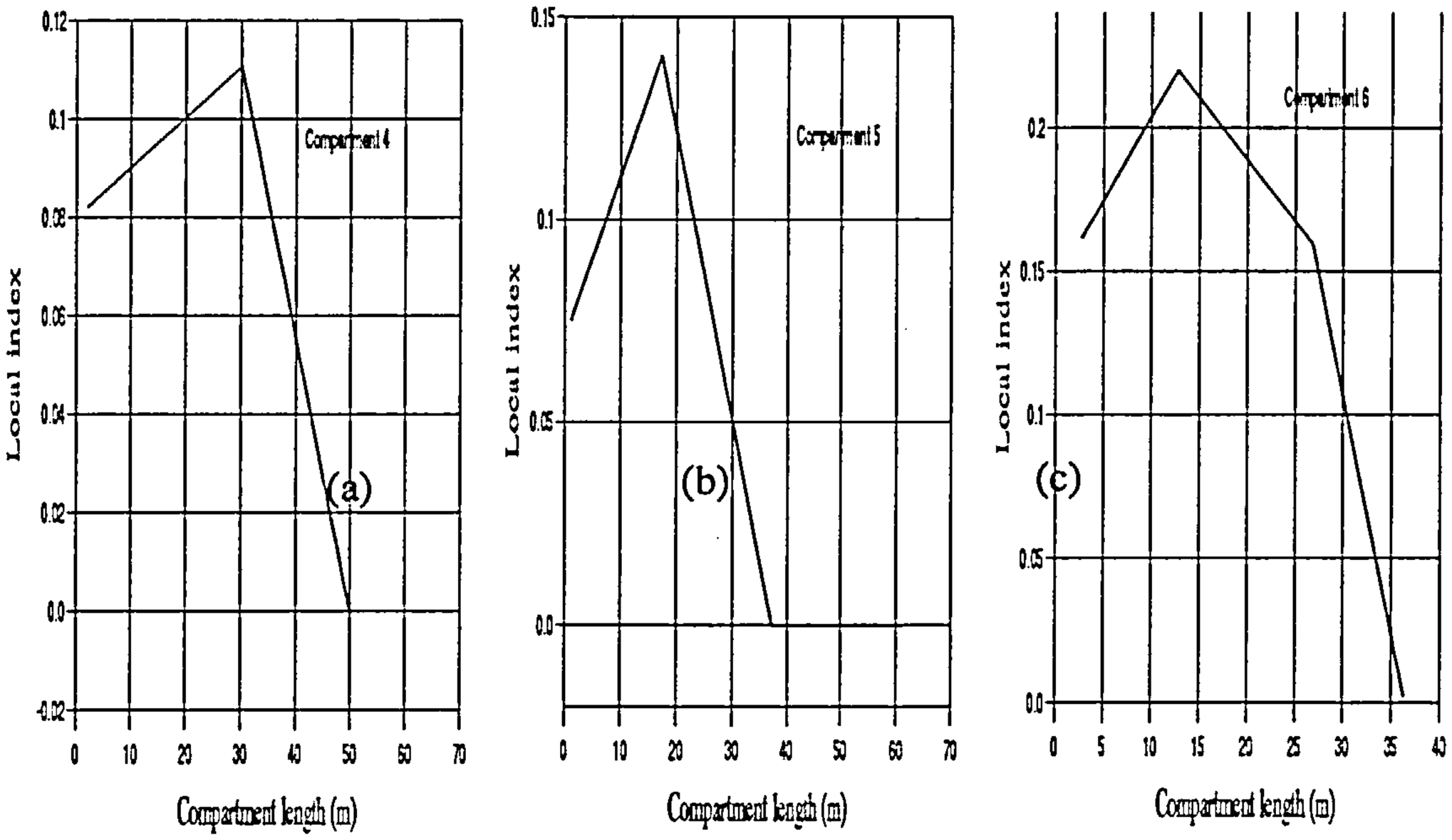

FIGURE 7.13. Variation of local index with length

In figure 7.12 (a), (b), (c) the product of the a and p values is plotted for compartments 4, 5 and 6 respectively for one, one and two and one, two and three compartments taken together. Figure 7.13 (a), (b) and (c) gives the local index variation for compartments 4, 5 and 6 respectively. As seen in Figure 7.12, the variation in the a p curves is very

smooth but the variation in the local index in Figure 7.13 is much more unpredictable and stepwise. This is principally due to the stepwise variation of the s values, as the rules currently stand.

The a, p and s values (Figure 7.10) were calculated for a fixed set of variations in the positions of the bulkheads. The a, p and s value for any arbitrary configuration of the bulkheads was then found by interpolation of the tabulated a, p and s values. Since there were seven compartments involved this resulted in an interpolation in seven dimensions to obtain the required a, p and s values for any arbitrary bulkhead configuration.

This interpolation technique was then used along with a genetic algorithm to determine different configuration of the bulkhead positions. These bulkhead configurations are a result of the interpolation of the a, p and s curves assuming that they are smoothly varying functions. The difference between the interpolated and actual results for a typical bulkhead layout determined by the GA are,

TABLE 7.3 : Bulkhead positions from the GA output

Bulkhead No.	Bulkhead position
1	-55.0
2	-39.1
3	-19.9
4	12.9
5	48.3
6	51.9

TABLE 7.4 : Comparison between interpolated and actual a, p and s values

Combn. No.	Interpolated			Actual		
	a	p	s	a	p	s
1	0.522758	0.083440	1.000000	0.52276	0.08261	1.00
2	0.728080	0.050348	1.000000	0.72808	0.04069	1.00
3	0.910347	0.069073	0.896587	0.91035	0.05727	1.00
4	1.142698	0.150577	1.000000	1.14270	0.14233	1.00
5	1.200000	0.163112	0.931313	1.20000	0.16026	0.00
6	1.200000	0.006257	1.000000	1.20000	0.00236	1.00
7	1.200000	0.082485	1.000000	1.20000	0.08189	1.00
8	0.605324	0.055366	0.787605	0.60532	0.06583	0.33
9	0.827782	0.040184	0.325000	0.82778	0.06023	0.00
10	1.042997	0.056182	0.434444	1.04300	0.07623	0.00

TABLE 7.4 : Comparison between interpolated and actual a, p and s values

Combn. No.	Interpolated			Actual		
	a	p	s	a	p	s
11	1.152512	0.074868	0.000000	1.15251	0.08596	0.00
12	1.200000	0.016007	0.000000	1.20000	0.02275	0.00
13	1.200000	0.015832	0.987506	1.20000	0.02014	1.00
14	1.200000	0.065338	0.000000	1.20000	0.06163	0.00
A-Index	0.678924			0.426005		

The bulkhead positions shown in Table 7.3 were used in the damage stability software to calculate the actual a, p and s values for this internal configuration. Table 7.4 compares the interpolated and their actual a, p, s values for the vessel for each of the 14 damage combinations involved. The a and p values show a very good match which is not surprising given the smooth variation in the a and p values. However the s values show a tremendous variation due to the stepwise variation in the s values with variation in the compartment length. The resultant A index values obviously and understandably do not compare well. However these step changes inherent in the regulations also make the case for the use of an adaptive optimisation method like GA's, as such methods are better able to deal with multimodality.

Wimalasiri [Wimalasiri'91] investigated this behaviour of the s curve. He reasoned that the main reason for this binary flip in the s-factor value in the cases of flooding is that the s factor reduces to 0 when the final waterline is above the subdivision deck. Wimalasiri termed them as the "cliff edge" effects and suggested remedial measures to smoothing out this phenomena.

The s-factor formulation adopted by Wimalasiri was that specified in the cargo ship regulations given as,

$$s_i = \sqrt{0.5(GZ_{max})(Range)} \qquad \text{(EQ 7.14)}$$

GZmax - maximum positive righting lever (in m) within the range as given below but not greater than 0.1m.

Range - range of positive levers beyond the angle of equilibrium but not more than 20° . However the range shall be determined at the angle where openings not capable of being closed weathertight

are immersed.

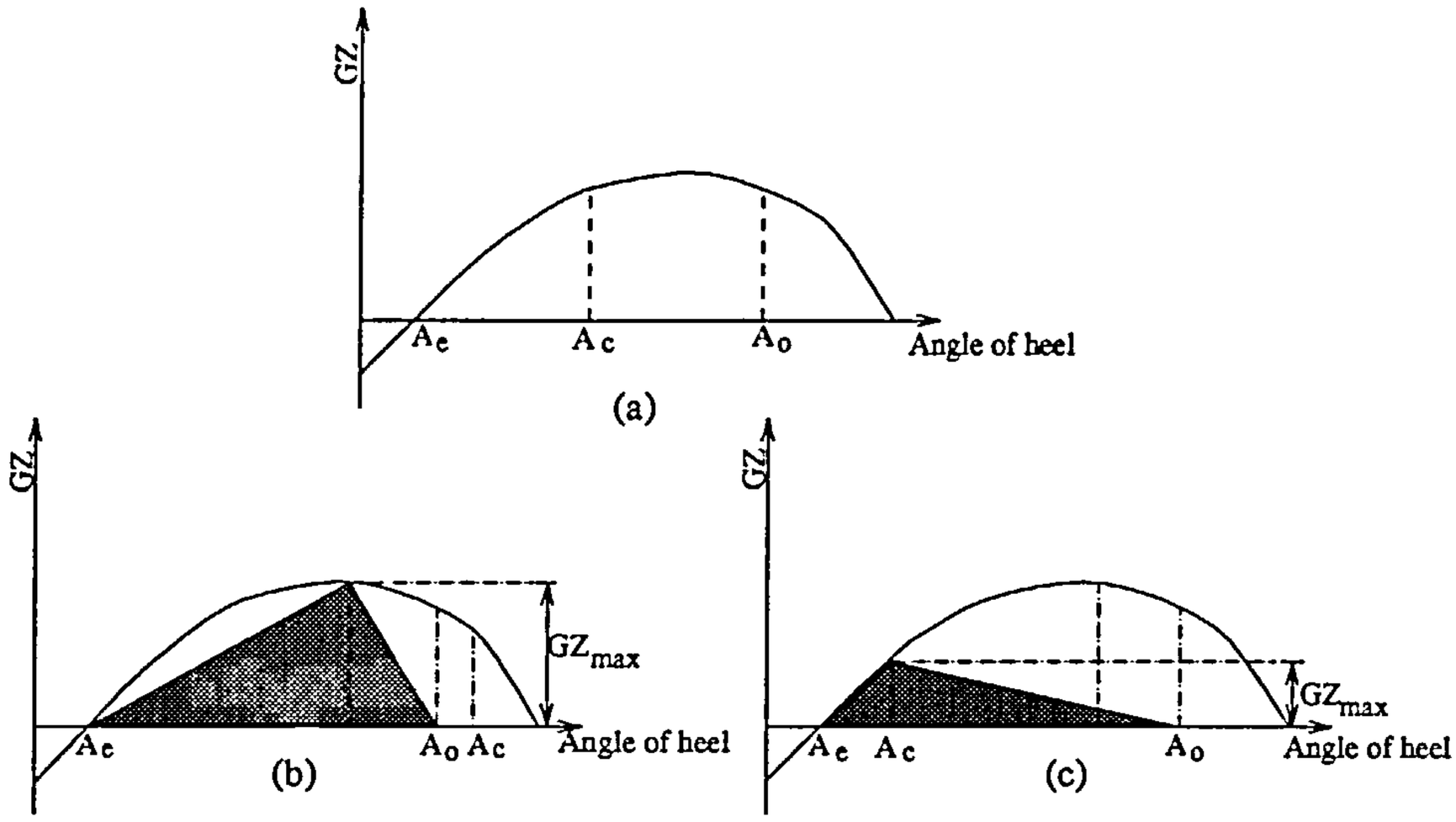

FIGURE 7.14. Modification of the s factor

In Figure 7.14(a)

A_e - angle of equilibrium

A_c - angle of immersion of openings closed weathertight

A_o - angle of immersion of openings which cannot be closed weathertight.

For cases where $A_o < A_c$, Figure 7.14(b), s is calculated as shown by the shaded area in accordance with the regulation. For cases where $A_o > A_c$, Figure 7.14(c), the definition of range remains according to that specified in the regulations but the maximum GZ value is measured within the range up to A_c but not more than 0.1m. With the help of this new formulation Wimalasiri demonstrated the smoothening of the s curve. The ruling idea is that if A_c approaches A_e the s-factor is gradually reduced, rather than in a stepwise variation. However since this modification was for the cargo ship formulation it could not be readily incorporated into the current model which was for passenger vessels.

7.7 Attained index optimisation

An even distribution of the local index, which can be thought of as a measure of "survivability" of a vessel, should in general result in an higher A-index value. The optimisation procedure for such a mathematical model should

i. evaluate the local index distribution for a given internal subdivision arrangement.

ii. evaluate the "performance" of this arrangement in terms of the A-index value.

iii. select the best internal configuration generated and if possible improve on it.

The first task was, however, to check the nature of the "performance landscape". The presence of multiple local maxima in the solution space would obviously require a more complex search technique than in a unimodal situation since in multi-modal domains there is always the danger of getting trapped in regions of local optima. The vessel shown in Figure 7.10 was used for this investigation.

TABLE 7.5 : Bulkhead positions

Bulkhead no.	Position 1	Position 2	Position 3
1	-65.2	-58.0	-50.8
2	-48.875	-38.75	-28.625
3	-26.125	-13.75	-1.375
4	1.375	13.75	26.125
5	28.625	38.75	48.875
6	51.1	61.0	70.9

Three distinct positions were chosen for each of the six bulkheads as shown in Table 7.5. Since there were three positions for each bulkhead and six bulkheads in total, this resulted in $3^6 = 729$ different internal configurations to be evaluated. For each of these configurations, the a, p and s values for all the damage combinations were determined. The A-index was then evaluated for all the 729 configurations..

TABLE 7.6 : Multimodality in the performance landscape

Configuration no.	A-index	Bulkhead position
24	0.34322	1 1 1 3 2 3
141	0.34369	1 2 3 1 2 3
351	0.34392	2 2 1 3 3 3
588	0.34398	3 2 1 3 1 3
86	0.44902	1 2 1 1 2 2
110	0.44964	1 2 2 1 1 2
262	0.44970	2 1 1 3 1 1
583	0.44985	3 2 1 2 3 1

In Table 7.6, the configuration number refers to one of the 729 internal configurations generated. The corresponding bulkhead position combination is represented in the table by a string of six numbers each of which refers to the respective bulkhead position listed in Table 7.5. Therefore, 1 1 1 3 2 3 = -65.2 -48.875 -26.125 26.125 38.75 70.9

As can be seen from Table 7.6, vastly different bulkhead positions give almost the same A-index value which confirmed the fact that the "performance landscape" was indeed many peaked. Also given the fact that the A-index formulation could not be expressed as a system of equations given the nature of the passenger ship regulations, this problem was best suited for the application of genetic algorithms.

The optimisation of the vessel shown in Figure 7.10 was carried out keeping bulkheads 1 and 6 fixed. The population size of the gene pool was taken as 50 and the bit string length that decoded to bulkhead positions was taken as 3. This meant that each bulkhead could not assume more than seven positions within its given range but even this resulted in $7^4 = 2401$ possible internal configurations to be evaluated. In order to achieve speed-ups the calculations were performed in parallel with the help of a cluster of UNIX machines with PVM as the message passing interface.

Table 7.7 lists the a, p and s values for generations 0, 6 and 15 respectively with 9 damage combinations for each case. Improvements in the a, p and s values for each successive generation can be seen but the most dramatic changes occur for the s value for combination 4.

TABLE 7.7 : a, p, s and A-index value for successive GA generations

Combn. no.	Generation 0			Generation 6			Generation 15		
	a	p	s	a	p	s	a	p	s
1	0.490	0.047	1.0	0.588	0.166	1.0	0.588	0.166	1.0
2	0.899	0.354	0.0	0.906	0.091	1.0	0.881	0.062	1.0
3	1.200	0.082	1.0	1.159	0.135	1.0	1.143	0.195	1.0
4	1.200	0.153	0.0	1.200	0.110	0.45	1.200	0.087	0.78
5	1.200	0.038	1.0	1.200	0.144	1.0	1.200	0.144	1.0
6	0.809	0.073	0.0	0.718	0.083	0.0	0.693	0.078	0.0
7	0.961	0.082	0.0	1.029	0.083	0.0	1.039	0.078	0.0
8	1.200	0.082	0.0	1.159	0.085	0.0	1.146	0.082	0.0
9	1.200	0.068	0.0	1.200	0.085	0.0	1.200	0.082	0.0
A-index	0.168			0.569			0.629		

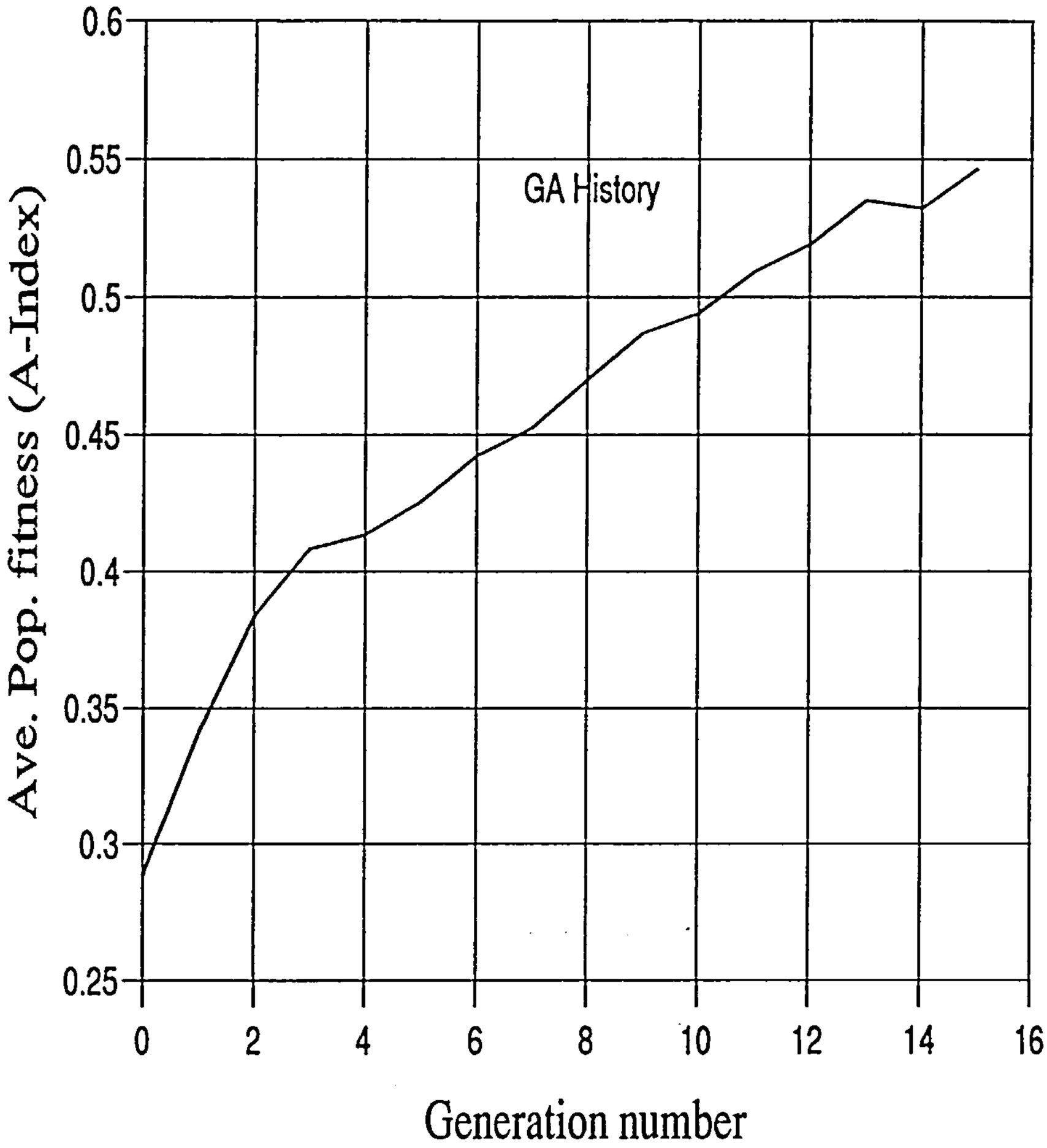

FIGURE 7.15. GA history

Figure 7.15 gives the iteration history of the optimisation process in terms of the average fitness value of the gene pool with every passing generation. As expected fitter members start dominating the gene pool as the generations progress resulting in increasing average population fitness values.

Figure 7.16 shows the variation in the local index values as the genetic algorithm progressed. The figures also displays the local index variation along with the bulkhead positions. The x-axis in each of the histograms represents the bulkhead position as shown in the top left graph of Figure 7.16. The height of the bar represent the local index value for each zone along the ship's length.

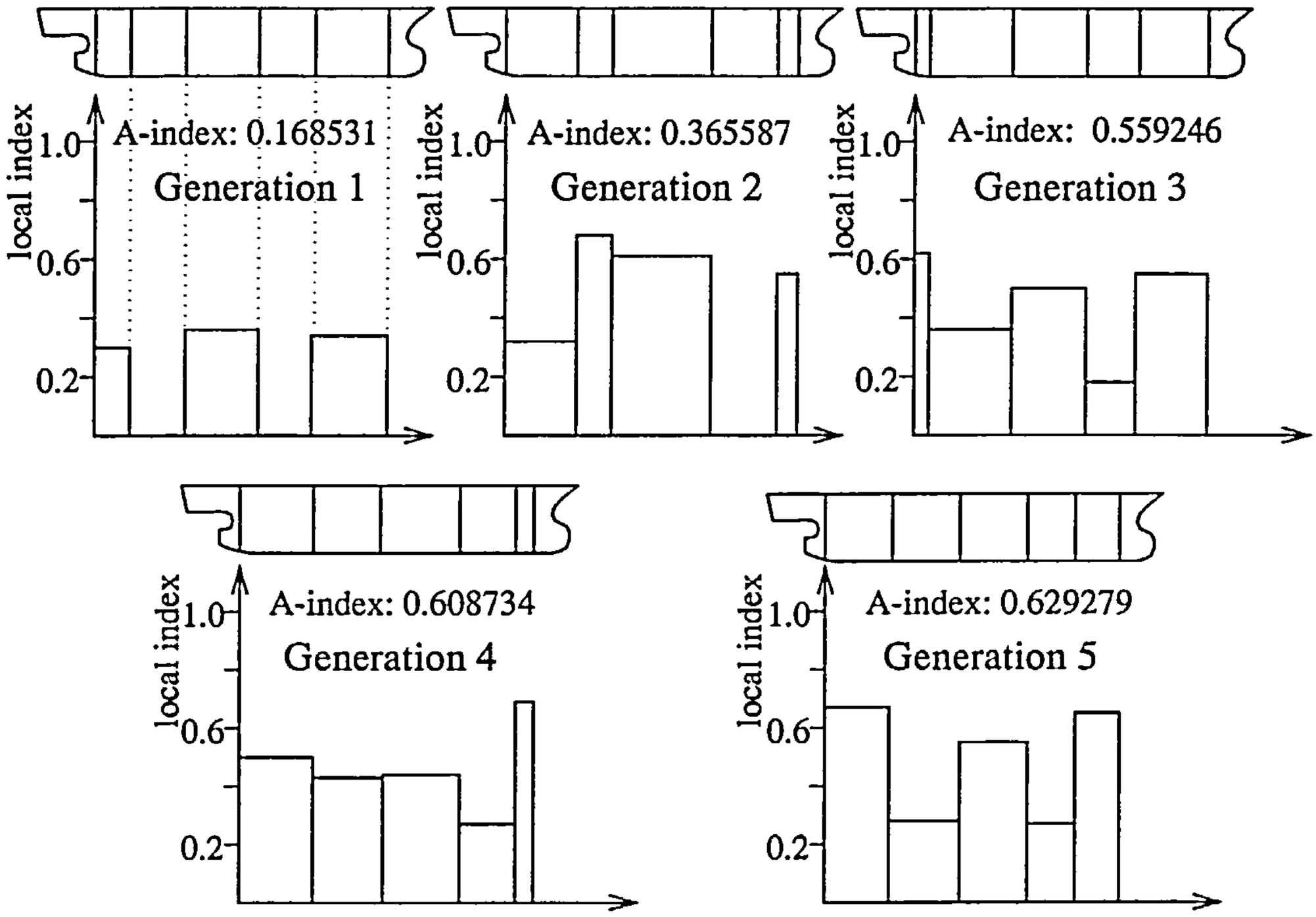

FIGURE 7.16. History of local index variation

There is no one-to-one correspondence between the movement of a bulkhead and the change in the local index value. This is due to the complex nature of the s factor for the passenger ship regulations which results in the "cliff edge" effect. When a compartment length exceeds a certain threshold value, then either that compartment taken singly or jointly with adjacent compartments fails to survive in the damaged condition. On the other hand the single compartment does survive but it fails to survive when combined with two or three adjacent compartments. This has a complex effect on the behaviour of the local index curve. However Figure 7.16 does demonstrate the fact that better A-index values can be achieved with a more even distribution of the local index value along the ship's length. This property allows designers to approach the design task with greater control than the arbitrary positioning of bulkheads and repeated analysis in terms of A-index values.

Chapter 8

Investigations into

Oil Tanker Subdivision

8.1 Introduction

The history of cargo ship probabilistic subdivision regulations shares a lot of its initial history with that for passenger vessels. The differing nature of their operation inevitably led to certain differences in the formulation of these rules.

The potential pollution problems associated with the use of double bottom tanks for fuel oil and ballast water was recognised in the early 50's [Tagg'82]. The problem included the oil pollution of harbours along with the problems of fuel contamination and tank cleaning problems. A conference on the prevention of pollution of the sea by oil in 1954 involving 32 nations banned the discharge of oil within 50 miles of land and called for the installation of oily ballast receiving facilities at all ports. Also in 1966, the international conference on load lines (ICLL) proposed a one compartment standard for tankships and other reduced freeboard cargo ships.

Concern regarding tanker safety grew over the sixties as the overall size of tankers grew along with the size of the cargo tanks, especially in the period following the closure of the Suez Canal in 1967. It wasn't until 1973 that the international conference on marine pollution (MARPOL'73) established a two-compartment standard for most tankships. It

also introduced new restrictions limiting the size of cargo tanks and more importantly made provision for a set of segregated ballast tanks (SBT). However the recommendations of MARPOL'73 were deterministic in nature because the requirements for tank size and location were based on specific damage assumptions. For instance it prescribed that the calculated hypothetical outflow anywhere along the length of the ship should not exceed $30{,}000m^3$ or $400\sqrt[3]{Deadweight}$ whichever is greater, subject to a maximum of $40{,}000m^3$.

TSPP'78, the IMO conference on tanker safety and pollution prevention convened in 1978, was driven by the US Administration due to the increasing concern amongst the US public after a series of tanker accidents in 76/77. Among the various proposals made were a minimum double bottom height of 2 metres or $B/15$, whichever is less, in all new tankers of 20,000 tonnes deadweight and over and the use of segregated ballast tanks in all tankers over 20,000 tonnes deadweight as a means of reducing oil outflow in the event of damage due to collisions. A "conflict of interest" between the legislators and the ship operators led to a compromise solution and resulted in what came to be known as the protective location (PL) of ballast tanks as an alternative to the fitting of double bottom tanks. The PL requirements of SBT was defined as [TSPP'78]:

$$\sum PA_C + \sum PA_S \geq J[L_T(B + 2D)]$$

where PA_C - side shell area (m^3) for each SBT for space other than an oil tank, based on projected moulded dimensions

PA_S - bottom shell area (m^3) for each such tank or space based on projected moulded dimensions

L_T - length (m) between forward and aft extremities of the cargo tank

B - maximum breadth of the ship (m)

D - moulded depth (m) from the top of the keel to the top of the freeboard deck beam at side amidship

J - 0.45 for oil tankers of 20,000 dwt

0.3 for oil tankers of 200,000 dwt

For intermediate values of deadweight the value of J shall be determined by linear interpolation.

In addition it was agreed that the minimum width of each tank or space shall not be less than 2 metres and the minimum depth of each double bottom tank or space shall be $B/15$ or 2 metres, whichever is less.

The Exxon Valdez incident of 1989 and its subsequent coverage by the media gave rise to public concern about oil pollution. This has led to the formulation of the Oil Pollution Act of 1990 (OPA'90) by the US Administration which makes it mandatory for vessels trading to US ports to have double hulls as a means of reducing accidental oil spills. Even though this is unilateral move, the fact that the US imports about 40% of its oil requirements (a demand which is expected to grow as indigenous sources start to deplete) makes it one of the more significant players in this market, making the impact of OPA'90 more global.

8.2 Review of Tanker Optimisation

Some of the early parametric studies identified the pertinent parameters involved in the design of oil tankers. For example, Buxton [Buxton'66] used the 1965 rules published by Lloyds register to obtain useful design rules on the basis of parametric studies. Price [Price'71] discussed the range of measures put forward by various delegations at IMO in terms of ship design and equipment to be incorporated into ships to prevent or mitigate pollution by oil or hazardous chemicals shipped in bulk. Price concluded that

> "Marine casualty analysis is a very difficult problem, chiefly because of inadequate and inconsistent collection of experience. The lack of management information system is what leads to the disaster-related response as the common means of correction in the maritime world. Lacking the means to consider antipollution measures from a system standpoint, they are being adopted without providing for the trade-off of operational restrictions against construction features, or the most appropriate mix of both".

Dillon [Dillon'71] presented an overview of measures that could be incorporated at the design stage in order to eliminate intentional oil discharges and to minimize accidental oil spills in the event of collision or stranding. A large part of the study concentrated on alternative solutions for coping with oily ballast and oily waste water discharge and their economic impact. Dillon also examined the effectiveness of antipollution procedures and equipment with respect to certain specific tanker designs. The longitudinal and

transverse extents of damage were specified (deterministic) and unlimited vertical extents were assumed. Dillon described the purpose of the study as "to give the reader a better insight into probabilities for oil pollution abatement through basic ship design"

Nowacki [Nowacki'70] modelled a non-linear optimisation problem for tanker design using Hooke and Jeeves direct search algorithm and a special version of Sequential Unconstrained Minimisation Technique (SUMT). The objective was to optimize the principal characteristics and the operating speed of tankers on the basis of a chosen economic measure of merit when subject to an arbitrary set of constraints (strength, stability, freeboard etc.). The study confirmed and quantified the economic reasons for the existing trends to larger, fuller tankers.

Fisher [Fisher'73] adopted the rules specified by IMCO (1971) which were mainly on

- Damage: the size of longitudinal and transverse damages were specified
- Oil outflow: the volume of oil outflow was described in terms of functions of total volume of the breached cargo tank and the relative width of wing tanks
- Limitation of tank size: volumetric limits were imposed along with restriction on tank lengths

to model the principal hull dimension, subdivision configuration, and major structural scantlings of a VLCC. Since the number of design variables involved were over 50, Fisher formulated and optimised them in smaller parameter groups using Nelder and Mead's algorithm. Fisher concluded that

> "In principle, there is no reason to prohibit the simultaneous optimisation of all those parameters. Difficulty will be encountered in finding an appropriately "strong" optimisation procedure, however. Since the number of trials necessary for the optimisation varies approximately as the square of the number of variables, it is realised that a considerable amount of computer time will be required for this 'total optimisation'. Further, the economic justification for such a study may not be readily apparent".

Mukherjee [Mukherjee'85] performed a parametric study into the subdivision characteristic of oil tankers with regards to pollution prevention. Using statistical data on damage location and damage extents Mukherjee formulated a set of density distribution functions using a curve fitting technique called E-splines. Mukherjee then obtained functions for longitudinal extents of damage and for damage penetration. Using these

functions he derived the expressions for the probability of flooding vessels with transverse and longitudinal subdivision. Mukherjee then ran a series of parametric evaluations, for what he termed as "identification of basic parameters", which involved

- variation in the length of the forepeak tank and machinery space
- investigation into segregated ballast in terms of amount of ballast, ballast in double skin and ballast in alternate wing tanks
- transverse subdivision of cargo space in terms of number of transverse bulkheads.
- position of longitudinal bulkheads in the case of two and four longitudinal bulkheads (that is, double skin with two longitudinal bulkhead)

Mukherjee tried to use the parametric study to establish a relationship between the number of transverse and longitudinal subdivisions by plotting lines of equal outflow for variations of transverse bulkheads in X-axis and variations of longitudinal bulkheads in the Y axis. He concluded that

> "From this diagram it may be observed that there is no fixed relation and it very much depends on the existing number of transverse subdivision. The efficiency of transverse subdivision in reducing outflow decreases as the number of transverse subdivisions increase."

Mukherjee also modelled the optimisation of subdivision design in terms of total weight of the subdivision members. He used the expression for defining the weight factors for transverse and longitudinal subdivision to examine their influence on volume of outflow. Some of the conclusion reached by Mukherjee were

- average volume outflow depends on location and number of transverse and longitudinal bulkheads inside cargo space and location and extent of non oil containing region
- best place for placing segregated ballast is within double skin
- optimal position of longitudinal bulkhead is largely independent of transverse subdivision
- the IMO formulation of hypothetical outflow was inadequate
- for minimum weight subdivision configurations, optimal number of longitudinal bulkheads is either one or two

Hook [Hook' 91] used the probabilistic approach to access the effectiveness of various constructional features in reducing accidental oil spills following collisions or grounding. Hook used published damage statistics to obtain probability density

functions for damage location, damage extent and damage penetration for the case of collision and grounding.

However in order to estimate the joint density function which represents the probability of damaging a compartment, Hook assumed the density functions of damage location, extents and penetration to be statistically independent. Thus the joint density function reduces to a simple multiplication of the individual density functions. However this may not be strictly true since the damage extents are related to damage location especially at the forward and after ends of the vessel (hence the triangular nature of their joint domain, Figure 7.3, chapter 7). Also damage penetration are related to damage extents due to the nature of ship bows. Vertical extents and locations of damage were not considered by Hook due to the lack of suitable damage statistics and unlimited vertical extents were assumed instead. This was justified on the basis that,

> "[though] for the arrangements considered with horizontal subdivision the probability would be effected but by assuming a vertical extent without limit, then the worst possible case is taken."

With the above formulation Hook examined six alternative designs for their probability of outflow and their expected outflow. Design (a) was of the conventional type using ballast tanks, designs (b), (c), (d) were designs with double bottoms, (e) was a double skin design and (f) was with horizontal subdivision akin to the mid-deck tanker design.

TABLE 8.1 : Variations in factor 'J'

Probability of outflow		Expected outflow	
Design	**J**	**Design**	**J**
(f)	0.458	(f)	0.458
(d)	0.654	(d)	1.0
(c)	0.694	(e)	0.654
(e)	1.0	(c)	1.0
(b)	0.727	(a)	0.698
(a)	0.308	(b)	0.727

Hook rated the designs according to their effectiveness in reducing oil pollution and calculated the corresponding 'J' factor, defined in the IMO regulations as being the ratio of the projected shell area to the total side and bottom shell area within the cargo tank

length. The ratings (in descending order) and the corresponding 'J' value is as shown in Table 8.1. To quote Hook,

> "From these tables it can be seen that there is no correlation between 'J' and the ranking of the alternatives on either probability of outflow or expected outflow"

The post OPA'90 legislation has seen a spate of new innovative tanker designs under the themes of "environmental designs" and "ecological designs". Van der Laan [Van der Laan'94] used an analysis procedure called Accident Sequence Model (ASM) for evaluating a set of tanker designs. ASM divided the damage process into several phases ranging from accident prevention to reducing outflow. This is followed by prevention measures such as collection of outflowing oil (or prevention of further outflow) to salvage and clean-up operations. Van der Laan defined various zones in the tanker as vulnerable zones or safe zones depending on the location of the zone within a tank. In the vulnerable zone such as wing tanks, outflow is sought to be reduced by

- double side structures for protection and greater energy absorption
- reduced cargo tank sizes
- initial outflow prevention by hydrostatic balance
- secondary outflow reduced by emergency transfer system.

In the safe zone such as central cargo tanks the following measures were thought to be necessary

- double bottom designed for protection (energy absorption)
- inner hull designed for penetration prevention.

This methodology was used to develop a comprehensively new design called Combination Of Basic Objectives (COBO). The COBO was evaluated against the double hull design in terms of oil outflow and a roughly estimated building cost measure and was found to be more competitive than the latter.

The E3 tanker was another post OPA'90 concept which was aimed as being Ecological, Economic and European [Paetow'94]. The tanker was a double skin vessel with two longitudinal bulkheads and with 8 tank sections in total. Apart from the passive measures (like those provided by proper subdivision), the design also incorporated active measures in the form of specialised equipment in order to reduce the net volume discharged after damage.

A lot of work has been undertaken in Japan sponsored by the major Japanese shipyards into evaluating the effectiveness of Mid-Deck Tankers (MDT) [Hirai'92]. Studies has also been carried out in the United States involving the U.S. Coast Guard (U.S.C.G) into evaluating MDT's against the double hull concept [Neyhart'92], [Karafaith'93]. The debate about which is more effective remains inconclusive, with each concept being more suited to some scenarios.

8.3 Recommendations on oil spill estimation

The United States submitted the proposals made by a study by Michel and Tagg [Michel'91] to the sub-committee on stability and load lines and on fishing vessel safety on its thirty-sixth session in December 1991 [SLF36'91]. These proposals have since become the basis for the most widely used measures for evaluating the effectiveness of a design against oil pollution. Michel and Tagg derived probability density functions for damage location, damage length and damage penetration from statistical data. The assumptions made for their evaluations were,

- the vessel is assumed fully loaded with cargo oil tankages at 98% of their capacity
- for each damage case, calculations are performed to determine the equilibrium condition and residual stability
- when a cargo tank is breached, oil is assumed to flow until hydrostatic pressure equilibrium is achieved
- at the equilibrium condition, the computed oil outflow for all affected tanks are summed to determine total outflow for that particular case
- if the damage fails to meet the damage stability survivability criteria, the ship and 100% of all oil is assumed lost

Michel and Tagg then described the following criteria for assessing the effectiveness of a design,

- *Probability of zero outflow* - the probability that no oil will be released into the environment which is a sum of the probabilities of damages to all those compartments that contain no oil
- *Mean outflow* - the sum of the product of each damage case probability and the computed outflow for that damage case. This was meant to be a good indication of the overall effectiveness of a particular design in limiting oil outflow

- *Extreme outflow* - this value represented the "worst case" spill scenario, and was the weighted average of the upper 10% of all casualties. This parameter was meant to provide a "snapshot" evaluation of the behaviour of a vessel subjected to extreme damage.

Neyhart et al. [Neyhart'92] discussed the merits and demerits of these parameters as proposed by Michel and Tagg. The authors argued against the approach which assumed that the "mean outflow" was the best in defining the effectiveness of a design,

> "This approach [of mean outflows] assumes that the environmental and economic impact of a single large spill is identical to a number of smaller spills whose total spill amounts add up to the large spill amount. This approach by itself is inadequate. The authors strongly believe that maximising the probability of zero outflow is one of the greatest importance of all three different approaches."

In addition to these Pawlowski [Pawlowski'92] introduced what could be termed as the local outflow index, defined as,

$$e_j = \frac{\sum_{i \in J} p_i v_i}{\sum_{i \in J} p_i} \qquad \text{(EQ 8.1)}$$

where p_i - probability of damaging a given compartment group
v_i - volume of oil contained in the compartment group
J - the set of all legal combinations that includes compartment j

A number of member countries, classification societies, shipbuilders and non-governmental organisations [NGO] were involved in the thirty-second session of the Marine Environmental Protection Committee convened in March 1992. A study by the NGO's OCIMF and INTERTANKO on double hull and mid-deck tankers [IMO'92] concluded that:

- operators believe that both the double hull and the mid-deck tanker can be operated satisfactorily but both types will be more difficult than the present single skin tankers.
- operators definitely expect that increased operational and safety problems will develop with older double hull tankers, but expect more difficult operation with mid-deck design from the day of delivery. Many problems can, however, be overcome by better detailed design, increased scantlings and generally greater safety margins.

The steering committee to the thirty-second Marine Environment Protection Committee [MEPC] however concluded that [IMO'92],

- when the whole range of probable collision and groundings are considered cumulatively, the oil outflow performance of mid-deck tankers is at least equivalent to that of double hull tankers, but the committee recognized that within this overall conclusion each design gives better or worse outflow performance under certain conditions.
- the steering committee recommends that the MPEC review existing requirements of MARPOL 73/78 covering tank size and bulkhead spacing to assess whether these requirements are adequate on all tankers.

8.4 Probability of vertical damage

The IMO formulation on probabilistic damage due to collision neglects the vertical extents of damage on the grounds of insufficient data. The same is also true of most studies on the effectiveness of oil tanker designs which assume unlimited vertical extents of damage. Such an assumption is envisaged to represent the worst case and is therefore justified as imposing a conservative estimate on the damage probabilities. However, to estimate the influence of alternative horizontal subdivision arrangements it would be meaningful to take the vertical distribution of damages into consideration.

Konstantinidis [Konstantinidis'86] collected casualty statistics for ro-ro cargo ships. The data collected was in two parts,

i. Casualty information systems of Lloyds Register of Shipping for the period January 1978 to March 1984 for ships registered with Lloyds and others.

ii. Information from Lloyds Register records section for ro-ro cargo ships for the period 1960-1983, gleaned from surveyor's reports.

Source (i) was limited and provided vessel details and the general failure modes that occurred. Source (ii) was considered to be more useful as it provided details such as damage location and extents, damage conditions and damage consequences.

Figure 8.1 and Figure 8.2 show the vertical location and extent of damage distribution respectively as obtained from the casualty statistics.The figures also show the assumed probability density functions respectively. The p.d.f for vertical damage location was assumed as,

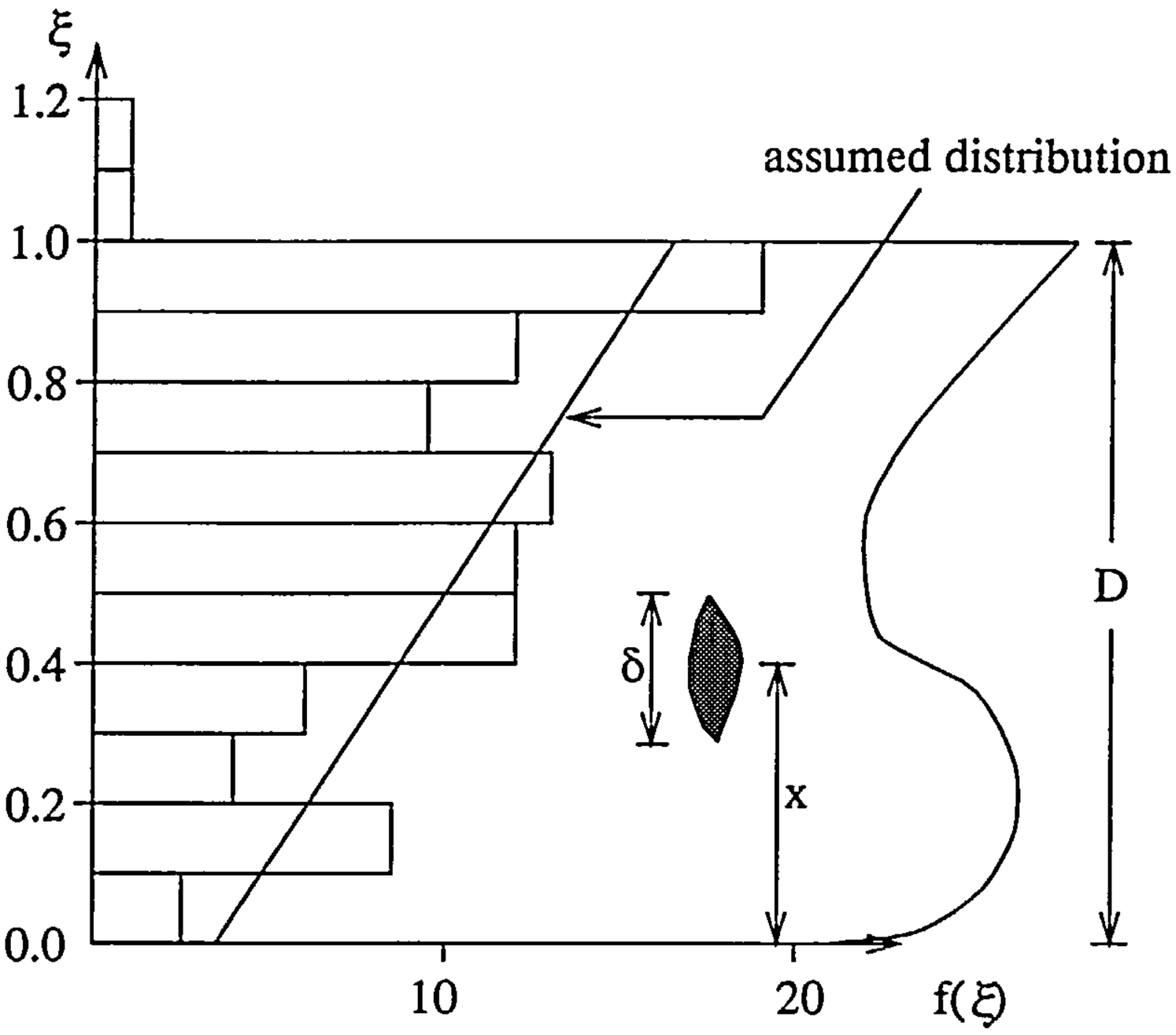

FIGURE 8.1. Distribution of damage location in the vertical direction (contacts and collision)

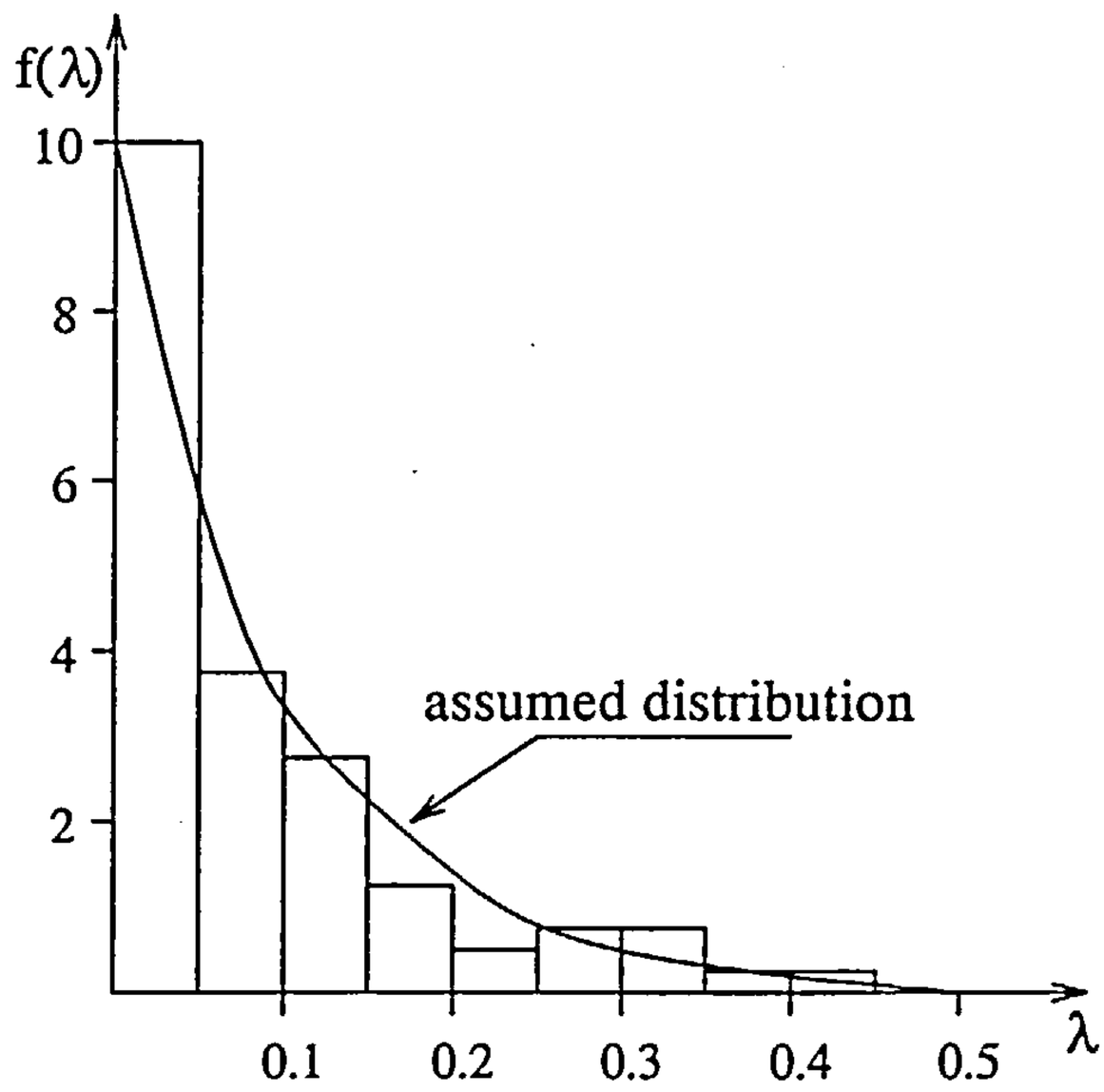

FIGURE 8.2. Distribution of damage extents in the vertical direction (contacts and collision)

$$f(\xi) = a + b\xi \qquad \text{(EQ 8.2)}$$

where $a = 0.35$

$b = 1.3$

$\xi = \frac{x}{D}$ is the non-dimensional vertical damage location (Figure 8.1)

and the p.d.f for vertical extents of damage was assumed to be,

$$g(\lambda) = ce^{-d\lambda} \qquad \text{(EQ 8.3)}$$

where $c = 10.0$

$d = 10.0$

$\lambda = \frac{\delta}{D}$ is the non-dimensional extent of damage (Figure 8.2)

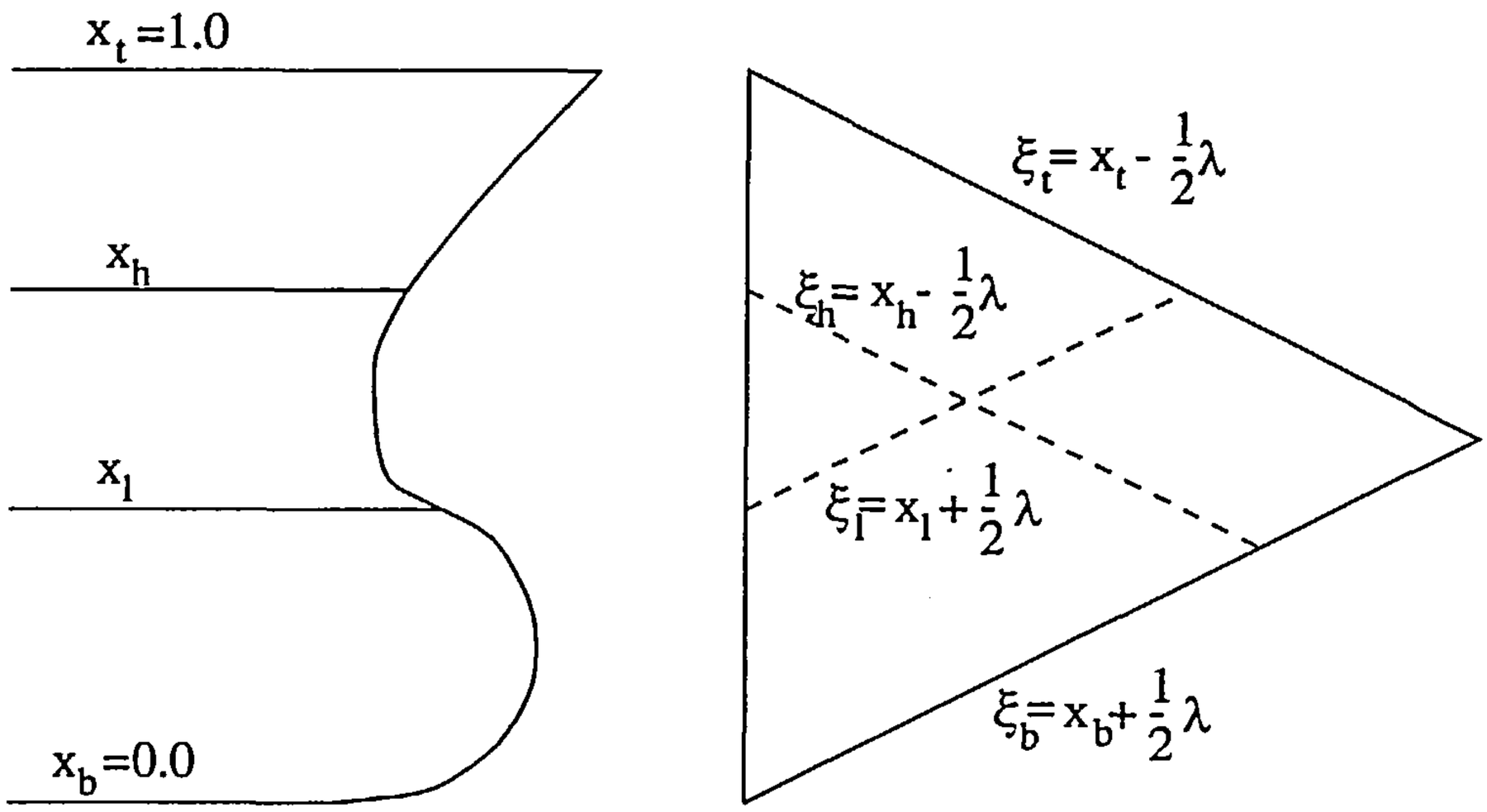

FIGURE 8.3. The domain of the joint density function

Figure 8.3 describes the domain over which the joint density function $f(\xi, \lambda)$ is defined. The domain is triangular because the damage is bound within the limits of the base (Keel) and the upper most deck of the vessel, implying that the variables ξ and λ are dependent on each other. In Figure 8.3,

x_t - the highest non-dimensional location in the vertical direction (equals 1.0 and corresponds to the height of the top-most deck)

x_b - the lowest non-dimensional location in the vertical direction (equals 0.0 and corresponds to the base line of the vessel)

x_h - the height of an intermediate deck defining the upper limit of that

compartment

x_l - the height of an intermediate deck defining the lower limit of that compartment

The upper and lower edges of the triangular domain can therefore be defined respectively as,

$$\xi_t = x_t - \frac{1}{2}\lambda \qquad \text{(EQ 8.4)}$$

$$\xi_b = x_b + \frac{1}{2}\lambda \qquad \text{(EQ 8.5)}$$

Thus the marginal distribution for the vertical location of damage given its vertical extent can be obtained as follows. Since,

$$\int_{\xi_b}^{\xi_t} f(\xi)d\xi = 1 \qquad \text{(EQ 8.6)}$$

Substituting (EQ 8.2) in (EQ 8.6)

$$\int_{\xi_b}^{\xi_t} (a + b\xi)d\xi = 1$$

$$a\xi + \frac{b}{2}\xi^2\Big|_{\xi_b}^{\xi_t} = 1$$

$$a(\xi_t - \xi_b) + \frac{b}{2}(\xi_t + \xi_b)(\xi_t - \xi_b) = 1 \qquad \text{(EQ 8.7)}$$

From (EQ 8.4) and (EQ 8.5)

$$\xi_t - \xi_b = x_t - x_b - \lambda \qquad \text{(EQ 8.8)}$$

$$\xi_t + \xi_b = x_t + x_b \qquad \text{(EQ 8.9)}$$

Substituting (EQ 8.8) and (EQ 8.9) in (EQ 8.7)

$$a(x_t - x_b - \lambda) + \frac{b}{2}(x_t - x_b - \lambda)(x_t + x_b) = 1 \qquad \text{(EQ 8.10)}$$

Since by definition $x_t = 1.0$ and $x_b = 0.0$, substituting these values in (EQ 8.10)

$$a = \frac{1}{1-\lambda} - \frac{b}{2}$$

Since only marginal distributions are available from damage statistics, the conditional distribution can be written on the basis of the above as,

$$f(\xi|\lambda) = \left(\frac{1}{1-\lambda} - \frac{b}{2}\right) + b\xi \qquad \text{(EQ 8.11)}$$

and since $b = 1.3$

$$f(\xi|\lambda) = \frac{1}{1-\lambda} - 0.65 + 1.3\xi \qquad \text{(EQ 8.12)}$$

Following the same process for the vertical damage extent distribution,

$$\int_0^{\lambda_m} ce^{-d\lambda} = 1 \qquad \text{(EQ 8.13)}$$

$$\frac{c}{d}[1 - e^{-\lambda_m d}] = 1 \qquad \text{(EQ 8.14)}$$

where λ_m, the maximum vertical extent of damage is defined as

$$x_t - \frac{1}{2}\lambda_m = x_b + \frac{1}{2}\lambda_m$$

In other words, the damage location at the upper vertical limit x_t minus half the maximum damage extent λ_m should be equal to the damage location at the lower vertical limit x_b plus half the maximum damage extent. Therefore,

$$\lambda_m = x_t - x_b = 1.0 \qquad \text{(EQ 8.15)}$$

From (EQ 8.14)

$$c = \frac{d}{1 - e^{-\lambda_m d}} \qquad \text{(EQ 8.16)}$$

Since $c = d = 10.0$ and $\lambda_m = 1.0$, the distribution function for the vertical extent of damage can be defined as,

$$g(\lambda) = k_3 e^{-10\lambda} \qquad \text{(EQ 8.17)}$$

where $k_3 = 10.000454$.

The joint density distribution function can be expressed as,

$$f(\xi, \lambda) = f(\xi|\lambda)g(\lambda) \qquad \text{(EQ 8.18)}$$

The probability of damage between limits x_h and x_l shown in Figure 8.3 can be expressed as,

$$p_i = \int_{\xi_l}^{\xi_h} \int_{0}^{\lambda_m} f(\xi, \lambda) d\xi d\lambda \qquad \text{(EQ 8.19)}$$

where $\xi_h = x_h - \frac{1}{2}\lambda$

$$\xi_l = x_l + \frac{1}{2}\lambda$$

Substituting from (EQ 8.12) and (EQ 8.17)

$$p_i = \int_{\xi_l}^{\xi_h} \int_{0}^{\lambda_m} \left(\frac{1}{1-\lambda} - 0.65 + 1.3\xi\right)(k_3 e^{-10\lambda}) d\xi d\lambda$$

$$p_i = \int_{0}^{\lambda_m} \left(\int_{\xi_l}^{\xi_h} \left(\frac{1}{1-\lambda} - 0.65 + 1.3\xi\right) d\xi \right)(k_3 e^{-10\lambda}) d\lambda \qquad \text{(EQ 8.20)}$$

The solution to

$$\int_{\xi_l}^{\xi_h} \left(\frac{1}{1-\lambda} - 0.65 + 1.3\xi\right) d\xi = \frac{k_1 - \lambda}{1-\lambda} + k_2(k_1 - \lambda) \qquad \text{(EQ 8.21)}$$

where $k_1 = x_h - x_l$

$k_2 = 0.65(x_h + x_l) - 0.65$

Substituting (EQ 8.21) in (EQ 8.20)

$$p_i = \int_{0}^{\lambda_m} \left(\frac{k_1 - \lambda}{1-\lambda} + k_2(k_1 - \lambda)\right)(k_3 e^{-10\lambda}) d\lambda \qquad \text{(EQ 8.22)}$$

(EQ 8.22) can be resolved into three separate integrals as,

$$p_i = I_1 + I_2 - I_3 \qquad \text{(EQ 8.23)}$$

where $I_1 = k_3 \int_0^{\lambda_m} \left(\frac{k_1 - \lambda}{1 - \lambda}\right) e^{-10\lambda} d\lambda$

$$I_2 = k_1 k_2 k_3 \int_{\lambda_m}^{0} (e^{-10\lambda}) d\lambda$$

$$I_3 = k_2 k_3 \int_0^{0} (\lambda e^{-10\lambda}) d\lambda$$

The solutions to integrals I_2 and I_3 can be readily obtained in a closed form as,

$$I_2 = \frac{k_1 k_2 k_3}{10}[1 - e^{-10\lambda_m}] \qquad \text{(EQ 8.24)}$$

$$I_3 = -\frac{k_2 k_3}{100}[e^{-10\lambda_m}(10\lambda_m + 1) - 1] \qquad \text{(EQ 8.25)}$$

Since a closed form solution cannot be obtained for integral I_1 a mathematical technique called Gaussian Quadrature [Gerald'84] was used. A simple case of a two-term formula (with four unknown parameters) can be defined as

$$\int_{l_1}^{l_2} f(t) = w_1 f(t_1) + w_2 f(t_2) \qquad \text{(EQ 8.26)}$$

where w_1, w_2, the weighting factors and the t-values have been tabulated. For integral I_1 a seven term gaussian quadrature was used.

TABLE 8.2 : gaussian quadrature accuracy for varying number of terms

Nos. of terms	Total probability
4	0.993091
5	0.999559
6	0.99998
7	0.99999

This was determined by numerically evaluating the integral in (EQ 8.23) till the result was close to 1.0. The results for increasing number of terms in the quadrature is listed in Table 8.2.

TABLE 8.3 : Values of weights and t-values

i	w_i	t_i
1	0.129484	-0.949107
2	0.279705	-0.741531
3	0.381830	-0.405845
4	0.417959	0.0
5	0.381830	0.405845
6	0.279705	0.741531
7	0.129484	0.949107

The t-values and the values of the weights used for the gaussian quadrature are as shown in Table 8.3. The integral I_1 can therefore be expressed as,

$$I_1 = \frac{k_3\lambda_m^2}{2}\left[\sum_{i=1}^{7} w_i f(t_i)\right] \quad \text{(EQ 8.27)}$$

where $w_i f(t_i) = \frac{q_i}{2 - r_i\lambda_m} e^{-s_i\lambda_m}$, the values of q_i, r_i and s_i is listed in Table 8.4

TABLE 8.4 : Values of q_i, r_i and s_i for the integral I_1

i	q_i	r_i	s_i
1	0.25238	0.05089	-0.2544
2	0.48712	0.25847	-1.2923
3	0.53679	0.59415	-2.9707
4	0.41796	1.0	-5.0
5	0.22687	1.0458	-7.0292
6	0.07230	1.7415	-8.7076
7	0.00659	1.9491	-9.7455

Substituting (EQ 8.24), (EQ 8.25) and (EQ 8.27) in (EQ 8.23)

$$p_i = \frac{k_3\lambda_m^2}{2}\left[\sum_{i=1}^{7} \frac{q_i}{2 - r_i\lambda_m} e^{-s_i\lambda_m}\right] + d(x_h + x_l - 1)[10(x_h - x_l) + e^{-10\lambda_m} - 1] \quad \text{(EQ 8.28)}$$

where $k_3 = 10.000454$

$\lambda_m = x_h - x_l$

and the values of q_i, r_i and s_i are as shown in Table 8.4.

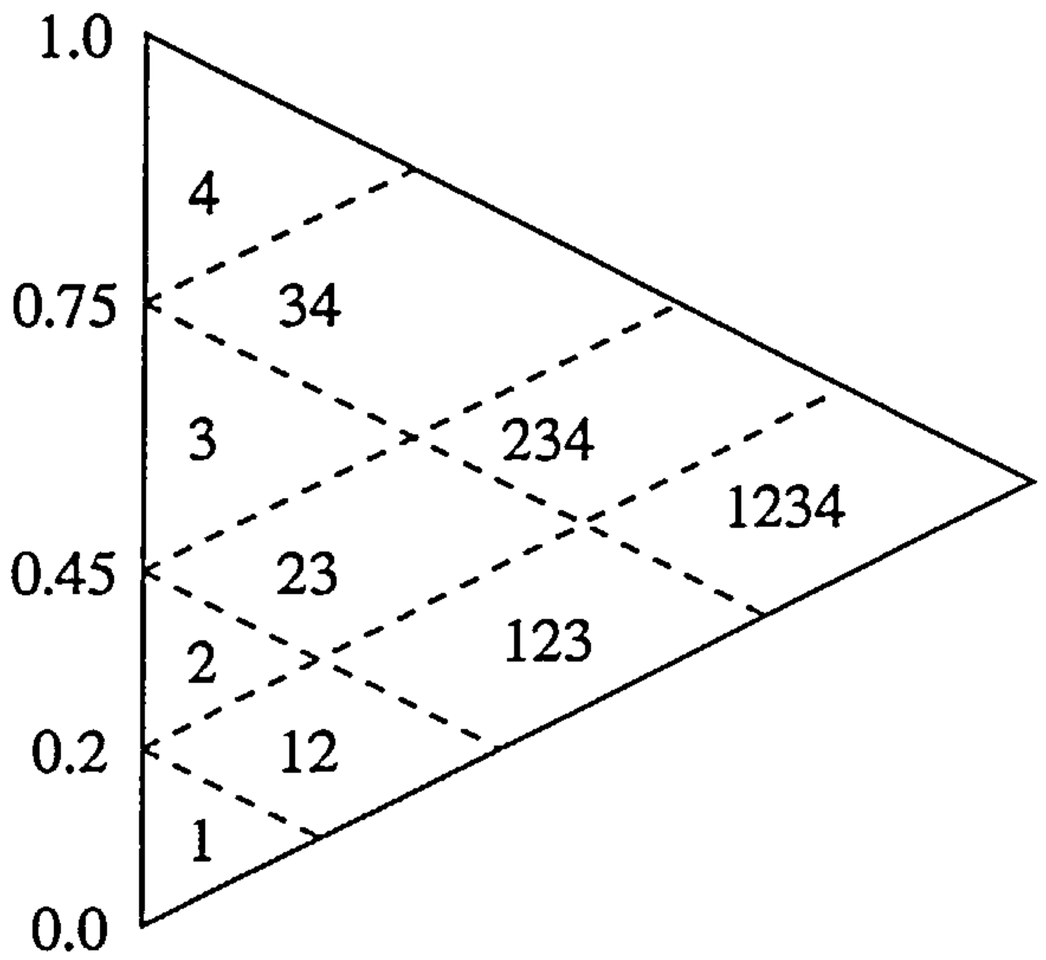

FIGURE 8.4. A three-deck compartment

Knowing the non-dimensional location of the decks, the probability of damaging single and groups of compartments bound by those decks can be obtained from (EQ 8.28). Figure 8.4 describes a situation where the compartment has a set of three decks. The probability of damaging compartment 1 and 2 is given as,

$$p_{1,2} = p_{12} - p_1 - p_2$$

and for compartments 1, 2 and 3 as,

$$p_{1,2,3} = p_{123} - p_{12} - p_{23} + p_2$$

where p_1 - probability of damaging horizontal compartment 1 (of length l_1)

p_2 - probability of damaging horizontal compartment 2 (of length l_2)

p_{12} - probability of damaging horizontal compartment 2 (of length l_{12})

p_{23} - probability of damaging horizontal compartment 2 (of length l_{23})

p_{123} - probability of damaging horizontal compartment 2 (of length l_{123})

where each of these probabilities can be obtained by using (EQ 8.28).

8.5 Oil tanker subdivision

In all four subdivision arrangements were examined.

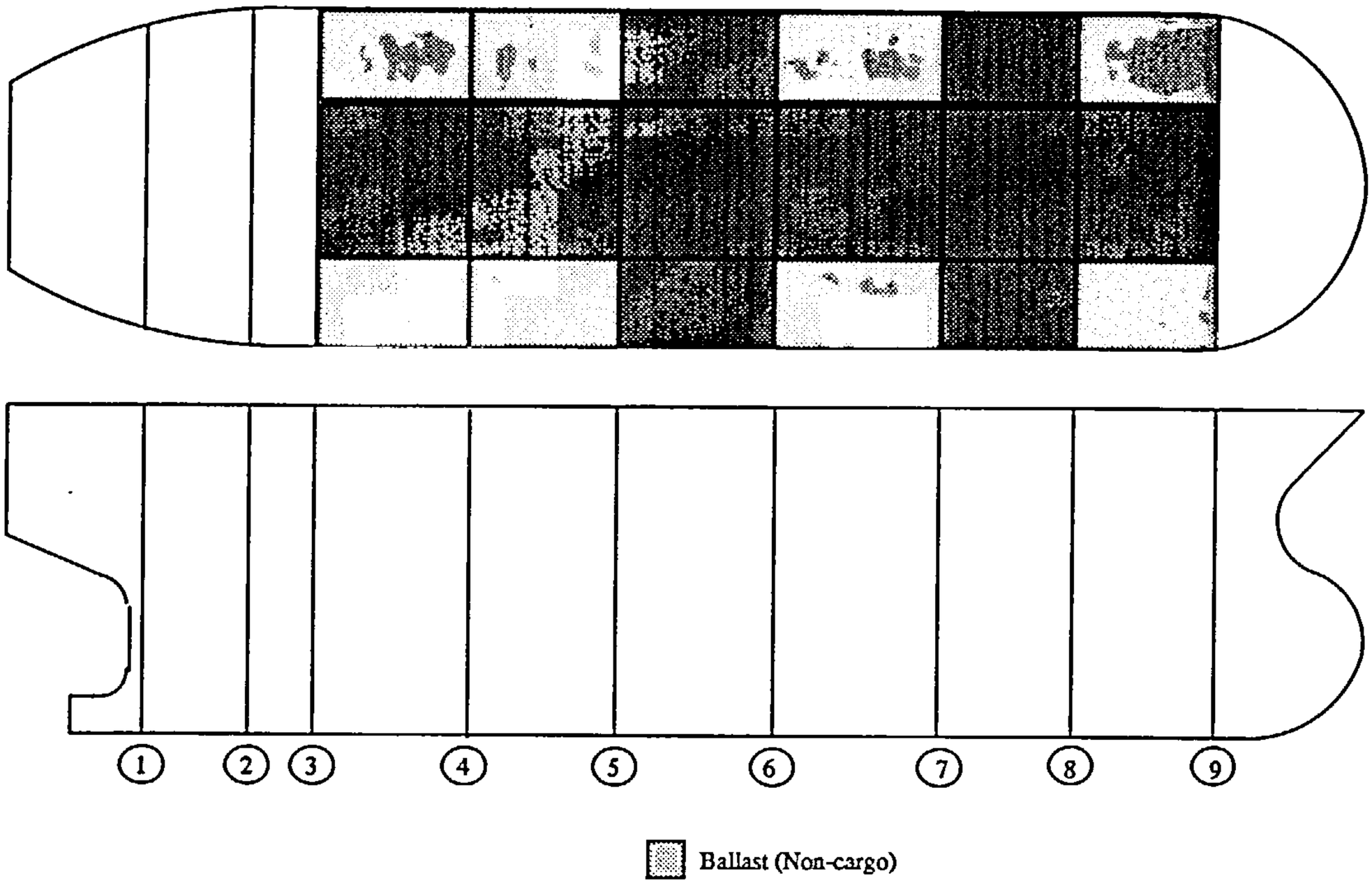

FIGURE 8.5. General arrangements for an oil tanker

TABLE 8.5 : Bulkhead positions

Bulkhead No.	Position
1	-101.68
2	-79.66
3	-66.0
4	-57.32
5	-38.64
6	-1.28
7	36.08
8	73.44
9	92.12

Figure 8.5 shows the general arrangements of the cargo oil tanks and the non-cargo spaces for the oil tanker to be analysed. The vessel particulars were as follows,

Length between perpendiculars	218m
Breadth	32m
Depth	19m
Draught	11.92m
Total ballast capacity	25,726 m^3
Total cargo capacity	72,036 m^3
c_b	0.87

In the three cases analysed, bulkheads 1, 2, 3 and 9 were kept fixed in their positions. The bulkhead positions for the actual (basis) vessel are as shown in Table 8.5. The longitudinal bulkheads were located at 7.6 metres from the centreline. The main objectives of the optimisation was to minimise the net oil outflow O_1 while maximising the total volume of cargo carried O_2. The following stability constraints were imposed [Michel'91]

- *Equilibrium heel angle* c_1 : Maximum 25 degrees if the deck edge is immersed, otherwise, 30 degrees.
- *Righting arm* c_2 : Maximum residual lever of at least 0.1 metre.
- *Range of positive stability* c_3 : range of positive stability beyond the equilibrium angle of at least 20 degrees.

In addition the MARPOL 73/78 restrictions on cargo tank lengths and cargo tank volumes were also imposed along with the segregated ballast requirements (see section 8.1),

- *Length restriction* c_4 : the length of the cargo tank shall not exceed 10 metres or one of the following whichever is greater

  0.1L when no longitudinal bulkhead is provided

  0.15L for a centreline longitudinal bulkhead

  0.2L when two or more longitudinal bulkheads are provided
- *Volume restriction* c_5 : cargo tanks of oil tankers shall be of such size and arrangement that the hypothetical outflow anywhere in the length of the ship does not exceed 30,000 m^3 or $400\sqrt[3]{DW}$ whichever is greater, subject to a maximum of 40,000 m^3 .
- Trim c_6 : the draughts at the forward and aft perpendiculars shall correspond to those determined by the draught at the midship (which shall not be less that $2.0 + 0.02L$) in association with trim by the stern not greater than 0.015L

The constrained optimisation problem was converted into an unconstrained one for the application of genetic algorithms by using the exterior penalty function formulation. The unconstrained objective function could therefore be stated as,

$$Min\left\{O_1 + (-O_2) + r_k \sum_{i=1}^{6} f(c_i)\right\} \qquad \text{(EQ 8.29)}$$

where r_k is the penalty term. Since the individual goals in this multiple criteria optimisation were normalised, they had almost equal weighting. The GA described earlier was used as the optimiser.

The values of mean outflow index and the probability of zero outflow was calculated for the base vessel. The mean outflow index is the ratio of the outflow volume to the total cargo carried..

Mean outflow index	0.06766
Probability of zero outflow	0.0136

8.5.1 Case (a)

In the first case that was analysed, bulkheads 4, 5, 6, 7 and 8 were allowed to vary within a set range with the longitudinal bulkheads kept fixed. This was to investigate for possible improvements in the basis design by the relocation of transverse bulkheads only.

The variables involved were as shown in Figure 8.6

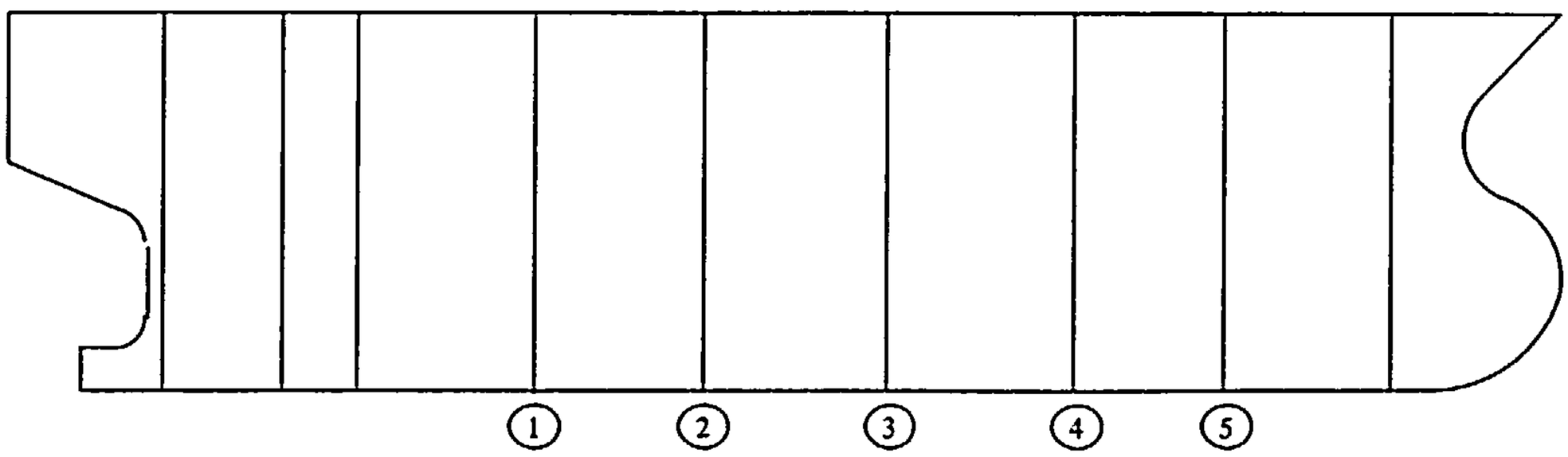

FIGURE 8.6. Variable description for case (a)

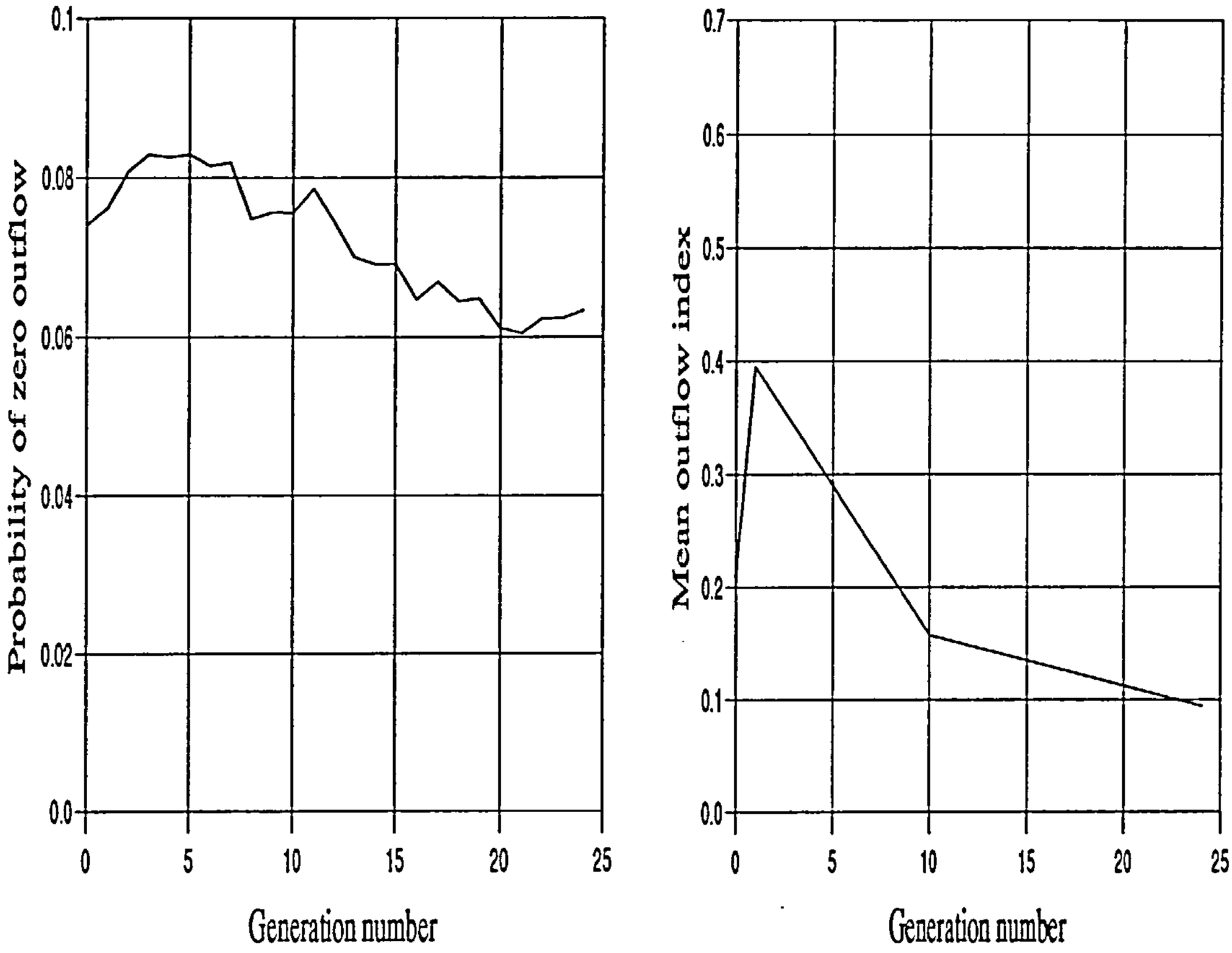

FIGURE 8.7. Zero outflow and Mean outflow index history, case(a)

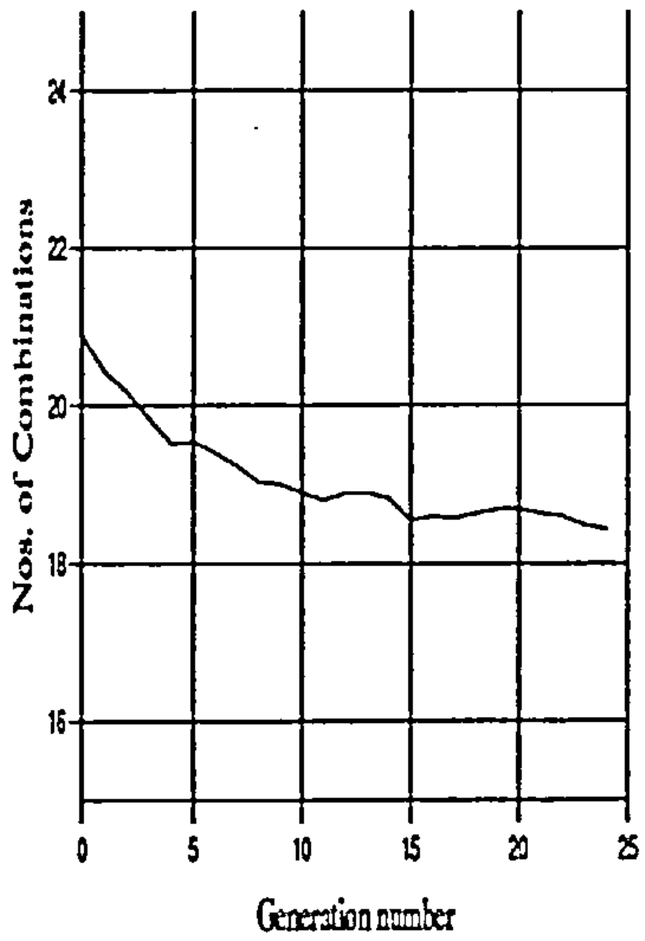

FIGURE 8.8. Average damage combination number history

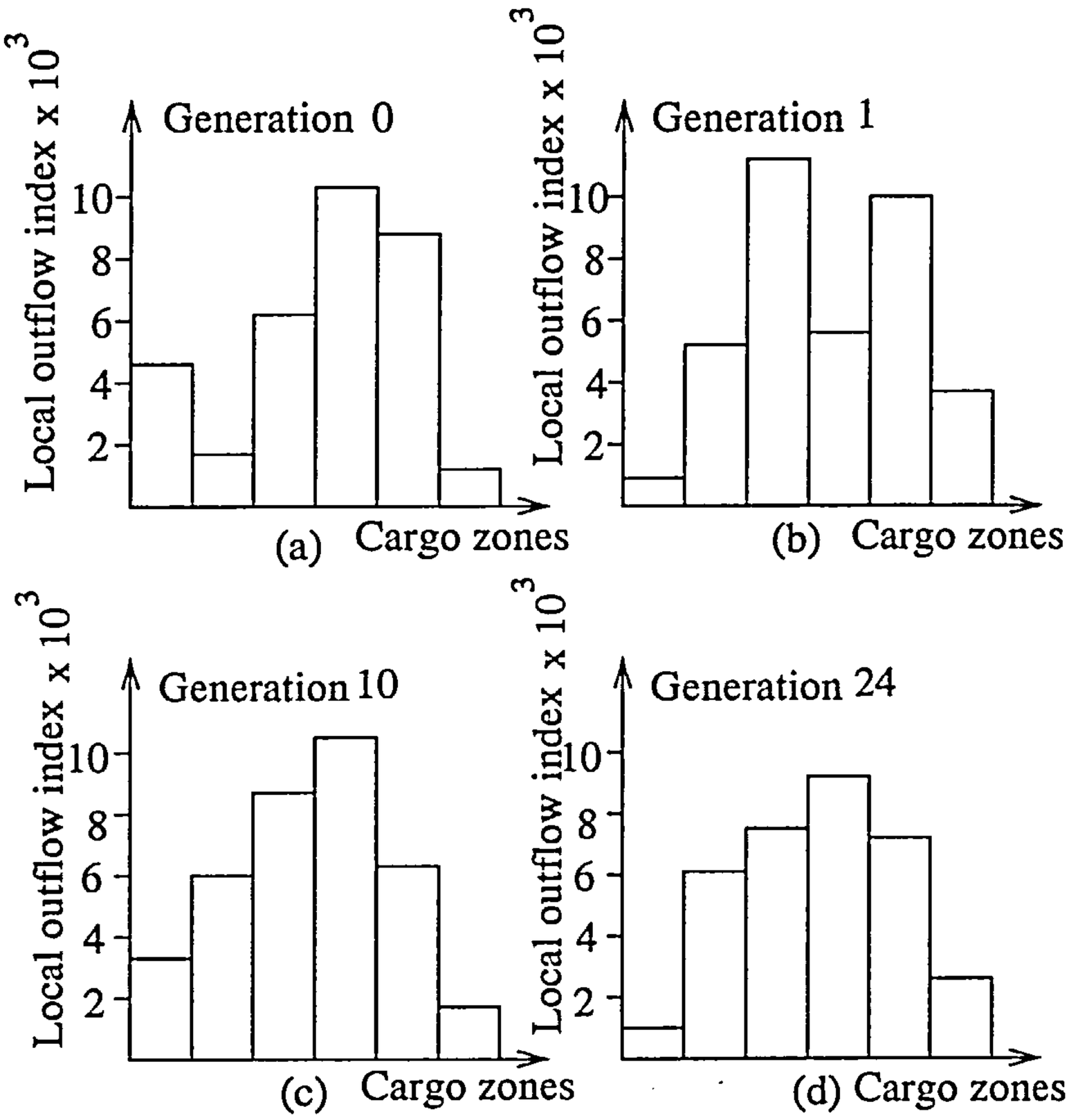

FIGURE 8.9. Variation of local outflow index, case(a)

The number of combinations for the first generation varied between 18 and 24 with the average value of around 21. Genes with lower damage combinations tended to dominate the gene pool. As the GA progressed the average value fell to around 18, Figure 8.8.

TABLE 8.6 : Parameters and results for the local index outflow cases

Gen. No.	Cargo vol. m^3	Ballast vol. m^3	Mean outflow m^3	Outflow index	Var 1	Var 2	Var 3	Var 4	Var 5
0	71,909	25,878	15,028	0.209	-51.2	-45.2	-15.4	19.2	63.5
1	82,381	15,408	32,514	0.395	-63.8	-45.9	9.7	28.4	79.2
10	72,086	25,664	11,358	0.157	-55.5	-35.3	8.2	43.4	74.9
24	72,931	24,854	6907	0.0947	-63.6	-43.4	-3.7	27.3	64.5

Figure 8.7 gives the GA history in terms of zero outflow probabilities and mean outflow index. Figure 8.9 shows the variation in the local outflow index distribution as the GA progresses with the details for each case given in Table 8.6.

Mean outflow for each generation is calculated by multiplying the volume of the damaged cargo compartments, in a given damage combination, by the probability of damage for that combination. If the vessel fails to satisfy the survival criteria for any damage combination, the entire cargo volume is assumed lost. The outflow index is the ratio of the mean outflow to the total cargo volume for that configuration.

TABLE 8.7 : Percentage changes in variables

Var. No.	Bulkhead	% change (+ve forwards)
1	4	-2.9
2	5	-2.2
3	6	-1.1
4	7	-4.0
5	8	-4.1

Table 8.7 gives the percentage variation with respect to the ships length in the transverse bulkhead positions as compared to the basic design. Though the change in bulkhead position is not substantial it has increased the probability of zero outflow as seen from Figure 8.7, though the increase in the number of damage combination has also caused an increase in the mean outflow index value when compared to the basis vessel.

For this case the GA was allowed to continue for 24 generations. The average time for evaluating a single damage combination was around two to three minutes for a gene during non-peak hours and hence for a ship with 18 combinations a single evaluation would take between 30 and 40 minutes. Hence the GA could not be run for longer durations. Figure 8.9 demonstrates the reduction in non-uniformity in the local outflow distribution as the GA progressed.

8.5.2 Case (b)

The next step was to introduce horizontal subdivision and to investigate the effect on the outflow parameters. For case (b) six additional decks were introduced, one in each of the central cargo tanks. It would have been simpler to use a single value for all decks but for this study it was considered to be of some interest to let the height of the deck vary. The location of the decks were allowed to vary within set limit (4 to 14 metres in this case). With the five transverse bulkheads as before the total number of design variable was 11.

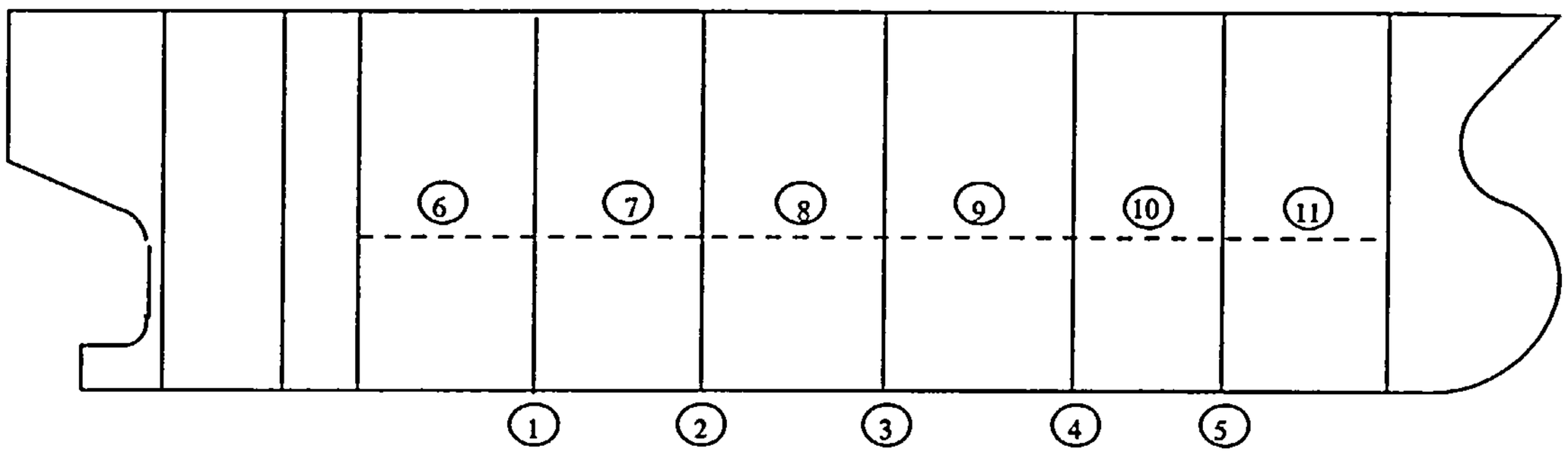

FIGURE 8.10. Variables for case (b)

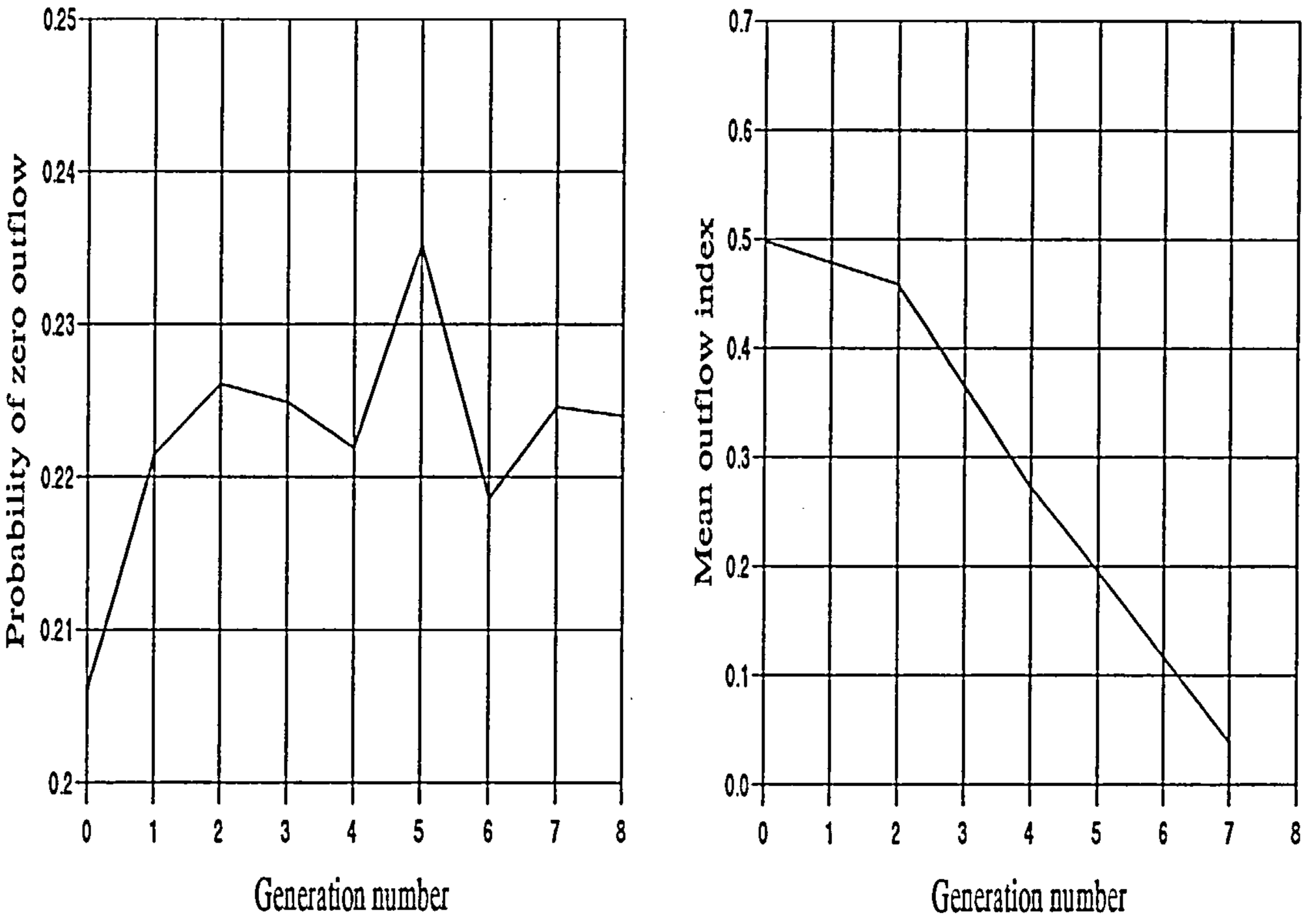

FIGURE 8.11. Zero outflow and Mean outflow index history, case(b)

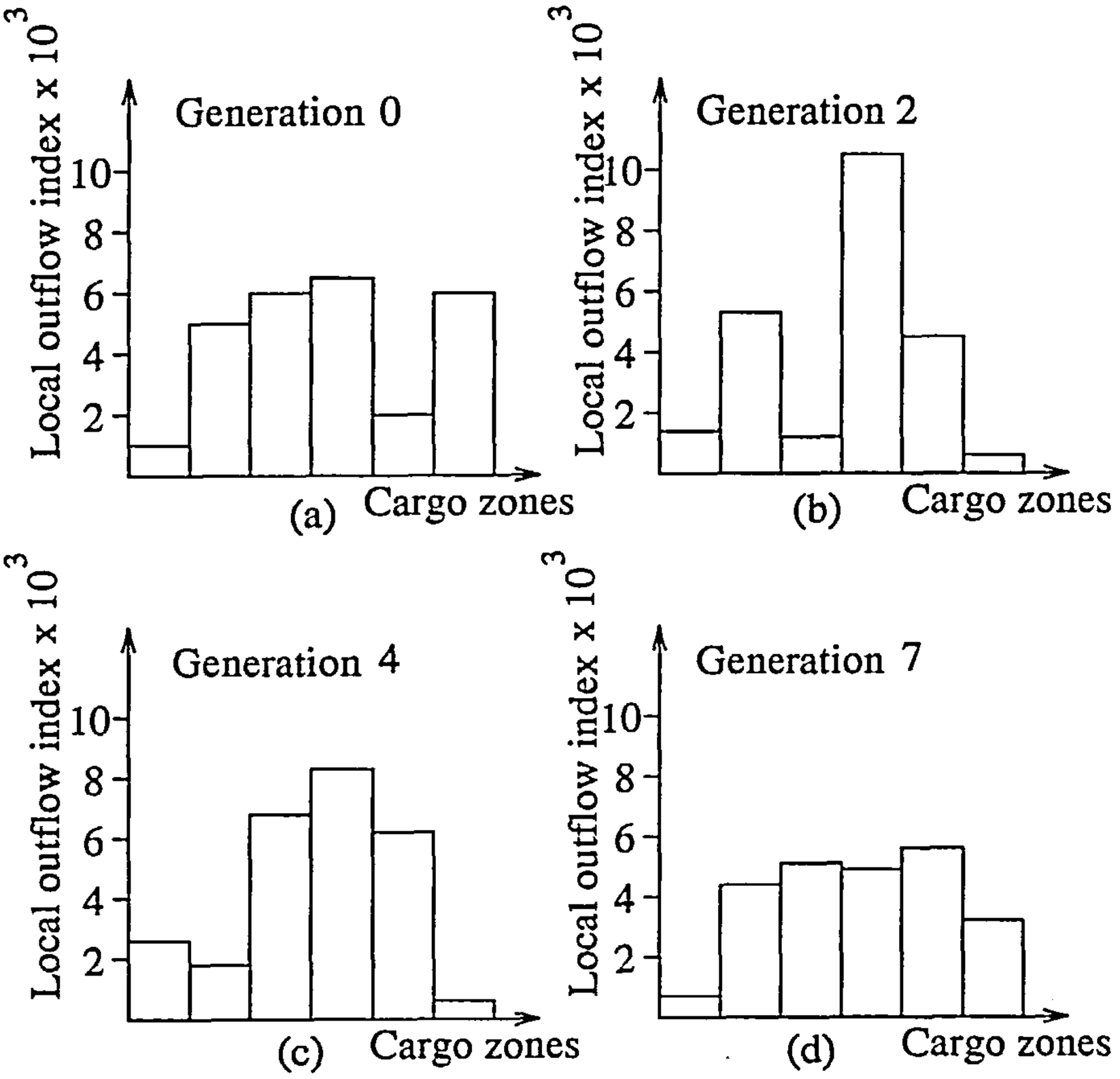

FIGURE 8.12. Variation of local outflow index, case (b)

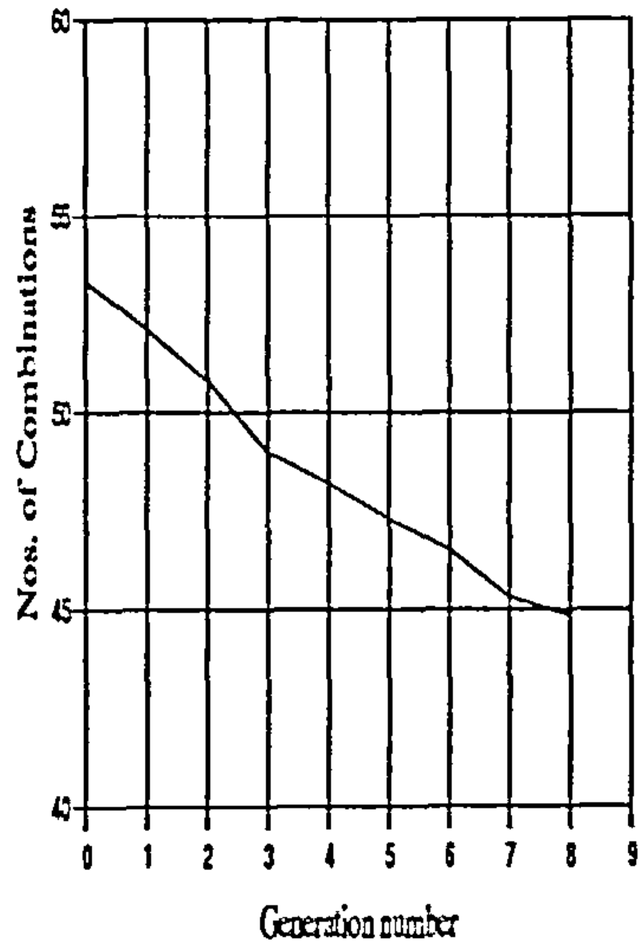

FIGURE 8.13. Average damage combination number history

TABLE 8.8 : Percentage changes in variables

Var. No.	Bulkhead	% change (+ve forwards)
1	4	0.36
2	5	2.3
3	6	1.4
4	7	-6.5
5	8	-4.9

TABLE 8.9 : Parameters and results for the local index outflow cases

Gen. No.	Cargo vol. m^3	Ballast vol. m^3	Mean outflow, m^3	outflow index	Var 1	Var 2	Var 3	Var 4	Var 5
0	62,984	34,780	31,378	0.498	-64.0	-28.4	6.3	43.5	56.0
2	62,490	35,294	28,650	0.458	-57.5	-21.0	-8.8	53.5	91.0
4	71,546	26,220	19,456	0.272	-53.2	-43.2	-3.7	53.5	91.0
7	70,775	27,004	2787	0.039	-61.8	-32.1	1.2	33.5	71.0

Var 6	Var 7	Var 8	Var 9	Var 10	Var 11
4.0	12.5	5.4	11.1	9.7	11.1
5.4	9.7	6.8	4.0	6.8	6.8
5.4	5.4	14.0	5.4	14.0	14.0
6.8	8.2	8.2	4.0	6.8	8.2

As seen from Figure 8.13 the introduction of additional subdivision members has had a dramatic increase in the number of damage combinations that need to be evaluated. The increase in the number of damage combinations had a two-fold effect on case (b).

The first was the increase in computation time for each gene and therefore for each generation. This meant that a lesser number of generations could be evaluated in a reasonable time frame.

The second effect of the increase in the number of combinations can be seen in the initial higher values of the mean outflow index as shown in Table 8.9. The outflow index fell quite dramatically over the seven generations as fitter members began to dominate the gene pool..

Table 8.8 lists the percentage variation in the transverse bulkhead positions for case (b). The pattern of variation for (aftwards) bulkheads 4 and 5 was opposite to that in case (a)

whereas the trends for (forward) bulkheads 6, 7 and 8 were quite similar to those in case(a) though of different magnitudes. However the more significant result is the increase in zero outflow probability which has occurred due to the introduction of additional subdivision members.

8.5.3 Case (c)

Case (c) was similar to case (b) in that no additional subdivision members were introduced In case (c), twelve additional design variables were introduced into the GA by allowing the twelve longitudinal bulkheads to vary within set limits (6.0 to 9.2 metres from the centreline).

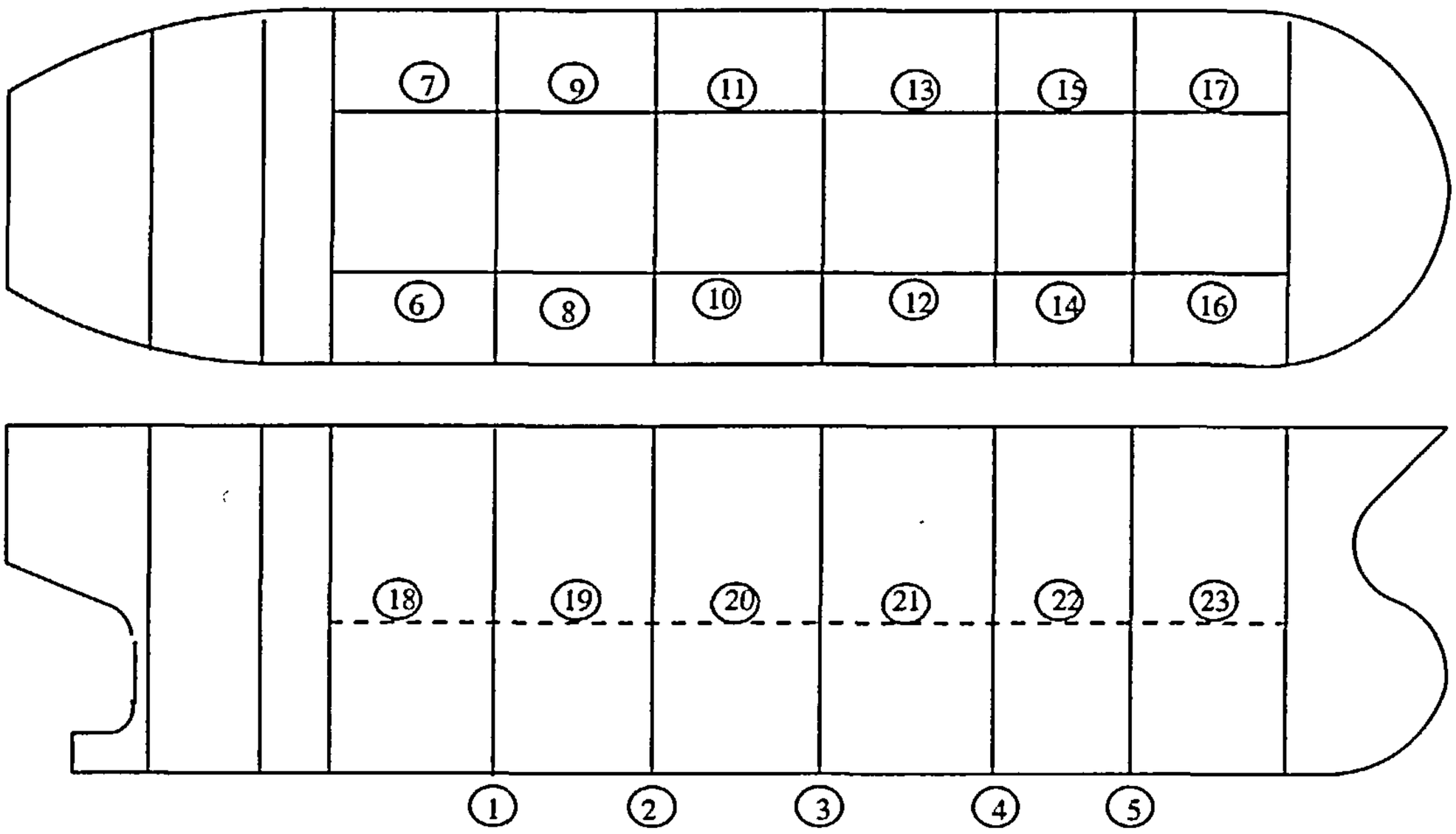

FIGURE 8.14. Variables for case (c)

Figure 8.14 describes the twenty three design variables for case (c).

Table 8.11 lists the percentage changes in the location of the subdivision members. The percentages for the longitudinal bulkhead has been calculated with respect to the beam of the vessel. Except for bulkheads 5 and 8, all other bulkheads share the same position as that for case (b). Figure 8.17 shows how the local index values again settle down as the GA progresses. The mean outflow index value have again increased for case (c) when compared to case (b) as seen in Table 8.10. But as seen from Figure 8.15 the outflow value has fallen substantially as the GA progressed and further reductions

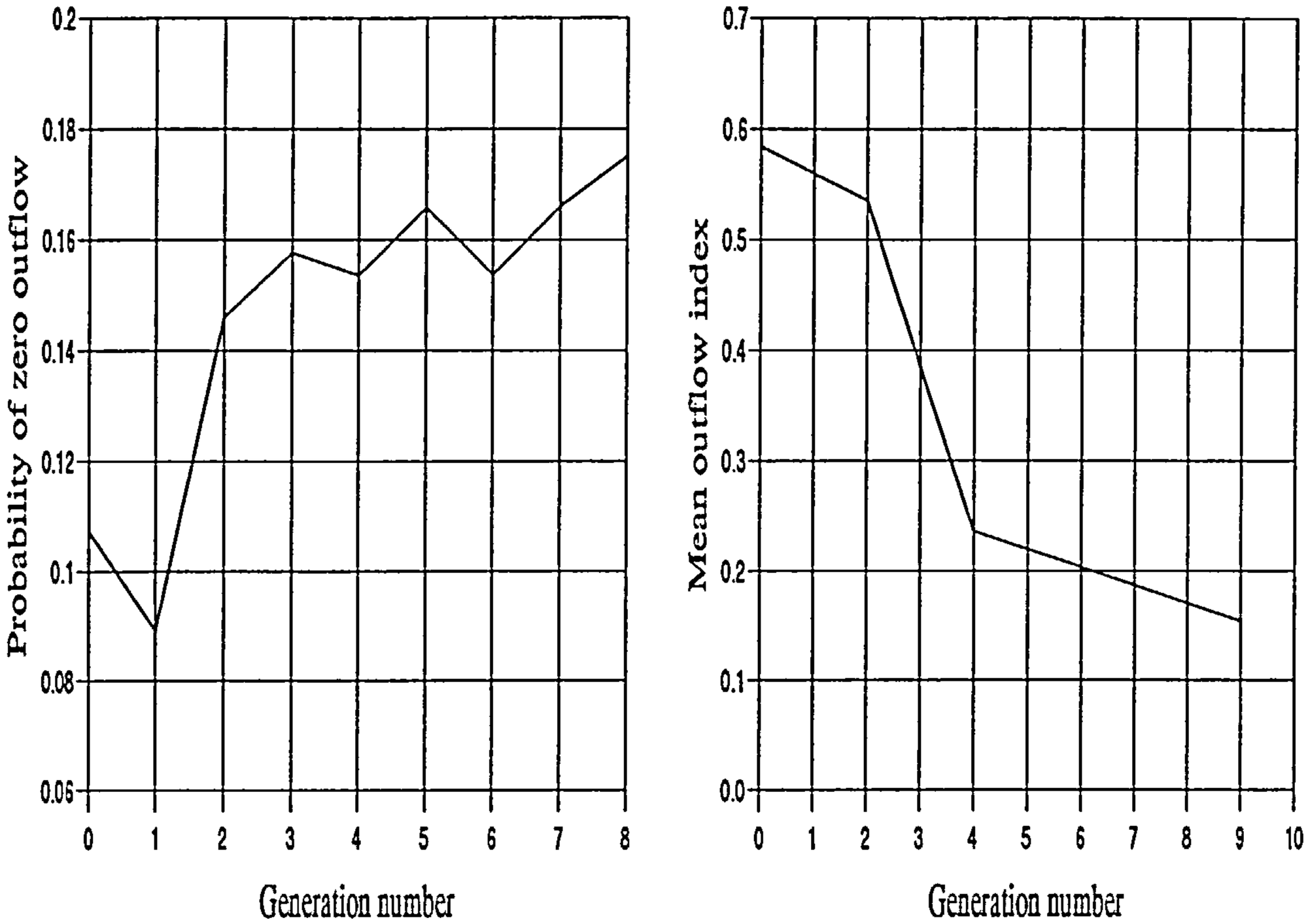

FIGURE 8.15. Zero outflow and Mean outflow index history, case(c)

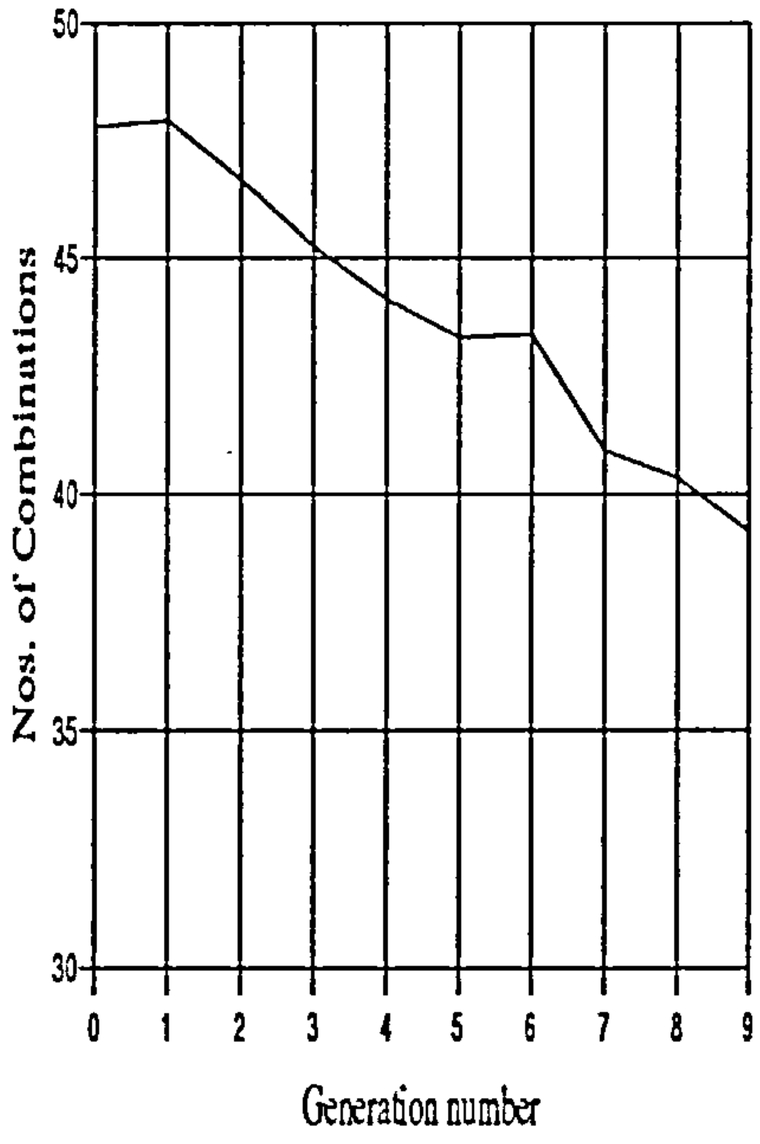

FIGURE 8.16. Average damage combination number history

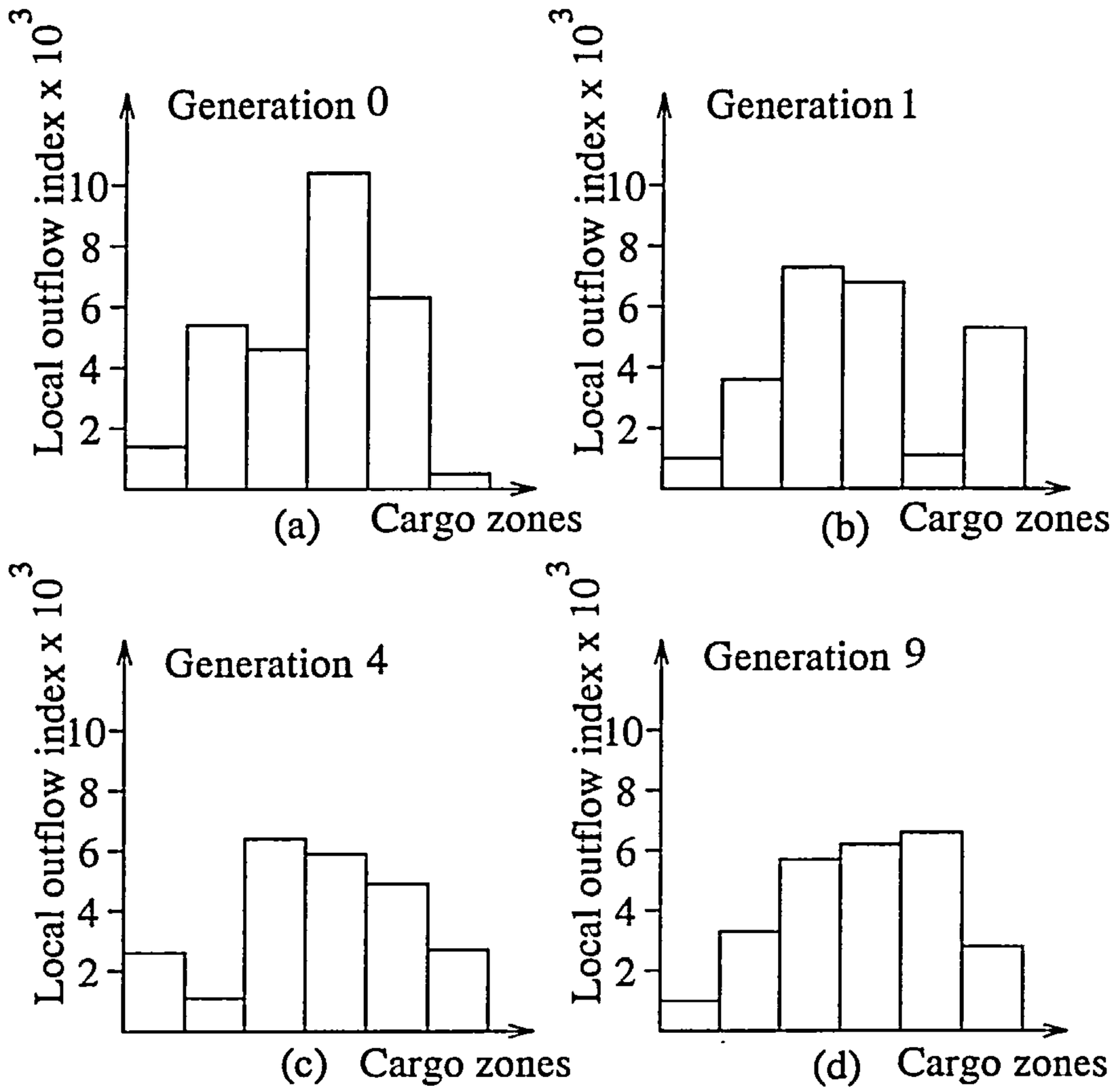

FIGURE 8.17. Variation of local outflow index, case (c)

can be expected if additional generations were evaluated. The larger mean outflow index was mainly due to the ship failing to meet the equilibrium condition since large wing compartment volumes caused considerable heel in the final damaged condition.

,

TABLE 8.10 : Parameters and results for the local index outflow cases

Gen. No.	Cargo vol. m^3	Ballast vol. m^3	Mean outflow, m^3	Outflow index	Var 1	Var 2	Var 3	Var 4	Var 5
0	66,869	30,170	39,053	0.584	-57.5	-35.8	-19.0	48.5	91.0
1	59,583	38,170	31,902	0.535	-59.7	-35.8	11.4	48.5	56.0
4	70,352	27,412	16,583	0.236	-49.0	-43.2	-3.7	43.5	76.0
9	74,309	23,468	11,414	0.154	-61.8	-35.8	1.3	33.5	76.0

Var 6	Var 7	Var 8	Var 9	Var 10	Var 11	Var 12	Var 13	Var 14	Var 15	Var 16	Var 17
8.7	8.7	7.8	7.8	8.2	8.2	7.8	7.8	7.8	7.8	7.3	7.3
7.3	7.3	6.4	6.4	6.9	6.9	9.2	9.2	7.8	7.8	6.9	6.9
7.8	7.8	8.7	8.7	8.3	8.3	6.4	6.4	6.0	6.0	9.2	9.2
9.2	9.2	6.4	6.4	8.7	8.7	8.3	8.3	8.3	8.3	8.7	8.7

Var 18	Var 19	Var 20	Var 21	Var 22	Var 23
12.5	6.8	9.7	8.2	11.1	11.1
6.8	4.0	14.0	8.3	12.5	6.8
12.5	5.4	6.8	12.5	14.0	9.7
4.0	12.6	4.0	4.0	12.6	14.0

TABLE 8.11 : Percentage changes in variables

Var. No.	Bulkhead	% change (+ve forwards)
1	4	0.36
2	5	2.3
3	6	1.4
4	7	-6.5
5	8	-4.9

Var. No.	% change (+ve away from centreline)
6, 7	5.0
8, 9	-3.7
10, 11	3.4
12, 13	2.2
14, 15	2.2
16, 17	3.4

8.5.4 case (d)

Case (d) was the same as case (c), in that all bulkheads and decks were allowed to vary with the resultant number of variables being 23. However the longitudinal bulkheads were all varied so that they all retained the same value so as to prevent a staggered

longitudinal bulkhead configuration for since such a configuration would be undesireable for many reasons.

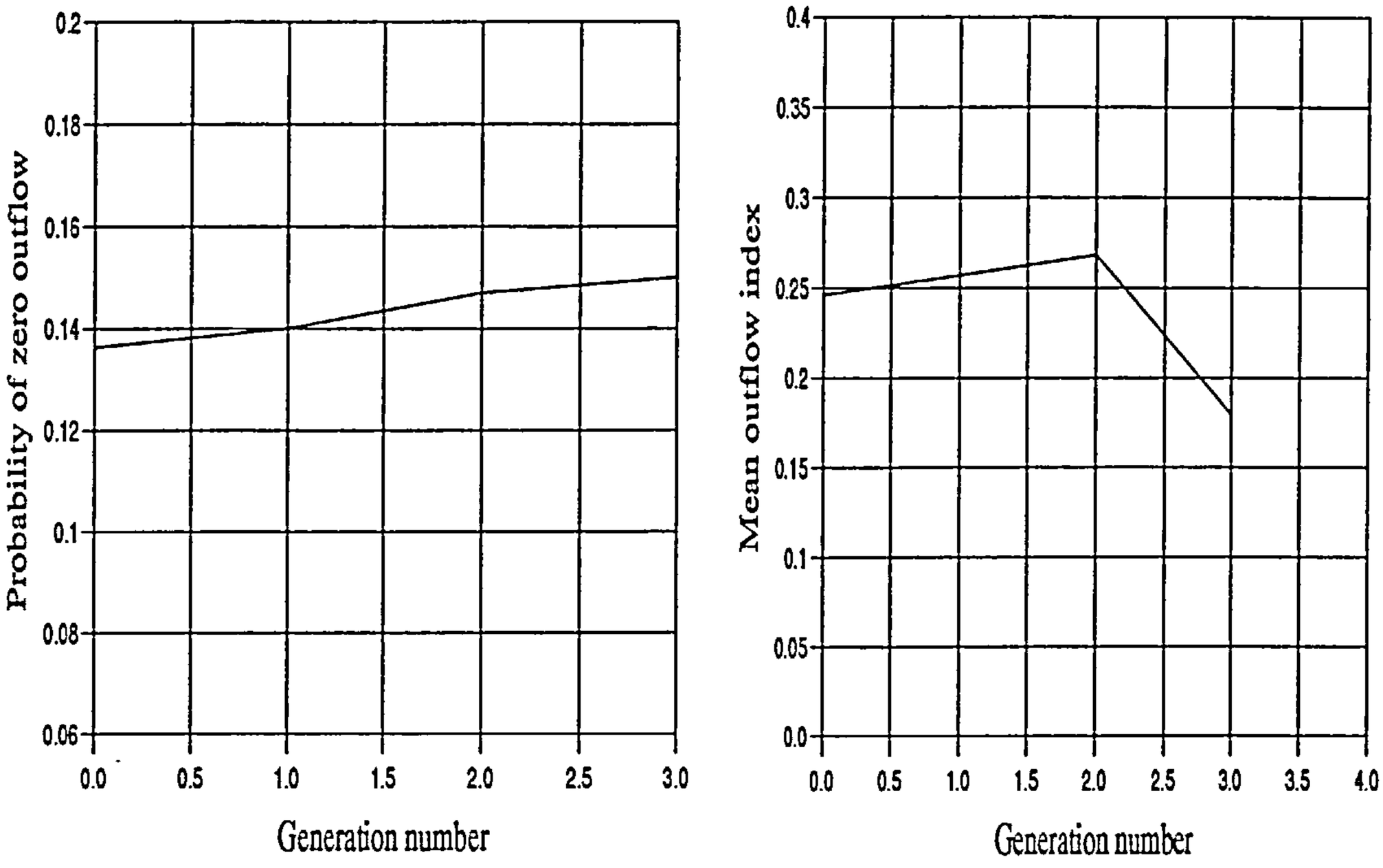

FIGURE 8.18. Zero outflow and Mean outflow index history, case(d)

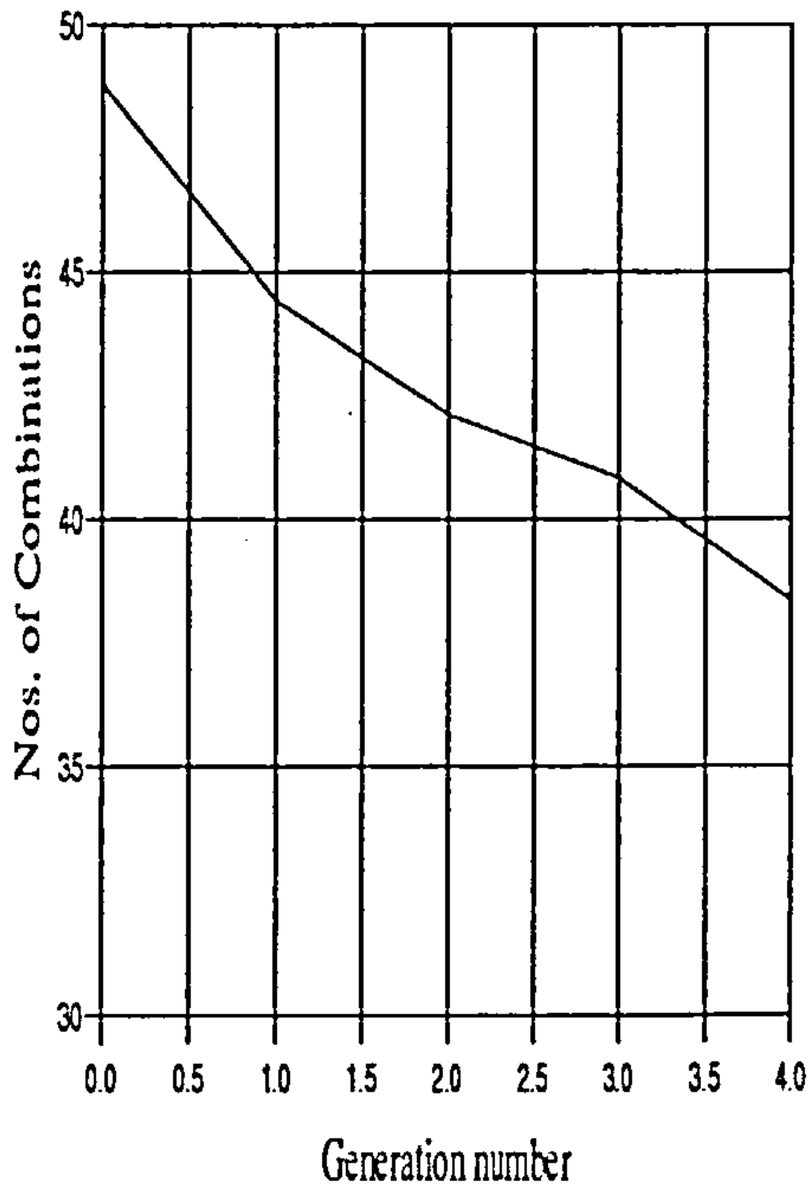

FIGURE 8.19. Average damage combination number history

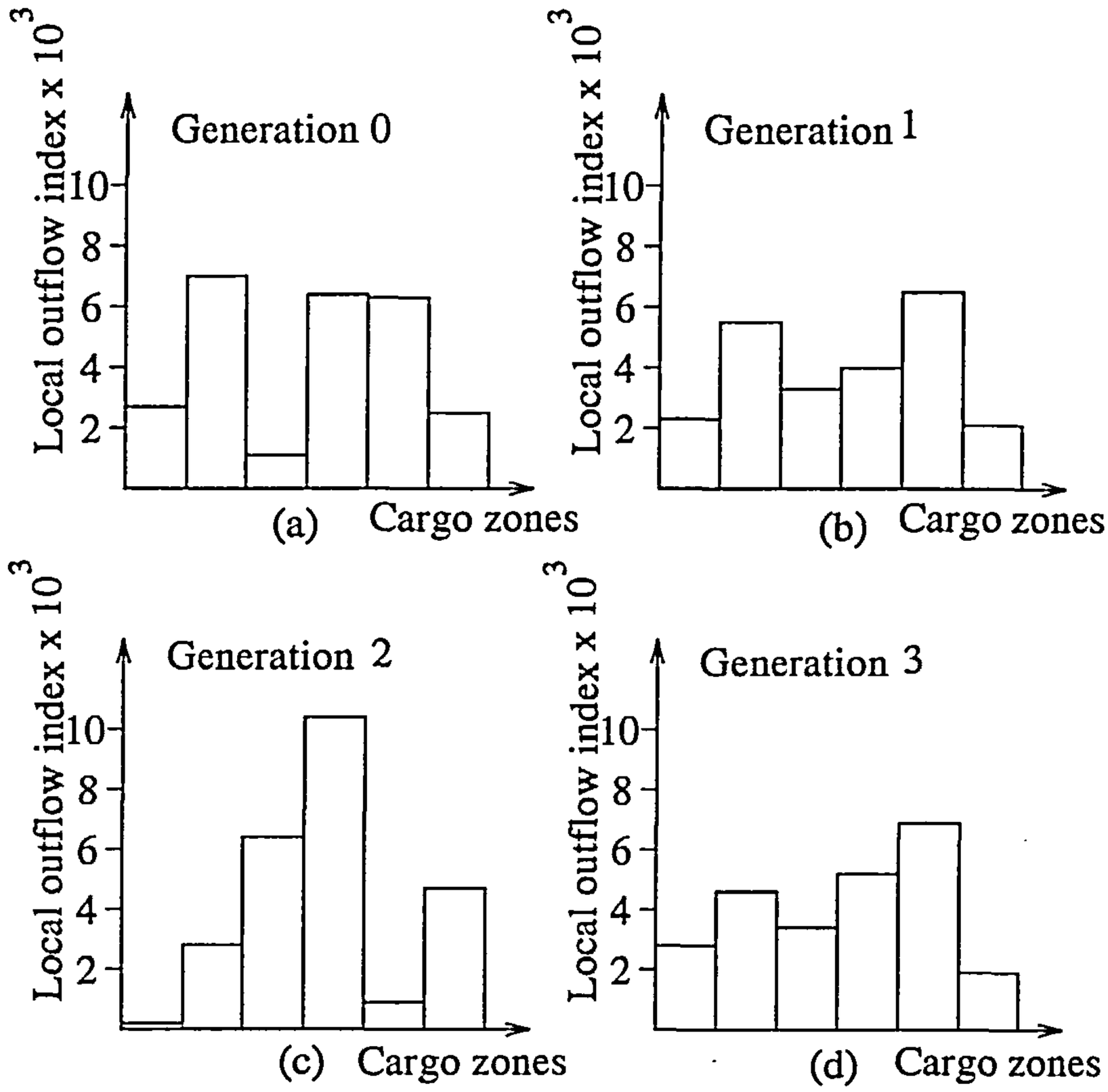

FIGURE 8.20. Variation of local outflow index, case (d)

TABLE 8.12 : Parameters and results for the local index outflow cases

Gen. No.	Cargo vol. m^3	Ballast vol. m^3	Mean outflow m^3	Outflow index	Var 1	Var 2	Var 3	Var 4	Var 5
0	70,023	27,766	17,266	0.246	-55.4	-21.0	-13.9	23.5	71.0
1	69,192	28,568	17,775	0.257	-57.5	-39.6	1.3	28.5	56.0
2	67,471	30,310	18,102	0.268	-64.0	-47.0	-8.85	53.5	61.0
3	68,885	28,904	12,319	0.179	-51.1	-28.4	-8.85	18.5	71.0

Var 6	Var 7	Var 8	Var 9	Var 10	Var 11	Var 12	Var 13	Var 14	Var 15	Var 16	Var 17
8.7	8.7	8.7	8.7	8.7	8.7	8.7	8.7	8.7	8.7	8.7	8.7
7.37	7.37	7.37	7.37	7.37	7.37	7.37	7.37	7.37	7.37	7.37	7.37
7.37	7.37	7.37	7.37	7.37	7.37	7.37	7.37	7.37	7.37	7.37	7.37
8.3	8.3	8.3	8.3	8.3	8.3	8.3	8.3	8.3	8.3	8.3	8.3

Var 18	Var 19	Var 20	Var 21	Var 22	Var 23
14.0	4.0	4.0	4.0	12.5	5.4
12.5	8.3	5.4	6.9	11.1	8.2
11.1	6.8	11.1	12.6	4.0	6.9
14.0	9.7	12.5	8.3	14.0	8.3

TABLE 8.13 : Percentage changes in variables

Var. No.	Bulkhead	% change (+ve forwards)
1	4	2.8
2	5	-4.7
3	6	3.5
4	7	8.1
5	8	1.1
Var. No.	**% change (+ve away from centreline)**	
6 to 17	2.2	

Due to the computational burden only the first five generations were evaluated, which was again due to the large number of combinations that were needed to be evaluated as shown in Figure 8.19. The mean outflow index values though almost steady over the first three generations has begun to fall from the fourth generation onwards. This trend can be expected to continue if the GA was allowed to progress. There is also a steady increase in the zero outflow probabilities. However the zero outflow probabilities have lower values than that for case (b) and (c) since the flexibility in the internal arrangement has been curtailed.

TABLE 8.14 :

Fitness value	1	2	3	4	5	6-17	18	19	20	21	22	23
23.97	-55	-25	16.5	48.5	91	6	12.6	12.6	4	14	4	7
23.19	-49	-43	-9	18.5	76	7.8	5.4	10	8	5.4	5.4	11
23.24	-53	-25	1.3	33.5	86	9.2	8	12.6	12.6	7	10	11

It was also interesting to note that almost similar fitness values were obtained for vastly different longitudinal bulkhead positions as shown in Table 8.14. As seen from Figure 8.20, the variations in the local outflow index have begun to assume a more uniform distribution as the GA progressed.

It must be borne in mind that the optimisation involved multiple goals with the priorities for each goal being almost equal. A parametric evaluation by varying the weights in this multi-objective optimisation could have perhaps been an interesting exercise but the limitation of time has prevented its undertaking. This is inspite of the fact that state-of-the-art computational tools such as message passing interface along with distributed computing paradigms have been used in order to speed up the calculations. GA by nature are wasteful in their evaluations. However given the multi-peaked nature of the performance landscape GA's are probably the most effective tool for such challenging problems because of the implicit parallelism that is built into their search strategy. The result emphasise how important it is to conduct detailed optimisation and parametric studies to produce good design rules if the probabilistic regulations are to be used effectively and intelligently. Also, an examination of the four cases above seem to indicate that a more uniform distribution of the local index results in a better overall index value rather than a staggered local index distribution.

Chapter 9

Conclusions

Safety seems to occupy an increasingly important role with every passing decade during the latter half of this century. A more environmentally aware population is beginning to become increasing vocal in its protestations against inadequate safety provisions. The work involved in this thesis was focused mainly on collision damage of ships and examination of the ship subdivision problems using the probabilistic methodology.

Pawlowski's theory on 'advanced stability' is a elegant method of modelling the behaviour of floating bodies under intact or damaged conditions [Pawlowski'91]. The method however requires clear visualisation of the parameters involved and precise definition of the vessel's form and compartmentation.

Though more complex and time-consuming to develop, B-splines have proved to be a superior method for hullform and compartment form definition. The flexibility of B-splines in terms of spline manipulation operations such as splitting and merging splines and properties such as convex hull property and affine transformation were important since the description of the intersection between the waterplane and the hullform was crucial to the development of the damage stability theory.

The use of equivolume waterplane theory, often underestimated in ship theory, provides the description of the new equivolume waterplane under conditions of free trim and the position of the centre of buoyancy in one single iteration. In comparison traditional methods use a great number of cross-sections to estimate the volume and its moments could be inaccurate due to the interpolations involved or much slower because of the iterative process involved. In addition the new theory can be applied to any floating vessel such as rigs or catamarans where the waterplanes are made up of separate and distinct areas.

Two aspect about this particular optimisation model made the problem suitable for the use of genetic algorithms (GA). The first was the presence of multiple peaks in the performance landscape but the second and the more important one was the inability to represent the probabilistic regulations in a closed form manner. Furthermore, a mathematical approach to this problem was definitely more efficient than a knowledge based approach given the degree of complexity in the rules, and an adaptive approach more effective than a hill-climbing search.

The coarse grained nature of the problem made it naturally suitable to a MIMD configuration. The availability of free public domain message passing interfaces such as PVM was also very useful. The granularity of the problem can be increased even further since every gene that gets farmed out again consists of several damage combinations which are again independent of each other. A careful evaluation of the parameters of parallelisation is however required because of the nature of certain Unix architectures whose performance drops rapidly as more and more processes are loaded onto the processor at a given time. This may have the effect of increasing the net processing time for a particular generation of the GA.

As the GA progressed a continuous improvement in the A-index value in the case of passenger vessels and a net reduction in mean oil outflows for oil tankers was obtained as expected as more efficient subdivision members started to dominate the gene pool and the non-uniformity in the local index variations also reduced. No exact correlation seemed to exist between the local index variation and the position of subdivision members, that is, the variation in the local index values cannot be used directly to drive the optimisation model towards superior subdivisions. However one of the conclusions that emerges from the analysis is that a general move towards uniformity in local index values is a worthwhile design objective. The effect of an even distribution of the local index

value seems to provide only an indirect measure of the efficiency of the subdivision arrangement. This largely reflects the complex nature of the theory behind the development of probabilistic regulations and it certainly makes the designer's task more difficult as the optimisation of subdivisions is currently a very time-consuming process.

The regulations were also found to be wanting in certain aspects and the author is aware of past and current work that is being done to address these problems. Some of the deterministic requirements that crept into A.265 (VIII) like the requirements for minimum standards for compartmentation (regulation 5) over some parts of the ship's length seem an unnecessarily imposed restriction. There also seem to be certain inconsistencies between the regulations for passenger and cargo ships. The regulation for passenger ships defines factors 'a' and 'p' which account for the longitudinal location and longitudinal extent of damage. As shown in the derivation for vertical extents in chapter 8, both these probabilities should be combined into a single factor and the cargo ship regulation seems to have addressed this with more rigour, as it has a single factor 'p' which combines the above two.

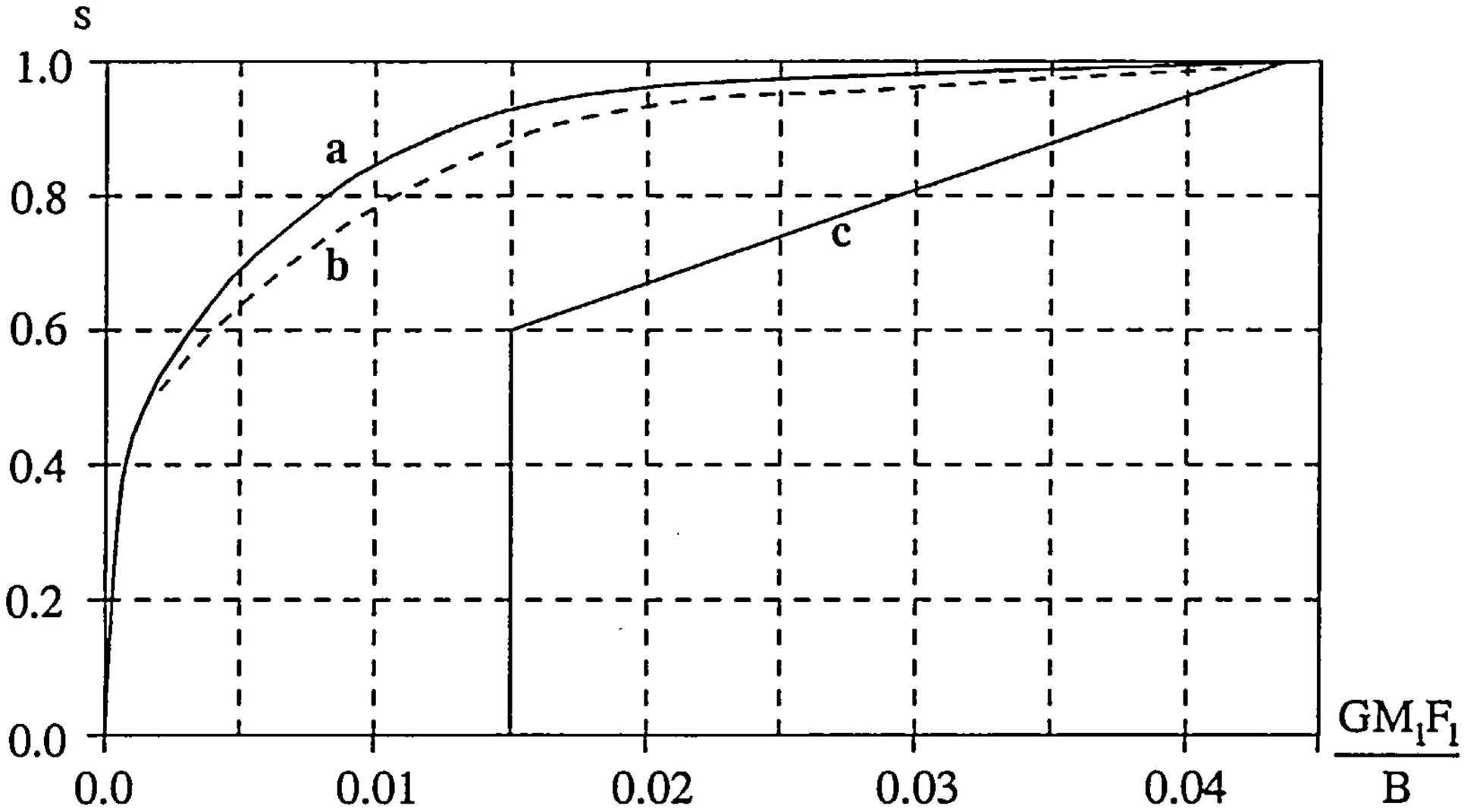

a – based on model tests and sea state distributions
b – as proposed by Pawlowski [Pawlowski'92]
c – approximation adopted by IMO

FIGURE 9.1. The 's' factor formulation

The 's' factor formulation for passenger ships also seems inconsistent with that for cargo ships. The 's' factor for passenger ships is based on the metacentric height (GM) and the

effective damage freeboard (F_e) instead of the righting arm curve. This was due to the fact that model tests conducted to estimate the damage stability characteristics of vessels based on the GZ-curve showed inconsistencies with regards to the direction of heel (whether away or towards the waves).

Figure 9.1 shows three curves based on the $\frac{GM_1F_e}{B}$ factor on which the 's' factor is formulated. Curve (a) is based on model tests, and curve (c) is the approximation adopted by IMO. Curve (b) as proposed by Pawlowski [Pawlowski'92] is based on the following relationship

$$s = 1.7\left(\frac{GM_1F_e}{B}\right)^{1/6} \qquad \text{(EQ 9.1)}$$

but not more than 1.0. The reasoning behind the IMO approximation was to reduce the amount of damage stability calculations involved, a consideration which is perhaps out-of-date in this age of computers. As can be seen from Figure 9.1, curve (b) is a good approximation of curve (a), based on model tests. Thus the current formulation of the 's' factor which has shortcomings in terms of stepwise variations is only a poor approximation of the true curve. Also the significance and the effectiveness of F_e, the mean damage freeboard, in the current 's' factor formulation seems ambiguous and contrived.

The stepwise variation in the s-curve as demonstrated in chapter 7 shows some of the shortcomings in the current formulation for the 's' factor. There seems to emerge a strong argument in favour of reformulating the 's' factor for the passenger ship regulations as a function of the GZ-curve which would harmonize the rules with that for cargo ships. Also certain modifications such as those proposed by Wimalsiri [Wimalsiri'91] could be incorporated so as to reduce the "cliff-edge" effects that seems to the cause for these stepwise variation in the 's' factor. The advantage of having a smooth 's' curve would eliminate the need for repeated damage stability calculations in order to determine the survival capability of a damage scenario as interpolations would be possible if the variations in the 's' factor were to be smooth. This would go a long way in reducing the computational burden that is imposed when attempting to use the probabilistic rules to a "satisfactorily" safe ship design from the subdivision point of view.

Vertical extents of damage are completely neglected by passenger ship regulations where damage is always assumed bottom upwards without limit. Placement of addi-

tional decks below the subdivision deck would therefore contribute to no merit in such a situation. .

The cargo ship regulations does include a factor 'v' which accounts for the probabilities of different vertical extents from the waterline upwards to the maximum vertical extent of damage, which conforms to the minimum bow height according to the 1966 load-line convention. However their formulation does not allow any credit for horizontal subdivisions below the waterline. The formulation for the probability of vertical extent of damage, as outlined in chapter 7, gives credit to all horizontal subdivision members that exist. Though the current formulation is based on the damage statistics for ro-ro cargo ships they can be easily replaced by other distributions as and when they become available, but the basic principle behind the formulation remains the same.

The need for harmonisation between cargo ship and passenger ship regulations cannot be overstated. Differing sets of rules for different ship types seems to alienate an already complex set of rules and poses a barrier to their universal endorsement and acceptance. This research has gathered state-of-the-art tools from various fields such as computer graphics, naval architecture, non-linear optimisation methods and distributed computing in an attempt to arrive at a satisfactory subdivision from the damage stability point of view. As seen from the performance landscapes for this problem, its multi-modal nature implies that there are a number of vastly different designs that can satisfy the same requirements for safety. The presence of multiple solutions may be of some advantage to designers since there are other theoretical and practical constraints that influence the position of subdivision members. The formulation of the probabilistic regulations has involved a considerable investment of time and effort and to a certain extent reflect a compromise between conflicting opinions that exists between nation states. But as pointed out there are a number of shortcoming that need to be addressed in order to make the regulations more acceptable and user friendly.

References

Andrews'91 — Andrews, G.R., Concurrent programming principles and practice, Benjamin/Cummings, California, 1991.

Back'91 — Back, T., Self-Adaptation in Genetic Algorithms, Proceedings of the First European Conference on Artificial Life, MIT Press, Paris, France, Deccember 11-13, 1991.

Baker'87 — Baker, J. E., Reducing Bias and Inefficiency in Selection Algorithms, Proceedings of the Second International Conference on Genetic Algorithms and their Applications, 1987, pp 14-21.

Bertsekas'89 — Bertsekas, D.P. and Tsitsiklis, J.N., Parallel and DistributedComputing, Prentice Hall, New Jersey, 1989.

Brindle'81 — Brindle, A., Genetic Algorithms for function optimization, Doctoral Dissertation, University of Alberta, Edmonton, 1981.

Buxton'66 — Buxton, I.L., The design of tanker hull structure by computer with particular reference to one midship cargo tank, Trans. RINA, vol.108, pp 405-420, 1966.

C-Linda'92 — C-Linda User Guide and Reference Manual, Scientific Computing Associates Inc., New Haven, CT, 1992.

Comstock'61 — Comstock, J.P. and Robertson, J.B., Survival of collision damage versus the 1960 convention on safety of life at sea, Trans. SNAME, vol. 69, pp. 461-522, 1961

Cox'71 — Cox,M.G., The numerical evaluation of B-splines, National Physical Laboratory DNAC 4, August 1971

Davis'87a — Davis, L., (Ed.) Genetic Algorithms and Simulated Annealing, Morgan Kaufmann Publishers Inc., Los Altos, CA, 1987.

Davis'87b — Davis, L. and Steenstrup, M., Genetic Algorithms and Simulated Annealing an overview, in [Davis'87a], pp. 1-11.

De Boor'72 — de Boor, C., On calculations with B-splines, J. approx. theory, Vol. 6, pp. 50-62, 1972

DeJong'75 — DeJong, K.A., An analysis of the behaviour of a Class of Genetic Adaptive Systems, Doctoral Dissertation, University of Michigan, 1975.

Dillon'71 — Dillon, E.S, Ship design aspects of oil pollution abatement, Marine Technology, SNAME, Vol. 8, No. 3, pp. 293-326, July 1971.

Farin'88 — Farin, G., Curves and Surfaces for Computer Aided Geometric Design, Academic Perss, Boston, MA, 1988.

Fischer'73 — Fischer, K.W., The inclusion of IMCO tanker design constraints in general optimisation procedures, Trans. SNAME , Vol. 81, pp 191-212, 1973.

Flynn'72 — Flynn, M.J., Some Computer Organisation and their effectiveness, IEEE transactions on Computers, C-12, No. 9, Sept. 1972, pp. 948-960.

Fog'85 — Fog, N.G., A B-spline surface system for Ship hull design, Proc. of the IFIP/IFAC figth Int. Conf. "Computer Application in the Automation of Shipyard Operations and Ship Design", 1985

Fogel'66 — Fogel, L.J., Owens, A.J. and Walsh, M.J., Artificial Intelligence through Simulated Evolution, Wiley, New York, 1966.

Garey'79 — Garey, M.R. and Johnson, D.S., Computers and Intractability A Guide to the theory of NP-completenesss, W.H.Freeman and Co., San Francisco, 1979.

Gerald'84 — Gerald, C. F. and Wheatley, P. O., Applied numerical analysis, Addison-Wesley, 1984.

Glover'77 — Glover, F.M., Heuristics for Integer Programming using Surrogate Constraints, Decision Sciences, Vol. 8, No. 1, 1977, pp. 156-166.

Goldberg'89 Goldberg, D.E., Genetic Algorithms in Search Optimization and Machine Learning, Addison Wesley, Reading, MA, 1989.

Grefensette'89 Grefensette, John J, How Genetic Algorithms Work: A Critical look at Implicit Parallelism, Proceedings of the Third International Conference on Genetic Algorithms, Morgan Kauffman, San Mateo, Calif, 1989, pp. 20-27.

Harel'87 Harel,D., Algorithms, the spirit of computing, Addison-Wesley, 1987

Hearn'94 Hearn, D. and Baker, M.P., Computer Graphics, Prentice-Hall, New Jersey, 1994.

Hestenes'69 Hestenes, M.R., Multiplier and Gradient methods, Journal of Optimization Theory and Applications, 1969, pp. 303-320.

Hirai'92 Hirai, A., The tanker design for prevention of oil pollution "Mid-deck tankers", Int. Symp. on the Practical Design of Ships and Mobile Units [PRADS'92], vol. 2, pp. 2.13944-2.1400, 1992.

Hockney'88 Hockney, R.W. and Jesshope, C.R., Parallel Computers 2, Arcitecture, Programming and Algorithms, IOP Pub., Philadelphia, 1988.

Holland'75 Holland, J., Adaptaions in Natural and Artificial Systems, University of Michigan Press, Ann Arbour, 1975.

Hook'91 Hook, J.P., The inqdequacies of the current approach to minimising oil outflow from damaged tankers, a proposed alternative, Trans. SNAME, vol. 99, pp. 421-462, 1991.

Horowitz'84 Horowitz, E., and Sartaj, S., Fundamentals of Computer Algorithms, Computer Science Press, Maryland, 1984.

Hwang'85 Hwang, K. and Briggs, F.A., Computer Architecture and Parallel Processing, McGraw-Hill, Singapore, 1985.

IMO'74 IMO, Regulations on subdivision and safety of passenger ships (as an equivalent to part B of chapter II of the Int. convention for the safety of life at sea 1960), London 1974.

IMO'92 IMO comparitive study on oil tanker design, IMO report, February 1992.

Izumida'79 — Iznumida, K. and Matida, Y., Ship hull definition by surface techniques for production use, Proc. of the IFIP/IFAC figth Int. Conf. "Computer Application in the Automation of Shipyard Operations and Ship Design", Univ. of Strathclyde, 18-21 June, 1979

Karafaith'93 — Karafaith, G. and Bill, R. M., Model tests of accidental oil spills due to grounding, Int. Conf. on Hydroscience and Engineering, June 7-11, 1993.

Kirkpatrick'83 — Kirkpatrick, S., Gelatt, C.D. and Vecchi, M.P., Optimization by Simulated Annealing, Science, Vol.220, No.4598, May 1983, pp. 671-681.

Konstantinidis'86 — Konstantinidis, C., Investigations into the damage survivability of ro-ro ships (with special reference to ro-ro cargo ships) M.Sc. thesis, Univ. of Newcastle upon Tyne, July, 1986.

Koza'90 — Koza, J.R., Genetic Programming: A Paradigm for Genetically Breeding Populations of Computer Programs to solve problems, Report No. STAN-CS-90-1314, Stanford University, 1990.

Michalewicz'92 — Michalewicz, Z., Genetic Algorithms + Data Structures = Evolution Programs, Springer-Verlag, New York, 1992.

Michel'91 — Michel, R. K. and Tagg, D., Probabilistic analysis of tanker oil outflow, The northern California section of SNAME, December 12, 1991.

Minoux'86 — Minoux, M., Mathematical Programming Theory and Applications, John Wiley and Sons, Chichester, 1986.

Mitchell'92 — Mitchell, M., Forrest, S. & Holland, J. H, The Royal Road for Genetic Algorithms: Fitness Landscapes and GA Performance Proceedings of the First European Conference on Artificial Life, 1992.

Motteler'93 — Motteler, F. C., Arbitrary precision floating point arithmetic, Dr. Dobb's Journal, vol. 18, issue 9, pp. 28-34, September 1993.

Mukherjee'85 Mukherjee, S., Investigation of tanker subdivision based on probability of pollution in case of collision, Ph.D. thesis, Ship Research Inst., Tech. Univ. Gdansk, Report No. 464/85, pp. 200, Gdansk, 1985.

Munchmeyer'79 Munchmeyer, F.C., Schubert, C. and Nowaki, H., Interactive design of fair hull surfaces using B-splines, Proc. of the IFIP/ IFAC figth Int. Conf. "Computer Application in the Automation of Shipyard Operations and Ship Design", Univ. of Strathclyde, 18-21 June, 1979

Newman'79 Newman, W.H. and Sproull, R.F., Principles of Interactive Computer Graphics, McGraw-Hill, New York, 1990.

Neyhart'92 Neyhart, T. L., Roseman, D. P., Sirkar, J., and Cojeen, P. H., Tanker design aspects following the OPA'90 legislation, Int. Symp. on the Practical Design of Ships and other Mobile units [PRADS'92], vol. 2, pp. 2.1407-2.1429, 1992

Nowacki'70 Nowacki, H., Brusis, F. and Swift, P.M., Tanker preliminary design - an optimisation problem with constraints, trans. SNAME, vol. 78,pp. 357-390, 1970.

Paetow'94 Paetow, K. H., The E3 tanker, Int. Marine Design Conf., Delft, Netherlands, pp. 3-22, 1994.

Pawlowski'91 Pawlowski, M., Advanced Stability Calculations for a Freely Floating Rig, report, Department of Marine Technology, University of Newcastle upon Tyne, p. 21, November, 1991 (also in 5th Int. Symp. on the Practical Design of Ships and mobile units [PRADS'92], vol. 2, pp. 2.1146-2.1160, May 1992).

Pawlowski'92 Pawlowski, M. and Sen, P., Probabilistic concept of ship subdivision: theory and application, report, Department of Marine Technology, University of Newcastle upon Tyne, pp. 117, 1992.

Payne'94 Payne, S., Tightening the grip on passenger ship safety: the evolution of SOLAS, The Naval Architect, pp. E482-E487, October 1994.

Petrie'94 Petrie, A. and Kerr, R., A Quantitative Comparison of Network Linda and PVM, Computing Service, University of Newcastle upon Tyne, July 1994 (anon. ftp from tuda.ncl.ac.uk [128.240.2.1] in /pub/parallel/ pvm_vs_linda.ps.Z).

Powell'69 Powell, M.J.D., A method for nonlinear constraints in minimization problems, Optimization (R. Fletcher, Ed.) Academic Press, New York, 1969, pp. 283-298.

Press'92 Press, W.H., Teukolsy, S.A, Vetterling, W.T. and Flannery, B.P., Numerical recipies in C, Cambridge University Press, MA, 1992.

Price'71 Price, R.I, Anti-pollution measure- IMCO subcommittee on ship design and equipment, Marine technology, SNAME, vol. 8, No. 3, pp. 1-7, July 1971.

PVM'93 PVM 3 User Guide and Reference Manual, Oak Ridge National Laboratory, Oak Ridge, Tennessee, 1993.

Rao'78 Rao, S.S., Optimization Theory and Applications, Wiley Eastern Limited, New Delhi, 1978.

Rawson'90 Rawson, K. J., Ethics and fashion in design, The Naval Architect, pp. 1-27, February 1990.

Riesenfeld'73 Riesenfeld, R. F., Application of B-spline approximation to geometric problems of computer aided design, Ph.D. dissertation, Syracuse Univ., Syracuse NY, 1972 (also available as U. of Utah, UTEC-CSc-75-126, March 1973).

Roberts'84 Roberts, F.S., Applied Combinatorics, Prentice-Hall, New-Jersey, 1984.

Robertson'74 Robertson Jr., J.B., Nickum, G. C., Price, R. I. and Middleton, E., H., The new equivalent international regulations on subdivision and stability of passenger ships, Trans. SNAME, vol. 82, pp. 344-351, 1974.

Rockafeller'73 Rockafeller, R.T., A dual approach to solving nonlinear programming problems by unconstrained optimization, Mathematical Programming, 1973, pp. 354-373.

Rogers'77 Rogers, D.F., B-spline Curves and Surfaces for Ship Hull Definition, Symp. on Comuter-Aided Hull Surface Definition [SCHAD'77], Annapolis, Sept. 26-27, 1977.

Ross'89 Ross, S.M., Introduction to probability models, Academic press, CA, 1989.

Schwefel'81 Schwefel, H.P., Numerical Optimization for Computer Models, Wiley, Chichester, UK, 1981.

Schwefel'88 Schwefel, Hans-Paul, Evolutionay learning, optimum-seeking on parallel computer architecture, Proceedings of the Int. Symp. on System Analysis and Simulation I : Theory and Foundations, Akademie der Wissenschaften der DDR, Kkademie-Verlag, Berlin, September 1988, pp. 217-225.

Sen'92 Sen, P. and Gerick, M.K., Some aspects of a knowledge based expert system for priliminary ship subdivision design for safety, Int. Symp. on the Practical Design of Ships and Mobile units [PRADS'92], vol. 2, pp. 2.1187-2.1197, 1992.

Shansky'63 Semyonov-Tyan-Shansky, V., Static and Dynamics of Ships, Peace Publishers, Moscow, 1963.

SIKOB'87 SIKOB-package for naval architect calculations, user's guide, May 1987.

Simon'69 Simon, H.A., The sciences of the artificial, Cambridge, MA, M.I.T Press, 1969.

SLF36'91 Review of the hypothetical oil outflow parameters, submitted by the United States, IMO document (in English only), SLF 36/INF.16, December 13, 1991.

Srinivas'94 Srinivas, M. and Patnaik, L.M., Computer, Vol.27, No. 6, June 1994.

Tagg'82 Tagg, R.D., Damage survivability of cargo ships, Trans. SNAME, vol. 90, pp 26-40, 1982.

TSPP'78 Final act of the Int. Conf. on Tanker Safety and Pollution Prevention, including attachments for SOLAS'74 and for the Int. conf. for the prevention of pollution from ships, 1973, IMO, London, 1978

Van del Laan'94 — Van der Laan, M., Innovative environmental tanker design, Imt. Marine Design Conference, Delft, Netherlands, pp. 23-37, 1994.

Volkov'63 — Volkov, B. N., Determination of probability of ship survival in the case of damage, Sudostrojenie, No. 5, pp 4-8, 1963.

Wendel'60 — Wendel, K., "Die Wahrscheinlichkeit des Uberstchens von Verletzungen, Schiffstechnik, Hamburg pp 47-61, 1960.

Wendel'68 — Wendel, K., Subdivision of ships, Proc. 1968 Diamond Jubilee Int.- 75th Aniversary, SNAME, New York, paper no. 12, pp. 27, 1968.

Wimalsiri'91 — Wimalsiri, W.K., Design of Ro-ro Cargo ships with Particular Reference to Damage Stability, Ph.D. thesis, University of Newcastle upon Tyne, 1991.

Appendix A

Transformation of Moments of Inertia

Figure A.1 shows two coordinate systems: (x, y) and (x', y'), having the same origin and inclined at an angle χ to each other. It is assumed that the moments about the former coordinate system are known and that the moments about the latter are to be found.

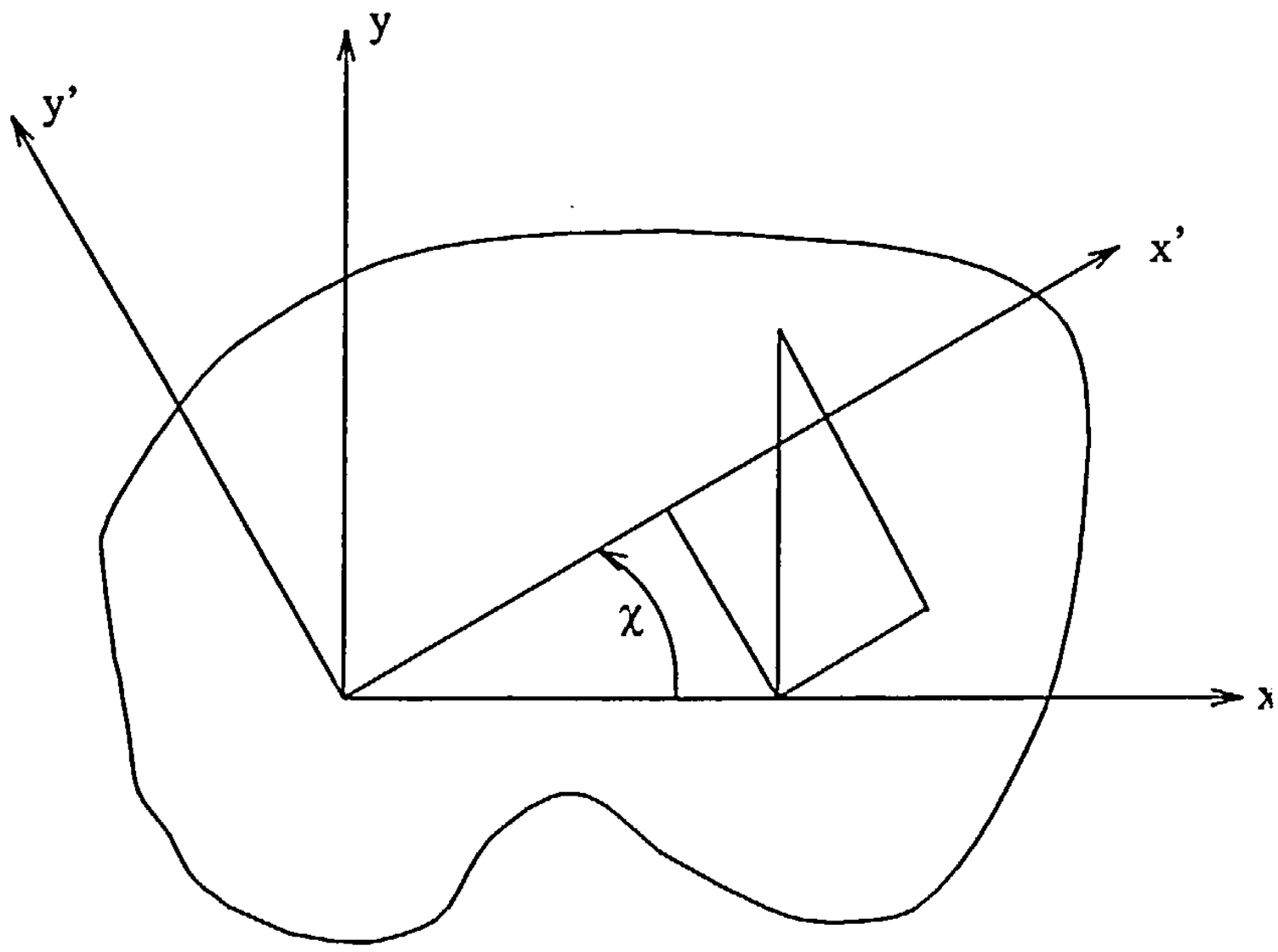

FIGURE A.1. Transformation of moments of inertia

The three sought moments of inertia are,

$$J_{x'} = \int_A y'^2 dA = \int_A (y^2(\cos\chi)^2 - xy\sin 2\chi + x^2(\sin\chi)^2)dA$$

$$J_{y'} = \int_A x'^2 dA = \int_A (x^2(\cos\chi)^2 + xy\sin 2\chi + y^2(\sin\chi)^2)dA$$

$$D' = \int_A x'y' dA = \int_A (xy\cos 2\chi + \sin\chi\cos\chi(y^2 - x^2))dA$$

D' is called the cross-product or the moment of deviation. Operating simultaneously on the above equations,

$$J_{x'} = J_x(\cos\chi)^2 + J_y(\sin\chi)^2 - D\sin 2\chi \qquad \text{(EQ A.1)}$$

$$J_{y'} = J_y(\cos\chi)^2 + J_x(\sin\chi)^2 + D\sin 2\chi \qquad \text{(EQ A.2)}$$

$$D' = \frac{J_x - J_y}{2}\sin 2\chi + D\cos 2\chi \qquad \text{(EQ A.3)}$$

where $J_x = \int_A y^2 dA$, $J_y = \int_A x^2 dA$ and $D = \int_A xy dA$.

Introducing the notations,

$$J = \frac{J_x + J_y}{2}$$

$$a = \frac{J_x - J_y}{2}$$

(EQ A.1) and (EQ A.2) become,

$$J_{x'} = J + a\cos 2\chi - D\sin 2\chi$$

$$J_{y'} = J - a\cos 2\chi + D\sin 2\chi$$

which can be written in a more compact form as,

$$J_{x'} = J + a' \qquad \text{(EQ A.4)}$$

$$J_{y'} = J - a' \qquad \text{(EQ A.5)}$$

where $a' = a\cos 2\chi - D\sin 2\chi$ and J is a constant. $J_{x'}$, $J_{y'}$ and D' are now dependent on just one variable a'. Therefore the problem is now reduced to finding just two variables, a' and D', given by,

$$a' = a\cos 2\chi - D\sin 2\chi \qquad \text{(EQ A.6)}$$

$$D' = a\sin 2\chi + D\cos 2\chi \qquad \text{(EQ A.7)}$$

which can be written in the form,

$$a' = r\cos(2\chi + 2\gamma) \qquad \text{(EQ A.8)}$$

$$D' = r\sin(2\chi + 2\gamma) \qquad \text{(EQ A.9)}$$

where $\cos 2\gamma = a$ and $r\sin 2\gamma = D$. These equations can be easily solved giving,

$$r^2 = a^2 + D^2 \qquad \text{(EQ A.10)}$$

$$2\gamma = \begin{cases} 2\gamma_o & \text{if } (a > 0) \\ 2\gamma_o + 180° & \text{otherwise} \end{cases} \qquad \text{(EQ A.11)}$$

$$2\gamma_o = \operatorname{atan}\frac{D}{a} \qquad \text{(EQ A.12)}$$

Knowing r and 2γ, the three sought moments can be easily found, using equations (EQ A.8) and (EQ A.9).

Equations (EQ A.4), (EQ A.5) and (EQ A.8), (EQ A.9) are the familiar expressions of analytical geometry for a circle of radius r with its centre at $(J, 0)$ and the phase angle equal to $2\gamma + 2\chi$ where χ is the parameter of variation in (EQ A.8) and (EQ A.9). Hence is a circle satisfying these equations is plotted for different angles of χ, the ordinate of a point on this circle corresponds to D' and the abscissa to $J_{x'}(= J + a')$. The other moment of inertia $J_{y'}(= (J - a'))$ corresponds to the abscissa of a point lying on the circle opposite to the given point whose phase angle is large by $180°$ (that is, the angle χ is larger by $90°$). The circle so constructed is known as the *Mohr's circle of inertia.*